

# DISSERTATION

## Study on Fluidization Phenomena Related to Gasification of Biomass in Fluidized Beds

ausgeführt zum Zwecke der Erlangung des akademischen Grades eines

Doktors der technischen Wissenschaften

unter der Leitung von

Univ.Prof.Dipl.-Ing.Dr.Techn. Hermann Hofbauer

am Institut für Verfahrenstechnik, Umwelttechnik und Technische Biowissenschaften  
(E166)

eingereicht an der Technischen Universität Wien  
Fakultät für Technische Chemie

von

**Master of Eng. Nguyen Xuan Quang**  
Matrikelnummer 0227478  
39/12 Le Thanh Nghi street, Hanoi, Vietnam

## **Abstract**

Being the most abundant sources of biomass energy in Vietnam and in Asia, rice husk and wood fuel at present are still not used properly. They are mainly used by direct burning in the cooking stove in household in remote areas that is very smoky and harmful to the health. Furthermore, biomass is used for direct burning with a low efficiency in some other heating applications such as in brick kiln and drying processes. A vast amount of rice husk is wasted to the river every year in Mekong Delta River in Vietnam every year.

Fluidized beds are one advanced technology that can be used for combustion and gasification processes. However, biomasses such as rice husk and wood pellets have particular characteristics so that they can not be fluidized alone. In order to process rice husk and wood pellets for fluidization applications, another fluidization material must be added to support the fluidization of the bed. Inert materials such as quartz sand, calcite, dolomite, olivine, etc. could be used as such fluidization bed materials. However, the fluidization behavior of the mixture of two different materials will be dependent on the percentage of biomass in the mixture.

Many experiments have been carried out to study the fluidization and mixing behavior of the mixtures of biomass and quartz sand. Furthermore, the knowledge was extended by a comprehensive literature review. Fluidization behavior becomes more complex and the characteristic values of the mixture (e.g.  $U_{mf}$ ) are not easy to determine. The standard deviation of pressure drop fluctuation is decreased when adding biomass to the sand bed depending on the percentage of biomass in the mixture. A good mixing is difficult to obtain when biomass and sand is initially in separated layers but becomes easier when biomass was continuously fed into the fluidized bed. Rice husk affected the fluidization behavior of the bed more than wood pellets due to its lower density and different shape.

Experiments were carried out also on gasification of rice husk and wood pellets in a laboratory scale fluidized bed gasifier. Gas product compositions and tar content were measured at different temperatures and equivalent ratios (ER). Temperatures inside reactor, gas compositions, and tar content in the producer gas were recorded or analyzed to understand the gasification process. While the gasification process occurs quite stable with wood pellets, some problems have been recognized when gasifying rice husk. Due to its low bulk density, high ash content and specific characteristic of rice husk ash, the problem of rice husk ash removal becomes significant. Furthermore, also the feeding of rice husk due to its low density and surface characteristics is not easy. This is a quite normal because there will be no existing gasifier that can be operated with every fuel. With the recognized problems in gasifying rice husk, some modifications have been proposed mainly on the feeding system and the ash removal for a properly operation of gasifying rice husk.

**Science is a form of competitive and aggressive activity, a contest of man against man that provides knowledge as a side product. That side product is its only advantage over football**

**Richard C. Lewontin  
Professor of biology, Harvard**

## **Acknowledgement**

I would like to express my sincere thanks to all who have contributed to this work.

Greatly, I acknowledge the coaching, the valuable suggestions and scientific support of Univ.Prof. Hermann Hofbauer who was very patient and motivating when supervising me in this work and gives me the option to attend the conference in Paris.

I would like to express my special thanks to Ass.Prof. Alexander Reichhold who is giving me many valuable suggestions during my work and supported me to build experimental equipments.

Greatly, I acknowledge the financial support from Austrian exchange service (OEAD) for three and a half year of this work and all the staffs who have given me many supports during the normal life in Austria.

My special thanks are also given to Bernhard Kronberger who was helping me in building and using the cold model test rig of fluidized bed and Jitka Hrbek who was guiding me for the first using of the laboratory gasifier.

I would like to thank Reinhard Rauch and Hermann Hüttler for their supports for measuring components and tar content of producer gas.

I would like to thank all my colleagues of the Institute of Chemical Engineering for the nice atmosphere. The "first skiing day" is always in my memory as the most beautiful day of my life.

I am grateful to my parents, my wife and my daughter who have given me an emotional support during all the time of this work. Their helps to transport the fuels (rice husk) from Vietnam to Austria was very important for my practical work.

The financial support of Renet- Austria is gratefully acknowledged.

**To: Đặng Thị Anh Đào  
and  
Nguyễn Vĩnh Xuân**

## Table of contents

Abstract.....	ii
Acknowledgement .....	iv
Table of contents.....	vi
List of figures.....	ix
List of tables.....	xii
List of symbols.....	xiii
1 INTRODUCTION .....	1
1.1 Biomass for energy generation in Vietnam .....	1
1.2 Aim of work.....	3
2 FLUIDIZATION TECHNOLOGY .....	6
2.1 Fluidization phenomenon and its essence.....	6
2.2 Characterization of particles .....	7
2.2.1 Shape and size of particles .....	7
2.2.2 Determination of mean diameter of particles.....	9
2.2.3 Particle density.....	9
2.2.4 Classification of particles.....	10
2.2.4.1 Groups of particles .....	10
2.2.4.2 Classification boundary between groups of particles .....	12
2.3 Onset of fluidization .....	15
2.3.1 Pressure drop through a fixed bed .....	15
2.3.2 Minimum fluidization velocity .....	15
2.3.3 Minimum fluidization velocity of binary particle mixture .....	20
2.3.4 Pressure drop fluctuation in fluidized bed .....	24
2.3.4.1 Standard deviation analysis.....	25
2.3.4.2 Frequency domain analysis.....	28
2.3.4.3 Wavelet analysis .....	29
2.3.4.4 Chaotic analysis .....	30
2.4 Solid mixing and segregation.....	32
2.4.1 Mixing and segregation process.....	32
2.4.2 Mechanism of mixing and segregation of binary mixture .....	36
2.4.3 Determination of mixing and segregation.....	39
2.4.3.1 Dispersion model .....	40
2.4.3.2 Counterflow solid circulation models.....	42
2.4.3.3 Mixing and segregation index.....	43
3 FLUIDIZATION BEHAVIOR OF BINARY MIXTURE BIOMASS AND SAND.....	49
3.1 Materials used in experiments .....	49
3.2 Experimental equipment and methodology .....	51
3.3 Basic concept and definitions .....	55
3.3.1 Minimum fluidization velocity .....	55
3.3.2 Standard deviation (or mean amplitude) of pressure drop fluctuation .....	55
3.3.3 “Real Volumes” of biomass in the mixture .....	55
3.3.4 Mixing Index.....	56
3.4 Results and discussions.....	58
3.4.1 Minimum fluidization velocity .....	58
3.4.2 Fluctuation of pressure drop through a fluidized bed .....	62
3.4.3 Mixing quality.....	65

3.4.3.1	Biomass initially in the bottom of the bed .....	65
3.4.3.2	Biomass initially placed at the top of the bed .....	66
3.4.3.3	Continuous feeding of biomass from the top of the bed .....	71
3.5	Conclusion .....	72
4	GASIFICATION TECHNOLOGY AND PRINCIPLE .....	74
4.1	Gasification today .....	74
4.2	Gasification process .....	74
4.3	Types of gasifier .....	78
4.3.1	Fixed bed gasifier .....	78
4.3.1.1	Updraft gasifier .....	79
4.3.1.2	Downdraft gasifier .....	80
4.3.1.3	Downdraft gasifiers: Open-core .....	81
4.3.1.4	Multi-stage gasifiers .....	81
4.3.1.5	Crossdraft gasifiers .....	82
4.3.1.6	Technical and operational problems with fixed bed gasifiers .....	82
4.3.2	Fluidized bed gasifier .....	83
4.3.2.1	Bubbling fluidized bed (BFB) .....	84
4.3.2.2	Circulating fluidized bed (CFB) .....	85
4.3.3	Entrained flow gasifiers (EF) .....	86
4.4	Gasification of Biomass .....	87
4.4.1	Biomass characteristics related to gasification .....	87
4.4.1.1	Moisture content .....	88
4.4.1.2	Ash content and ash composition .....	88
4.4.1.3	Elemental composition .....	88
4.4.1.4	Heating value .....	88
4.4.1.5	Bulk density and morphology .....	89
4.4.1.6	Volatile matter content .....	89
4.4.2	Problems in using biomass as a fuel for gasification process .....	89
4.5	Gasification of rice husk .....	93
4.5.1	Fixed bed gasifier .....	93
4.5.2	Fluidized bed rice husk gasifier .....	94
5	FLUIDIZED BED GASIFICATION OF RICE HUSK AND WOOD PELLETS	
	101	
5.1	Characteristic of fuel and fluidization materials .....	101
5.1.1	Fuels characteristics .....	101
5.1.2	Characteristics of the fluidization bed material .....	103
5.2	Gasification equipments .....	105
5.2.1	Biomass feeding system .....	105
5.2.2	The reactor .....	107
5.2.3	Producer gas distribution system .....	108
5.2.4	Measuring and analysis equipments .....	108
5.2.4.1	Thermal analysis .....	108
5.2.4.2	Pressure measurements .....	109
5.2.4.3	Producer gas analysis .....	109
5.2.4.4	Tar sampling and analysis .....	109
5.3	Operation procedure of biomass gasification in the unit .....	110
5.4	Results and discussion of biomass gasification .....	111
5.4.1	Gasification of milled wood pellets .....	111
5.4.1.1	Procedure of gasification experiments .....	111
5.4.1.2	Gas composition and heating values .....	113

5.4.1.3	Tar content in the producer gas.....	116
5.4.2	Experiments with rice husk.....	117
5.4.2.1	Procedure of gasification experiments.....	117
5.4.2.2	Producer gas composition and heating value for different conditions 119	
5.4.2.3	Tar content in the producer gas.....	121
5.4.2.4	Problems of rice husk gasification.....	122
5.4.2.5	Proposed ideas for the rice husk gasification.....	127
5.5	Conclusions.....	130
6	CONCLUSION AND RECOMMENDATION.....	131
	Reference .....	133

## List of figures

Figure 1.1 Share of power sources in 2002 (total capacity of 9149,2 MW) ( <i>Cuong, 2004</i> ) .....	3
Figure 2.1 Various forms of fluidization phenomena ( <i>Kunii and Levenspiel, 1991</i> ) .....	6
Figure 2.2 Particle density .....	10
Figure 2.3 The Geldart classification of particles for air at ambient condition .....	12
Figure 2.4 Dimensionless superficial gas velocity vs. dimensionless particle diameter ( <i>Grace, 1986</i> ) .....	13
Figure 2.5 . Pressure drop and bed height fluctuation in fluidized bed ( <i>Kang et al., 1967</i> ) .....	24
Figure 2.6 Standard deviation of differential pressure fluctuations for FCC particles ( <i>Bi and Grace, 1996</i> ) .....	26
Figure 2.7 Definition of $U_c$ and $U_k$ .....	26
Figure 2.8 Two-dimensional bubble rising from an under-layer of black particles ( <i>Loeffler, 2001 adapted from Rowe, 1971</i> ) .....	33
Figure 2.9 General pattern of movement of emulsion ( <i>Kunii and Levenspiel, 1991 adapted from Werther and Molerus, 1973</i> ) .....	33
Figure 2.10 Movement of solids in bubbling fluidized beds ( <i>Kunii and Levenspiel, 1991</i> ) .....	34
Figure 2.11 Typical bubbling condition in the fluidization of coarse particles ( <i>Kunii and Levenspiel, 1991</i> ) .....	35
Figure 2.12 Movement of large cylinders of various densities in fine particle beds ( <i>Kunii and Levenspiel, 1991</i> ) .....	35
Figure 2.13 Experimental setup used by Brötz 1956 to study the horizontal movement of solids ( <i>Kunii and Levenspiel, 1991</i> ) .....	40
Figure 2.14 Horizontal movement of solids ( <i>Kunii and Levenspiel, 1991</i> ) .....	41
Figure 2.15 Schematic diagram for the counter-current back-mixing model considering solids movement only ( <i>Kunii and Levenspiel, 1991</i> ) .....	42
Figure 2.16 Model mechanism of interchange of solids between downflowing emulsion solids and upflowing wake solids ( <i>Kunii and Levenspiel, 1991</i> ) .....	43
Figure 2.17 Mass fraction of jetsam in the mixture along the height of the bed in different situations to describe the mixing index .....	44
Figure 2.18 Definition of mixing index (MI) ( <i>Chiba et al., 1980</i> ) .....	46
Figure 3.1 Rice husk shape (microscope) .....	50
Figure 3.2 Wood pellets particle (microscope) .....	50
Figure 3.3 Quartz sand particles (microscope) .....	51
Figure 3.4 Schematic diagram of cold model test rig for fluidization .....	52
Figure 3.5 Cold model test rig for fluidization experiments .....	52
Figure 3.6 Pressure drop through the distribution plate .....	53
Figure 3.7 Mass fraction determination along height of the bed column .....	54
Figure 3.8 Deviding binary mixture into sections along the height of the bed column .....	54
Figure 3.9 Determination of the minimum fluidization velocity .....	55
Figure 3.10 "Real bulk density" of biomass in the mixture .....	56
Figure 3.11 Mixing index calculation .....	57
Figure 3.12 Pressure drop through 300g wood pellets .....	58
Figure 3.13 Pressure drop through 100 g rice husk .....	59

Figure 3.14 Comparison of fluidization behavior of different way sand-rice husk mixture .....	60
Figure 3.15 Pressure drop through a mixture of sand1 and rice husk.....	61
Figure 3.16 Pressure drop through a mixture of sand1 and wood pellets.....	61
Figure 3.17 Pressure drop through a bed of sand 2 and rice husk .....	61
Figure 3.18 Pressure drop through a mixture of sand2 and wood pellets.....	62
Figure 3.19 Pressure drop through 200 g sand 1 .....	62
Figure 3.20 Standard deviation of pressure drop fluctuation through mixtures sand1-rice husk.....	63
Figure 3.21 Standard deviation of pressure drop fluctuation through mixtures sand1-wood pellets .....	64
Figure 3.22 Standard deviation of pressure drop fluctuation through mixtures sand2-rice husk.....	64
Figure 3.23 Standard deviation of pressure drop fluctuation through the bed materials of sand2-wood pellets .....	64
Figure 3.24 Pressure drop through a bed of 200g sand1 when continuous feeding 30g wood pellets to the bed in 2 minute with $U=23,5\text{cm/s}$ ( $3,3 U_{mf}$ ).....	65
Figure 3.25 Volume fraction of sand in the mixture of 300g sand+6,98% rice husk when rice husk is initially placed at the bottom.....	66
Figure 3.26 Volume fraction of sand in the mixture of sand and rice husk (200g sand+2,44% rice husk; $U=3 U_{mf}$ ).....	67
Figure 3.27 MI of mixture 200g sand1+2,44% rice husk ( $U=3 U_{mf}$ ) .....	67
Figure 3.28 Volume fraction of sand in the mixture 200g sand+2,44% rice husk when changing air supply velocity (fluidization time 6 minutes) .....	68
Figure 3.29 MI of mixture 200g sand+2,44% rice husk when changing air supply velocity (fluidization time 6 minutes).....	68
Figure 3.30 Volume fraction of sand in the mixture of 200g sand and rice husk with the variation of percentage of rice husk in the mixture ( $U=3U_{mf}$ , fluidization time = 6 minutes).....	68
Figure 3.31 MI in the case of variation of rice husk amount in the mixture .....	69
Figure 3.32 Volume fraction of mixture sand-wood pellets when changing air supply velocity (200g sand+ 9,1% wood pellets and fluidization time: 1minute) .....	69
Figure 3.33 MI calculated for the mixture sand1-wood pellets in case of changing air supply velocity (200g sand, 9,1% wood pellets and fluidized for 1minute).....	69
Figure 3.34 Volume fraction of sand in the mixture 200g sand1+9,1% wood pellets when changing fluidization time ( $U=3U_{mf}$ ).....	70
Figure 3.35 MI calculated for the mixture 200g sand1+9,1% wood pellets when changing fluidization time.( $U=3U_{mf}$ ).....	70
Figure 3.36 Volume fraction of sand in the mixture 200g sand1+ 9,1% wood pellets when changing fluidization time ( $U=2 U_{mf}$ ).....	70
Figure 3.37 MI calculated for the mixture 200g sand1 + 9,1% wood pellets when changing fluidization time ( $U=2 U_{mf}$ ).....	71
Figure 3.38 Volume fraction at different air supply velocity for continuous feeding of 30g wood pellets into the bed of 200g sand1 for 3 minutes. ....	72
Figure 3.39 MI calculated for the mixture of sand1-wood pellets for continuous feeding of 30g wood pellets into the bed of 200g sand for 3 minutes .....	72
Figure 4.1 Cumulative worldwide gasification capacities ( <i>Stiegel and Maxwell, 2001</i> ) .....	74
Figure 4.2 C-O-H diagram of gasification processes ( <i>Bolhar-Nordenkamp, 2004</i> )....	75
Figure 4.3 Sequential steps of biomass gasification ( <i>Bolhar-Nordenkamp, 2004</i> ) ....	76

Figure 4.4 Influence of the gasification temperature on the reaction constants ( <i>Bolhar-Nordenkamp</i> , 2004) .....	77
Figure 4.5 Updraft gasifier.....	79
Figure 4.6 Downdraft gasifier.....	81
Figure 4.7 Cross-draft gasifier.....	82
Figure 4.8 Bubbling fluidized bed gasifier .....	85
Figure 4.9 Circulating fluidized bed gasifier .....	86
Figure 4.10 Entrained flow gasifier .....	87
Figure 4.11 Chinese rice husk gasifier.....	94
Figure 4.12 Dual distributor type feeding mechanism for rice husk into fluidized beds ( <i>Mansaray et al.</i> , 1999).....	100
Figure 5.1 Milled wood pellets .....	103
Figure 5.2 Rice husk .....	103
Figure 5.3 Quartz sand used as bed material .....	104
Figure 5.4 Pressure drop of a bed of quartz sand at 660 °C.....	105
Figure 5.5 Laboratory scale fluidized bed gasifier .....	106
Figure 5.6 Fluidized bed gasifier .....	107
Figure 5.7 Scheme of tar measuring arrangement .....	110
Figure 5.8 Typical gasification run for wood pellets.....	113
Figure 5.9 Composition of the producer gas for different reactor temperatures (ER=0,22).....	114
Figure 5.10 Heating value of the producer gas for different reactor temperatures (ER=0,22).....	114
Figure 5.11 Composition of the producer gas for different equivalent ratios (ER) (T <sub>2</sub> =725-728 °C; T <sub>3</sub> = 607-617 °C; T <sub>4</sub> =679-682 °C).....	115
Figure 5.12 Heating values of the producer gas for different equivalent ratios (ER) (T <sub>2</sub> =725-728 °C; T <sub>3</sub> = 607-617 °C; T <sub>4</sub> =679-682 °C).....	115
Figure 5.13 Composition of the producer gas at higher temperatures when changing ER (T <sub>2</sub> =803-817 °C; T <sub>3</sub> =704-712 °C; T <sub>4</sub> =754-762 °C) .....	116
Figure 5.14 Heating value of the producer gas at higher temperatures when changing ER (T <sub>2</sub> =803-817 °C; T <sub>3</sub> =704-712 °C; T <sub>4</sub> =754-762 °C) .....	116
Figure 5.15 Tar content with ER = 0,22 .....	117
Figure 5.16 Tar content with ER = 0,2 .....	117
Figure 5.17 Typical example of a gasification run with rice husk.....	118
Figure 5.18 Composition of the producer gas dependent on ER .....	120
Figure 5.19 Heating value of the producer gas dependent on ER .....	120
Figure 5.20 Composition of the producer gas when gasification process of rice husk takes place at the top of the bed .....	121
Figure 5.21 Heating value of the producer gas when gasification process of rice husk takes place at the top of the bed .....	121
Figure 5.22 Tar content in the producer gas .....	122
Figure 5.23 Outer surface of rice husk particle.....	123
Figure 5.24 Screw feeder after 20 hours of feeding rice husk .....	123
Figure 5.25 Shape of one a rice husk ash particle.....	124
Figure 5.26 Rice husk ash remaining in the bed after one experiment.....	125
Figure 5.27 Fluidization behavior of rice husk ash and sand .....	126
Figure 5.28 Rice husk ash particle stucked together in a small spot .....	127
Figure 5.29 Rice husk ash agglomerated together to form a block .....	127
Figure 5.30 Proposed improvements for the laboratory scale gasifier for rice husk gasification.....	129

## List of tables

Table 1.1 Share of biomass energy consumption in the total national energy consumption. (Cuong, 2004).....	1
Table 1.2 Consumption of biomass energy by type and end-use in 2000 in Vietnam (Cuong, 2004) .....	2
Table 1.3 Potential of biomass for electricity generation (Cuong, 2004) .....	2
Table 2.1 Equivalent diameter of particles (Hoffbauer, 2004) .....	7
Table 2.2 Shape factor of some technical interesting materials (Hoffbauer, 2004) .....	8
Table 2.3 Various calculation for $U_{mf}$ .....	16
Table 2.4 Correlations for calculating minimum fluidization of the binary mixture $U_{mfM}$ (superscript S refers to the particles that fluidized at lower velocity whereas superscript L refer to those that fluidized at higher velocity). (Wu and Baeyerns, 1998) .....	20
Table 2.5 The different calculations of $U_c$ , $U_k$ (Loeffler, 2001) .....	26
Table 2.6 Material used in various experiments of binary mixtures (concluded from Rowe et al., 1972a) .....	36
Table 2.7 Correlation for mixing index calculation .....	44
Table 3.1 Characteristic of materials used in experiments .....	49
Table 3.2 Calculation of "real bulk density" ( $\rho_{Br}$ ) of biomass.....	56
Table 3.3 MI of sand-rice husk mixture when rice husk is initially placed at the bottom .....	66
Table 4.1 Gasification characteristic of various fuels in downdraft gasifier (Yogi Goswami 1986) .....	90
Table 4.2 Literature review on the fluidized bed gasification of rice husk (Natarajan et al., 1998) .....	94
Table 5.1 Fuel Characteristics of rice husk and wood pellets.....	101
Table 5.2 Melting behavior of rice husk ash.....	102
Table 5.3 Rice husk ash analysis (Pham, 1999) .....	102
Table 5.4 Gas analysis equipments .....	109

## List of symbols

Symbols	Name	Equation	Unit
$a$	scale parameter	2-52	-
$A$	cross sectional area of bed column	2-25	$m^2$
$A_b$	amplitude of pressure fluctuation in the bed	2-38	Pa
$A_j(t_i)$	approximation of multi-resolution decomposition at level $j$	2-54	-
$Ar$	Archimedes number	2-12	-
$b$	transition parameter	2-54	s
$C_1, C_2$	Constant value	2-27	-
$C_{hi}$	Distributed concentration of material at the height of $h$	2-80	$kg/m^3$
$C_{oi}$	Even distributed concentration of material along the bed height	2-80	$kg/m^3$
$C_s$	Concentration of tagged particles at position $z$ at time $t$	2-60	$kg/m^3$
$C_{sd}$	Concentration of solid downward	2-65	$kg/m^3$
$C_{su}$	Concentration of solid upward	2-66	$kg/m^3$
$d_b$	Effective bubble diameter	2-63	m
$d_B$	Diameter of bigger particles	2-74	$\mu m$
$D_j(t_i)$	detail of multi-resolution decomposition at level $j$	2-54	-
$d_m$	average particle size of bed material particle	2-84	mm
$d_p$	Mean sieving diameter of particles	Table 2.1	m
$d_p^*$	dimensionless particle diameter	2-10	-
$dp_{eff}$	effective particle diameter	2-36	m
$dp_i$	Sieving diameter of solid $i$ in the mixture	2-7	m
$d_s$	Surface area equivalent diameter	Table 2.1	m
$d_s$	Diameter of smaller particles	2-74	$\mu m$
$D_{sh}$	horizontal dispersion coefficient	2-63	$m^2/s$
$d_{si}$	even particle size of simulating material particle	2-84	mm
$d_{sv}$	Surface area/volume ratio equivalent diameter	Table 2.1	m
$D_{sv}$	Vertical dispersion coefficient averaged over the entire cross section of the bed	2-60	$m^2/s$
$D_T$	Bed diameter	2-56	m
$d_v$	Volume equivalent diameter	Table 2.1	m
$E(z)$	Expectation of $z$ (dimension of $z$ )	2-50	$z$
$f_d$	Fraction of flowing down solid in the bed ( $m^3$ solid down/ $m^3$ bed)	2-65	-
$f_u$	Fraction of flowing up solid in the bed ( $m^3$ solid up/ $m^3$ bed)	2-66	-
$f_w$	Volume fraction of wake region	2-69	-
$G(i\omega)$	Transfer function	2-42	-
$G_p(f)$	power spectral density function (defined by Zhanyong Li et al., 2005)	2-47	$[Pa^2/Hz]$
$H$	Height of the bed column	2-21	m
$h$	distance above distribution plate	2-75	m
$h$	Sampling time interval	2-49	s
$H_s$	Settled bed height	2-56	m
$k$	constant value	2-37	-

Symbols	Name	Equation	Unit
K	Kolmogorov entropy	2-56	bits/s
$K_s$	interchange coefficient for solids in beds with clouded bubbles	2-68	$s^{-1}$
$L_f$	Heigh of bubbling fluidized bed	2-52	m
$m_B$	weigh of biomass in a bed	3-5	kg
MI	Mixing index	2-71	-
$M_p$	Mass of particle	2-8	kg
$m_s$	Mass of sand	3-7	kg
n	Length of time series signal	2-55	s
n	the maximum time lag number	2-49	
p	Pressure measured at different place		Pa
$p(x_i)$	Probability of every component in the signal	2-55	-
$P(xx)$	Power spectral density of each measurement position (defined by <i>Schaaf et al., 1999</i> )	2-50	$[kPa^2/Hz]$
$P(xy)$	cross power spectral density between two measurement positions x and y (defined by <i>Schaaf et al., 1999</i> )	2-51	$[kPa^2/Hz]$
$R_d$	relative particle size rate	2-84	-
Re	Reynolds number	2-13	-
$R_p$	relative density. $R_p = \rho_{si}/\rho_m$	2-83	-
$R_p(\tau)$	autocorrelation function for a time lag $\tau$	2-47	$[Pa^2]$
$R_{yy}(\tau)$	Autocorrelation function of a continuous time series	2-44	-
S	Shannol Entropy	2-55	dB
s	sum of all the positive Lyapunov exponents	2-59	-
SI	Segregation index	2-77	-
$S_p$	Surface area of particle	Table 2.1	$m^2$
$S_{yy}(j\omega)$	power spectra density function (defined by <i>Brue and Brown, 2001</i> )	2-43	-
t	time	2-44	second
U	Gas supply velocity	2-24	m/s
$U^*$	Dimensionless air velocity	2-9	-
$U_b$	Minimum bubble velocity	2-16	m/s
$U_{br}$	Rise velocity of the bubble with respect to emulsion phase	2-63	m/s
$U_c$	Transition velocity (Air velocity that corresponding to maximum standard deviation of pressure drop)	table 2.5	m/s
$U_F$	minimum fluidizaiton velocity of fluid particle	2-31	m/s
$U_f$	$=U_{mf}/\varepsilon_{mf}$ upward velocity of gas at minimum fluidizing condition	2-63	m/s
$U_k$	Air velocity corresponding to levelling out of pressure fluctuation amplitude as ; is increased, m/s	table 2.5	m/s
$U_{mf}$	Minimum fluidization velocity	2-19	m/s
$U_{mfM}$	minimum fluidization velocity of the mixture	Table 2.4	m/s
$U_p$	minimum fluidization velocity of parked particles	2-31	m/s
$U_{sd}$	Velocity of solid flowing down	2-65	m/s
$U_{su}$	Velocity of solid flowing up	2-66	m/s
$U_{vf}$	Visual minimum fluidization velocity of the mixture	2-31	m/s
V	Bed volume	3-6	$m^3$
$V_B$	Volume of biomass in a bed	3-5	$m^3$
$V_{Br}$	Real volume of biomass in the mixture	3-6	$m^3$

Symbols	Name	Equation	Unit
$V_p$	Volume of particle	2-1	$m^3$
$V_s$	Volume of sand in the bed	3-6	$m^3$
$W_\varphi x(a,b)$	wavelet coefficient (dimensionless)	2-52	-
$W_F$	weight fraction of fluid component (sand) in the bed	2-34	-
$W_p$	mass fraction of packed component	2-36	-
$x$	Mass or volume fraction of jetsam in the sample	2-72	-
$x(t)$	pressure signal in time domain		Pa
$x(t_i)$	Orthogonal wavelet series approximates to a continuous signal	2-54	Pa
$x_c$	volume fraction of coarse particles	2-77	-
$X_F$	Real volume fraction of fluid component (sand) in the bed	2-33	-
$x_i$	Mass fraction of solid i in the mixture	Table 2.1	-
$y$	general time series function	2-44	-
$Y$	Sand/biomass ratio	3-9	-
$z$	Distance above the distribution plate	2-60	m
$z_f$	Distance above a mean surface of fluidized bed	2-61	m
$\overline{p}$	Mean pressure measured		Pa
$\overline{\Delta p}$	Mean pressure drop measured at a certain air supply velocity		Pa
$\overline{u_{s,up}}$	mean upward velocity of solid	2-61	m/s
$\overline{t_s}$	Mean residence time of solid	2-61	s
$\overline{x}$	Mass or volume fraction of jetsam in the whole bed	2-73	-
$\phi$	form factor	Table 2.1	-
$\mu$	Viscosity of fluidization agent	2-9	kg/ms
$\varepsilon$	Porosity of the bed	2-21	-
$\varepsilon_f$	Void fraction of fluidized bed as a whole	2-67	-
$\varepsilon_i(0)$	distances between two nearby trajectories along the principal axis i at time 0	2-57	s
$\varepsilon_i(t)$	distances between two nearby trajectories along the principal axis i at time t	2-57	s
$\varepsilon_{mf}$	porosity of the bed at minimum fluidization condition	2-19	-
$\omega$	angular frequency	2-42	rad/s
$\omega_n$	Characteristic angular frequency	2-42	rad/s
$\tau$	time shift	2-43	second
$\delta$	Bubble fraction in a fluidized bed	2-63	-
$\sigma$	standard deviation of pressure fluctuation	2-39	Pa
$\alpha$	Ratio of effective diameter of the wake to diameter of the bubble	2-63	-
$\Im(i\omega)$	is the Fourier transform	2-46	-
$\varphi_{ab}^*(t)$	complex conjugation of $\varphi_{ab}(t)$	2-52	-
$\rho_0$	density at incipient fluidization	2-38	$kg/m^3$
$\rho_B$	Density of the bed	2-23	$kg/m^3$
$\rho_{eff}$	$\rho_{eff}$ : effective density of the mixture	2-36	$kg/m^3$
$\rho_f$	particle density of fluid component	2-36	$kg/m^3$
$\rho_g$	gas density	2-9	$kg/m^3$

<b>Symbols</b>	<b>Name</b>	<b>Equation</b>	<b>Unit</b>
$\rho_p$	particles density of packed component	2-36	$\text{kg/m}^3$
$\rho_m$	density of basic bed material	2-85	$\text{kg/m}^3$
$\rho_p^*$	dimensionless particle density	2-11	-
$\rho_p$	particle density	2-9	$\text{kg/m}^3$
$\rho_s$	Bulk density of sand in the bed	3-7	$\text{kg/m}^3$
$\rho_{si}$	density of simulating material particle	2-85	$\text{kg/m}^3$
$\rho_B$	Bulk density of biomass	3-5	$\text{kg/m}^3$
$\rho_{Br}$	Real density of biomass in the mixture	3-8	$\text{kg/m}^3$
$\rho_H$	Particle density of the heavier material	2-74	$\text{kg/m}^3$
$\rho_L$	Particle density of the lighter material	2-74	$\text{kg/m}^3$
$\varphi_{ab}(t)$	basic wavelet function	2-53	-
$\lambda_i$	Lyapunov exponent	2-57	-
$\Delta p$	Pressure drop through 2 place of measurement	2-21	Pa
$\Delta P_b$	Pressure drop in the bed	2-38	Pa
$\mathfrak{T}_x(f)$	Fourier transform of the time series x, denotes complex conjugate	2-50	[kPa/Hz]

## 1 INTRODUCTION

Biomass in the term of ecology refers to the cumulation of living matter. However, recently with the increasing role of biomass for energy generation, biomass is understood as living biological materials which can be used as fuel for energy generation or industrial production. Most commonly biomass refers to plant matter grown for use as biofuel, but also includes plant or animal matter used for production of fibres, chemicals or heat.

Biomass is solar energy which has been stored by means of photosynthetic capabilities of the chlorophyll molecules present in the leaves of green plants. The larger leaves, the larger amount of chlorophyll and in general, the greater amount of biomass.

Since biomass has a short life cycle, abundant potential of energy resources, it is refer to one of the most effective renewable energy resources in the world today.

The diversification of biological living matter leads to the diversification of biomass fuel resources in local areas.

### 1.1 Biomass for energy generation in Vietnam

Being a tropical weather country, Vietnam is a high biological diversification area with many leaving species that result multiform of biomass resources which are distributed throughout the ecological areas in the country. The major sources of biomass energy in Vietnam may come from forest wood, rubber wood, logging residues, saw mill residues, plywood, sugar cane residues, rice residues, coconut residues, coffee residues, etc.

Being a developing country where the level of industrialization is still very low, the energy consumption of biomass is still considered as high share in the total national final energy consumption and it account for over 50% of total energy demand as shown in table 1.1.

**Table 1.1 Share of biomass energy consumption in the total national energy consumption. (Cuong, 2004)**

Year	Total national final energy consumption (KTOE)	Total biomass energy consumption (KTOE)	Share of biomass energy in the national final energy consumption (%)
1990	16879,3	12390	73
1995	20594	13480	65
2000	26007	14000	54

*Note. 1KTOE = 10000\*10<sup>6</sup> kcal.*

It is estimated that about more than 50 million tons of biomass is generated every year from agricultural residues. However, so far only from 30-40% of biomass is used for energy purposes, mainly as fuel for cooking in house holds and small amount used for about 150MW<sub>e</sub> electricity generation in 42 sugar mills (Cuong, 2004)

## Chapter 1. Introduction

Current status of biomass use for energy production which is categorized by type of biomass and end-use is summarized and presented in table 1.2.

**Table 1.2 Consumption of biomass energy by type and end-use in 2000 in Vietnam**  
(Cuong, 2004)

By type of end-use		By type of biomass					Total
		Fuel wood	Rice husk	Rice straw	Bagasse	Others	
Heat	Cook stoves	6997	665	1950	165	890	10667
	Small kilns	663	140	-	-	100	903
	Bigger kilns	1145	110	-	100	698	2053
Electricity	Co-generation	-	-	-	377	-	377
<b>Total</b>		8805	915	1950	642	1688	14000

Unit: KTOE

With so large biomass energy resources, the use of biomass for electricity generation is quite small as shown in figure 1.1.

As shown in figure 1.1, biomass for electricity generation is only 1,639% and mainly from cogeneration of sugar plants that use biogases as fuel for electricity generation. Although, there are only 3 in 42 sugar mills can supply electricity to the grid. Potential of electricity generation based on biomass is about 250-400 MW electricity as shown in table 1.3.

**Table 1.3 Potential of biomass for electricity generation** (Cuong, 2004)

Type of biomass	Total main biomass amount produced (‘000 tons)	Total available biomass amount (‘000 tons)	Potential of estimated electricity capacity (MW)
Rice husk	6600	2500	70-150
Bagasse	5500	4 600	150-200
Wood residues	480	-	5
Wastes and other biomass	-	-	30--50

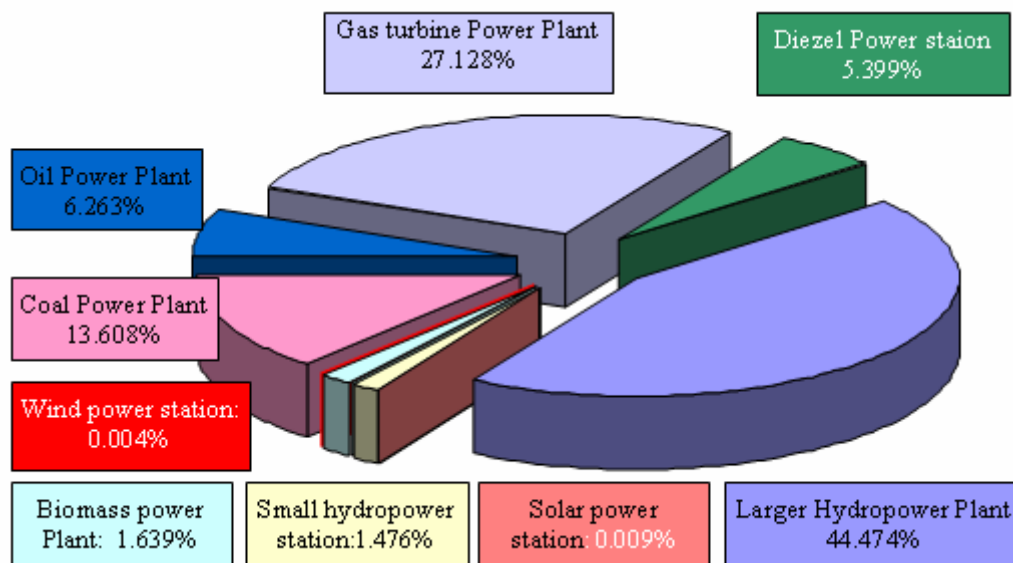


**Figure 1.1 Share of power sources in 2002 (total capacity of 9149,2 MW) (Cuong, 2004)**

Being the most abundant sources of biomass in Vietnam, rice husk potential is high mainly in the provinces of Red river and Mekong River deltas. Rice husk has been produced as by product from rice mill and was not properly used. The main uses of rice husk are:

- Fuel in cooking stove
- Burnt directly in the field to obtain ash for improving the quality of cultivated land
- Fertilizer
- Fuel in brick kiln
- Being a waste to the river and affecting environment

It is estimated that there are about 140 000 tons of rice husk every year wasted to rivers in Vietnam.

Wood fuel resources represent also a high potential as biomass energy and it is summarized as follows (Lien, 2001)

- From natural forest: approximately 41 million tons / year
- From dispersed forest, bushed, etc.: approximately 35 million tons/ year
- From planted forest: approximately 1-2 million tons /year
- From scattered trees: approximately 8-10 million tons/years.

Total quantity of fuel wood is about 75 - 80 million tons/year that equivalent to 26-28 million TOE/year.

## **1.2 Aim of work**

Among the most commonly used biomass, wood and rice husk are the most abundant resources in Vietnam and even in the world. While wood has been used more

commonly in industrial application and energy generation, rice husk with abundant amount in some areas is not so commonly used due to some following reasons.

- Rice husk resource is mostly located in the developing countries with backward technologies and limited in know-how.
- Rice husk is really difficult to operate due to its particular characteristics as high ash content and low bulk density.
- Rice mills in developing countries are mostly small scale with backward technology. Rice husk produced by these rice mills can not be used economically for cogeneration.

Biomass gasification is not a well known technique in Vietnam. Except some recognized charcoal gasifier that used for public buses in remote area in Vietnam at around 1990, the gasification technology still is an unknown technique.

With the high application of biomass for cooking stoves and other small scale heating applications such as drying in rice mill itself, brick kiln, etc. the potential of using biomass gasification for heating in industry in Vietnam is also very high with many advantages compared to direct burning in the furnaces. Some major application could be recognized:

- Small gasifier to use gas product for cooking stove in household
- Central gasifier with larger scale to supply gas for cooking of one village
- Using gasification of rice husk in small scale rice mill and use gas product for drying purpose in rice mill
- Using gasification of rice husk or other biomass for brick kiln and ceramic kiln

With the thermal application, the problem of tar content in product gas could be negligible.

With the high rate of economic development, the electricity demand is also increasing very fast. Many fossil fuel power plants are being built and even a nuclear power plant will be built in around the year 2020. In this case, cogeneration with biomass gasification technology in a large rice mill, sugar mill and wood mill is a good choice to contribute to the power generation of the country. The biomass power station using replanting forest should be taken into account.

With the aim of future developing of thermal biomass conversion technology in Vietnam, the study of this dissertation focuses mainly on:

- Literature study on fluidization technology which is related to bed particles, fluidization behavior of the single materials and the mixture of 2 different materials.
- Experimental studies on fluidization behavior of the biomass mixture which is represented by wood pellets, rice husk and sand at different conditions.
- Literature study on gasification technology of biomass with some regarding to rice husk gasification.
- Experimental study on gasification of rice husk and wood pellets in a small scale laboratory fluidized bed. Gas compositions and tar content will be measured at different conditions to study the dependencies with the change of

temperatures and equivalent ratio (ER). Reactor temperatures and CO, CO<sub>2</sub> will be recorded to understand the gasification process sequences occurring in the reactor.

This dissertation should give some understanding about fluidization phenomena as well as the gasification process occurring in the fluidized bed gasifier. The observations can provide helpful knowledge when designing a gasifier for the different types of fuels in general and particularly for rice husk which is known as most difficult to apply.

## 2 FLUIDIZATION TECHNOLOGY

### 2.1 Fluidization phenomenon and its essence

Fluidization is a phenomenon that solid particles are transformed into a fluid like state through suspension in a gas or liquid. Depending on solid particles characteristic, velocity of supplying fluidization agent, and characteristic of fluidization agent, fluidization behavior would be different. Figure 2.1 shows different forms of fluidization when introducing gas or liquid through a bed of particles. Forms of fluidization phenomena have been described as following (Kunii and Levenspiel, 1991)

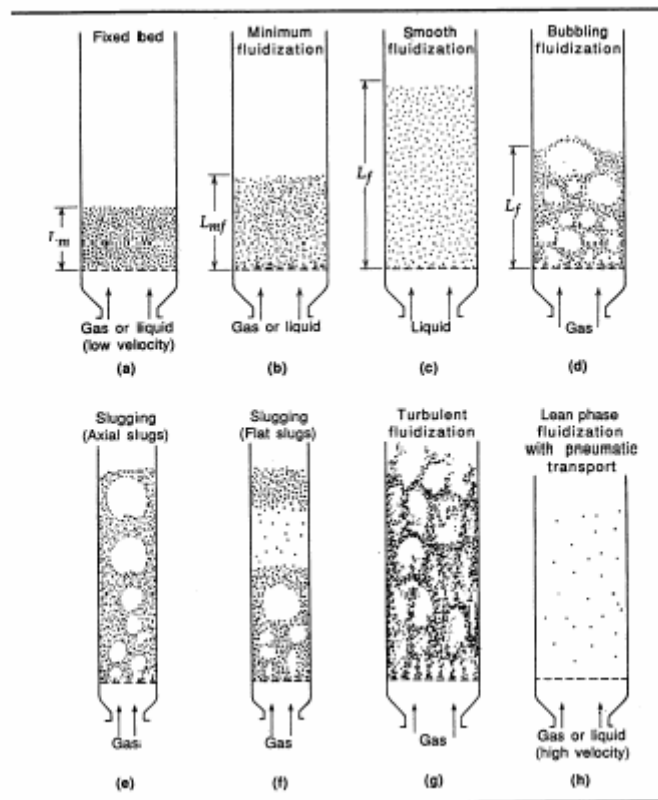


**Figure 2.1 Various forms of fluidization phenomena** (Kunii and Levenspiel, 1991)

- When a fluid (gas or liquid) is passed upward through a bed of particles, at a low flow rate, the fluid merely percolates through the void spaces between stationary particles. This is a fixed bed.
- When increasing flow rate, particles move a part and a few vibrate and move in restricted regions. This is the expanded bed.
- Supplying more flow rate, all the particles are suspended by the upward flowing gas or liquid. At this point, the frictional force between particles and fluid is counterbalances the weight of the particles, the vertical component of the compressive force between adjacent particles disappears and the pressure drop through any section of the bed equals to the weight of fluid and particles in that section. The bed start fluidized and it is an incipiently fluidized bed

- d) At higher flow rates, agitation becomes more violent and the movement of solids becomes more vigorous. In this state, the bed does not expand much
- e) Beyond its volume at incipiently fluidized bed but bubbles appear in the bed. Such bed called aggregative fluidized bed or bubbling fluidized bed.
- f) With the increasing of air, bubbles coalesce and grow as they rise and in a deep enough bed of small diameter, they may become large enough to spread across the vessel. In the case of fine particles, they flow smoothly down by the wall around the rising void of gas. This is called slugging, with axial slugs.
- g) For the coarse particles, the portion of the bed above the bubble is pushed upward as by a piston. Particles rain down from the slug, which finally disintegrates. At about this time another slug forms, and this unstable oscillatory motion is repeated. This is called a flat slug.
- h) When fine particles are fluidized at a sufficiently high flow rate, the terminal velocity of the solids is exceeded, the upper surface of the bed disappears, the entrainment becomes appreciable, and, instead of bubbles, one observes a turbulent motion of solid clusters and voids of gas of various sizes and shapes. This is the turbulent fluidized bed.
- i) With further increase of gas velocity, solids are carried out of the bed with the gas. In this state we have dispersal, dilute, or lean phase fluidized bed with pneumatic transport of solids.

Fluidized bed is a well known technique that has many applications in combustion, gasification and drying etc. Many researches have done in different aspects in fluidization phenomenon. The details discussed latter will show an overview of the fluidized bed technology.

## 2.2 Characterization of particles

The form of fluidization in the fluidized bed is depending on the characteristic of the particles. In most cases, characteristics of particles are defined by sharp, size and density of particles.

### 2.2.1 Shape and size of particles

In case of spherical particles, size of particles can be measured easily through a diameter of the sphere; however, in most of a reality cases, particles are irregular in shape and the methodology to determine the size of particles is more difficult. In practical some equivalent particles diameter are defined as shown in table 2.1.

**Table 2.1 Equivalent diameter of particles** (Hoffbauer, 2004)

Symbol	Diameter name	Description
$d_p$	Sieving diameter	Dimension of square sieving hole that particles can be sieved through.
$d_v$	Volume equivalent diameter	Diameter of the sphere with the equal volume as the

Symbol	Diameter name	Description
		particle. $V_p = V_{sphere} = \frac{d_v^3 \Pi}{6} \Rightarrow d_v = \left( \frac{6V_p}{\Pi} \right)^{1/3}$
$d_s$	Surface area equivalent diameter	Diameter of the sphere with the equal surface area as the particle. $S_p = S_{sphere} = d_s^2 \Pi \Rightarrow d_s = \left( \frac{S_p}{\Pi} \right)^{1/2}$
$d_{sv}$	Surface area/volume ratio equivalent diameter	Diameter of the sphere with the equal surface area/volume ratio as the particle. $\frac{S_p}{V_p} = \frac{S_{sphere}}{V_{sphere}} = \frac{d_{sv}^2 \Pi}{\frac{d_{sv}^3 \Pi}{6}} = \frac{6}{d_{sv}} \Rightarrow d_{sv} = \frac{6V_p}{S_p}$

To unify the equivalent diameter of particles, the concept of shape factor has been used as following:

$$\phi = \frac{\text{Surface area of equivalent volume sphere}}{\text{Surface area of the particle}} = \left( \frac{d_v}{d_s} \right)^2 \quad (\text{Equation 2-1})$$

With the concept of shape factor, the sphere particles will have a shape factor  $\phi = 1$  and other particles will have the shape factor in between  $0 < \phi < 1$ .

Table 2.2 shows the shape factor of some technical interesting materials

**Table 2.2 Shape factor of some technical interesting materials** (Hoffbauer, 2004)

Material name	Form factor ( $\phi$ )
Broken coal grinded	0,7 - 0,75
Broken sand grinded	0,7 - 0,85
spherical sand	0,9 - 0,95
lime stone	0,65 - 0,75
iron catalyst	0,6 - 0,65
common salt	0,8 - 0,85
Technical glass sphere	0,98 - 1

With the definition of shape factor ( $\phi$ ) and the equivalent diameters ( $d_v$ ,  $d_s$ ,  $d_{sv}$ ) by mathematical calculation, we can have following relations:

$$\frac{S_p}{V_p} = \frac{6}{d_{sv}} = \frac{d_s^2 \Pi}{\frac{d_v^3 \Pi}{6}} = 6 \left( \frac{d_s}{d_v} \right)^2 \frac{1}{d_v} \Rightarrow d_{sv} = d_v \left( \frac{d_v}{d_s} \right)^2 = \phi d_v \quad (\text{Equation 2-2})$$

In practice, sieve analysis is the most convenient way to measure particle size. Numerous calibrated sieves are available for analyzing the size of particles. Since

there is no general relationship between  $d_{sv}$  and  $d_p$ , the best we can say without doing experiments is following:

For irregular particles with no seemingly longer or shorter dimension (hence, isotropic in shape)

$$d_{sv} = \phi d_{\text{sphere}} \approx \phi d_p \quad (\text{Equation 2-3})$$

For irregular particles with one somewhat longer dimension, but with a length ratio not greater than 2:1 we can have

$$d_{sv} = \phi d_{\text{sphere}} \approx d_p \quad (\text{Equation 2-4})$$

For irregular particles with somewhat shorter dimension, but with a length ratio not less than 1:2, then roughly,

$$d_{sv} = \phi d_{\text{sphere}} \approx \phi^2 d_p \quad (\text{Equation 2-5})$$

For the sphere form or near sphere form particles,

$$d_{sv} \approx d_v \approx d_p \quad (\text{Equation 2-6})$$

At present, there exists no exact method for determination of the shape factor. The values showed in table 2.2 are only a mean values from empirical studies. The value of  $\phi$  is normally in between of 0,6 and 1.

### 2.2.2 Determination of mean diameter of particles

In reality, particles will have irregular shape and a size distribution. Determination of mean diameter of particles is very important for predicting fluidization behavior of fluidization materials. Using a sieving analysis with various calibrated sieve is the most convenient way to determine particles diameter. Particles that passing through a larger sieve size and remaining on a smaller sieve size will have a size in between. For example, particles passing through a sieve with apertures of 104 $\mu\text{m}$  and resting on a sieve with apertures of 74 $\mu\text{m}$  will have mean diameter.

$$d_p = (104+74)/2 = 89 \text{ } (\mu\text{m})$$

The mean diameter of various size distributions could be determined by using equation 2-7.

$$d_p = \sum \frac{100}{x_i / d_{pi}} \quad (\text{Equation 2-7})$$

### 2.2.3 Particle density

One particle can have pores inside. These pores can be open or closes as seen in figure 2.2. The definition of particle density with respect to fluidization is as following:

$$\rho_p = \frac{M_p}{V_p} \quad (\text{Equation 2-8})$$

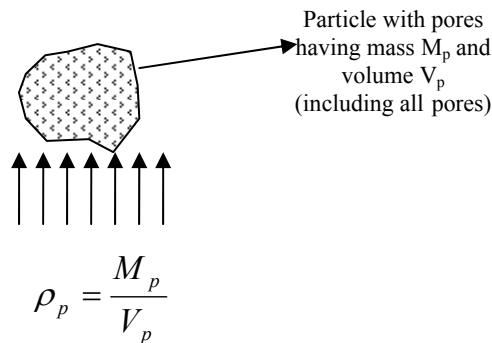


**Figure 2.2 Particle density**

This definition of particle density is for hydrodynamic density based on the shape and volume of particle that including all the pores. It is different with material density where the pores volume is excluded from calculation.

## 2.2.4 Classification of particles

### 2.2.4.1 Groups of particles

To classify particles into groups with similar behavior when fluidized by gas is a practical way of generalization. Based on experimental work and some other previous reports, Geldart, 1973 had classified particles into four groups described as following:

**Group A.** Materials having a small size and/or a low particle density (less than  $1,4\text{g/cm}^3$ ). The fluidization characteristic of group A as following:

Bed of powders in this group expands considerably before bubbling commences. When the gas supply is suddenly cut off the bed collapses slowly, typically at a rate of  $0,3\text{-}0,6\text{cm/s}$ , this being similar to the superficial velocity of the gas in the dense phase. Gross circulation of the powder occurs even when few bubbles are present, producing rapid mixing. Bubbles in a two dimensional bed appear to split and re-coalesce very frequently. All bubbles rise more rapidly than the interstitial gas velocity, but in freely bubbling beds the velocity of small bubbles appears to be about  $30\text{-}40\text{cm/s}$  regardless of bubble size, suggesting that the gross circulation referred to controls the rise velocity. There is some evidence that the mean size of bubbles may be reduced in two ways, i.e. by having a wide particle size distribution and/or a small mean particles size. A maximum bubble size does appear to exist. Considerable back mixing of gas in the dense phase occurs and gas exchange between bubble and dense phase is generally high; however, the ratio (volume of cloud/volume of bubble) is negligible. When the superficial gas velocity is sufficiently high to cause the formation of slugging conditions, the slugs produced are axi-symmetric; as the superficial gas velocity is further increased slug flow breaks down into a turbulent regime with "tongues of fluid darting zig-zag fashion up the bed". The velocity at which this occurs appears to decrease with particle size.

**Group B.** Group B contains most materials in the mean size and density ranges  $40\mu\text{m} < d_{sv} < 500\mu\text{m}$ ;  $4\text{g/cm}^3 < \rho_p < 1,4\text{g/cm}^3$ , sand being the most typical powder.

Bubbles start to form in this type of powder at or only slightly above minimum fluidization velocity. Bed expansion is small and the bed collapses very rapidly when

the gas supply is cut off. There is little or no powder circulation in the absence of bubbles burst at the surface of the bed as discrete entities. Most bubbles rise more quickly than the interstitial gas velocity and bubble size increases linearly with bed height and excess gas velocity ( $U-U_{mf}$ ); coalescence is the predominant phenomenon. There is no evidence of a maximum bubble size, although few studies have involved bed sufficiently deep or large enough to allow bubbles to reach the maximum size predicted by theory. It has been shown recently that when comparisons are made at equal values of bed height and  $U-U_{mf}$ , bubble sizes are independent of both mean particle size and size distribution. Back mixing of dense phase gas is relatively low as is gas exchange between bubbles and dense phase; the cloud volume/bubble volume ratio is generally not negligible. When the gas velocity is so high that slugging commences, the slugs are initially axial symmetry, but with further increase in gas velocity and increasing proportion become asymmetric, moving up the bed wall with an enhanced velocity rather than up the tube axis. There is no evidence of the breakdown of slugging into turbulent flow.

### ***Group C***

Powders which are in any way cohesive belong in this category. "Normal" fluidization of such powders is extremely difficult; the powder lifts as a plug in small diameter tubes, or channels badly, i.e. the gas passed up voids extending from distributor to bed surface. This difficulty arises because the inter-particle forces are greater than those which the fluid can exert on the particle, and these are generally the result of very small particle size, strong electrostatic charges or the presence in the bed of very wet or sticky material. Particle mixing and consequently heat transfer between a surface and the bed is much poorer than with powders of groups A or B.

Fluidization can generally be made possible or improved by the use of mechanical stirrers or vibrators which break up the stable channels, or, in the case of some powders, by the addition of fumed silica of sub-micron size. Where agglomeration occurs due to excessive electrostatic charging some improvement can generally be effected by humidification of the incoming gas, or by making the equipment walls conducting, for example, by coating glass with a very thin layer of tin oxide. An equally effective but less permanent technique is to coat the particles with a conducting substance such as graphite.

### ***Group D***

The justification of this further category of powders, confined to large and/or very dense particles, is not as readily apparent as in the other three cases since relatively little published information is available.

Certainly all but the largest bubbles rise more slowly than the interstitial fluidizing gas, so that gas flows into the base of the bubble and out of the top, providing a mode of gas exchange and by-passing different from that observed with group A or B powders. The gas velocity in the dense phase is high, solids mixing relatively poor; consequently back mixing of the dense phase is small. The flow regime around particles in this group may be turbulent, causing some particle attrition with rapid elutriation of the fines produced. Relatively sticky materials can be fluidized since the high particle momentum and fewer particle-particle contacts minimize agglomeration. There is some evidence that bubble size may be similar to those in group B powders at equal values of bed height and  $U-U_0$  but that bubble formation does not commence

until about 5 cm above the distributor. However, it does appear that if gas is admitted only through a centrally positioned hole, group D powders can be made to spout.

Boundary between those groups was proposed by Geldart in the form of a dimensional plot of  $(\rho_p - \rho_g)$  and mean particles size  $d_{sv}$  as showing in figure 2.3 and valid only for air under atmospheric conditions.

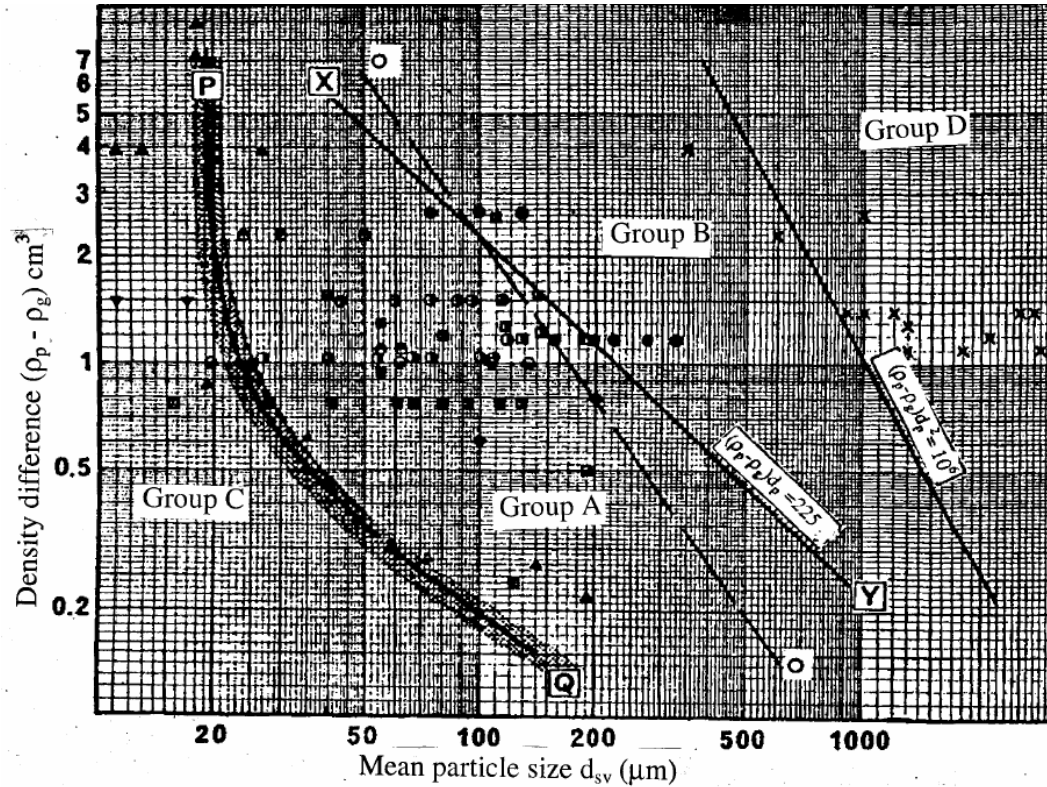


Figure 2.3 The Geldart classification of particles for air at ambient condition

#### 2.2.4.2 Classification boundary between groups of particles

The boundary between groups have been discussed by Geldart and some other authors such as *Abrahamsen and Geldart, 1980a, b; Grace, 1986*. The classification of Grace based on definition of dimensionless velocity, dimensionless diameter, and density ratio as following:

$$U^* = U \left( \frac{\rho_g^2}{\mu_g (\rho_p - \rho_g) g} \right)^{1/3} = \frac{Re}{Ar^{1/3}} \quad (\text{Equation 2-9})$$

$$d_p^* = d_p \left( \frac{\rho_g (\rho_p - \rho_g) g}{\mu^2} \right)^{1/3} \quad (\text{Equation 2-10})$$

$$\rho^* = \frac{\rho_p - \rho_g}{\rho_g} \quad (\text{Equation 2-11})$$

Archimedes number (Ar) and Reynolds number (Re) from that can be calculated by following correlation

$$Ar = \frac{\rho_g (\rho_p - \rho_g) g d_p^3}{\mu^2} = (d_p^*)^3 \quad (\text{Equation 2-12})$$

$$\text{Re} = \frac{\rho_g d_p U}{\mu} = d_p^* U^* \quad (\text{Equation 2-13})$$

Figure 2.4 show the dimensionless superficial gas velocity vs. dimensionless particle diameter for upflow through solid particles showing region in which industrial reactors operate, approximate boundaries between groups C, A, B, in Geldart's classification and a proposed boundary between group B and D.

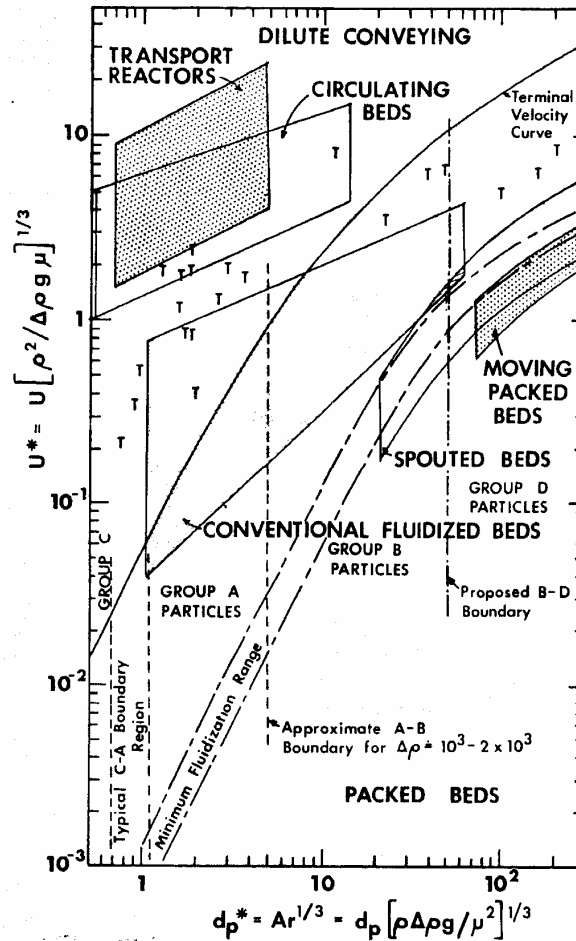


Figure 2.4 Dimensionless superficial gas velocity vs. dimensionless particle diameter  
(Grace, 1986)

**C-A boundary:** Powder in group C do not fluidize properly when the gas flow through them is increased. They may be distinguished qualitatively by the formation of channels and quantitatively by having a pressure drop across them substantially less than required to support their weight. The boundary between group A and C is strongly influenced by inter particulate forces including Van der Waals forces, capillary forces, electrostatic forces and magnetic forces. These forces depend on number of properties including size, surface asperities, and hardness of material, humidity, melting or softening point, electrical conductivity and magnetic susceptibility. By the balance between hydrodynamic forces and the Van der Waals forces at the point where the former are just sufficient to break up bed structures, *Molerus, 1982* defined the boundary of group C as

$$d_p^* \approx 0,68 - 1,1 \text{ or } \text{Ar} = 0,31 - 1,3. \quad (\text{Equation 2-14})$$

**A-B boundary.** The distinguishing feature between groups A and B is based on the concept that the bed powder of group A expand considerably before bubbling commences. That mean for group A powders,  $U_{mb} > U_{mf}$  whereas  $U_{mb} = U_{mf}$  for group B powders. Group A powder will have a region of bubble free fluidization  $U_{mf} < U < U_{mb}$ . With those criteria, for the ambient conditions, *Geldart, 1973* give criteria for group A in equation

$$(\rho_p - \rho_g)d_p \leq 225 \quad (\text{Equation 2-15})$$

With the new development on the determination of  $U_{mf}$  and  $U_{mb}$  for higher pressure and a small number of data also for gases other than air and for elevated temperatures, *Grace, 1986* give the equation of boundary between group A and B using equation

$$d_p^* = 101 \left( \frac{\rho_p - \rho_g}{\rho_g} \right)^{-0.425} \quad (\text{Equation 2-16})$$

or

$$Ar = 1.03 \times 10^6 \left( \frac{\rho_p - \rho_g}{\rho_g} \right)^{-1.275} \quad (\text{Equation 2-17})$$

**B-D boundary.** The distinction between groups B and D is not as clear as that between A and B. *Geldart, 1973* divided in two way, one theoretical and one empirical. The theoretical way based on the different mode of gas by-passing described by characteristic of group D. The calculation of *Geldart, 1973* leads to the equation to distinguish group D as following:

$$(\rho_p - \rho_g)d_p^2 \geq 10^6 \quad (\text{Equation 2-18})$$

The empirical way based on a recent suggestion that group D powders are capable of maintaining a stable spout in a bed more than 30cm deep. Experimental investigations are in progress on this and will be reported in due course.

*Grace, 1986* based on the supposition of *Geldart, 1973* was that bubbles in group B should have clouds (or be "fast bubbles" as they are sometimes misleadingly called), while those in group D should be cloudless (or "slow bubbles") and give criteria for the boundary as following:

$$U_b = \frac{U_{mf}}{\varepsilon_{mf}} \quad (\text{Equation 2-19})$$

With combination of other researches on  $U_{mb}$ ,  $U_{mf}$ , the criteria for boundary between group B and D are

$$d_p^* = 53 \text{ or } Ar = 1.45 \times 10^5 \quad (\text{Equation 2-20})$$

This equation is valid in case  $(\rho_p - \rho_g)/\rho_g > 219$  and in principle the equation should apply to gas properties other than air, i.e. to the temperatures and pressure which differ from atmospheric.

## 2.3 Onset of fluidization

### 2.3.1 Pressure drop through a fixed bed

When introducing a flow of gas through a bed of particles at low velocity, the gas goes through a void between stationary particles in the fixed bed and depending on the gas velocity supply. In case of  $Re < 1$ , pressure drop through a bed could be calculated using Carman-Kozeny equation as following:

$$\frac{\Delta p}{H} = 180 \frac{(1-\varepsilon)^2}{\varepsilon^3} \frac{\mu U}{d_{sv}^2} \quad (\text{Equation 2-21})$$

Where the porosity of the bed  $\varepsilon$  is defined as:

$$\varepsilon = \frac{\text{total volume} - \text{particle volume}}{\text{total volume}} \quad (\text{Equation 2-22})$$

From this definition we can obtain

$$\varepsilon = 1 - \frac{\rho_B}{\rho_P} \quad (\text{Equation 2-23})$$

In case of higher gas velocity supply, when  $Re > 1$  the flow of gas becomes turbulent, the frictional pressure drop was calculated using Ergun equation:

$$\frac{\Delta P}{H} = 150 \frac{(1-\varepsilon)^2}{\varepsilon^3} \frac{\mu U}{d_{sv}^2} + 1.75 \frac{1-\varepsilon}{\varepsilon^3} \frac{\rho_g U^2}{d_{sv}} \quad (\text{Equation 2-24})$$

### 2.3.2 Minimum fluidization velocity

Above a certain level of gas supply velocity, when the drag force of the upward moving gas is equal to the weight of particles, the bed expands and acts like a fluid. The corresponding gas velocity is called minimum fluidization velocity. Consider a bed of particles resting on a distributor designed for uniform up flow of gas, the onset of fluidization occurs when:

$$\left( \begin{array}{c} \text{Drag force by} \\ \text{upward moving gas} \end{array} \right) = \left( \begin{array}{c} \text{Weight of} \\ \text{particles bed} \end{array} \right)$$

or

$$\left( \begin{array}{c} \text{Pressure drop} \\ \text{across bed} \end{array} \right) \left( \begin{array}{c} \text{Cross sectional} \\ \text{area of tube} \end{array} \right) = \left( \begin{array}{c} \text{Volume} \\ \text{of bed} \end{array} \right) \left( \begin{array}{c} \text{Fraction} \\ \text{consisting} \\ \text{of solid} \end{array} \right) \left( \begin{array}{c} \text{specific} \\ \text{weight} \\ \text{of solid} \end{array} \right)$$

or

$$\Delta P A = W = A H_{mf} (1-\varepsilon_{mf}) (\rho_p - \rho_g) g \quad (\text{Equation 2-25})$$

Applying Ergun equation for the minimum fluidization phenomena point we can write:

$$\Delta P = H_{mf} \left( 150 \frac{(1 - \varepsilon_{mf})^2}{\varepsilon_{mf}^3} \frac{\mu U_{mf}}{d_{sv}^2} + 1,75 \frac{1 - \varepsilon_{mf}}{\varepsilon_{mf}^3} \frac{\rho_g U_{mf}^2}{d_{sv}} \right) = H_{mf} (1 - \varepsilon_{mf}) (\rho_p - \rho_g)$$

(Equation 2-26)

Multiplying left hand side and right hand side of an equation 2-26 with  $\left( \frac{\rho_g d_{sv}^3}{\mu^2} \right)$ , then calculated, we can have equation

$$Ar = C_1 Re_{mf} + C_2 Re_{mf}^2 \quad (\text{Equation 2-27})$$

Where  $Ar$ ,  $Re_{mf}$  are Archimedes number and Reynolds number respectively at minimum fluidization point.

$$C_1 = 150 \frac{1 - \varepsilon_{mf}}{\varepsilon_{mf}^3} \quad (\text{Equation 2-28})$$

$$C_2 = \frac{1,75}{\varepsilon_{mf}^3} \quad (\text{Equation 2-29})$$

Finally the following general expression for the calculation of minimum fluidization velocity can be obtained:

$$U_{mf} = \frac{\mu}{\rho_g d_{sv}} \left( \sqrt{C_1^2 + C_2 Ar} - C_1 \right) \quad (\text{Equation 2-30})$$

Calculations for  $C_1$ ,  $C_2$  to estimate minimum fluidization velocity of particles have been proposed by many authors using empirical data obtained from experiments. Table 2.3 gives some results recommended to determine  $U_{mf}$  of the particles.

**Table 2.3 Various calculation for  $U_{mf}$**

Reference	Determination of $U_{mf}$
Miller and Logwinuk, 1951	$U_{mf} = \frac{0,0125 d_p^2 (\rho_p - \rho_g)^{0,9} \rho_g^{0,1} g}{\mu}$
Leva et al., 1956	$U_{mf} = \frac{7,39 d_p^{1,82} (\rho_p - \rho_g)^{0,94}}{\rho_g^{0,06}}$
Goroshkov et al., 1958	$U_{mf} = \frac{\mu}{\rho_g d_p} \left( \frac{Ar}{1400 + 5,2 \sqrt{Ar}} \right)$
Leva, 1959	$U_{mf} = \frac{7,169 \cdot 10^{-4} d_p^{1,82} (\rho_p - \rho_g)^{0,94} g}{\rho_g^{0,06} \mu^{0,88}}$

Reference	Determination of $U_{mf}$
Bena, 1960	$U_{mf} = \frac{\mu}{\rho_g d_p} \left( \frac{1,38 \cdot 10^{-3} Ar}{(Ar + 19)^{0,11}} \right)$
Rowe and Henwood, 1961	$U_{mf} = \frac{8,1 \cdot 10^{-3} d_p^2 (\rho_p - \rho_g) g}{\mu}$
Frantz, 1966	$U_{mf} = \frac{1,065 \cdot 10^{-3} d_p^2 (\rho_p - \rho_g) g}{\mu}$
Davies and Richardson, 1966	$U_{mf} = \frac{7,8 \cdot 10^{-4} d_p^2 (\rho_p - \rho_g) g}{\mu}$
Wen and Yu, 1966	$U_{mf} = \frac{\mu}{\rho_g d_p} \left( \sqrt{33,7^2 + 0,0408 Ar} - 33,7 \right)$
Bourgeois and greneir, 1968	$U_{mf} = \frac{\mu}{\rho_g d_p} \left( \sqrt{25,46^2 + 0,038 Ar} - 25,46 \right)$
Kunii and Levenspiel, 1969	$U_{mf} = \frac{\mu}{\rho_g d_p} \left( \frac{\phi^2 \varepsilon_{mf}^3 Ar}{150(1 - \varepsilon_{mf})} \right)$
Pillai and Rao, 1971	$U_{mf} = \frac{7,01 \cdot 10^{-4} d_p^2 (\rho_p - \rho_g) g}{\mu}$
Baeyens, 1973	$U_{mf} = \frac{9,4 \cdot 10^{-4} d_p^{1,8} (\rho_p - \rho_g)^{0,934} g^{0,934}}{\rho_g^{0,066} \mu^{0,87}}$
Baeyens and Geldart, 1974	$Ar = 1823 Re_{mf}^{1,07} + 21,27 Re_{mf}^2$
Broadhurst and Becker, 1975	$U_{mf} = \frac{\mu}{\rho_g d_p} \left( \frac{Ar}{2,42 \cdot 10^5 \cdot Ar^{0,85} \left( \frac{\rho_p}{\rho_g} \right)^{0,13} + 33,7} \right)^{0,5}$
Saxena and Vogel, 1977	$U_{mf} = \frac{\mu}{\rho_g d_p} \left( \sqrt{25,28^2 + 0,0571 Ar} - 25,28 \right)$

Reference	Determination of $U_{mf}$
Babu et al., 1978	$U_{mf} = \frac{\mu}{\rho_g d_p} \left( \sqrt{25,25^2 + 0,0651 Ar} - 25,25 \right)$
Richardson and Jeronimo, 1979	$U_{mf} = \frac{\mu}{\rho_g d_p} \left( \sqrt{25,7^2 + 0,0365 Ar} - 25,7 \right)$
Doichev and Akhmakov, 1979	$U_{mf} = \frac{\mu}{\rho_g d_p} \left( 1,08 \cdot 10^{-3} \cdot Ar^{0,947} \right)$
Thonglimp, 1981	$U_{mf} = \frac{\mu}{\rho_g d_p} \left( \sqrt{31,6^2 + 0,0425 Ar} - 31,6 \right)$ $U_{mf} = \frac{\mu}{\rho_g d_p} \left( 7,54 \cdot 10^{-4} \cdot Ar^{0,98} \right) \text{ For } Re_{mf} < 30$ $U_{mf} = \frac{\mu}{\rho_g d_p} \left( 1,95 \cdot 10^{-2} \cdot Ar^{0,66} \right) \text{ For } 30 < Re_{mf} < 180$
Grace, 1982	$U_{mf} = \frac{\mu}{\rho_g d_p} \left( \sqrt{27,2^2 + 0,0408 Ar} - 27,2 \right)$
Chitester et al., 1984	$U_{mf} = \frac{\mu}{\rho_g d_p} \left( \sqrt{28,7^2 + 0,0494 Ar} - 28,7 \right)$
Wu and Baeyens, 1991	$U_{mf} = \frac{\mu}{\rho_g d_p} \left( \sqrt{30,85^2 + 0,0379 Ar} - 30,85 \right)$
Adanez and Abanades, 1991	$U_{mf} = \frac{\mu}{\rho_g d_p} \left( \sqrt{25,18^2 + 0,0373 Ar} - 25,18 \right) \text{ for limestone}$ $U_{mf} = \frac{\mu}{\rho_g d_p} \left( \sqrt{9,88^2 + 0,0297 Ar} - 9,88 \right) \text{ for coal and char}$
Lucas et al., 1986	$U_{mf} = \frac{\mu}{\rho_g d_p} \left( \sqrt{29,5^2 + 0,0357 Ar} - 29,5 \right)$
Davtyan et al., 1976	$U_{mf} = \frac{\mu}{\rho_g d_p} \left( \frac{Ar}{1040 + 4,86 \sqrt{Ar}} \right)$

Reference	Determination of $U_{mf}$
Sathyanarayana and Rao, 1989	$U_{mf} = \frac{\mu}{\rho_g d_p} \left( \sqrt{30,1^2 + 0,0417 Ar} - 30,1 \right)$
Nakamura et al., 1985	$U_{mf} = \frac{\mu}{\rho_g d_p} \left( \sqrt{33,953^2 + 0,0465 Ar} - 33,953 \right)$
Zheng et al., 1985	$U_{mf} = \frac{\mu}{\rho_g d_p} \left( \sqrt{18,75^2 + 0,03125 Ar} - 18,75 \right)$
Sangeetha et al., 2000	$U_{mf} = \frac{\mu}{\rho_g d_p} \left( \sqrt{60,407^2 + 0,1536 Ar} - 60,407 \right) \text{ for group A}$ $U_{mf} = \frac{\mu}{\rho_g d_p} \left( \sqrt{15,898^2 + 0,0201 Ar} - 15,898 \right) \text{ for group B}$ $U_{mf} = \frac{\mu}{\rho_g d_p} \left( \sqrt{17,612^2 + 0,02613 Ar} - 17,612 \right) \text{ for group D}$
Coltter and Rivas, 2004	<p>Giving <math>X = \frac{d_p^2 (\rho_p - \rho_g) g}{\mu} \left( \frac{\rho_p}{\rho_g} \right)^{1,23}</math>. The equations for several type of particles are as following:</p> <p><b>Metal :</b> <math>U_{mf} = (4,7673 \times 10^{-6}) X^{(0,71635 \pm 0,02213)}</math></p> <p><b>Alumina:</b> <math>U_{mf} = (2,7568 \times 10^{-6}) X^{(0,81455 \pm 0,02845)}</math></p> <p><b>Glass</b> <math>23 \mu m &lt; d_p &lt; 569 \mu m</math>  <math>U_{mf} = (4,3384 \times 10^{-7}) X^{(0,89029 \pm 0,1888)}</math>  <math>569 \mu m &lt; d_p &lt; 3000 \mu m</math>  <math>U_{mf} = (2,4624 \times 10^{-3}) X^{(0,46943 \pm 0,01190)}</math></p> <p><b>Sand:</b> <math>95 \mu m &lt; d_p &lt; 800 \mu m</math>  <math>U_{mf} = (9,7119 \times 10^{-7}) X^{(0,84268 \pm 0,01601)}</math>  <math>800 \mu m &lt; d_p &lt; 2800 \mu m</math>  <math>U_{mf} = (2,4624 \times 10^{-3}) X^{(0,46943 \pm 0,01190)}</math></p> <p><b>Coal:</b> <math>710 \mu m &lt; d_p &lt; 1000 \mu m</math>  <math>U_{mf} = (4,7731 \times 10^{-6}) X^{(0,87117 \pm 0,01513)}</math>  <math>1000 \mu m &lt; d_p &lt; 3578 \mu m</math></p>

Reference	Determination of $U_{mf}$
	$U_{mf} = (8,5557 \times 10^{-3}) X^{(0,46093 \pm 0,28872)}$
<b>Catalyst:</b>	$25 \mu m < d_p < 2250 \mu m$
	$U_{mf} = (1,145 \times 10^{-5}) X^{(0,71957 \pm 0,1422)}$
<b>Metallic ores:</b>	$101 \mu m < d_p < 1250 \mu m$
	$U_{mf} = (3,1108 \times 10^{-8}) X^{(0,93283 \pm 0,03451)}$
<b>Polymer:</b>	$116 \mu m < d_p < 1000 \mu m$
	$U_{mf} = (1,145 \times 10^{-5}) X^{(0,71957 \pm 0,1422)}$
<b>Minerals belong to orthorhombic system</b>	
$512 \mu m < d_p < 2828 \mu m$	$U_{mf} = (4,427 \times 10^{-3}) X^{(0,47851 \pm 0,0393)}$
<b>Mineral belong to hexagonal system</b>	
$0,89 \mu m < d_p < 2300 \mu m$	$U_{mf} = (7,9265 \times 10^{-4}) X^{(0,50953 \pm 0,01379)}$
<b>Minerals belong to cubic system</b>	
$106 \mu m < d_p < 2474 \mu m$	$U_{mf} = (7,1187 \times 10^{-5}) X^{(0,61787 \pm 0,04099)}$

### 2.3.3 Minimum fluidization velocity of binary particle mixture

With the development of fluidized bed applications in drying, combustion, gasification and even separation, multi-component fluidized beds are more practically applied. A lot of combinations of particles with different size, density and shape may be found in such fluidized beds, but great insight into their general behavior can be found from studying binary systems. The equations for prediction of minimum fluidization velocity have been presented in the previous part are only valid for particles with a small difference in size and of equal density. According to *Wen and Yu, 1966*, the maximum difference in size  $d_b/d_s$  for which the equations for  $U_{mf}$  are valid is not higher than  $\sqrt{2}$ .

When a binary mixture is fluidized, in general one species will have a lower  $U_{mf}$  than the other. For the component which has the lower  $U_{mf}$ , we name its minimum fluidization velocity as  $U_F$  (the fluid component) and the higher  $U_{mf}$ , we name as  $U_p$  (the packed component). Many authors have investigated in different ways to determine minimum fluidization velocity of the mixture. Some of the results are shown in table 2.4.

**Table 2.4 Correlations for calculating minimum fluidization of the binary mixture  $U_{mfM}$**  (superscript S refers to the particles that fluidized at lower velocity whereas superscript L refer to those that fluidized at higher velocity). (*Wu and Baeyerns, 1998*)

Reference	Correlation, Definition and Comments
Otero et al., 1971	$U_{mfM} = U_{mf}^S x^S + U_{mf}^L (1 - x^S)$

Reference	Correlation, Definition and Comments
	$U_{mfM} = \frac{\mu}{\rho_g d_M} \left( \sqrt{33,7^2 + 0,0408 Ar} - 33,7 \right)$ $Ar = Ga^* Mv$
Goossens et al., 1971	$Ga = \frac{d_M^3 \rho_g^2 g}{\mu^2} ; Mv = \frac{\rho_M - \rho_g}{\rho_g}$ $d_M = \frac{R_0}{R_t} d^L d^S ; \frac{1}{\rho_M} = \frac{x^S}{\rho^S} + \frac{1-x^S}{\rho^L}$ $R_0 = (1-x^S) \rho^S + x^S \rho^L ; R_t = (1-x^S) \rho^S d^S + x^S \rho^L d^L$
Kumar and Sen Gupta, 1974	$U_{mfM} = \frac{54 \cdot 10^{-4} d_M^{1,34} (\rho_M - \rho_g)^{0,78} g}{\rho_g^{0,22} \mu^{0,56}}$ $d_M = \frac{1}{\frac{x^S}{d^S} + \frac{x^L}{d^L}} ; \rho_M = x^S \rho^S + x^L \rho^L$
Cheung et al., 1974	$U_{mfM} = U_{mf}^S \left( \frac{U_{mf}^L}{U_{mf}^S} \right)^{(x^L)^2} ; \frac{d^L}{d^S} \langle 3$
Rowe and Nienow, 1975	$U_{mfM} = U_{mf}^S \left\{ \left( \frac{\varepsilon_{mf}}{\varepsilon_{mf}^S} \right)^3 \left( \frac{1 - \varepsilon_{mf}^S}{1 - \varepsilon_{mf}} \right)^{0,947} \right\}^{0,950} \left\{ x^S + \left( \frac{U_{mf}^S}{U_{mf}^L} \right)^{0,54} (1 - x^S) \right\}^{-1,85}$
Chiba, 1977	$U_{mfM} = \left\{ f_V^S + (1 - f_V^S) \frac{\rho^L}{\rho^S} \right\}^{0,95} \left\{ x^S + \left( \frac{\rho^L U_{mf}^S}{\rho^S U_{mf}^L} \right)^{0,54} (1 - x^S) \right\}^{-1,85}$ $f_V^S = \frac{1}{\left\{ 1 + \left( \frac{1}{x^S} - 1 \right) \frac{\rho^S}{\rho^L} \right\}}$
	With perfectly mixed particles
Chiba et al., 1979	$U_{mfM} = U_{mf}^S \frac{\rho_M}{\rho^S} \left( \frac{d_M}{d^S} \right)^2 ; \rho_M = f_V^S \rho^S + (1 - f_V^S) \rho^L$ $d_M = \left[ f_N^S (d^S)^3 + (1 - f_N^S) (d^L)^3 \right]^{1/3} ; f_N^S = \frac{1}{1 + \left( \frac{1}{f_V^S} - 1 \right) \left( \frac{d^S}{d^L} \right)^3}$

Reference	Correlation, Definition and Comments
	$f_N$ : Number fraction of particles; $f_V$ : Volume fraction of particles With completely segregated particles. $U_{mfM} = \frac{U_{mf}^S}{\left(1 - \frac{U_{mf}^S}{U_{mf}^L}\right)x^S + \frac{U_{mf}^S}{U_{mf}^L}}$
Thonglimp et al., 1981	First form: $Re_M = 3,4 \cdot 10^{-3} Ga^{0,2} M_V^{0,1}, Re < 20$ $\rho_M = \frac{\rho^S \rho^L}{x^L \rho^S + x^L \rho^L}$ $Re_M = 2,88 \cdot 10^{-2} Ga^{0,63} M_V^{0,626}, Re > 20$ $d_M \frac{x^S \rho^L + x^L \rho^S}{x^S \rho^L d^L + x^L \rho^S d^S} d^L d^S$ Second form: $Re_M = (19,9^2 + 0,03196 Ar)^{0,5} - 19,9$
Obata et al., 1982	$U_{mfM} = \left( \sum \frac{x_i}{U_{mf_i}} \right)^{-1}$
Uchida et al., 1983	$U_{mfM} = \frac{U_{mf}^S U_{mf}^L (1 - V_f)^m}{U_{mf}^S}; \quad m = 0,17 \left( \frac{d^L \rho^S}{d^S \rho^L} \right)^{0,437}$ $V_f$ : Volume fraction of smaller particle
Noda et al., 1986	$Ar = A Re_M^2 + B Re_M$ In Re and Ar, Use $d_M$ and $\rho_M$ $\frac{1}{\rho_M} = \frac{x^S}{\rho^S} + \frac{x^L}{\rho^L}$ $\frac{1}{d_M \rho_M} = \frac{x^S}{d^S \rho^S} + \frac{x^L}{d^L \rho^L}$ $A = 36,2 \left( \frac{d^L \rho^S}{d^S \rho^L} \right)^{-0,196}$ In general case: $B = 1397 \left( \frac{d^L \rho^S}{d^S \rho^L} \right)^{0,296}$ If $d^L/d^S > 3$ ; $\rho^L/\rho^S \approx 1$ , $B = 6443 \left( \frac{d^L \rho^S}{d^S \rho^L} \right)^{-1,86}$
Rincon et al., 1994	$\frac{1}{U_{mfM}} = \frac{1}{U_{12...n}} = \sum_{i=1}^n \frac{x_i}{U_{mf_i}}$

All determinations of  $U_{mf}$  of the binary mixture mentioned above are based on the selected particles and  $U_{mf}$  of each component is known. Even though, the agreement

between theory and experiment is very variable. Experimental values are extremely sensitive to voidage, which is a function both of bed composition and experimental technique. This makes simplified theoretical equations which do not include a voidage term.

In some cases, the proposed equations are not possible to apply due to some special characteristics of one component in binary mixture. *Bilbao et al., 1987* studied with the binary mixture of straw and sand and some problems had been pointed out:

- The maximum of straw that could be added to a fluidizing mixture was found to be of 15wt%. Beyond this point, fluidization of the whole mixture could not be achieved.
- Straw does not fluidize on its own, its minimum fluidization velocity (known as  $U_p$ ) can not be previously determined.
- The  $U_{mf}$  values obtained from the plot  $\Delta P$  vs.  $U$  are always lower than the actual velocity needed to fluidize the mixture.

Due to those reasons, *Bilbao et al., 1987* defined a visual minimum fluidized bed velocity  $U_{vf}$  as the minimum velocity needed for the whole mixture start fluidizing. These values are obtained visually. By experiments,  $U_{vf}$  obtained in all cases of the same mixtures when complete mixing, complete segregation, increasing and decreasing air flow rate give the same results. By experiments, *Bilbao et al., 1987* give the equation for calculating  $U_{vf}$  as following:

$$U_{vf} = U_p - (U_p - U_F)X_F \quad (\text{Equation 2-31})$$

where

$$U_p = 50d_p^{0.84} \quad (\text{Equation 2-32})$$

$U_F$  was calculated using Wen and Yu correlation (see table 2.3)

$$X_F = \frac{W_F}{W_F + \frac{\rho_F}{\rho_p}(1 - W_F)} \quad (\text{Equation 2-33})$$

$$W_F = \frac{M_F}{M_p + M_F} \quad (\text{Equation 2-34})$$

*Aznar et al., 1992a, b* studies fluidization of various biomasses including sawdust, wood chips, chars from sawdust and wood chip gasification, straw, ground thistle in the mixture of various size of sand. The results of actual fluidization velocities of the mixture measured did not agree with the mathematical extrapolation of *Bilbao et al., 1987*. The results of research concluded that a single mathematical equation to fit all of the experimental data obtained, is impossible to create and all the existing equations for predicting or correlating  $U_{mf}$  of the mixture of biomass and another second solid are inapplicable since most biomasses are not fluidizable without a second solid.

However, most recently, *Rao and Bheemarasetti, 2001* studied fluidization behavior of binary mixtures of biomass such as rice husk, sawdust, groundnut shell powder and sand to develop equation for predicting  $U_{mf}$  of the mixture as following.

$$U_{mf} = \frac{d_{p_{eff}}^2 (\rho_{eff} - \rho_g)}{1650\mu} \quad (\text{Equation 2-35})$$

Where

$$\rho_{eff} = \frac{w_F \rho_F + w_p \rho_p}{w_1 + w_2} ; \quad d_{p_{eff}} = kd_F \left( \frac{\rho_F d_p}{\rho_p d_F} \right)^{w_p/w_F} \quad (\text{Equation 2-36})$$

$$k = \sqrt{20d_F + 0,36} \quad (\text{Equation 2-37})$$

### 2.3.4 Pressure drop fluctuation in fluidized bed

From the initial use of fluidized bed, researchers have recognized the link between a fluidized bed's performance and its pressure fluctuations. When the supplying gas velocity is increased above minimum fluidization velocity, pressures measured in different heights of the bed start to fluctuate. The amplitude and frequency of the pressure fluctuations are dependent on various conditions of the fluidized bed. Researches on amplitude and frequency of pressure fluctuations of fluidized beds have taken place from earliest studies of pressure fluctuations in fluidized beds. *Tamarin, 1964* and *Hiby, 1967* have used visual observation of the pressure signals with time to determine the frequency of the pressure fluctuations. *Kang et al., 1967* produce a simultaneous plot of pressure and bed height fluctuations against time. Figure 2.5 shows a slight negative correlation between two values. He is also among the first to use signal analysis techniques to describe the time and frequency characteristics of the pressure fluctuations. These techniques included probability density functions, the root mean square of the pressure fluctuation and the powder spectral density.

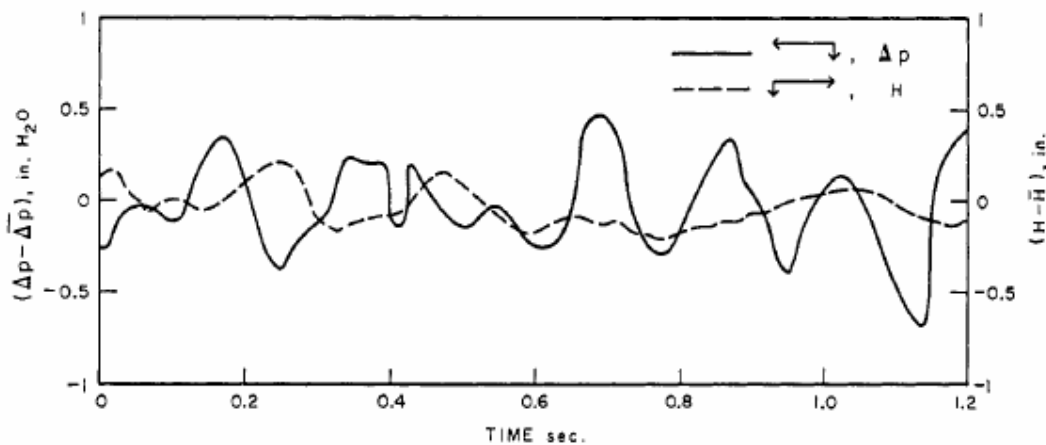


Figure 2.5 . Pressure drop and bed height fluctuation in fluidized bed (*Kang et al., 1967*)

*Baskakov, 1986* studied the relation of gravitational oscillations of the fluidized bed material and pressure drop fluctuation in a bubbling bed and found out that the major effect on pressure fluctuation is exerted by the bubbles that rise through the bed. They entrain solids, causing the surface to rise at the site of bubble emergence and cause the bed height to vary in adjacent regions. The research gives the relation:

$$\frac{A_b}{\Delta P_b} = 1,5 \left[ \frac{\rho_0 (U - U_{mf})^2}{\Delta P_b} \right]^{0,42} \quad (\text{Equation 2-38})$$

In general, until now, there are several main methods for researching pressure drop fluctuation in fluidized bed has been used as following.

#### 2.3.4.1 Standard deviation analysis

In probability and statistic, the standard deviation is defined as the square root of the variance. This means it is the root mean square (RMS) deviation from the arithmetic mean. The standard deviation is always a positive number (or zero) and is always measured in the same units as the original data. In case of pressure fluctuation, the standard deviation will have a unit as pressure unit such as Pascal, N/m<sup>2</sup>, bar, etc.

Standard deviation of the pressure fluctuation signals or mean amplitude of pressure fluctuation could be expressed as following.

$$\sigma = \sqrt{\frac{1}{N} \sum_{i=1}^N (p_i - \bar{p})^2} \quad (\text{Equation 2-39})$$

Average pressure,

$$\bar{p} = \frac{1}{N \sum_{i=1}^N p_i} \quad (\text{Equation 2-40})$$

When superficial velocity in a fluidized bed is increased, bubbling starts to become more and more vigorous and pressures are fluctuated. Exceeding a critical velocity, commonly named as transition velocity,  $U_c$ , the amplitude of pressure fluctuation start to decrease. Then, the further increasing of velocity results the decreasing of amplitude of pressure fluctuations. Figure 2.6 shows an experimental result of standard deviation of pressure fluctuation vs. air supply velocity in the fluidized bed of FCC particles.

The decreasing of amplitude of pressure fluctuation then becomes constant with further increasing of air supply velocity. At that point, superficial velocity is called  $U_k$  at which significant solid circulation is reached (*Bi and Fan, 1992*).

The gas velocity,  $U_c$ , at which the standard deviation of pressure fluctuation reached a maximum was said to mark the beginning of the transition from bubbling fluidization to turbulent fluidization while  $U_k$ , where the standard deviation of the pressure fluctuation levels off, was said to denote the end of the transition (*Bi et al., 2000*). The definition of transition velocity  $U_c$  and  $U_k$  is shown in figure 2.7.

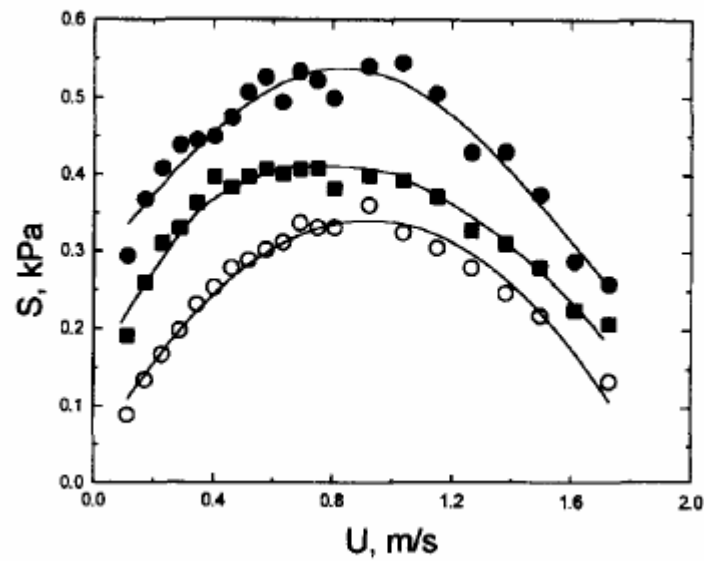


**Figure 2.6** Standard deviation of differential pressure fluctuations for FCC particles (*Bi and Grace, 1996*)

- (●) Vertical interval  $z = 0.20$  to  $0.28$  m with both probes at the axis;
- (■) vertical interval over  $z = 0.20$  to  $0.28$  m with both probes at the wall;
- (○) between wall and axis at  $z = 0.28$  m. (*Bi and Grace 1996*)

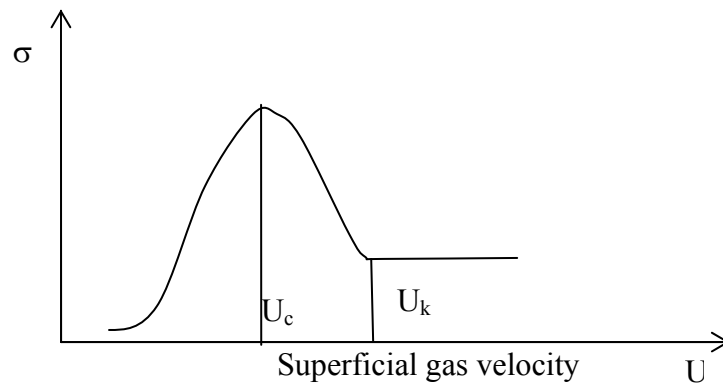


**Figure 2.7** Definition of  $U_c$  and  $U_k$

During the recent years, many investigations have been carried out to determine  $U_c$  and  $U_k$ . Many applications of turbulent fluidized bed have been realized in industry for chemical and metallurgical processes. A survey of calculations of  $U_c$  and  $U_k$  is shown in table 2.5.

**Table 2.5** The different calculations of  $U_c$ ,  $U_k$  (*Loeffler, 2001*)

Reference	Proposed correlation	Note.
Yeruschalmi and Cankurt 1979	$U_c = 3 \cdot \sqrt{\rho_p d_p} - 0,17$ $U_k = 7 \cdot \sqrt{\rho_p d_p} - 0,77$	$\rho_p \cdot d_p = 0,05 \div 0,7$ kg/m <sup>2</sup>

Reference	Proposed correlation	Note.
Yang 1984	$U_c = U_i \cdot \left( \frac{m-1}{m} \right)^m$ $\frac{U_i}{U_t} = 25,49 \cdot \text{Re}_t^{-0,485}$ $m = 2,31 \cdot \text{Re}_t^{-0,0457}$	$33 < d_p < 49 \text{ } \mu\text{m}$ $1070 < \rho_p < 1450 \text{ kg/m}^3$
Han et al., 1985	$U_c = 60 \cdot \rho_p^{0,56} \cdot d_p^{0,29} \cdot D^{0,52}$ $U_k = 45,24 \cdot \rho_p^{0,96} \cdot d_p^{0,18} \cdot D^{0,52}$	$24 < d_p < 2600 \text{ } \mu\text{m}$ $1070 < \rho_p < 2920 \text{ kg/m}^3$ $0,0779 < D < 0,305 \text{ m}$
Rhodes and Geldart, 1986	$U_k = C \cdot \rho_p^x \cdot d_p^y$	C, x, y depends on conditions
Jin et al., 1986	$U_c = \sqrt{g \cdot d_p} \cdot \left[ KD_f \cdot \frac{\rho_p - \rho_g}{d_p \cdot \rho_g} \right]^{0,27}$ $KD_f = 0,00367 \text{ for free bed}$	$50 < d_p < 1050 \text{ } \mu\text{m}$ $700 < \rho_p < 2600 \text{ kg/m}^3$
Horio et al., 1986	$\text{Re}_c = 0,936 \cdot \text{Ar}^{0,472}$ $\text{Re}_k = 1,41 \cdot \text{Ar}^{0,562}$ $\text{Re}_k = 1,46 \cdot \text{Ar}^{0,472}$	$54 < d_p < 2600 \text{ } \mu\text{m}$ $54 < d_p < 650 \text{ } \mu\text{m}$ $650 < d_p < 2600 \text{ } \mu\text{m}$
Lee and Kim, 1989	$\text{Re}_c = 0,7 \cdot \text{Ar}^{0,485}$	
Cai et al., 1989	$\frac{U_c}{\sqrt{g \cdot d_p}} = \left( \frac{0,211}{D^{0,27}} + \frac{2,42 \cdot 10^{-3}}{D^{1,27}} \right) \cdot \left( \frac{\rho_p - \rho_g}{\rho_g} \cdot \frac{D}{d_p} \right)^{0,27}$	
Sun and Chen, 1989	$U_c = 1,74 \cdot d_p^2 \cdot \left( \frac{\frac{\rho_p}{\rho_p - \rho_g} - \varepsilon_{mf}}{1 - \varepsilon_{mf}} \right) \cdot \left( \frac{\sqrt{g}}{Z_c^{1,5}} \right) + U_{mf}$ $Z_c = 2,25 \cdot \left( \frac{0,6 \cdot D}{d_{b,max} + 0,6 \cdot D} \right)^{0,5} \cdot d_{b,max}$	$0,03 < d_p \rho_p < 40 \text{ kg/m}^3$ $0,05 < D < 0,8 \text{ m}$
Lee and Kim, 1990	$\text{Re}_c = 0,7 \cdot \text{Ar}^{0,485}$	$0,44 \leq \text{Ar} \leq 4,4 \cdot 10^7$
Leu et al., 1990	$\text{Re}_c = 0,568 \cdot \text{Ar}^{0,578}$	
Nakajima et al., 1991	$\text{Re}_c = 0,633 \cdot \text{Ar}^{0,467}$	
Perales et al., 1991	$\text{Re}_k = 1,95 \cdot \text{Ar}^{0,453}$	
Horio, 1991	$\text{Re}_c = 0,936 \cdot \text{Ar}^{0,472}$ $\text{Re}_k = 1,41 \cdot \text{Ar}^{0,56}$ $\text{Re}_k = 1,46 \cdot \text{Ar}^{0,472}$	$\text{Ar} < 10^4$ $\text{Ar} > 10^4$
Bi and Fan, 1992	$\text{Re}_k = 0,601 \cdot \text{Ar}^{0,695}$ $\text{Re}_k = 2,28 \cdot \text{Ar}^{0,419}$	$\text{Ar} \leq 125$ $\text{Ar} > 125$
		$\text{Ar} \leq 125$

Reference	Proposed correlation	Note.
	$Re_k = 16,31 \cdot Ar^{0,136} \cdot \left( \frac{U_t}{\sqrt{g \cdot D}} \right)^{0,941}$ $Re_k = 2,274 \cdot Ar^{0,419} \cdot \left( \frac{U_t}{\sqrt{g \cdot D}} \right)^{0,0015}$	Ar>125
Dunham et al., 1993	$Re_c = 1,201 \cdot Ar^{0,386} \cdot \left( \frac{H}{D} \right)^{0,128 \cdot \ln(\rho_p \cdot d_p) + 0,264}$ $Re_c = 1,027 \cdot Ar^{0,450} \cdot \left( \frac{H}{D} \right)^{0,128 \cdot \ln(\rho_p \cdot d_p) + 0,264}$	Group A and B solids Group D solids
Bi and Grace, 1994	$Re_c = 1,24 \cdot Ar^{0,45}$	
Gonzalez et al., 1994	$\frac{U_c}{\sqrt{g \cdot D}} = 0,262 \cdot Ar^{0,1} \cdot \left( \frac{\mu_g}{\mu_{g,20}} \cdot \frac{\rho_{g,20}}{\rho_g} \right)^{0,27}$	0,4<Ar<123316 293<T<1063
Gonzalez et al., 1995	$\frac{U_c}{\sqrt{g \cdot d_p}} = 0,463 \cdot Ar^{0,145}$	
Tsukada, 1995	$Re_c = 0,791 \cdot Ar^{0,435}$ $Re_k = 1,31 \cdot Ar^{0,45}$	
Bi and Grace, 1995	$Re_c = 1,243 \cdot Ar^{0,447}$ $Re_c = 0,565 \cdot Ar^{0,461}$	based on differential pressure measurements based on absolute pressure measurements

#### 2.3.4.2 Frequency domain analysis

The frequency domain analysis is mainly based on a Fourier analysis of the frequency. For the frequency analysis, most of the researchers specify sample rates of 50 to 100Hz. The most effective way of frequency analysis is using power spectral density that describes how energy of a signal or time series is distributed with frequency. *Brue and Brown, 2001* using Bode plots to study power spectra of fluidized bed. The Bode plot technique consists of the logarithm of the power spectrum plotted against the logarithm of the frequency that based on equation:

$$10 \log S_{yy}(i\omega) = 20 \log |G(i\omega)| - 20 \log \sigma \quad (\text{Equation 2-41})$$

$$G(i\omega) = \frac{1}{1 + i\omega / \omega_n} \quad (\text{Equation 2-42})$$

The power spectra density function,  $S_{yy}(i\omega)$ , is defined as the Fourier transform of the autocorrelation function.

$$S_{yy}(i\omega) = \int_{-\infty}^{\infty} R_{yy}(\tau) e^{-i\omega\tau} d\tau \quad (\text{Equation 2-43})$$

$$R_{yy}(\tau) = \lim_{T \rightarrow \infty} \frac{1}{T} \int_{-T/2}^{T/2} y(t) y(t + \tau) dt \quad (\text{Equation 2-44})$$

In practice, time series are finite in duration and only an estimated of  $S_{yy}$  can be obtained:

$$S_{yy}(i\omega) = \lim_{T \rightarrow \infty} E \left\{ \frac{1}{2T} |\mathfrak{T}(i\omega)|^2 \right\} \quad (\text{Equation 2-45})$$

Where  $E$  is the expected value operator and  $\mathfrak{T}(i\omega)$  is the Fourier transform of the continuous time series  $y(t)$ :

$$\mathfrak{T}(i\omega) = \int_{-\infty}^{\infty} y(t) e^{i\omega t} dt \quad (\text{Equation 2-46})$$

*Li et al., 2005* gives the concept of power spectral density function  $G_p(f)$  computed via the Fast Fourier transform of the autocorrelation function of a series of pressure signals.

$$G_p(f) = 2 \int_{-\tau_m}^{\tau_m} p(t) p(t + \tau) dt \quad (\text{Equation 2-47})$$

Where  $R_p(\tau)$  is an autocorrelation function for a time lag  $\tau$

$$R_p(\tau) = \lim_{T \rightarrow \infty} \frac{1}{T} \int_1^T p(t) p(t + \tau) dt \quad (\text{Equation 2-48})$$

$$\tau_m = nh \quad (\text{Equation 2-49})$$

$n$ : the maximum time lag number;

$h$ : the sampling time interval.

*Schaaf et al., 1999* gives concepts of power spectral density of each measurement position  $P_{xx}$  [ $\text{kPa}^2/\text{Hz}$ ] and the cross power spectral density  $P_{xy}$  [ $\text{kPa}^2/\text{Hz}$ ] between two measurement positions  $x$  and  $y$  were calculated with

$$P_{xx}(f) = \frac{1}{T} E(\mathfrak{T}_x(f) \mathfrak{T}_x^*(f)) \quad (\text{Equation 2-50})$$

$$P_{xy}(f) = \frac{1}{T} E(\mathfrak{T}_x(f) \mathfrak{T}_y^*(f)) \quad (\text{Equation 2-51})$$

Where  $\mathfrak{T}_x(f)$  is the Fourier transform of the time series  $x$ , denotes complex conjugate [ $\text{kPa}/\text{Hz}$ ],  $E(z)$  is the expectation of  $z$  and  $T$  is the window for which the Fourier transformation is determined.

### 2.3.4.3 Wavelet analysis

Wavelet transformations play an important role in the investigation of self-similar signals system. A wavelet transformation can decompose a signal into multi-resolutions components. The components at fine and coarse resolutions indicate the

fine and coarse scale features of the signal. In theory, the wavelet transformation constitutes as natural a tool for the manipulation of self-similar or scale-invariant signals as the Fourier transformation does for translation invariant signals such as stationary, cyclostationary, and periodic signals. In practice, fast discrete wavelet transform (DWT) algorithms can be employed to perform wavelet transformations of self-similar signals. *Quingjie Guo et al., 2002*

According to *Ming-Chang Shou and Lii-Ping Leu, 2005*, the wavelet transformation of a continuous signal  $x(t)$  can be defined as:

$$W_{\varphi}x(a,b) = \int_{-\infty}^{\infty} x(t)\varphi_{a,b}^*(t)dt \quad (\text{Equation 2-52})$$

Where  $W_{\varphi}x(a,b)$  is the wavelet coefficient,  $\varphi_{ab}^*(t)$  is a basic wavelet function,  $a$  and  $b$  are the continuous dilation and translation parameters, respectively, they take values in the range of the amplitude function  $-\infty < a, b < \infty$  with  $a \neq 0$ .

Wavelet functions form a family of functions with high frequency and small duration that are all normalized dilations and translation of a prototype "wavelet basic" function. Thus,

$$\varphi_{ab}(t) = \frac{1}{\sqrt{|a|}} \varphi\left(\frac{t-b}{a}\right) \quad a \neq 0 \quad (\text{Equation 2-53})$$

An original signal is decomposed into its approximations and details with different frequency bands by means of a wavelet transformation. The decomposition process is repeated until the desired decomposition level,  $J$ , is obtained. The orthogonal wavelet series approximate a continuous signal  $x(t_i)$  at a discrete time  $t_i$  express as

$$x(t_i) \approx A_j(t_i) + D_j(t_i) + D_{j-1}(t_i) + \dots + D_1(t_i) \quad (\text{Equation 2-54})$$

where  $D_1(t_i)$ ,  $D_2(t_i)$ , ...,  $D_j(t_i)$  represent detailed signals of multi-resolution decomposition at different resolution  $2^j$ , and  $A_j(t_i)$  the approximation signal of multi-resolution decomposition at resolution  $2^j$ .

*Ming-Chang Shou and Lii-Ping Leu, 2005* when doing a research on Geldart group B sand particles found that the result from the maximum energy of the approximations by wavelet transform analysis agreed with the result of the standard deviation analysis of pressure fluctuation. The research proved that the wavelet analysis was an effective tool to identify the existence of the transition velocity.

#### **2.3.4.4 Chaotic analysis**

Traditionally, time-dependent fluctuations of pressure or solids concentration in fluidized beds are analyzed using amplitude analysis or spectral analysis (e.g. power spectral density and autocorrelation function). Implicitly, these analysis techniques assume that the fluctuations can be described, respectively, by a distribution of random variations or by a linear summation of different periodic waves. *Stringer 1989*, however, was the first to suggest that the irregular, *aperiodic* behavior of the fluidized bed's dynamics is due to the fact that it is a *non-linear*, chaotic system. For that reason, it also seems appropriate to characterize fluidized bed time series with specific techniques that take the periodicity and non-linearity of the dynamics into account. This is done with chaos analysis. Many research have been done for chaos analysis of pressure fluctuation of fluidized bed such as *Schouten et al., 1996*, *Letzel*

*et al.*, 1997; *Lin et al.*, 2001a and b, *Ellis et al.*, 2003; *Ming-yan liu and Zong ding hu*, 2004; *Briens and Ellis*, 2005, *Zhong and Zhang*, 2005. Chaotic systems are governed by nonlinear interactions between the system variables and for this reason they are sensitive to small changes in initial conditions. Therefore, information about some initial state of the system is lost when it evolves in time and the system is characterized by a limited predictability. The dynamics of the system are reflected by its attractor in phase space. This attractor forms a fingerprint of the dynamical behavior of the system and is characterized by invariants like the Kolmogorov entropy, Shannon entropy, and Lyapunov exponents.

### Shannon entropy

Shannon entropy is concept of entropy in information theory. Shannon entropy is a measurement of the amount of information in a certain information source and the degree of indeterminacy in a certain system resulting in it enriching the meaning of entropy. The Shannon entropy can be utilized to express the degree of uncertainty involved in predicting the output of a probabilistic event. That is to say, if one predicts the outcome exactly before it happens, the probability will be a maximum value and, as a result, the Shannon entropy will be a minimum. If one is absolutely able to predict the outcome of an event, the Shannon entropy will be zero. The Shannon entropy of any differential pressure time series in a spout-fluid bed can be defined as following (*Zhong and Zhang*, 2005)

$$S = - \sum_{i=1}^n p(x_i) \lg[p(x_i)] \quad (\text{Equation 2-55})$$

Where,  $n$  is the length of time series signal,  $p(x_i)$  is the probability of every component in the signal, satisfying the constraint  $\sum_{i=1}^n p(i) = 1$ .  $p(x_i)$  can be estimated by joint probability density formula. The unit of  $S$  is decibels (dB). It can be seen that the more disorder in a system, the larger the information entropy. The Shannon entropies in spout-fluid beds reflect the dynamic behavior (e.g. turbulent motion of the gas or particles, intensive interactions between particles and gas, flow instability, chaos)

### Kolmogorov entropy

Kolmogorov entropy is one of the most important chaos characteristics, which measures the rate of loss of information and quantifies the limited predictability of chaotic system. Kolmogorov entropy is large for very irregular dynamic behavior, while it is small in case of more regular, periodic like behavior. Formal definition of Kolmogorov entropy is given e.g. in *Schouten et al.*, 1996 presented an interesting attempt to relate the Kolmogorov entropy to bubbling bed design parameters. They used the time series of pressure fluctuations in bubbling bed for direct calculation of Kolmogorov entropy and derived the following equation:

$$K = 19.3(U - U_{mf}) \frac{0.4D_T}{H_s^{1.6}} \quad (\text{Equation 2-56})$$

The correlation of experimental data using Equation 2-56 was fairly good for a given type of particle in a wide range of superficial gas velocities and bed ratios ( $H_s = D_T$ ). The investigation of data from various particle systems however revealed that correspondence only could be obtained when the correlation was changed in the following way:

$$K = 1,07 \left( \frac{U - U_{mf}}{U_{mf}} \right) \frac{D_T^{1,2}}{H_s^{1,6}} \quad (\text{Equation 2-57})$$

### **Lyapunov exponent**

The Lyapunov exponent providing a qualitative and quantitative characterization of dynamical behavior represents the exponentially fast divergence of nearby orbits in the phase space. A system with one or more positive Lyapunov exponents is defined to be chaotic.

After the chaotic attractor is successfully obtained, the evolution of the trajectories and the distribution of attractor's phase points enable the calculations of the chaotic measures. The most important measure to decipher is the set of Lyapunov exponents, or the Lyapunov spectrum. The Lyapunov exponent characterizes the large-time average of the exponentially divergent rate of two nearby trajectories. At least one positive Lyapunov exponent represents chaos. In the d-dimensional phase space, there are d principal axes where expansion or contraction occurs in each axis, respectively. The Lyapunov exponents are given as follows to determine the average rate of divergence along each principal axis (*Lin et al., 2001a*)

$$\lambda_i = \lim_{n \rightarrow \infty} \log \frac{\varepsilon_i(t)}{\varepsilon_i(0)} \quad (\text{Equation 2-58})$$

Where  $\varepsilon_i(0)$  and  $\varepsilon_i(t)$  are the distances between two nearby trajectories along the principal axis i at time 0 and t. Computation of the Lyapunov exponents not only can determine whether a system is chaotic but also provides the other chaotic measure. Metric entropy is the sum of all the positive Lyapunov exponents:

$$s = \sum_{i=1}^K \lambda_i \quad (\text{Equation 2-59})$$

The evaluations of the negative Lyapunov exponents are unreliable due to the extremely small numbers uncounted which are often contaminated by noise from experimental measurements or computer truncations. The value of metric entropy obtained from the Lyapunov exponents is similar to the Kolmogorov entropy or the other thermodynamic entropy

## **2.4 Solid mixing and segregation**

### **2.4.1 Mixing and segregation process**

The mixing of the solid in the fluidized bed is very important since it influences the gas-solid contacting, thermal gradients within the bed, heat transfer coefficients, position and number of solids feed and withdrawal points, the presence and extent of dead zones at distributor level. In the fluidized bed, the mixing behavior is connected to the solid movement mechanism in the bed. A good knowledge of the particle movement in fluidized beds assists in the understanding of solids mixing, erosion of immersed surfaces and the determination of the optimum location for feeding and withdrawing solids in fluidized beds. The movement of bubbles transporting solids in the wake provides a good axial mixing. In the group D particles, the large size of particles giving a small wake bubble leads to the poor mixing in these systems. Bubbles transport particles also due to the drift where the spike is approximately one third of bubble volume. At the very beginning, *Rowe and Partridge, 1962 and 1965*

investigated the mechanisms where the bed of particles colored and colorless were mixed by inducing bubble in a two dimensional bed. Figure 2.8 shows how the solid moves due to wake and drift of the bubble.



**Figure 2.8 Two-dimensional bubble rising from an under-layer of black particles**  
(Loeffler, 2001 adapted from Rowe, 1971)

By investigation on emulsion movement of Geldart B and A particles, *Kunii and Levenspiel, 1991* found out that when the solids move upwards due to the upward flow of bubbles, there must be downward flow of solid forming a poor bubble region. It summarizes the observation of *Whitehead, 1985, Yamazaki et al., 1986, and Lin et al., 1985. Tsutsui et al., 1980 Werther and Molerus, 1973* observed a strong upflow of emulsion solids close to the vessel walls and starting close to the bottom of the bed. Higher up the bed this upflow region shifts toward the center of the bed. Figure 2.9 shows the general pattern of movement of emulsion.

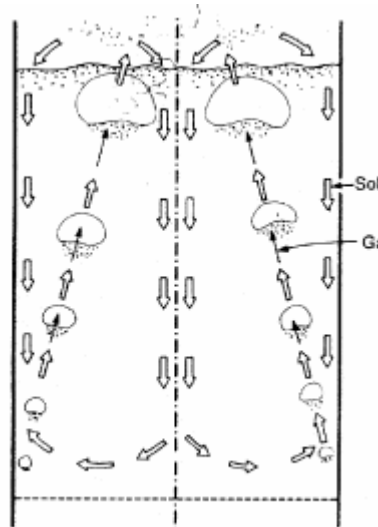


**Figure 2.9 General pattern of movement of emulsion** (*Kunii and Levenspiel, 1991 adapted from Werther and Molerus, 1973*)

With some other related studies, *Kunii and Levenspiel, 1991* tentatively make the following schemes regarding the emulsion flow in the fluidized bed of Geldart B solids that is shown in figure 2.10.

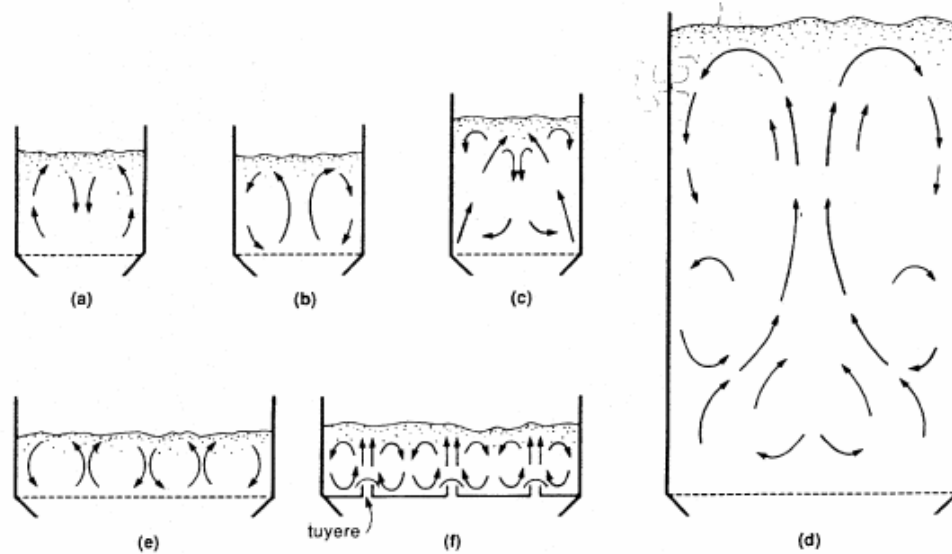


**Figure 2.10 Movement of solids in bubbling fluidized beds** (*Kunii and Levenspiel, 1991*)

*Note : a)  $H/D \cong 1$ , low  $U$ ; b)  $H/D \cong 1$ , high  $U$ ; c)  $H/D \cong 2$ , high  $U$ ; d) general pattern in deep beds; e) shallow bed, uniform distributor; f) shallow bed, with tuyeres.*

- At low fluidizing velocity in beds of aspect ratio (height/diameter) close and below unity, the emulsion solids circulate as a vortex ring with upflow at the wall and downflow at the center of the bed (figure 2.10a).
- When gas flow rates increasing this flow pattern may reverse because of the large rising bubbles in the bed (figure 2.10b)
- When the bed aspect ratio higher than unity, emulsion solids begin to move down the wall near the bed surface (figure 2.10c)
- In the deeper bed, a second vortex ring forms above the original vortex ring with upflow at the centerline of the bed (figure 2.10 d). At higher gas flows, the solid circulation in the upper vortex ring becomes more vigorous and dominates the overall movement of the emulsion.
- In very shallow bed with aspect ratio  $< 0,5$  supported on uniform distributors, vortex rings of aspect ratio  $H/D \cong 1$  may develop (figure 2.10 e).
- With higher pressure drop tuyeres, these distributors may determine the circulation pattern of the emulsion (figure 2.10 f)
- In beds of Geldart A FCC catalyst, the transition to upflow of emulsion occurs much closer to  $U_{mf}$  than in bed of Geldart B solids.

For the large particles (Geldart D), *Kunii and Levenspiel, 1991* describe the mixing mechanism as showing in figure 2.11. As seen in the figure, long lenticular cavities are formed close to the perforated plate distributor. These cavities move slowly upward to transform into nearly spherical bubbles higher up the bed. These bubbles grow rapidly and do not follow any preferred path. The bubble above nearly spherical and have very small wake, in contrast to what one finds with small particle systems.

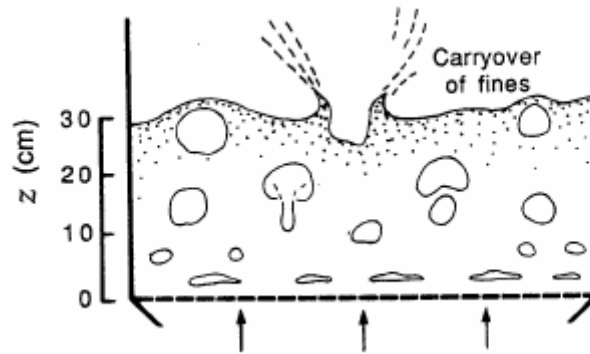


**Figure 2.11 Typical bubbling condition in the fluidization of coarse particles (Kunii and Levenspiel, 1991)**

The mixing behavior of "second solid" with different shape and density is also connected to the movement of the solids in the bed. Depending on the shape and density of second solids, movement of second solid would be different.

Figure 2.12 shows the movement of large cylinder particles in the bubbling fluidized bed. Observations are as following (Kunii and Levenspiel, 1991).

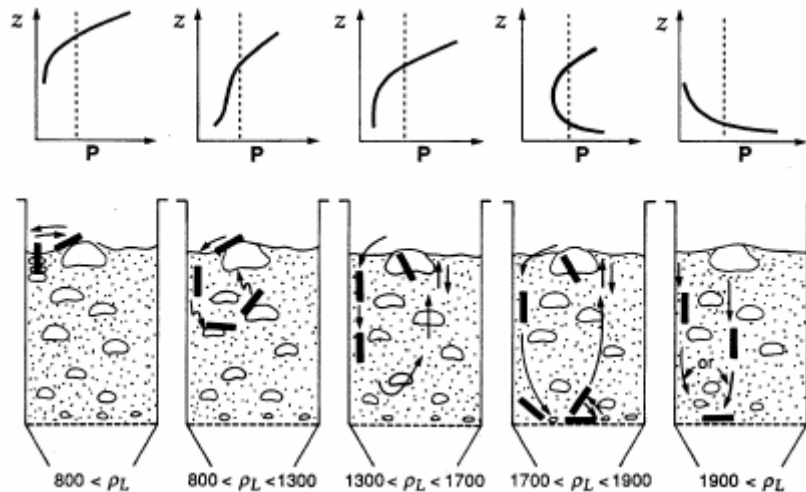


**Figure 2.12 Movement of large cylinders of various densities in fine particle beds (Kunii and Levenspiel, 1991)**

Note: Particles 11mm outside dia. , 45mm long;  $U_{mf} = 0,096\text{m/s}$ ;  $U = 2,8 U_{mf}$ ;  $\rho_L$ : density of cylinder;  $P$  = probability of having the cylinder present at level  $z$  in bed;  $\rho_{bulk} = 1490\text{kg/m}^3$ .

- For the large body of very low density,  $\rho_L < 800\text{kg/m}^3$ , the large body is swept up by the roof of the bubbles and remains near the top of the bed.
- At density  $800 < \rho_L < 1300 \text{ kg/m}^3$ , the body occasionally descends into the bed where rising bubble roofs push it back up. Sometimes several bubbles are needed to return it to the top of the bed.
- For a density comparable to the bed density, or  $1300 < \rho_L < 1700 \text{ kg/m}^3$ , the large body penetrates the bubble roofs; however, the bubble wakes are still able to push the body up
- For density between 1700 and 1900  $\text{kg/m}^3$ , the large body falls to the distributor from time to time. It stays there until a swarm of bubbles exert a lifting effort

great enough to push it toward the top of the bed. Once caught by this swarm of bubbles, the large body is often conveyed rapidly all the way to the top of the bed.

- For very dense objects,  $\rho_L > 1900 \text{ kg/m}^3$ , or with a density ratio greater than 1.3:1, the large body falls to the bottom of the bed and stays there.

It is recognized that mixing in a fluidized bed occur in distinct mechanism that are moderately well understood depending on shape, size, density of particles and also fluidization mechanism of the bed.

#### **2.4.2 Mechanism of mixing and segregation of binary mixture**

Rowe *et al.*, 1972a carried out various experiments with the binary mixture of six different combinations of particles as following:

- Heavy, Big, Packed combined with Light, Small, Fluid (HBP/LSF)
- Heavy, Small, Packed combined with Light, Big, Fluid (HSP/LBF)
- Heavy, Small, Fluid combined with Light, Big, Packed (HSF/LBP)
- Big, Packed combined with Small, Fluid (BP/SF)
- Heavy, Packed combined with Light, Fluid (HP/LF)
- Heavy, Small combined with Light, Big (HS/LB)

The materials used are shown in table 2.6

**Table 2.6 Material used in various experiments of binary mixtures** (concluded from Rowe *et al.*, 1972a)

Mixture	Material name	Particle density ( $\text{kg/m}^3$ )	$d_p$ ( $\mu\text{m}$ )
HBP vs. LSF	Steel shot (HBP)	7500	333
	Ballotini (LSF)	2940	189
HSP vs. LBF	copper shot (HSP)	8860	275
	Ballotini (LBF)	2940	460
HP vs. LF	Steel shot (HP)	7500	278
	Ballotini (LF)	2940	271
HSF vs. LBP	Copper shot (HSF)	8860	82 or 114
	Ballotini (LBP)	2940	271
BP vs. SF	Ballotini (BP)	2940	642
	Ballotini (SF)	2940	96

Mixture	Material name	Particle density (kg/m <sup>3</sup> )	d <sub>p</sub> (μm)
HS vs. LB (1)	Copper shot(HS)	8860	114
	Ballotini (LB)	2940	189
HS vs. LB (2)	Copper shot (HS)	8860	82
	Polystyrene (LB)	1050	267
HS vs. LB (3)	Copper shot (HS)	8860	82
	Ballotini (LB)	2940	163

Mixing mechanism was observed in experiments visually and if necessary by surface dyeing. Some observations were made using two dimensional bed where the whole sequence of particle movement could be seen and filmed. The observation of mixing mechanism can be concluded as following:

#### **HBP vs. LSF**

##### *Flotsam initially at the top*

Since  $U_{mf}$  of LSF is smaller compare to  $U_{mf}$  of HBP, when increasing air flow from zero, LSF begins to fluidize in the upper part of the bed while HBP remain static and act roughly as a porous distributor.

At higher air supply velocity, during the formation of bubbles in the flotsam the wake of bubbles may carried few HBP particles to the surface of the bed even the velocity still lower than  $U_{mf}$  of HBP. At this state, HBP remain pure in the bottom while LSF contain some HBP particles in the upper part of the bed.

When increasing air supply velocity, no dramatic change occurs until the bubble formed in the HBP part. The wake of bubbles carried up HBP particles in to the flotsam and interface become uneven. The mixing mechanism when increasing air supply velocity is the increasing of proportion of HBP in the flotsam whilst the bottoms remain essentially pure until all the jetsam was pulled up by the wake of bubbles.

##### *Jetsam initially at the top*

When increasing air velocity, the bed is remaining static until  $U$  exceeds  $U_{mf}$  of LSF. The bubbles then, appear in the bottoms, originating at the distributor and quenched at a height that increases with the gas velocity.

At a critical velocity, which is not precise and reproducible but is markedly less than the  $U_{mf}$  of HBP, the upper part of the bed consisting of static LSF particles over-layered by the HBP layer, is lifted bodily before it collapses. It can remain in this lifted position indefinitely if it is not disturbed but the ultimate collapse is sudden.

The HBP then rapidly sinks as jetsam even without any increase in velocity by falling through bubbles or their disturbed wakes.

##### *Jetsam initially in the middles*

When increasing air velocity, At first only the upper layer of LSF fluidized and few HBP particles going to LSF area in the upper part of the bed.

The bottom layer of LSF then fluidized and at this stage, still there is an inert layer in the middle.

The HBP layer may move and distort but remain coherent until it collapses and eventually sinks to the bottom of the bed.

### **HSP vs. LBF and HP vs. LF**

The mechanism is similar to HBP vs. LSF system

HSP or HP became jetsam very rapidly with the same mechanism described above.

The mechanisms by which relative movement occurs are essentially independent of size except for the gross differences.

### **HSF vs. LBP**

Experiments have been performed when HSF initially was placed at the top.

With the increasing of air velocity, HSF fluidize and bubbles formed from the interface between HSF and LBP in usual way and slowly sinks and steadily to become submerged beneath a totally static layer of mainly LBP even  $U < U_{mf}$  of LBP particles. Some LBP particles could be dragged up to the upper part due to the wake of HSF.

At fixed velocity between the  $U_{mf}$  of the two components, the HSF particles come to rest at a relatively clearly marked interface below which there is only LBP. Above this is a fairly crude mixture of both components.

When HSF particles too small, basically with the diameter smaller than 1/2,4 or 1/3,3 diameter of LBP, HSF can sink through the static of LBP particles.

Bubbles of HSF gather some LBP particles in their wake and deposited them on the surface where they effectively float. In this way, the bubbling layer covers itself with static particles until the weight of this overburden is sufficient to suppress fluidization and all further movement ceases.

If the air velocity is increased until the LBP particles fluidize, then segregation occurs rapidly and the HSF become jetsam. Mixing then occurs by wake entrainment and equilibrium is established with fairly pure jetsam and contaminates flotsam.

### **BP vs. SF**

Ballotini with different size was used in these experiments (see table 2.6). 10% BP particles was initially in the top of the bed.

The inert overburden at first suppresses fluidization and then the bed begins to fluidize from the bottom supporting a quasi-stable inert bed above it. Eventually the top collapses and BP particles fall through bubbles at an air velocity well below their own  $U_{mf}$ .

The behavior exactly as the case of HBP particle initially in the tops except that, in spite of the much larger difference in  $U_{mf}$ 's, collapse is less dramatic and segregation much slower. The BP particles become jetsam but even so, at a velocity only one quarter of their  $U_{mf}$ , a large proportion is distributed through the bed.

Although BP particles become a jetsam, the effect of size on segregation is small compared with the effect of density.

**HS vs. LB**

Three pairs of particles were used to study mixing mechanism (table 2.6)

Density dominates the tendency to segregate.

HS particles easy to sink largely with the passage of each bubble as described above and also by interstitial penetration.

Experiments with an approximation uniform mixture was made by forming alternate thin layers of equal parts by weight of the same two kinds of particles have done in two dimensional bed. The flotsam and jetsam form rapidly at velocity little in excess of the common  $U_{mf}$  but some re-mixing occurs at higher velocities.

**Mixing and segregation mechanism**

Differences in particle density readily lead to segregation in fluidized beds. The denser particles become jetsam and the lighter particles become flotsam.

The difference in size of the same density particles also leads to segregate with large one settling in the bottom however the effect of size different is slight

Some different mechanisms of mixing and segregation observed including:

- Particles lifting in the enclosed wake of rising bubble
- Particles falling through bubbles to descend in the bed.
- Small particles may descend by inter-particle percolation.
- Quasi-hydrostatic effect that caused particles to float on a fluidized bed of denser one.

**2.4.3 Determination of mixing and segregation**

Various techniques have been used to study the mixing of solids have been concluded by *Kunii and Levenspiel 1991* as following:

- Following the paths of individual tagged particles for long periods of time as they move about the bed.
- Measuring the extent of intermixing of two kinds of solids originally located one above the other in the bed.
- Measuring the vertical spread of thin horizontal slice of tracer solid
- Finding the residence time distribution of the flowing stream in a bed with a through flow of solids, using a variety of tracer techniques such as step or pulse injection.
- Measuring the axial heat flow in a bed with a heated top section and cooled bottom section. This technique assumes that heat transport is caused solely by the movement of solids.

And also, various models describing the solids mixing in fluidized bed have been presented in literature. These are reviewed recently by *Kunii and Levenspiel, 1991*, *Lim et al., 1995*, and *Costa and de Souza Santos, 1999*. The models that have been used to interpret the experimental findings on the vertical moment of solids are discussed in the next section.

### 2.4.3.1 Dispersion model

The dispersion model was first used by *May, 1959* to fit the experimental mixing data through an effective solid diffusion coefficient *Kunii and Levelspiel, 1991* represented as following:

$$\frac{\partial C_s}{\partial t} = D_{sv} \frac{\partial^2 C_s}{\partial z^2} \quad (\text{Equation 2-60})$$

Equation 2-60 may take several forms. For a step input of tracer introduced into the stream of solids entering the bottom of a fluidized bed and leaving at the top or vice versa, the use of the appropriate boundary and initial conditions give

$$\frac{C_s(\text{at exit})}{C_s(\text{at } t = \infty)} = f\left(\frac{D_{sv}}{u_{s,up} z_f}, \frac{t}{t_s}\right) \quad (\text{Equation 2-61})$$

For a pulse of tracer introduced into a bed with no through flow of solids,

$$\frac{C_s(t)}{C_s \text{ if well mixed in the bed}} = f\left(\frac{D_{sv} t}{L_f^2}, \frac{z}{L_f}\right) \quad (\text{Equation 2-62})$$

As understanding of the hydrodynamics of fluidized beds grew, attempts were made to relate the dispersion model to more mechanistic models so that more fundamental measurements could be used for the design of large-scale units.

For the horizontal movement of solids, the study of *Brötz, 1956* in a shallow rectangular bed as shown in figure 2.13. When measuring the rate of approach to uniformity after removal of the dividing plate, the information was evaluated using horizontal dispersion coefficient  $D_{sh}$ .

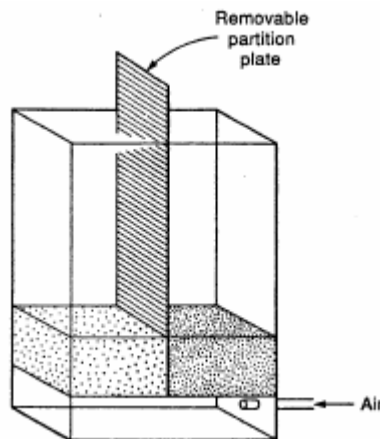


**Figure 2.13** Experimental setup used by *Brötz 1956* to study the horizontal movement of solids (*Kunii and Levelspiel, 1991*)

The mechanism for the horizontal movement of solids is shown in figure 2.14. When a bubble rises, it pushed emulsion aside. However, the solids passing close to the bubble enter its cloud and are then drawn into the wake. Solids mix uniformly in the wake and leave the wake from random positions, thereby giving rise to horizontal mixing. Solids from the bubble move aside when the bubble passes, but they return close to their original position.

For this mechanism the horizontal dispersion coefficient  $D_{sh}$  in terms of Einstein random is expressed by *Kunii and Levenspiel, 1991*:

$$D_{sh} = \frac{(\text{fraction of solids that mix})(\text{mean square distance moved})}{4(\text{time interval considered})}$$

$$D_{sh} = \frac{1}{4} \left( \frac{\text{fraction of bed solids that enter bubble wakes}}{\text{to mix there per unit time}} \right) \overline{\Delta r^2}$$

The calculation of horizontal dispersion finally leads to the equation:

$$D_{sh} = \frac{13}{16} \frac{\delta}{1-\delta} \alpha^2 d_b U_{br} \left[ \left( \frac{U_{br} + 2U_f}{U_{br} - U_f} \right)^{1/3} - 1 \right] \quad (\text{Equation 2-63})$$

For fast bubbles with thin clouds typical of fine particle systems ( $U_{br} \gg U_f$ ),  $D_{sh}$  could be simplified to:

$$D_{sh} = \frac{13}{16} \frac{\delta}{1-\delta} \frac{\alpha^2 U_{mf} d_b}{\varepsilon_{mf}} \quad (\text{Equation 2-64})$$

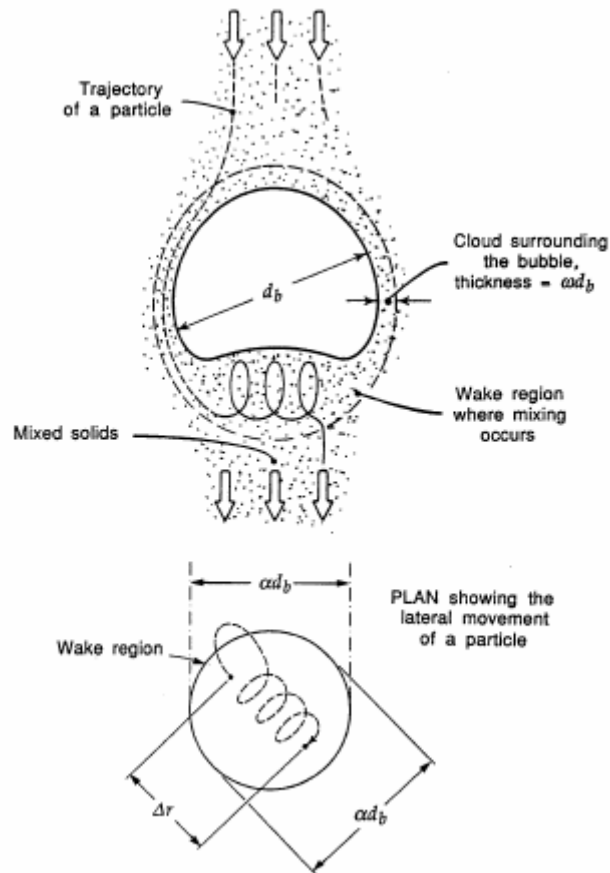
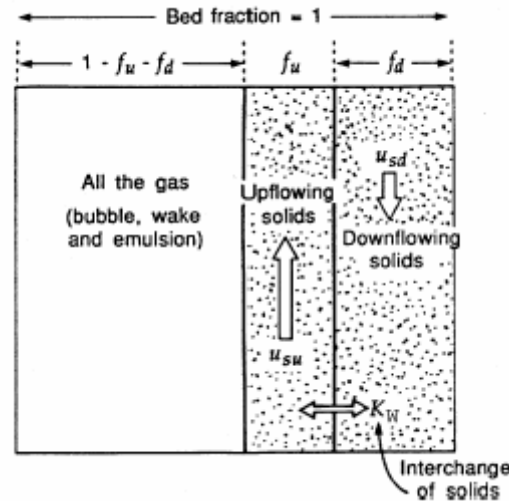


Figure 2.14 Horizontal movement of solids (*Kunii and Levenspiel, 1991*)

### 2.4.3.2 Counterflow solid circulation models

The counterflow models or counter current back mixing model was originally proposed by *van Deemter, 1961* and has been refined and generalized by *Gwyn et al., 1970*. It has gained great acceptance due to its good representation of the transport process in a bubbling bed (*Lim et al., 1995*). This model is based on the hypothesis that the fluidized bed can be divided into three distinct phases (refer to figure 2.15):



**Figure 2.15 Schematic diagram for the counter-current back-mixing model considering solids movement only (*Kunii and Levenspiel, 1991*)**

- An ascending gaseous phase free of particles (i.e. bubbles)
- An ascending phase including gas and solids (i.e. wake)
- A descending phase including gas and solids (i.e. emulsion)

The solids flowing up at a velocity  $U_{su}$ , the other flowing down at velocity  $U_{sd}$  with  $f_u$  and  $f_d$  ( $\text{m}^3 \text{ solids/m}^3 \text{ bed}$ ) is the bed fractions consisting of these streams. Consider the movement of some labeled or tagged solids that constitute a fraction  $X_{su}$  and  $X_{sd}$  ( $\text{m}^3 \text{ tagged solid/m}^3 \text{ total solid stream}$ ) of the up and down flowing streams. The different equation describing the vertical movement of these tagged solids and their interchange is then

$$f_d \frac{\partial C_{sd}}{\partial t} + f_d U_{sd} \frac{\partial C_{sd}}{\partial z} + K_s (C_{sd} - C_{su}) = 0 \quad (\text{Equation 2-65})$$

and

$$f_u \frac{\partial C_{su}}{\partial t} + f_u U_{su} \frac{\partial C_{su}}{\partial z} + K_s (C_{su} - C_{sd}) = 0 \quad (\text{Equation 2-66})$$

Where the solids interchange coefficient  $K_s$  ( $\text{m}^3 \text{ tracer/m}^3 \text{ bed.s}$ ) represents the transfer of tagged solid from one stream to the other.

For a tall enough bed of fine particles and sufficiently large values of elapsed time, *van Deemter* showed that the changes in concentration of labeled solids could be represented by an effective dispersion coefficient given by

$$D_{sv} = \frac{f_d^2 U_{sd}^2}{K_s (f_d + f_u)} = \frac{f_d^2 U_{sd}^2}{K_s (1 - \delta)(1 - \epsilon_f)} \quad (\text{Equation 2-67})$$

Since the circulation of cloud gas cause a rapid movement of solids around a clouded bubble as shown in figure 2.16, *Kunii and Levenspiel, 1969* assumed that all the solids from the lower part of the cloud are swept into the wake, mix with the solid already there, and eventually leak back into the emulsion.

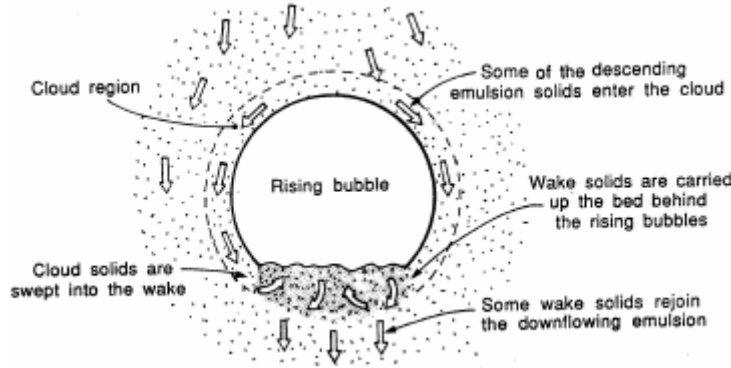


**Figure 2.16 Model mechanism of interchange of solids between downflowing emulsion solids and upflowing wake solids (*Kunii and Levenspiel, 1991*)**

By this process, slowly downflowing emulsion solids are swept into the rising bubble wake and then return to the downflowing emulsion. From this mechanism the interchange coefficient for solids in beds with clouded bubbles is

$$K_s = \frac{\text{volume of solids transferred from the emulsion to the wake}}{(\text{volume of bubble})(\text{time})}$$

$$K_s \approx \frac{3(1 - \varepsilon_{mf})U_{mf}}{(1 - \delta)\varepsilon_{mf}d_b} \quad [\text{s}^{-1}] \quad (\text{Equation 2-68})$$

With somewhat similar model, *Chiba and Kobayashi, 1977* derived the following expression for the interchange coefficient:

$$K_s = \frac{3}{2} \left( \frac{f_w}{1 + f_w} \right) \frac{U_{mf}}{\varepsilon_{mf}d_b} \quad (\text{Equation 2-69})$$

Introducing  $K_s$  from equation 2-68 into equation 2-67 and simplifying leads to the following expression for the vertical dispersion coefficient in term of measurable bubble and bed properties.

$$D_{sv} \cong \frac{f_w^2 \varepsilon_{mf} \delta d_b U_b^2}{3U_{mf}} \quad (\text{Equation 2-70})$$

#### 2.4.3.3 Mixing and segregation index

In the fluidized bed of the mixture of a particles with different size and density, particles with bigger size and higher density have tendency to sink down to the bottom of the bed and vice versa.

Many experiments on determination of mixing quality have done with measuring mass fraction of solids along the high level of the bed. The convenient way of represent the mixing quality is using mixing index (MI). *Rowe et al., 1972b* give the first definition of a mixing index as described in figure 2.17.

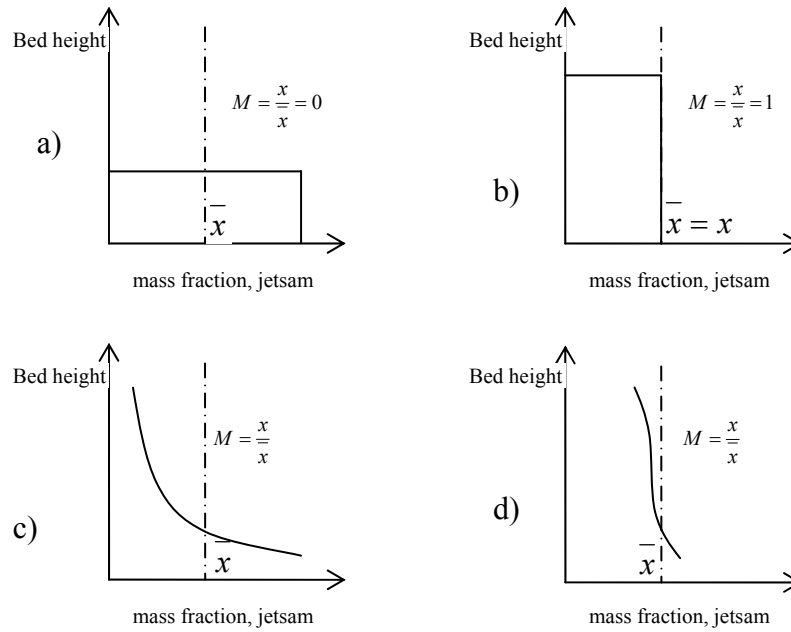


**Figure 2.17 Mass fraction of jetsam in the mixture along the height of the bed in different situations to describe the mixing index**

Note: a) completely segregation; b) completely mixed; c) Low quality mixing; d) high quality mixing.

He proposed using mixing index defined as

$$MI = \left( \frac{\text{Fraction of jetsam in the top portion of the bed}}{\text{fraction in a completely mixed bed}} \right) = \frac{x}{\bar{x}} \quad (\text{equation 2-71})$$

$$x = \frac{M_{\text{jetsam}}}{M_{\text{jetsam}} + M_{\text{flotsam}}} (\text{in the top portion of the bed}) \quad (\text{Equation 2-72})$$

$$\bar{x} = \frac{M_{\text{jetsam}}}{M_{\text{jetsam}} + M_{\text{flotsam}}} (\text{in the whole bed}) \quad (\text{Equation 2-73})$$

By this definition, MI has a range between 0 and 1 with that MI = 0 relating to complete segregation while MI = 1 is related to completely mixed.

By doing experiments with a bed of 141mm diameter, 100 to 150mm deep, with different materials, Rowe *et al.*, 1972b has given the equation to calculate x as following

$$x = f(U - U_{mf(\text{flotsam})}) (\rho_H / \rho_L)^{-2.5} (d_B / d_S)^{-1/5} \quad (\text{Equation 2-74})$$

Several authors have given governing equations for mixing index calculation as shown in table 2.7.

**Table 2.7 Correlation for mixing index calculation**

Reference	Equation
-----------	----------

Reference	Equation
Nienow et al., 1978	$M = \frac{1}{1 + \exp(-F)}$ $F = \frac{U - U_{TO}}{U - U_{mf,l}} \cdot \exp\left(\frac{U}{U_{TO}}\right)$ <p>With:</p> $\frac{U_{TO}}{U_{mf,l}} = \left(\frac{U_{mf,h}}{U_{mf,l}}\right)^{1,2} + 0,9 \cdot \left(\frac{\rho_{p,h}}{\rho_{p,l}} - 1\right)^{1,1} \cdot \left(\frac{\varphi_h \cdot d_{p,h}}{\varphi_l \cdot d_{p,l}}\right)^{0,7} - 2,2 \cdot \sqrt{X} \cdot \left[1 - \exp\left(-\frac{H}{D}\right)\right]^{1,4}$
Rice and Brainovich, 1986	$MI = \frac{1}{1 + \exp(-F)} \quad \text{with definition} \quad U_{TO} = \sqrt{U_{mf,l} \cdot U_{mf,h}} \cdot \left(\frac{2 \cdot H}{D}\right)^{-0,2}$ $F = \pm \sqrt{\frac{ U - U_{TO} }{U - U_{mf,l}}} \cdot \exp\left(\frac{U}{U_{TO}}\right) \sqrt{f_s} \quad \text{for } U > U_{TO}: +, f_s = \frac{3 \cdot d_{p,h}}{d_{p,l}}$ $\text{for } U < U_{TO}: -, f_s = \frac{3 \cdot d_{p,l}}{d_{p,h}}$
Nienow et al., 1987	$MI = \frac{1}{1 + \exp(-F)}$ $F = \pm \sqrt{\frac{ U - U_{TO} }{U - U_{mf,l}}} \cdot \exp\left(\frac{U}{U_{TO}}\right) \quad \text{for } U > U_{TO}: +$ $\text{for } U < U_{TO}: -$ <p>with</p> $U_{TO} = \left(\frac{U_{mf,h}}{\bar{U}_{mf}}\right)^{0,46} + 0,047 \cdot \left(\frac{d_{p,h}}{\bar{d}_p}\right)^{-0,26} \quad \text{or} \quad U_{TO} = \bar{U}_{mf} \cdot \sqrt{\frac{U_{mf,h}}{\bar{U}_{mf}}}$
Peeler and Huang, 1989	$MI = \frac{1}{1 + \exp(-F)}$ $F = \pm \sqrt{\frac{ U - U_{TO} }{U - U_{mf,l}}} \cdot \exp\left(\frac{U}{U_{TO}}\right) \quad \text{for } U > U_{TO}: +$ $\text{for } U < U_{TO}: -$ <p>with</p> $U_{TO} = \sqrt{U_{mf,l} \cdot U_{mf,h}} \cdot D \cdot d_{b,TO}^{-0,21}$
Fan, 1990	$MI = K \left(\frac{\bar{d}_p}{d_F}\right)^k \left(\frac{U}{U - U_F}\right)$

Reference	Equation
	$MI = \frac{1}{1 + \exp(-F)}$
Wirsum and Fett, 1997	$F = \frac{U - U_{TO}}{U - U_{mf,l}} \cdot \exp\left(\frac{U}{U_{TO}}\right)$ <p>with <math>\left(\frac{U_{TO}}{U}\right)^2 = \left(0,01 \cdot \frac{d_{p,f}}{d_{p,j}} \cdot \frac{U_{mf,f}}{U_{mf}}\right)^{1,6} \cdot 0,0045 \cdot \left(\frac{1000}{\rho_{p,f}}\right)^{3,7} + 12,4 \cdot \bar{X}_f</math></p>
Wu and Baeyens, 1998	$MI = 1 - 0,0067 \frac{d_{p,h}}{d_{p,l}} \cdot 1,33 \cdot \left(\frac{Q_b}{A}\right)^{-0,75}$
Sahoo and Roy, 2005	$MI = C_j \frac{W}{J} \text{ where } C_j = \int e^{-\int \left(\frac{FU}{FD_{sv}D_{SH}}\right) dZ} dZ; F = \frac{W\rho_s}{2V_B}$ <p>W, J: weight of total bed materials and of Jetsam particles taken in the bed  D<sub>SV</sub>, D<sub>SH</sub> : Vertical and horizontal dispersion coefficient (m<sup>2</sup>/s)</p>

Besides the definition of the mixing index from Rowe *et al.*, 1972b, there are different definitions for a mixing index considering the axial concentration profile of the respective solids.

Chiba *et al.*, 1980 proposed mixing index modified as shown in figure 2.18 and equation 2-75

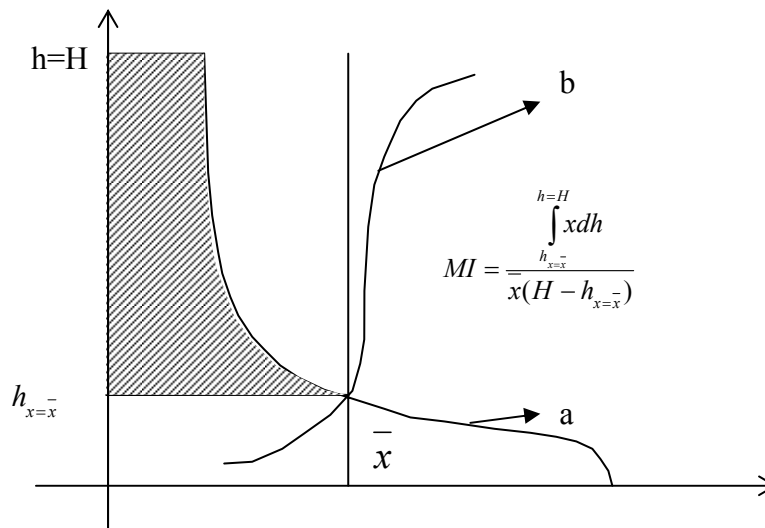


**Figure 2.18 Definition of mixing index (MI) (Chiba *et al.*, 1980)**

$$MI = \frac{\int_{h=\bar{x}}^{h=H} x dh}{x(H - h_{x=\bar{x}})} \quad (\text{Equation 2-75})$$

The definition is used in two cases when  $x$  represents a mass fraction of jetsam (line a), then  $0 < MI < 1$  and when  $x$  represents a mass fraction of flotsam (line b), then  $1 < MI < \infty$ .

*Bilbao et al., 1991* studies on mixing of sand and straw in fluidized bed and gives definition of mixing index based on the real volume fraction of sand in bed as following

$$MI = \frac{\frac{\int_{h=\bar{x}}^H x dh}{1 - h_{x=\bar{x}}}}{\bar{x}} \quad (\text{Equation 2-76})$$

Where,  $\bar{x}$ ,  $\bar{x}$  are volume fraction and mean volume fraction of sand in the bed.

*Nakagawa et al., 1994* investigate segregation of particles in circulating fluidized bed in a bed of 0,097 m and 0,15 m diameter and 3m height. He gives definition of segregation intensity as following

$$SI = \frac{1}{H} \int_0^H \left( \frac{x - \bar{x}}{\bar{x}} \right)^2 dz \quad (\text{Equation 2-77})$$

$$\text{Where } \bar{x} = \frac{1}{H(1 - \varepsilon)} \int_0^H (1 - \varepsilon) x dz \quad (\text{Equation 2-78})$$

With this definition, the larger of the value of  $S$ , the stronger is the segregation of particles and vice versa.

*Li Xiaodong et al., 2001* studied on mixing performance of municipal solid waste with different densities fluidized beds. Five kinds of materials have been investigated such as plastic, wood, candle, coal and coal-stone. The mixing index was defined as following:

$$MI = \int_{0,5}^1 \bar{C}_h dz - \int_0^{0,5} \bar{C}_h dz \quad (\text{Equation 2-79})$$

$$\text{Where } \bar{C}_h = \frac{\sum C_{hi}}{\sum C_{oi}} \quad (\text{Equation 2-80})$$

$$\text{With this definition, } \int_0^{0,5} \bar{C}_h dz = 1 - \int_{0,5}^1 \bar{C}_h dz \quad (\text{Equation 2-81})$$

$$\text{Therefore, } MI = 2 \int_{0,5}^1 \bar{C}_h dz - 1 \quad (\text{Equation 2-82})$$

$MI = 0$ , complete mixing in the bed

$MI > 0$ , mass concentration of material is higher in the upper part of the bed and material has a tendency to float.

$MI < 0$ , mass concentration of material is concentrated in the lower part of the bed and material has a tendency to sedimentation.

$MI = 1$  or  $MI = -1$  corresponds to material completely float or sedimentation and complete segregate to fluidization material.

Various experiments were performed to determine the mixing index of the bed depending on gas velocity, type of material, size of material.

Regression analysis of experimental data leads to equation to determine mixing index as following

$$MI = 3,09(0,55e^{-(R_d - 1)/3} - R_p + 0,45] + 0,028 \quad (\text{Equation 2-83})$$

Where,

$$R_d = d_{si}/d_m \quad (\text{Equation 2-84})$$

$$R_p = \rho_{si}/\rho_m \quad (\text{Equation 2-85})$$

### 3 FLUIDIZATION BEHAVIOR OF BINARY MIXTURE BIOMASS AND SAND

Fluidization technology is a well known technology that has many applications e.g. in drying, combustion and gasification process. For proper using of biomass in combustion or gasification in fluidized beds, understanding of fluidization behavior of biomass in the fluidized bed is very important since it is closely related to the heat and mass transfer process occurring inside reactors. In this chapter, experiments have been carried out to understand the fluidization and mixing behavior when fluidizing biomass or mixtures of biomass and sand in a fluidized bed. Biomasses used in the experiments are rice husk and milled wood pellets.

#### 3.1 Materials used in experiments

Materials used in the experiments are shown in table 3.1. Particles density of materials was measured by using a pyknometer.

**Table 3.1**Characteristic of materials used in experiments

Materials	$d_p$ ( $\mu\text{m}$ )	Bulk density ( $\text{kg/m}^3$ )	Particles Density ( $\text{kg/m}^3$ )	Calculated $U_{mf}$ (cm/s)	$\epsilon$ (fixed bed)
Sand 1	295,9	1607,6	2605,3	7,14	0,383
Sand 2	450	1473,6	2605,3	15,77	0,434
Rice husk	2x1x7 mm cylind. shape	130	638,72	NA	0,796
wood pellets	2036	442,1	1208,1	NA	0,634

By microscope analysis of particles itself, the observations on the characteristic of materials used in the fluidized bed are as following:

**Rice husk.** The microscope picture of rice husk is shown in figure 3.1.

- - Rice husk has a lozenge shape with shaft pointed at two ends, rounded with a thin layer and empty inside. Weight of two ends is not balance. The structure is like a boat. With this aerodynamics shaft, it is quite difficult to blow upward rice husk particles. The bulk density of rice husk is very low. Due to the low density, rice husk affects the fluidization behavior even at small mass contents.
- - There are a lot of thorns in the surface of the particle so when many particles stay together in a bed, they have a cohesive nature.

**Wood pellets.** Figure 3.2 shows the wood pellets particle. The main characteristics are:

- Shapelessness
- Soft and rough in surface can create a cohesive nature and easy to agglomerate.
- The particle is solid so the bulk density is higher compare to rice husk.



**Figure 3.1 Rice husk shape (microscope)**

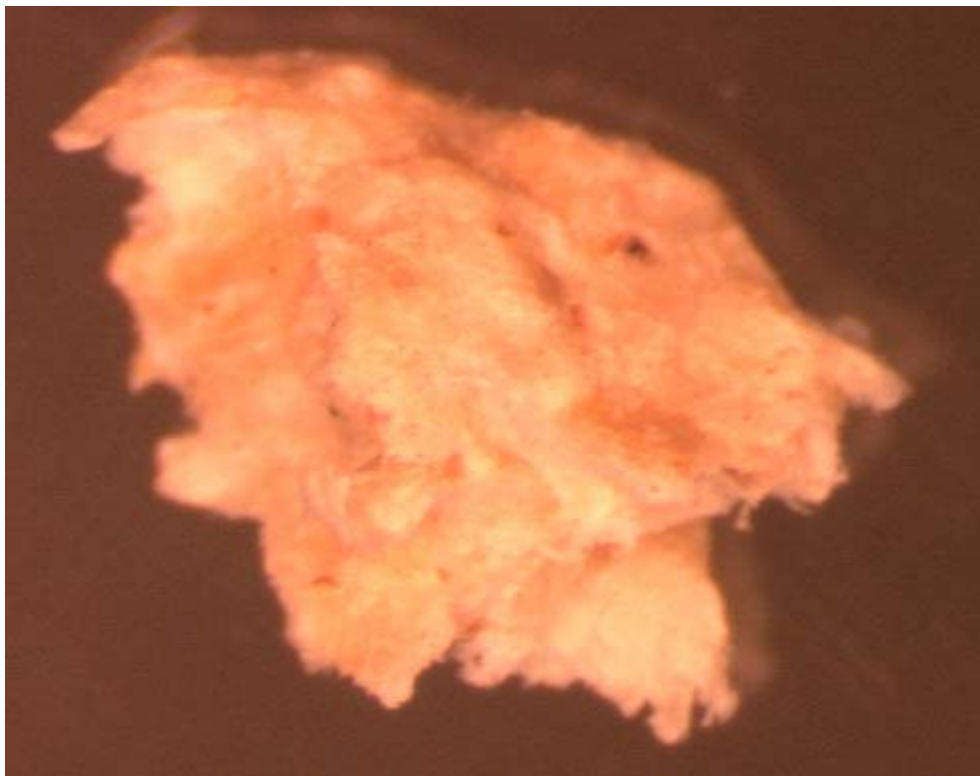


**Figure 3.2 Wood pellets particle (microscope)**

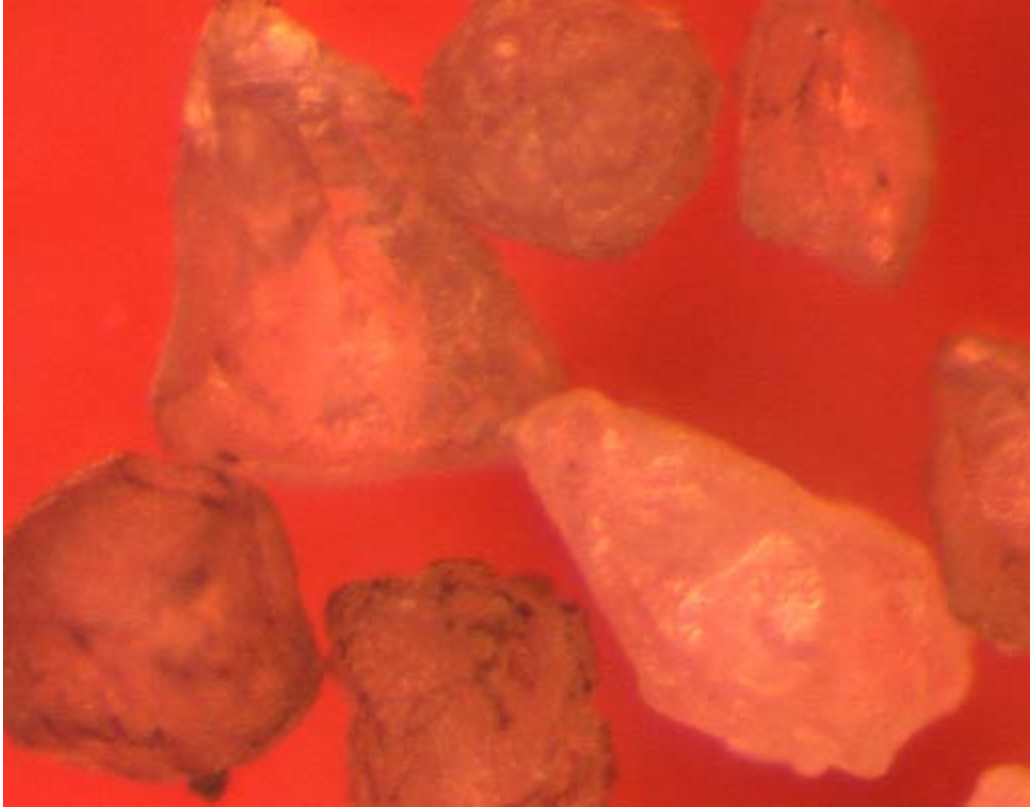


**Figure 3.3 Quartz sand particles (microscope)**

**Quartz sand.** Figure 3.3 shows quartz sand particles. The particle is solid with hard surface and also shapelessness. With hard surface, and not so rough, they do not have a cohesive characteristic and are therefore easy to fluidize.

### **3.2 Experimental equipment and methodology**

The experimental equipment used for investigation of the fluidization behavior of binary mixtures of sand and biomass is a cold test rig modeling fluidized bed with the bed chamber of 95cm height and 6cm inner diameter made of Plexiglas. Figure 3.4 shows the schematic diagram of the equipment and figure 3.5 shows the system in the laboratory.

Distribution of fluidizing air is accomplished by using a porous plate and the volume flow of the air can be controlled and recorded. The pressure is measured and recorded automatically. 5 values per second were taken at above the bed surface and the wind box where the air is introduced. The pressure drop through the bed materials is calculated by using following equation:

$$\Delta p = (p_{\text{winbox}} - p_{\text{chamber}}) - \Delta p_{\text{plate}}. \quad (\text{Equation 3-1})$$

By experiments measurements, the pressure drop through a porous plate ( $\Delta P_{\text{plate}}$ ) could be determined with the relation showed in figure 3.6 and the equation 3-2. The correlation was used to calculate  $\Delta P_{\text{plate}}$

$$\Delta p_{\text{plate}} = 47,636U + 48,986 \quad (\text{Equation 3-2})$$

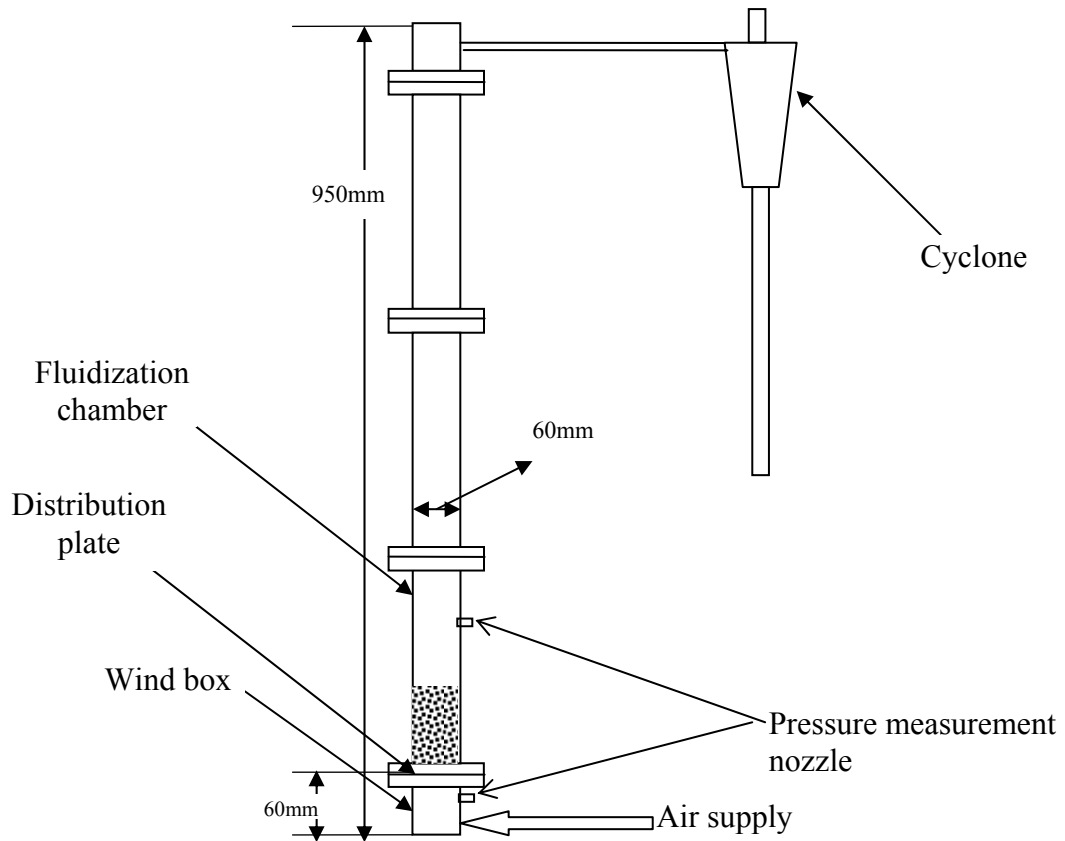


**Figure 3.4 Schematic diagram of cold model test rig for fluidization**



**Figure 3.5 Cold model test rig for fluidization experiments**

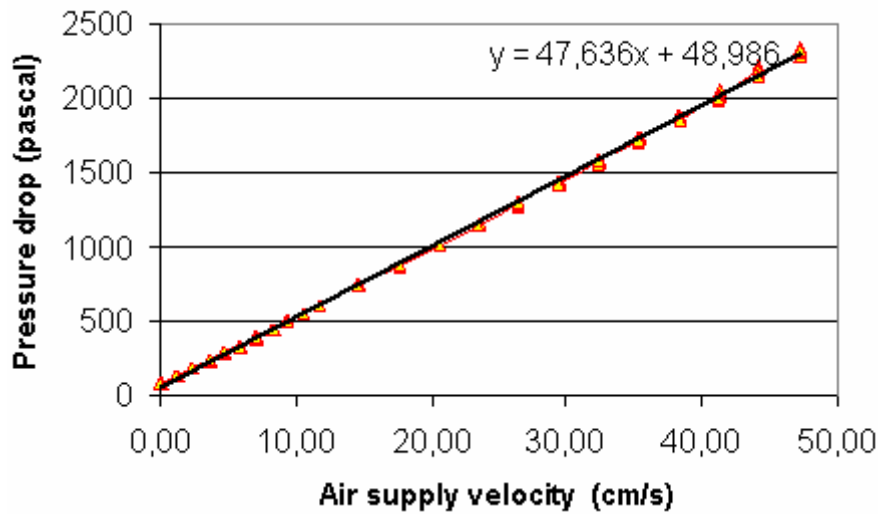


**Figure 3.6 Pressure drop through the distribution plate**

Mixing quality between biomass and sand in different conditions was determined by measuring mass fraction of each material at different height level of the bed column. The procedure for measuring the mass fraction includes following steps:

- Put sand and biomass in certain layers and amounts into the fluidization chamber.
- Supply air to fluidize the materials at a certain velocity for a certain time.
- Stop supplying air and allow the materials to form a fixed bed again.
- Uninstall and take out a part of the chamber containing materials. Then divide materials in the bed into sections throughout the height of the bed column as showing in figure 3.7 and figure 3.8.
- Separate biomass and sand in each section using sieving method
- The mass fraction of sand and biomass in each section could be used for analyzing the mixing quality.

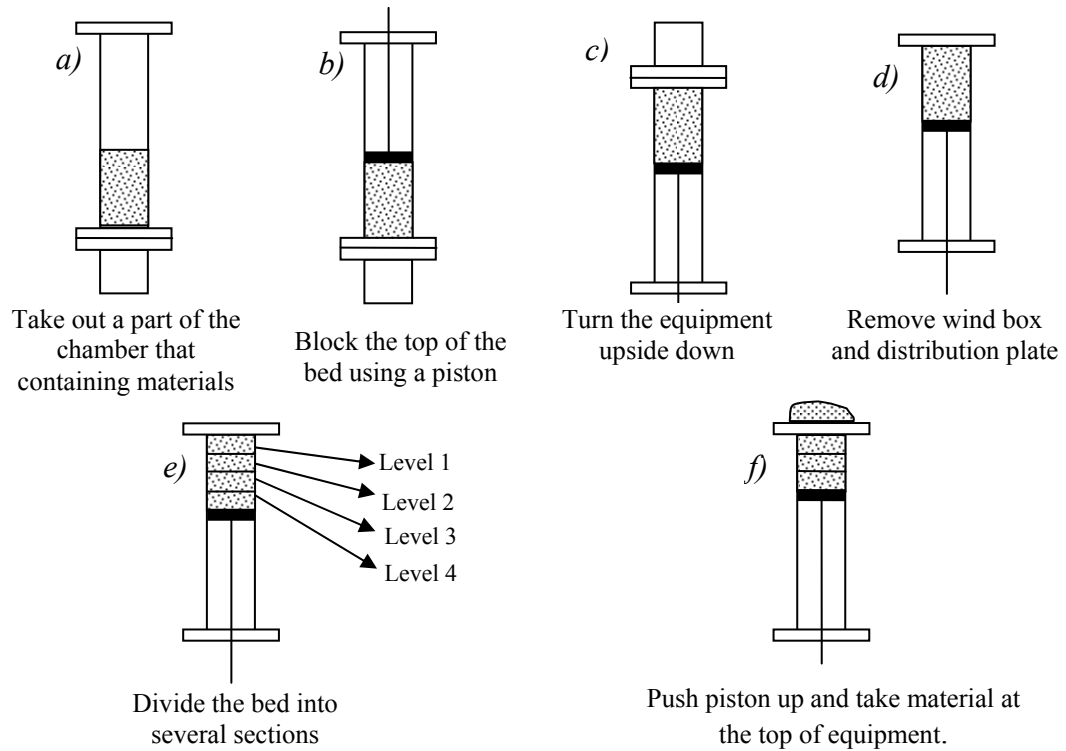


**Figure 3.7 Mass fraction dertermination along height of the bed column**



**Figure 3.8 Deviding binary mixture into sections along the height of the bed column**

### 3.3 Basic concept and definitions

#### 3.3.1 Minimum fluidization velocity

Minimum fluidization velocity is the minimum velocity of the gas supply that can make the drag forces balance the buoyed weight of the bed and the particles are suspended in the flow. By experimental determination, the minimum fluidization velocity is obtained from the intersection of the pressure curve for the fixed bed and for the fluidized bed as seen in figure 3.9.

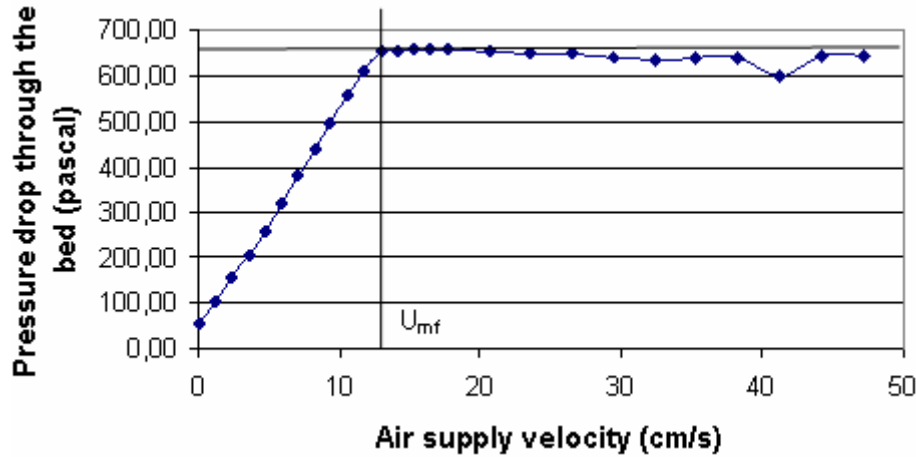


Figure 3.9 Determination of the minimum fluidization velocity

#### 3.3.2 Standard deviation (or mean amplitude) of pressure drop fluctuation

The standard deviation (or mean amplitude) of pressure drop fluctuation is defined as following

$$\sigma = \left[ \frac{1}{n-1} \sum_{i=1}^n (\Delta p(t_i) - \overline{\Delta p})^2 \right]^{1/2} \quad (\text{Equation 3-3})$$

Where

$\Delta p(t_i)$ : pressure drop through a bed materials at the time  $t_i$

$\overline{\Delta p}$ : Mean pressure drop measured at a certain superficial velocity.

$$\overline{\Delta p} = \frac{1}{n} \sum_{i=1}^n \Delta p(t_i) \quad (\text{Equation 3-4})$$

#### 3.3.3 “Real Volumes” of biomass in the mixture

“Real Volumes” are defined as those volumes which would correspond to real voidage in the mixture of the bed. Biomass alone has a volume which can be calculated from equation:

$$V_B = m_B / \rho_B \quad (\text{Equation 3-5})$$

In case of biomass and sand mixtures, sand particles fill the voids between biomass particles since biomass particles have a bigger size compared to sand particles. The “Real Volume” for the mixture of biomass and sand can be calculated:

$$V_{Br} = V - V_S \quad (\text{Equation 3-6})$$

$$V_S = m_s / \rho_s \quad (\text{Equation 3-7})$$

$$V_{Br} \leq V_B \rightarrow \rho_B \leq \rho_{Br} \quad (\text{Equation 3-8})$$

Experiments have been carried out with different mass fractions of biomass. The correlation of "real bulk density" of biomass ( $\rho_{Br}$ ) and sand/biomass ratio is shown in figure 3.10.

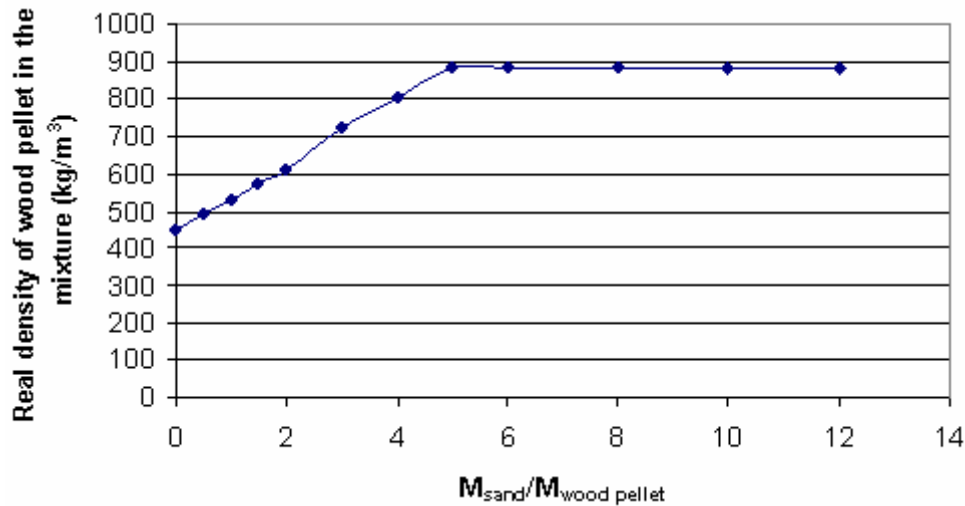


Figure 3.10 "Real bulk density" of biomass in the mixture

Many experiments have been done with different mixture of sand1, sand2 with rice husk and wood pellets. The equations used in table 2 could be used to calculate real density of rice husk and wood pellets in the mixture.

Table 3.2 Calculation of "real bulk density" ( $\rho_{Br}$ ) of biomass

	Rice husk	Wood pellets
Sand 1	$14,773Y + 122,21 \quad Y \leq 15$ $353,677 \quad \text{when } Y \geq 15$	$89,42Y + 442,54 \quad Y \leq 5$ $884,1941 \quad \text{when } Y \geq 5$
Sand 2	$8,0672Y + 127,91 \quad Y \leq 15$ $353,677 \quad \text{when } Y \geq 15$	$73,81Y + 463,74 \quad Y \leq 5$ $803,8128 \quad \text{when } Y \geq 5$

Y is the sand/biomass ratio defined as:

$$Y = \frac{M_{sand}}{M_{biomass}} \quad (\text{Equation 3-9})$$

### 3.3.4 Mixing Index

As already described in section 2.4.3.3, many definitions of a mixing index have been given by different authors to evaluate mixing quality along the height of the bed column. Among those definitions, *Chiba et al., 1980* defined MI as the ratio of the integral of mass fraction of jetsam particles in the top of the bed and the average mass fraction of jetsam. In this research work, due to the large difference in the density of biomass and sand, definition of MI based on mass fraction may be not suitable to

represent mixing quality. The calculation for MI in this research work is based on the volume fraction with the concept of "real volume" already explained in section 3.3.3. The description of MI definition is shown in figure 3.11

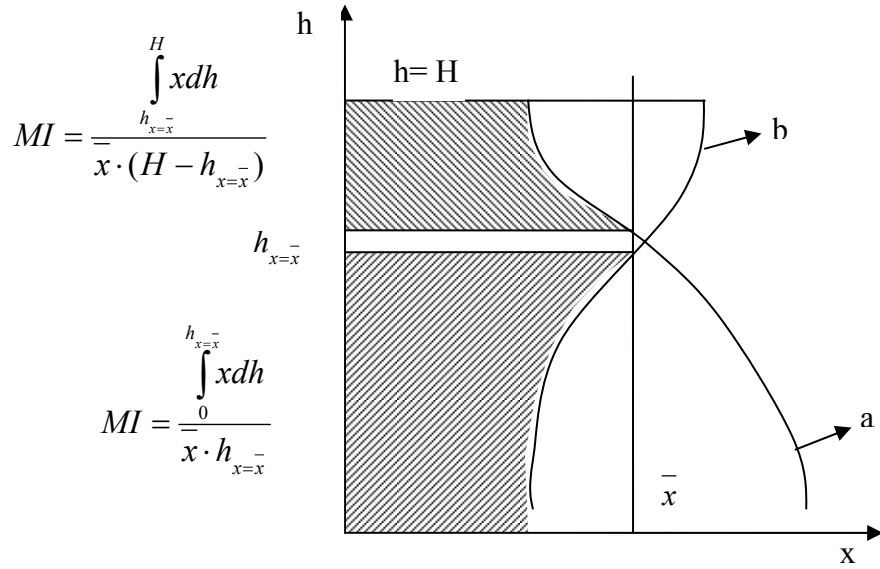


Figure 3.11 Mixing index calculation

In the normal case when the volume fraction of sand in the top of the bed is smaller than the mean value of volume fraction of sand in the whole bed (line a with  $x < \bar{x}$ ), then the MI can be calculated as following:

$$MI = \frac{\int_{h_{x=\bar{x}}}^H x dh}{\bar{x} \cdot (H - h_{x=\bar{x}})} \quad (\text{Equation 3-10})$$

In the special case (occured at some experiments where biomass was initially placed at the bottom of the bed) when the volume fraction of sand in the top after experiments is higher than the mean volume fraction of sand in the whole bed (line b with  $x > \bar{x}$ ) then the MI can be calculated as following:

$$MI = \frac{\int_0^{h_{x=\bar{x}}} x dh}{\bar{x} \cdot h_{x=\bar{x}}} \quad (\text{Equation 3-11})$$

In the equation 3-10 and 3-11

$$x = \frac{V_{sand}}{V_{sand} + V_{biomass}} \quad (\text{Equation 3.12})$$

H: total height of the bed after fluidization.

x: Volume fraction of sand in the mixture

h: height position of the experiment point.

### 3.4 Results and discussions

#### 3.4.1 Minimum fluidization velocity

Experiments have been carried out to understand fluidization behavior of rice husk and wood pellets only. By gradually increasing the air velocity through the rice husk bed and wood pellets bed, the behavior of biomass can be described as following:

- At low air supply velocity, biomass remains stable in the bed. This is a fixed bed.
- When the air velocity is increased, at about 15 cm/s with wood pellets and at about 20cm/s with rice husk, channeling appeared.
- At higher velocities, the channels are clearer and form a long and complicated track. When the bed column is high (>25cm), sometimes, the bed was separated into two parts with a gap in the middle.
- When the air velocity reaches 30cm/s with rice husk and 35cm/s with wood pellets, some particles in the top of the bed were blown upwards.
- In the case of a not very high bed column (< 15cm with rice husk and <10cm with wood pellets), a big hole appeared at high air velocities and reduced the pressure drop through the bed.

Figure 3.12 and 3.13 show the pressure drop through a bed of rice husk and wood pellets.

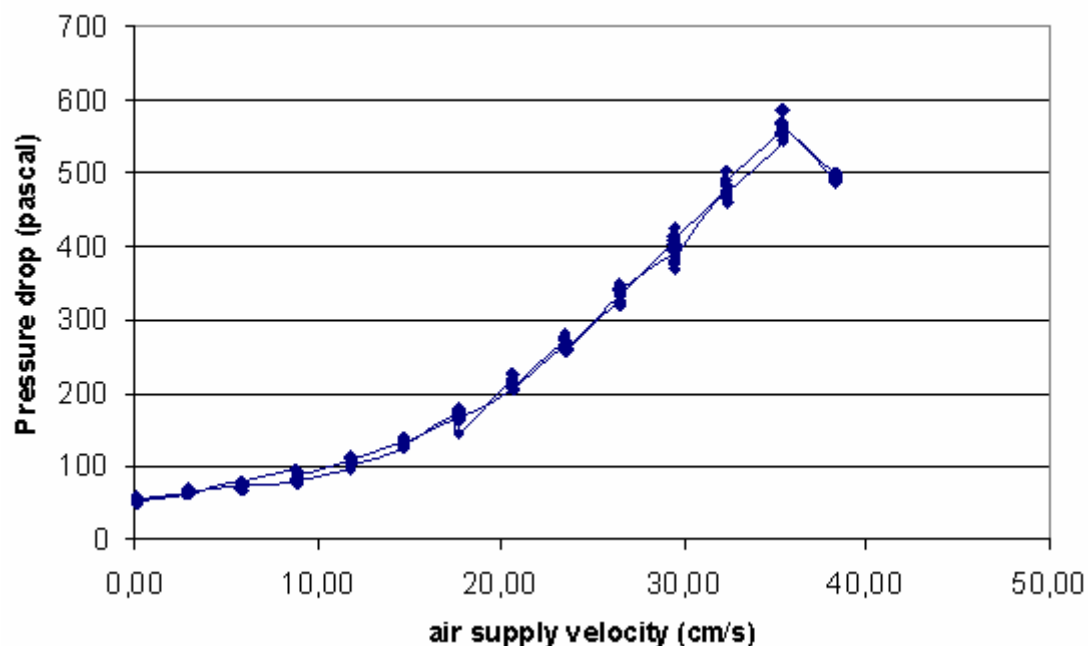
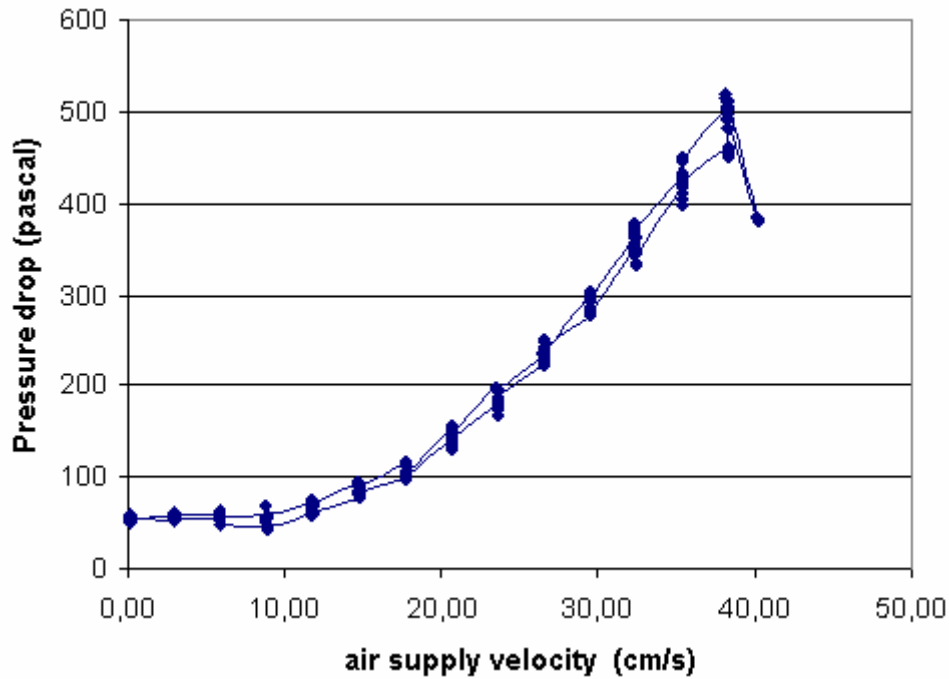


Figure 3.12 Pressure drop through 300g wood pellets



**Figure 3.13 Pressure drop through 100 g rice husk**

When using sand as fluidization material, the mixtures of sand-biomass could be fluidized easier depending on the percentage of biomass in the mixture. The fluidization behavior of the sand- biomass mixture can be described as following:

In case of initial segregation with biomass placed at the top of the bed, sand in the bottom of the bed starts to fluidize nearly the same way as with sand alone, only a little higher pressure drop occurs. However, when the mixing occurs ( $U > 23,55$  cm/s), fluidization behavior is affected. Figure 3.14 shows the pressure drop vs. air supply velocity for different mixtures.

In case of an initially mixed bed, biomass particles in the mixture can change the porosity of the bed; the fluidization behavior is quite different as shown in figure 3.14.

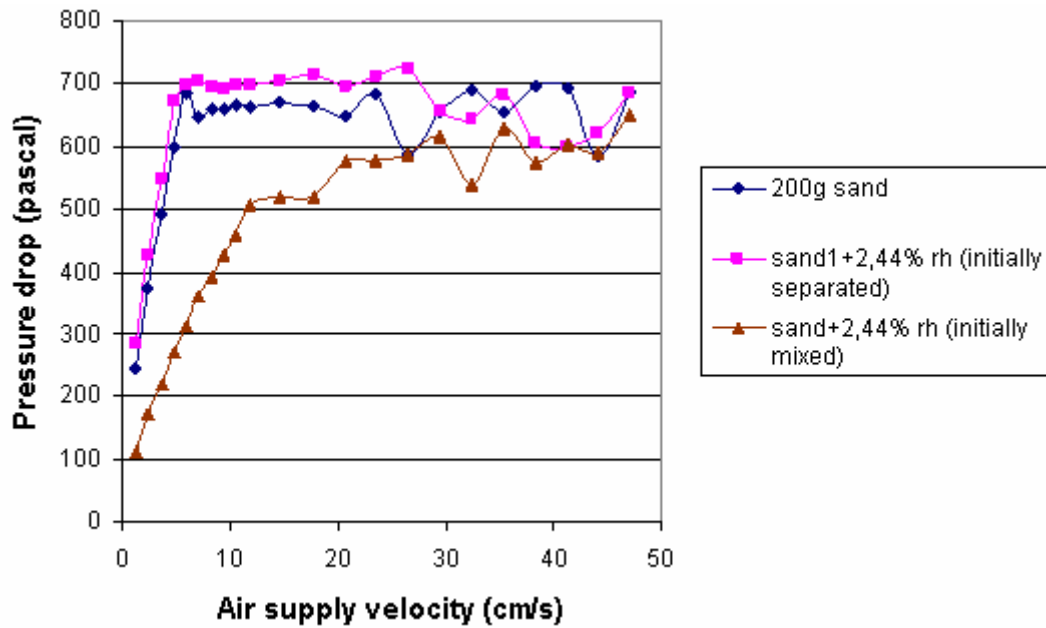


**Figure 3.14 Comparison of fluidization behavior of different way sand-rice husk mixture**

Various experiments have been carried out with initially mixed bed of sand-wood pellets and sand-rice husk. Following conditions were considered for understanding the fluidization behavior of the mixtures

- Mixing with different sand size
- Increasing and then decreasing air supply velocity
- Mixing with different mass of rice husk or wood pellets in the mixture

Figures 3.15-3.18 show the pressure drop vs. superficial velocity of those experiments. Observations are as following:

- The curve of pressure drop vs. superficial velocity shows no clear region of fixed bed and fluidized regime to identify minimum fluidization velocity accurately.
- $U_{mf}$  of the mixtures is depending on the  $U_{mf}$  of fluidization materials. The fluidization materials with higher  $U_{mf}$  result in higher  $U_{mf}$  of the mixture.
- $U_{mf}$  of the mixtures is always higher than  $U_{mf}$  of the fluidization materials only.
- Pressure drop through the bed of the mixture is different when increasing and decreasing air supply velocity. This difference is increasing when the percentage of biomass in the mixture is increased.
- Values for  $U_{mf}$  are smaller from experiments with increasing superficial velocity compared to experiment with decreasing superficial velocity.
- Due to its lower bulk density, rice husk influences strongly the fluidization behavior of the mixture. Small mass of rice husk can occupy a larger volume of the bed and so cause a serious change of the fluidization behavior.

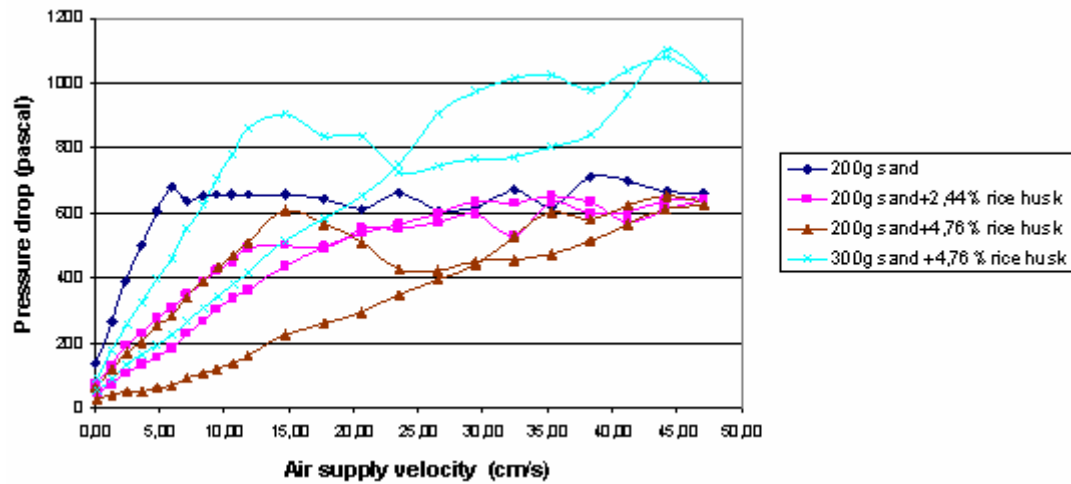


Figure 3.15 Pressure drop through a mixture of sand1 and rice husk

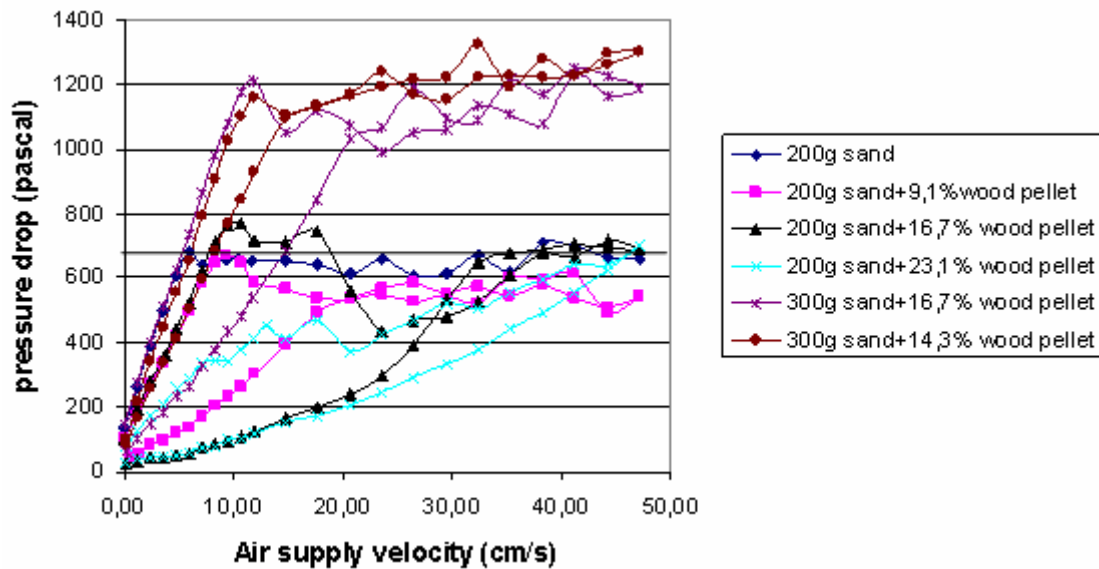


Figure 3.16 Pressure drop through a mixture of sand1 and wood pellets

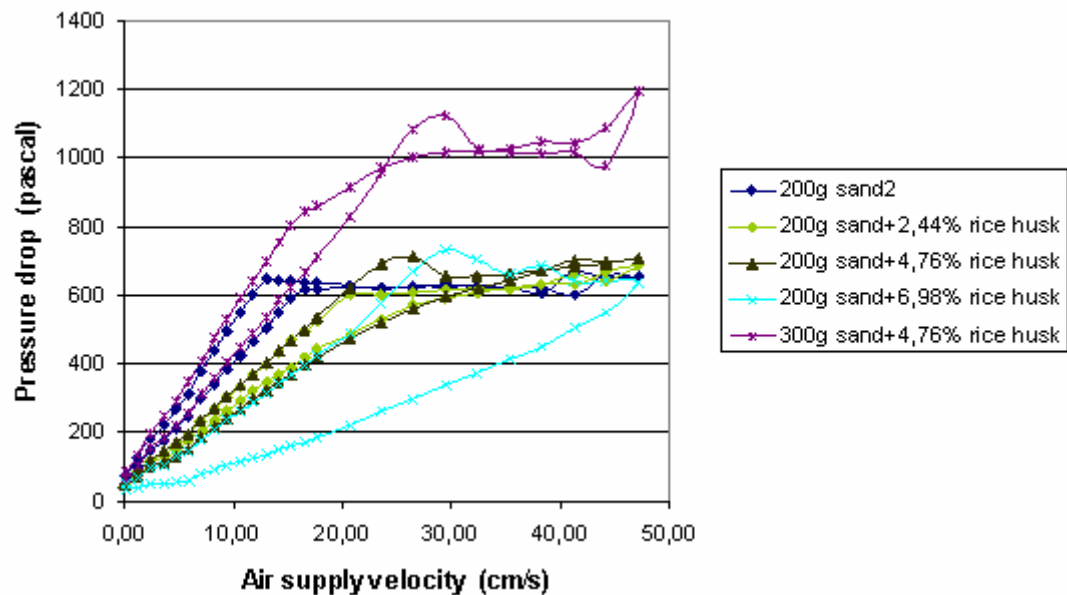


Figure 3.17 Pressure drop through a bed of sand 2 and rice husk

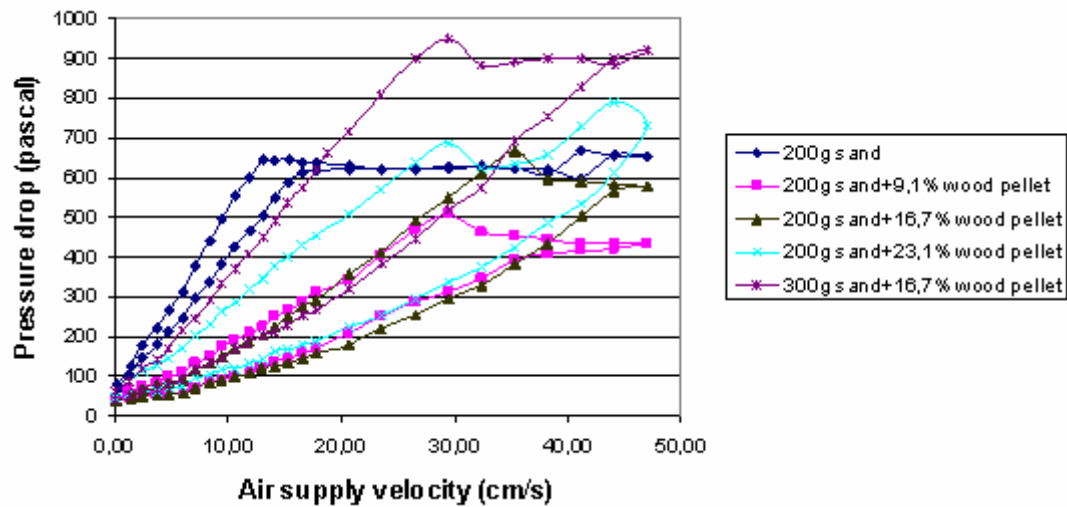


Figure 3.18 Pressure drop through a mixture of sand2 and wood pellets

### 3.4.2 Fluctuation of pressure drop through a fluidized bed

The pressure drop through the bed also fluctuated at high air supply velocity due to the bubble forming and releasing as explained in section 2.3.4. Figure 3.19 shows how the pressure drop through a bed of 200g sand1 fluctuated. The starting point of high pressure drop fluctuations is when air supply velocity reached 17,7 cm/s and it is continuously increased with increasing the superficial velocity. The limitation of the system equipment does not allow determining a point where deviation starts to decrease.

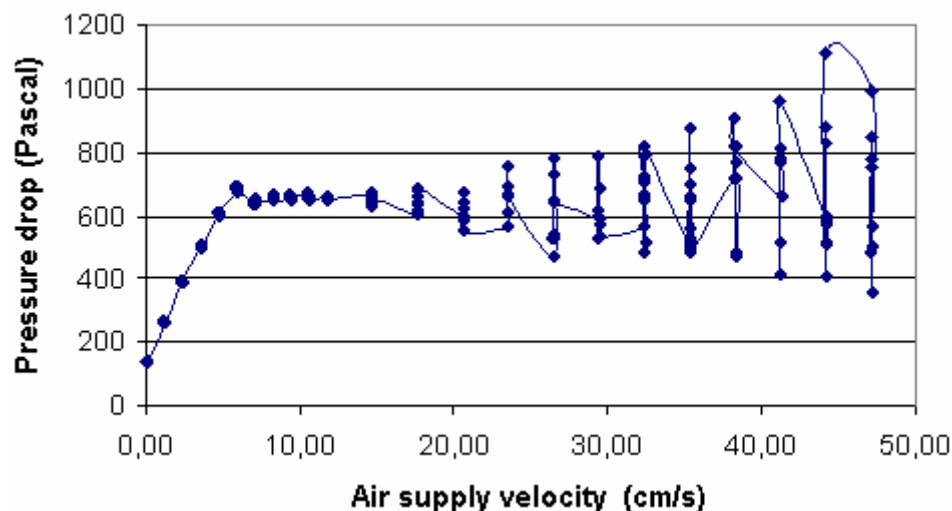


Figure 3.19 Pressure drop through 200 g sand 1

In the mixture of sand-rice husk the pressure drop is also fluctuating at high air velocity. Figures 3.20-3.23 show the standard deviation of pressure drop fluctuation at different conditions (determined using equation 3-3). Observations are as following

- When the bed stays as fixed bed, fluctuation of pressure drop is small and negligible. The standard deviation of pressure drop fluctuation is higher when bubbles appear and increasing when the air velocity is increasing.

- When biomass is added to the bed, the increasing of bed porosity can reduce the formation of bubbles. At the same air supply velocity,  $\sigma$  of the mixture is lower than  $\sigma$  of the sand bed only.
- When increasing and decreasing air supply velocity, the arrangements of biomass particles in the bed are different and lead to different fluctuations. The values of  $\sigma$  determined when increasing air velocity are higher compared to experiments with decreasing air velocity.
- With the same percentage of biomass in the mixture,  $\sigma$  of the bed was increasing with the increasing of sand in the bed.
- The results of calculated  $\sigma$  are related to the curve of pressure drop vs. air velocity to show the fluidization behavior of the mixture. It can give a simple way to evaluate the fluidization of the bed materials in the actual situation when the systems are not visible.

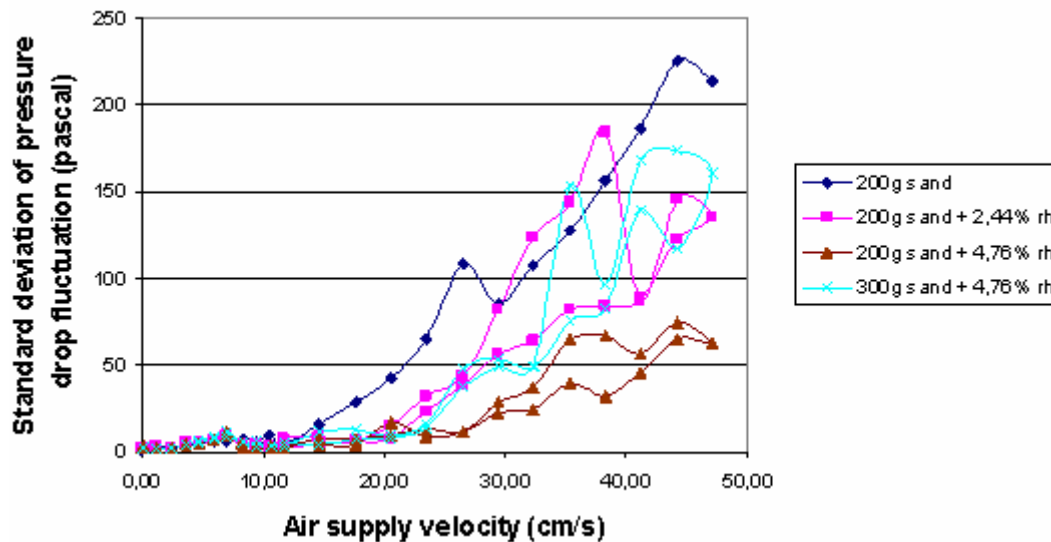


Figure 3.20 Standard deviation of pressure drop fluctuation through mixtures sand1-rice husk

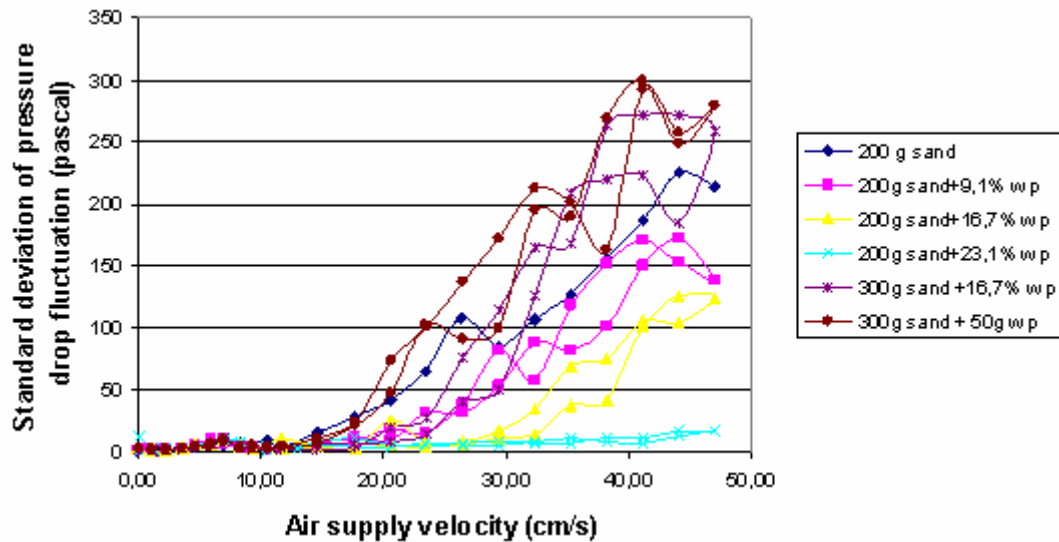


Figure 3.21 Standard deviation of pressure drop fluctuation through mixtures sand1-wood pellets

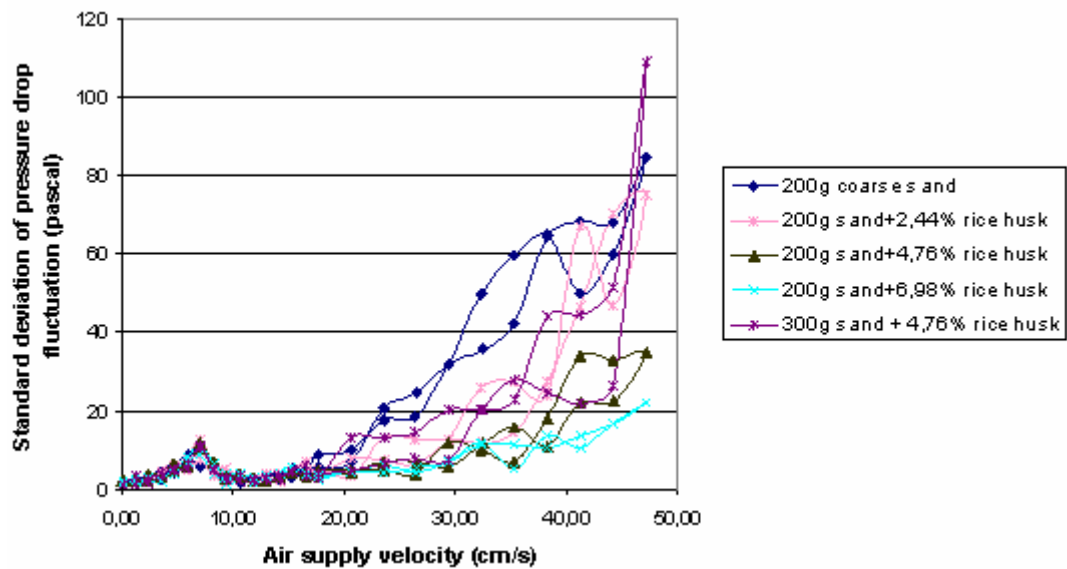


Figure 3.22 Standard deviation of pressure drop fluctuation through mixtures sand2-rice husk

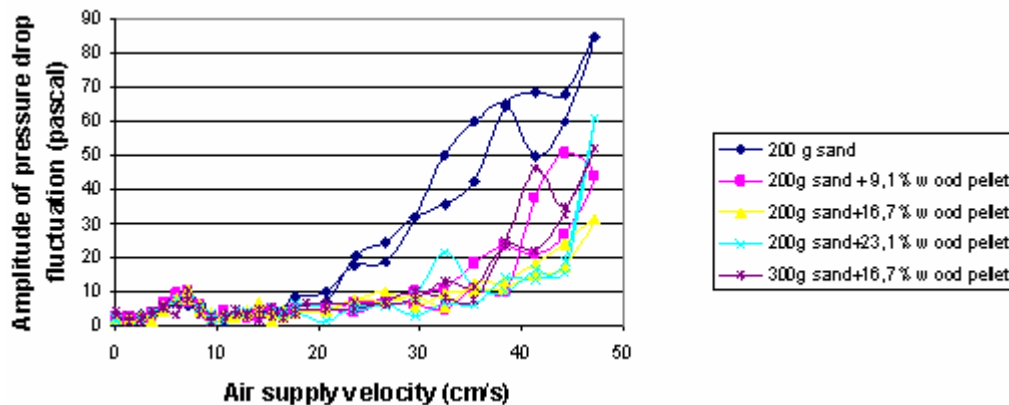


Figure 3.23 Standard deviation of pressure drop fluctuation through the bed materials of sand2-wood pellets

Further experiments have been carried out with continuous feeding biomass into the fluidized bed of sand1 at  $U = 23,5\text{cm/s}$ . The result is shown in figure 3.24. The figure presents the slight increasing of pressure drop through the bed while the amplitude of fluctuations is decreasing.

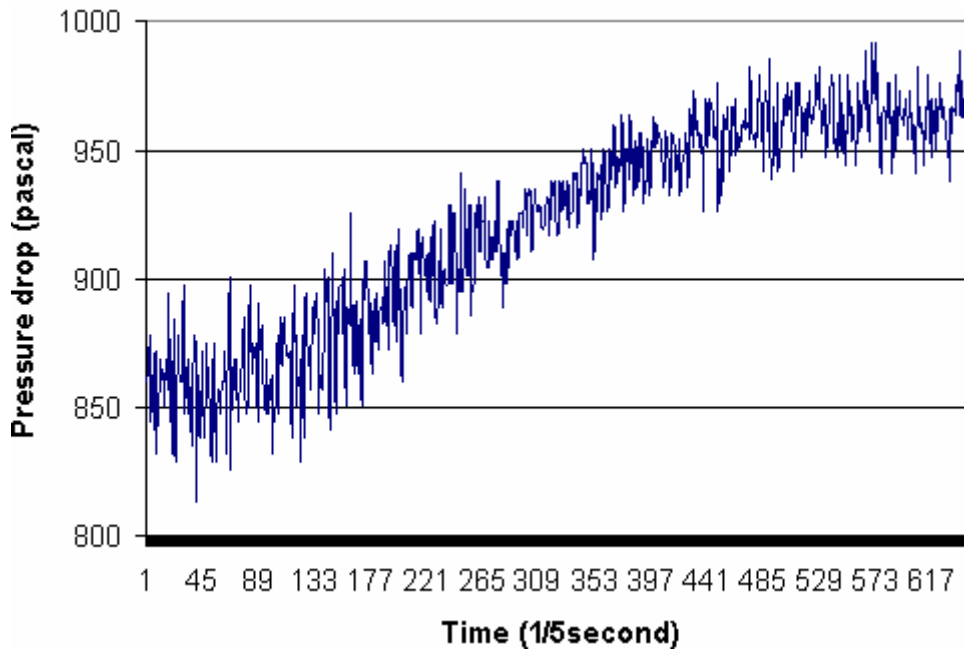


Figure 3.24 Pressure drop through a bed of 200g sand1 when continuous feeding 30g wood pellets to the bed in 2 minute with  $U=23,5\text{cm/s}$  ( $3,3 U_{mf}$ )

### 3.4.3 Mixing quality

In binary systems by size and density, mixing is only achieved under specific hydrodynamic conditions. Experiments have been performed with binary mixtures of sand1 and rice husk or wood pellets to understand mixing mechanism and examine the mixing quality in different conditions as following:

- Biomass is initially placed at the bottom of the bed
- Biomass is initially placed at the top of the bed
- Continuous feeding of biomass to the fluidized bed of sand1
- Changing percentage of biomass in the mixture, air supply velocity, fluidization time.

#### 3.4.3.1 Biomass initially in the bottom of the bed

According to *Nienow et al., 1978*, mixing is caused solely by bubbles. Each bubble gathers a wake of material from near the bottom of the bed and draws the material upwards to the surface although with some spillage en route. Each bubble also draws a spout of material below itself upwards as a result of the pseudo-streamlined flow of particles around the rising bubble. However, biomasses such as rice husk and wood pellets have a strong cohesive nature due to some particular particles characteristic as described in section 3.2. In the bed column, particles agglomerate easily to become a block. A block of rice husk or wood pellets settled in the bottom of the bed has a high porosity and acts similar as a distribution plate. The air goes through the biomass layer and fluidizes the fluidization materials (sand) above. With increasing air

velocity, sand placed on the top begins to fluidize and bubble in the usual way. Bubbles in the fluidized bed of sand above are not possible to draw the biomass particles upwards. The agglomeration of biomass in the block is increasing with the height of the biomass block in the bed column. When the air supply velocity is increased until it can break the block of biomass, then mixing occurs rapidly and biomass becomes flotsam in the mixture, Sand and biomass are then quickly mixed even in good quality. Figure 3.25 shows the volume fraction of sand in the mixture of sand and rice husk; table 3.3 shows the result MI calculated based on the concept as shown in the sections 3.4.3 and 3.4.4.

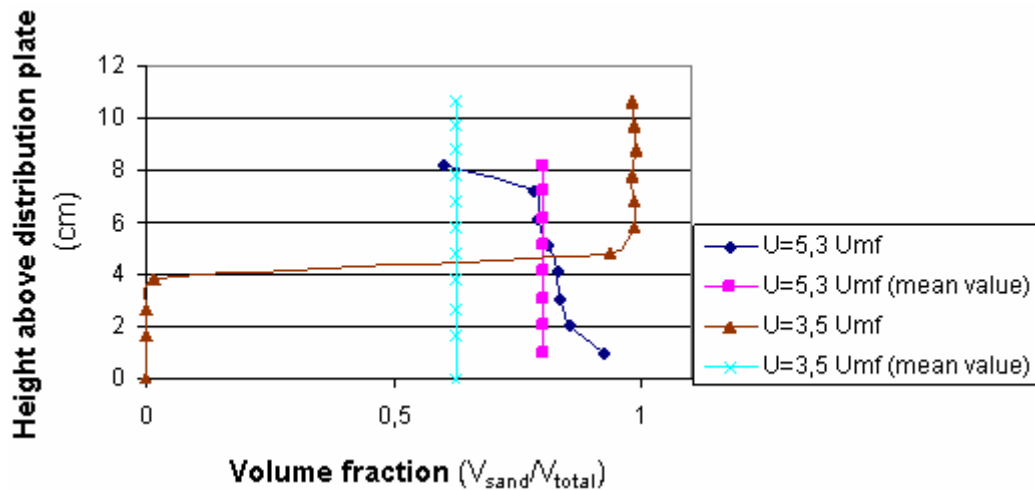


Figure 3.25 Volume fraction of sand in the mixture of 300g sand+6,98% rice husk when rice husk is initially placed at the bottom

Table 3.3 MI of sand-rice husk mixture when rice husk is initially placed at the bottom

Situation	MI
300g sand+6,98% rice husk (15g); rice husk at the bottom; U=38cm/s	0,9
300g sand+6,98% rice husk (15g); rice husk at the bottom; U=24,76 cm/s	0,15

#### 3.4.3.2 Biomass initially placed at the top of the bed

When rice husk or wood pellets particles are placed at the top of the bed, they are also easily agglomerated to become a block. At the air velocity just above minimum fluidization of sand, bubbles appear with small size and less quantity. This does not lead to a mixing process. When increasing air supply velocity, quantity and size of the bubbles are increasing. Bubbles when going to the top of the sand bed can create a chaotic area in the border of sand bed and biomass bed. In the chaotic area, sand particles penetrate into biomass bed and separate biomass particles from the block of biomass. Separated biomass particles are easy moving downward or upward following the movement of sand particles around. The chaotic area expands and the mixing quality is increasing with the time. Many experiments with the mixture of sand+rice husk and sand+wood pellets have been carried out and MIs have been calculated for various conditions as following:

- Changing the fluidization time while air supply velocity and percentage of biomass are kept in constant as shown in figure 3.26; 3.27; 3.34; 3.35; 3.36; 3.37
- Changing the air supply velocity while fluidization time and percentage of biomass in the mixture are kept constant as shown in figure 3.28; 3.29; 3.32; 3.33.
- Changing the mass of biomass in the mixture while keeping fluidization time and air supply velocity at a constant value as shown in figure 3.30; 3.31.

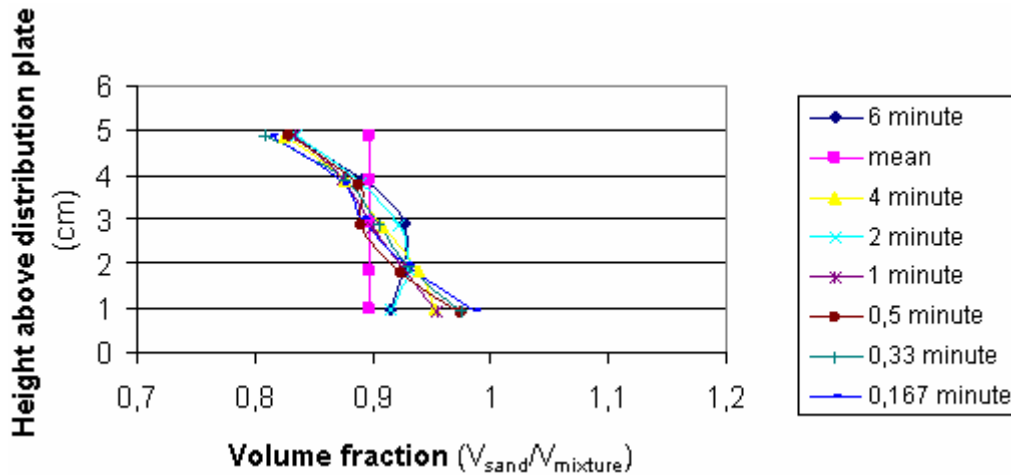


Figure 3.26 Volume fraction of sand in the mixture of sand and rice husk (200g sand+2,44% rice husk;  $U = 3 U_{mf}$ )

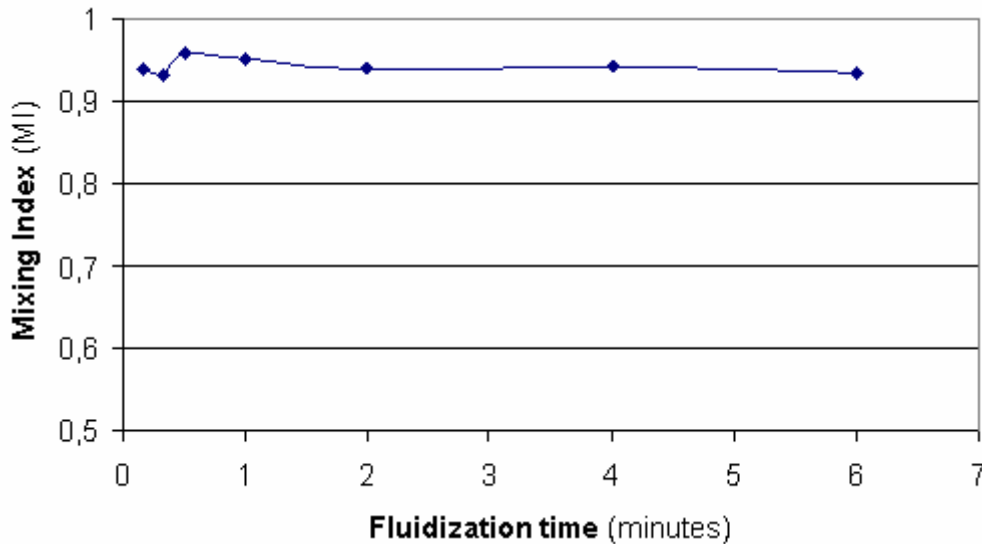


Figure 3.27 MI of mixture 200g sand+2,44% rice husk ( $U = 3 U_{mf}$ )

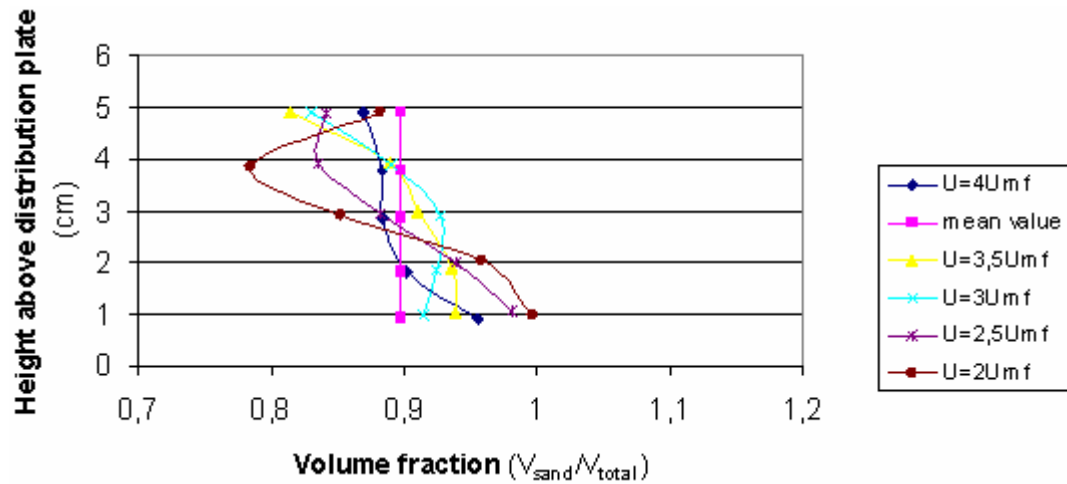


Figure 3.28 Volume fraction of sand in the mixture 200g sand+2,44% rice husk when changing air supply velocity (fluidization time 6 minutes)

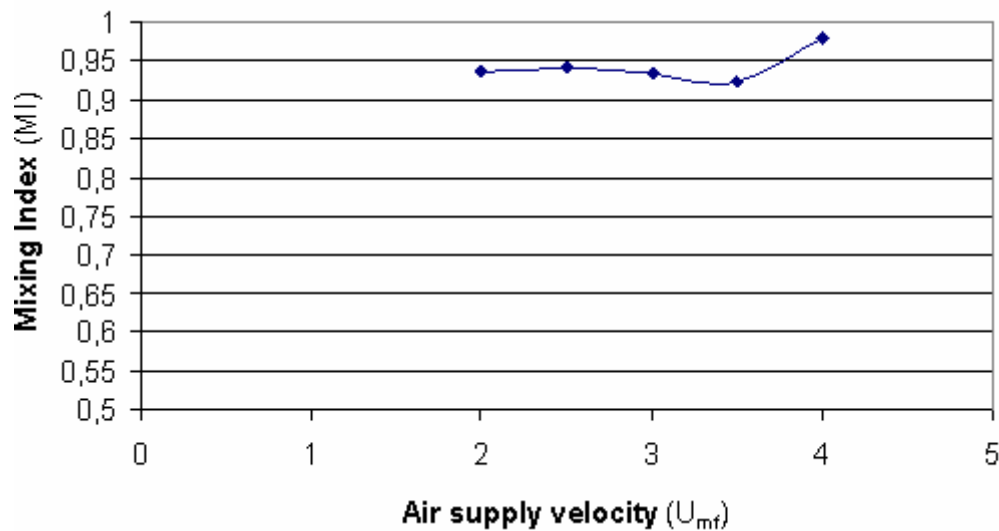


Figure 3.29 MI of mixture 200g sand+2,44% rice husk when changing air supply velocity (fluidization time 6 minutes)

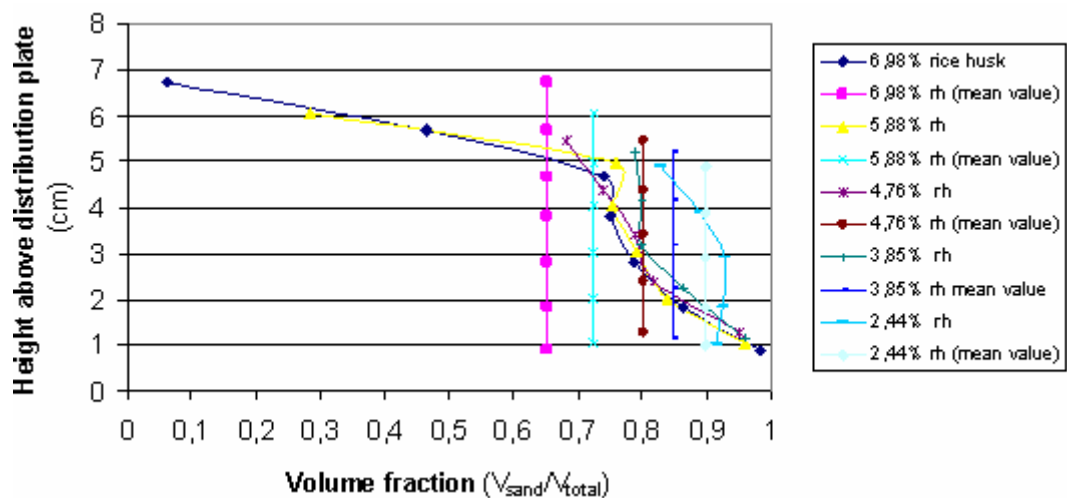


Figure 3.30 Volume fraction of sand in the mixture of 200g sand and rice husk with the variation of percentage of rice husk in the mixture ( $U=3U_{mf}$ ; fluidization time = 6 minutes)

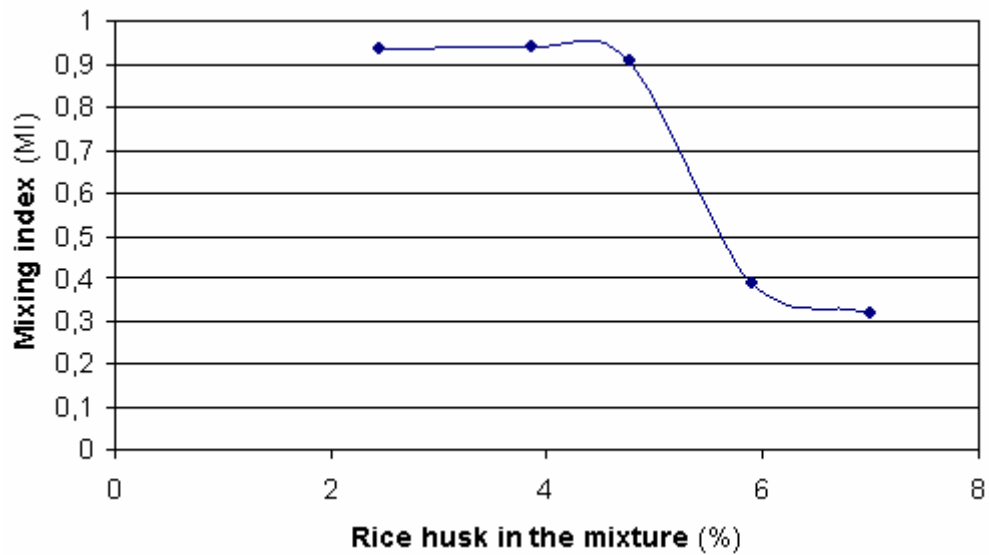


Figure 3.31 MI in the case of variation of rice husk amount in the mixture

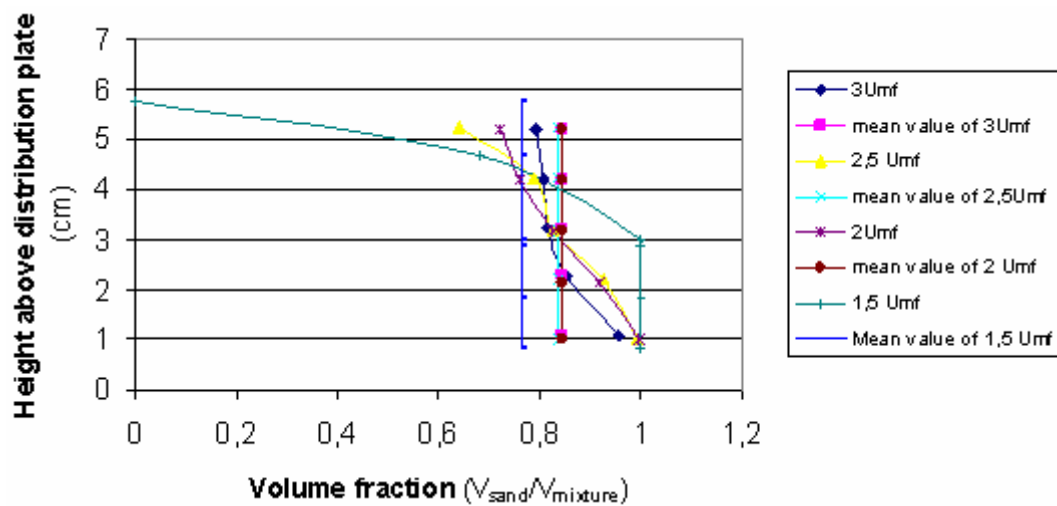


Figure 3.32 Volume fraction of mixture sand-wood pellets when changing air supply velocity (200g sand+ 9,1% wood pellets and fluidization time: 1minute)

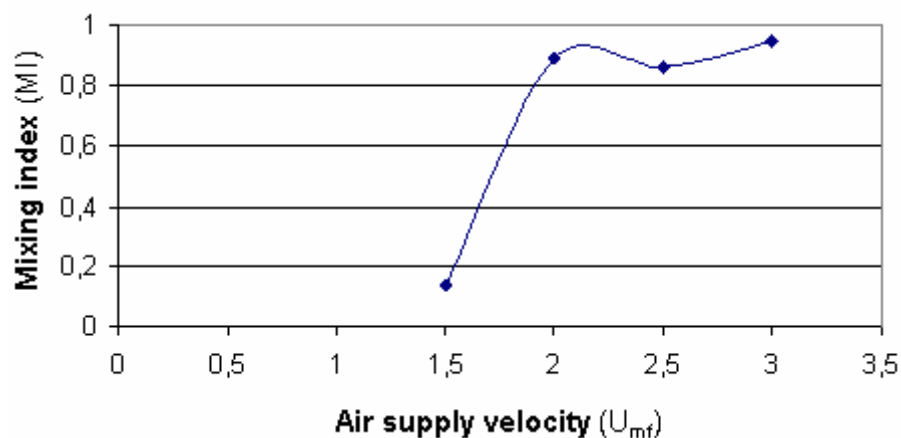


Figure 3.33 MI calculated for the mixture sand1-wood pellets in case of changing air supply velocity (200g sand, 9,1% wood pellets and fluidized for 1minute)

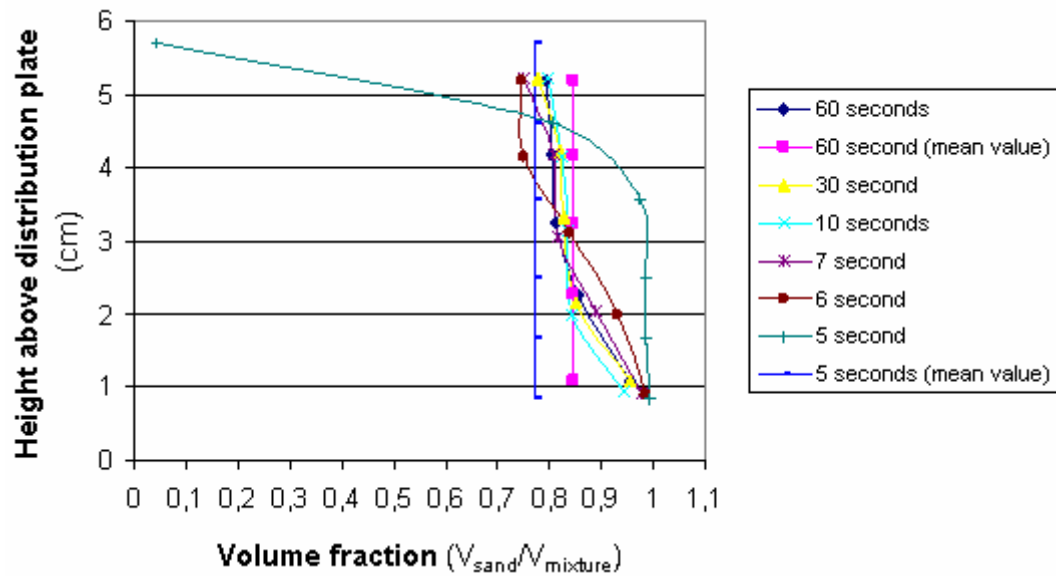


Figure 3.34 Volume fraction of sand in the mixture 200g sand1+9,1% wood pellets when changing fluidization time ( $U=3U_{mf}$ )

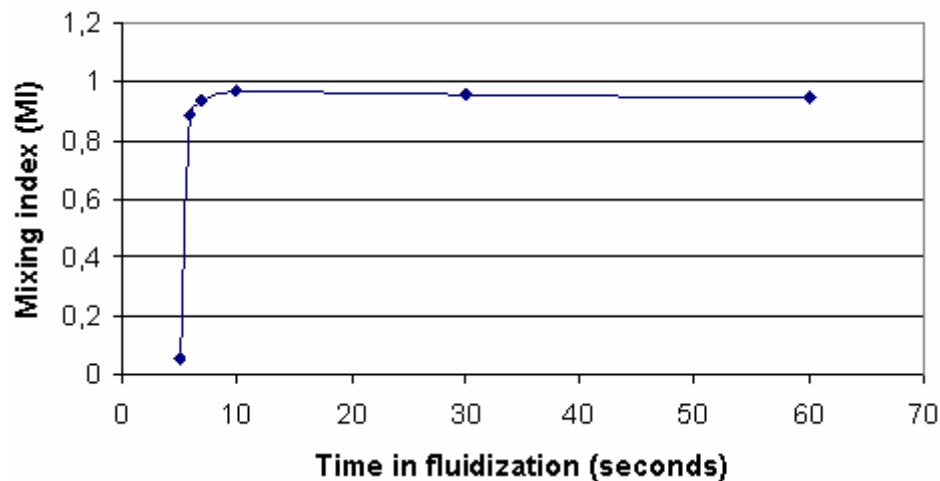


Figure 3.35 MI calculated for the mixture 200g sand1+9,1% wood pellets when changing fluidization time. ( $U=3U_{mf}$ )

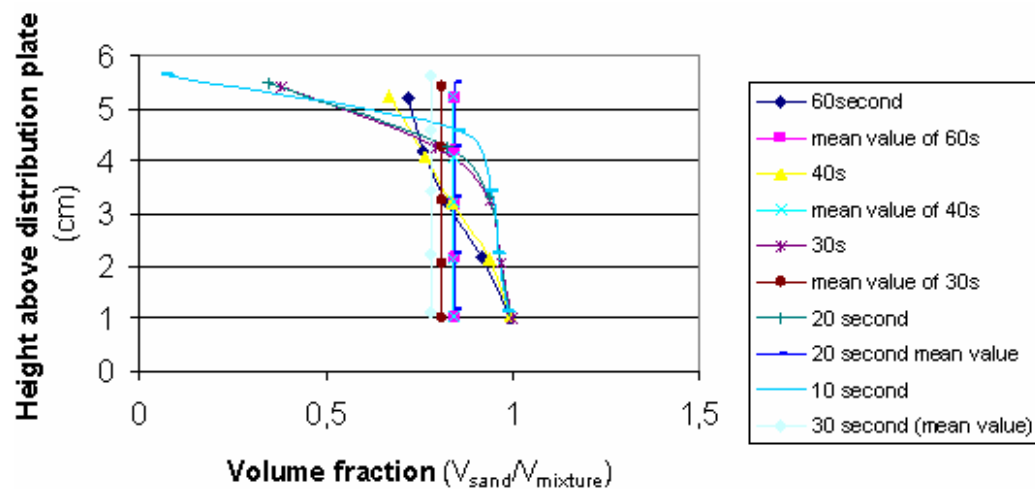
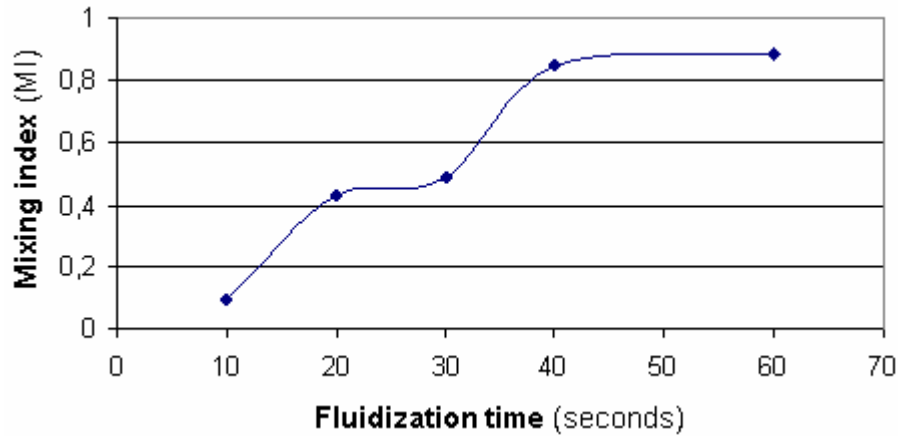


Figure 3.36 Volume fraction of sand in the mixture 200g sand1+ 9,1% wood pellets when changing fluidization time ( $U=2 U_{mf}$ )



**Figure 3.37 MI calculated for the mixture 200g sand1 + 9,1% wood pellets when changing fluidization time ( $U=2 U_{mf}$ )**

The observations are as following:

- Due to the low density of rice husk, even a relatively small amount of rice husk can affect the mixing quality of the mixture. Only 6.98% by mass of rice husk (15g) in the bed of 200g sand lead to a very poor mixing even fluidized at high velocity and quite long fluidization time (figure 3.30 and 3.31) while 9,1% by mass wood pellets (20g) give an essential mixing at the same conditions (figure 3.34 and 3.35).
- Very small amount rice husk (2,44% by mass) in the mixture of 200g sand could be easy mixed well (figure 3.26; 3.27; 3.34; 3.35). But we could not find a correlation to describe this mixing behavior.
- The potential to form agglomerates of wood pellets is very strong. With 25g wood pellets in the mixture of 200g sand, the mixing does not occur when the whole wood pellets layer was blown upwards and separated from the sand which stays at the bottom of the bed.
- The increasing of biomass in the mixture resulted in poorer mixing. When the percentage of biomass reached a certain value (figure 3.30 and 3.31), no further decrease of the mixing quality could be observed.
- The quality of mixing when changing air supply velocity also sudden when the biomass amount is small (figure 3.28; 3.29; 3.32; 3,33)
- For the mixture of 200g sand with 9,1% of wood pellets, at an air velocity of about  $2U_{mf}$  we can observe a transient region between nearly no mixing when the velocity is lower and very quickly and well mixing when the velocity is significantly higher than  $2U_{mf}$ . For this transient region we can observe some dependency of the mixing index on the fluidization time (see figure 3.36 and 3.37). If the air velocity is increased to values of more than  $3U_{mf}$ , mixing occurs more or less immediately.

#### **3.4.3.3 Continuous feeding of biomass from the top of the bed**

Due to the agglomeration characteristics of biomass, the mixing occurs hardly when biomass and sand initially are placed at separated layers in the bed. In case of continuous feeding biomass to the fluidized bed of sand, small rate of biomass are easy to mix with the sand bed. Experiments have been performed by continuously

feeding 30 g wood pellets to the fluidized bed of 200g sand for 3 minutes. Experiments were carried out at different air supply velocities. Results are shown in figures 3.38 and 3.39. Observations are as following:

With 30g wood pellets and 200g sand, the mixing can not occur in case of initially separated layer even at quite high air velocities ( $U=5U_{mf}$ ). However, in case of continuous feeding, the mixing occurs even with quite low air velocities ( $U=1,5U_{mf}$ )

Higher air supply velocity results in a better mixing quality. However, the mixing quality is not stable and can vary at each experiment. Experiments at the same conditions of air velocity and fluidization time give different results.

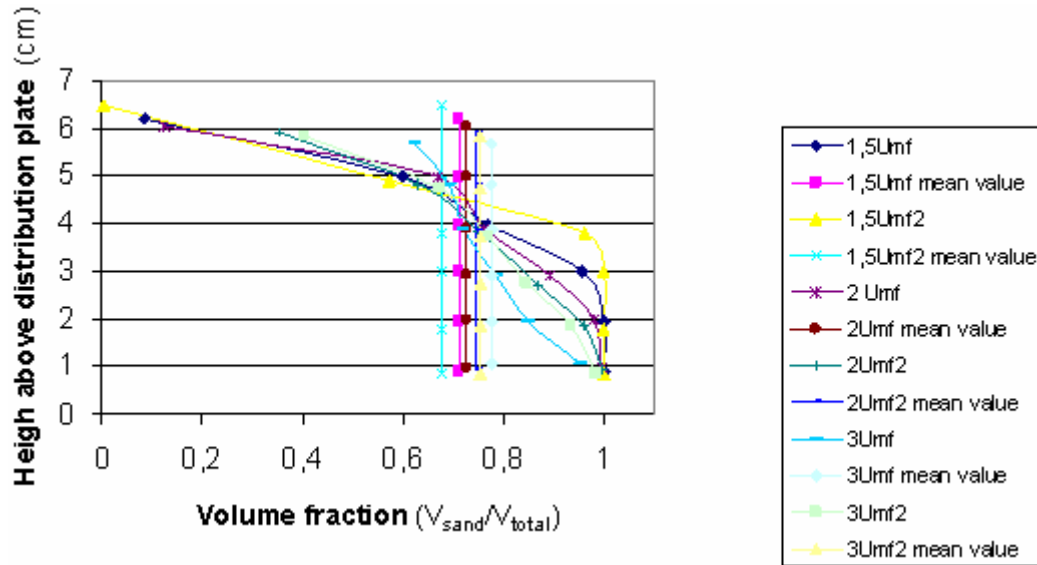


Figure 3.38 Volume fraction at different air supply velocity for continuous feeding of 30g wood pellets into the bed of 200g sand1 for 3 minutes.

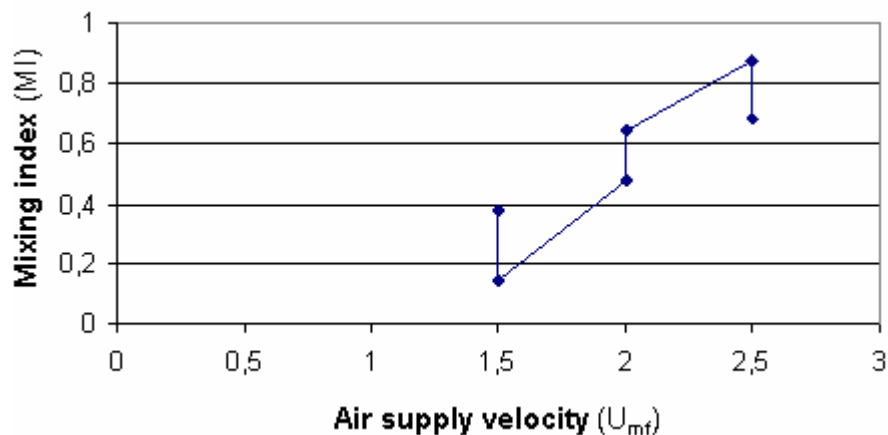


Figure 3.39 MI calculated for the mixture of sand1-wood pellets for continuous feeding of 30g wood pellets into the bed of 200g sand for 3 minutes

### 3.5 Conclusion

The fluidization behavior of mixtures of biomass and sand can be described as complex. Research on minimum fluidization velocity, fluctuation of pressure drop and mixing at different conditions has taken place by carrying out many experiments.

Determining the exact value of minimum fluidization velocity using the curve of pressure drop vs. air supply velocity is not really possible because of the complex behavior of the pressure fluctuations. The differences of the curve when increasing and decreasing the air supply velocity are quite big. The reason for this phenomenon is that the biomass in the mixture can change the porosity of the bed when it is mixed with the sand. Depending on the location of biomass particles in the bed, it can be easy or more difficult to create channels in the bed that can affect the fluidization behavior. The distribution of biomass particles when gradually decreasing air velocity from a high value is more uniform compared to when increasing the air velocity, which leads to a higher porosity resulting in a lower pressure drop.

Fluctuations of pressure drop occur when bubbles appear in the bed. The standard deviation of pressure drop is decreasing by adding biomass into the bed. The percentage of biomass in the mixture also affects negatively the fluctuations of pressure drop. Understanding the relation between pressure drop fluctuations and fluidization behavior at different conditions will help to control the fluidized bed system in industrial applications.

Mixing of biomass (rice husk and wood pellets) and sand in a fluidized bed can not be performed at a high quality when biomass and sand initially are separated in two layers in the bed, especially when the biomass is placed at the bottom of the bed, due to the agglomeration characteristics of rice husk and wood pellets particles. The mixing quality is much higher when biomass was fed continuously in to the fluidized bed of sand. Many experiments have been carried out to understand mechanisms of mixing at different conditions. Parameters such as air supply velocity, fluidization time, and percentage of biomass in the mixture were taken into account. In general, higher air velocity, longer fluidization time, and less percentage of biomass in the mixture result in a better mixing. However, experiments showed that the gap between very good mixing and very poor mixing when changing conditions is very small. Mixing quality can vary quite a lot even for experiments at the same conditions (figure 3.38 and 3.39). Thus a prediction of the mixing quality based on conditions such as biomass percentage in the mixture, air velocity and fluidization time is not easy possible.

## 4 GASIFICATION TECHNOLOGY AND PRINCIPLE

### 4.1 Gasification today

The basic principles of gasification have been known since the late 18th century. Commercial applications were first recorded in 1830. By 1850, large parts of London had gas lights, and an established industry had grown up using heat gasifier to make producer gas, mainly from coal and biomass fuels, to supply the lights. During World War II, biomass gasifiers appeared in force in Europe, Asia, Latin America, and Australia. Because of the general scarcity of petroleum fuels, many charcoal or wood fueled gasifier-powered vehicles helped to keep transport systems running. However, after the war, the availability of petroleum fuels supply was leading to the disappearance of those gasifier systems due to their inconvenient and unreliable operation. During the energy crises in 1973 and 1980, a renewed interest in biomass gasification to substitute for petroleum products appeared. From 1990, the problem of global environment leads to the trend of using renewable energy for power generation and biomass gasification also has a great development. Figure 4.1 illustrates the worldwide historical growth in gasification capacity since 1970. Gasification technologies are capable of processing any carbon based feed stock e.g. biomass to produce synthesis gas for the production of heat, electricity, steam, hydrogen, transportation fuels and chemicals.

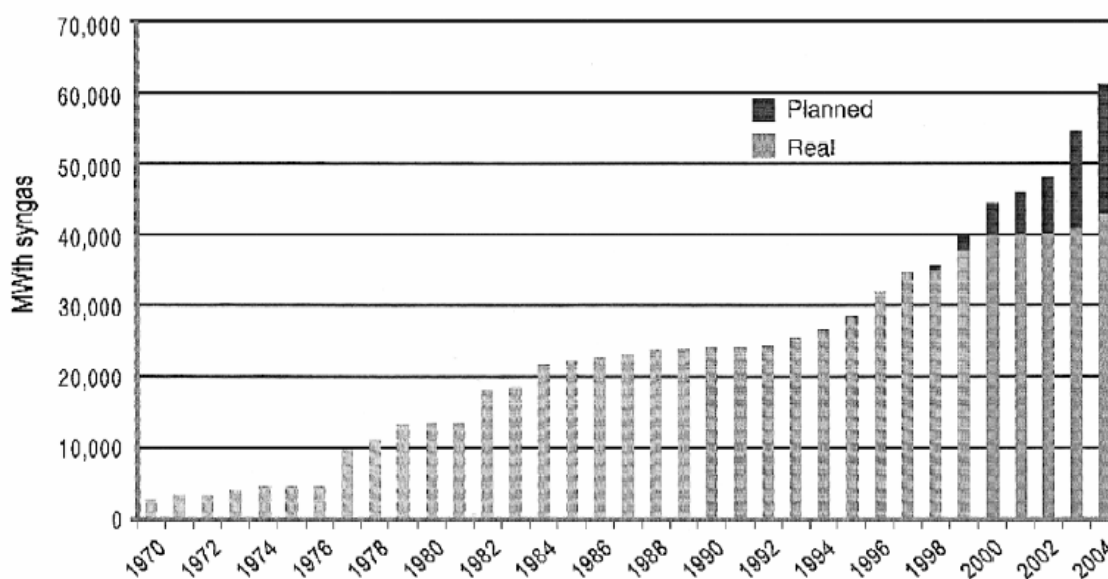


Figure 4.1 Cumulative worldwide gasification capacities (Stiegel and Maxwell, 2001)

### 4.2 Gasification process

Thermochemical gasification is the conversion by partial oxidation at elevated temperature of a carbonaceous feed stock such as biomass or coal into a gaseous energy carrier. Product of the process is a combustible gas containing carbon monoxide, carbon dioxide, hydrogen, methane, and trace amounts of higher hydrocarbons such as ethane, ethene. Depending on the particular process and the fuel characteristic, the concentration of each component could be varied and other components could be existent in the producer gas such as nitrogen, hydrogen sulphide, ammonia, char particles, ash, and tars. The partial oxidation is carried out

using air, oxygen, steam or a mixture of these gases. Figure 4.2 shows the conversion paths for the formation of the different gasification products from biomass with the indication of the relevant processes in C-O-H diagram.

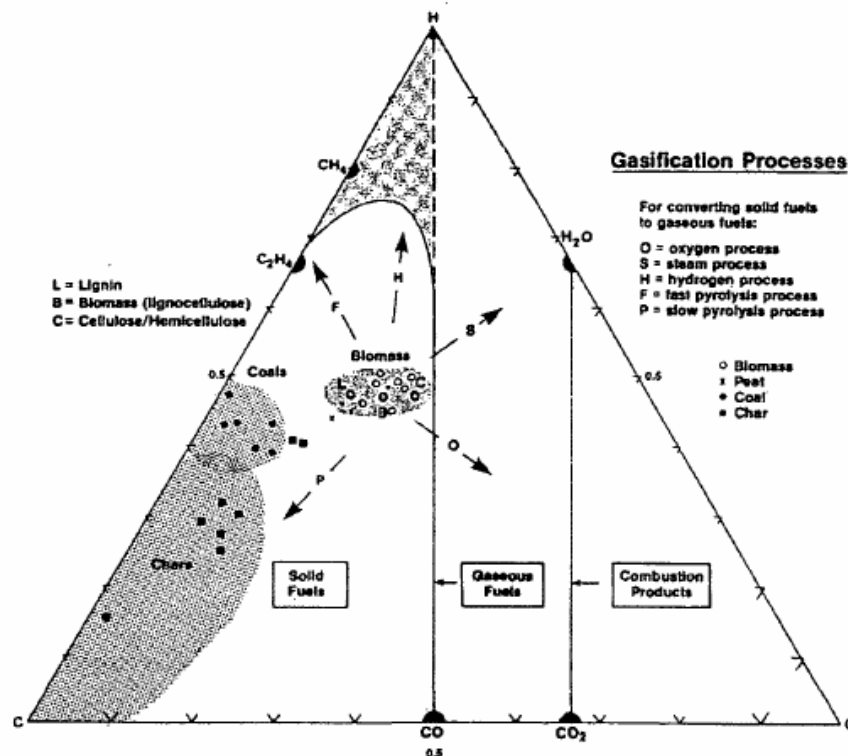
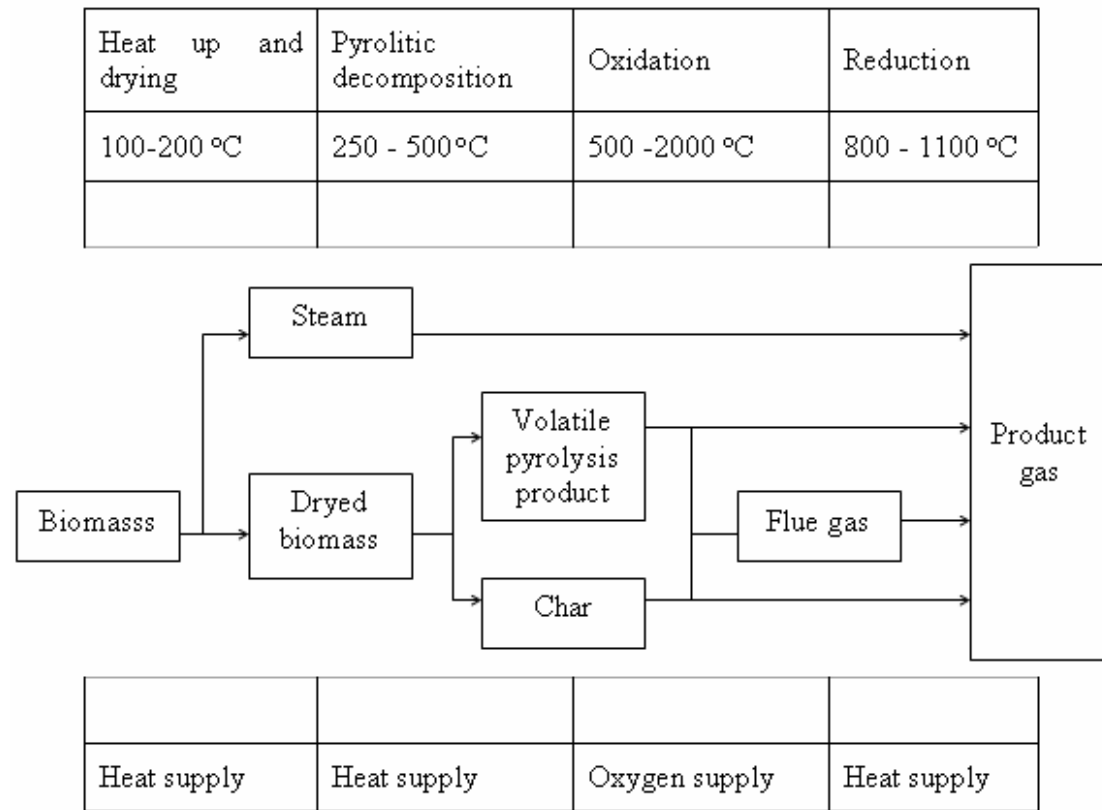


Figure 4.2 C-O-H diagram of gasification processes (Bolhar-Nordenkamp, 2004)

If oxygen is used as gasification agent the conversion path points in the oxygen corner. This path leads to a lowering of the hydrogen content and an increase on the carbon based compounds such as CO and CO<sub>2</sub>. If steam is used instead the path is pointing into the formation of water, which causes an increase of hydrogen in the produced compounds.

In general, gasification occurs in sequential steps as show in figure 4.3, which can be found in most gasification reactors:

- Drying: The drying process leads to the evaporation of moisture out of the pores of the fuel particle.
- Pyrolysis: During pyrolysis a gas, tars and a solid char residue is produced by thermal degradation
- Oxidation: Oxidation or partial oxidation of the solid char, pyrolysis tars and pyrolysis gases takes place where free oxygen is present.
- Reduction: Reduction is the formation of the producer gas, by a reduction of the combustion compounds on fixed carbon.



**Figure 4.3 Sequential steps of biomass gasification** (Bolhar-Nordenkamp, 2004)

Once the biomass enters the reactor it is first heated up and dried, releasing its water content as steam. Temperature of this period is 100 - 200 °C. When the dried biomass is heated further in the absence of an oxidizing agent, pyrolysis process occurs to release volatile matter from dried biomass. Products of this process are solid char and volatile pyrolysis products such as condensable hydrocarbons, tar, and gases. The relative yields of gas, liquid and char depend mostly on the rate of heating and the final temperature.

The products of the pyrolysis process then react with oxidizing agent at over 500 °C to produce permanent gases such as CO, CO<sub>2</sub>, H<sub>2</sub> and lesser quantities of hydrocarbon gases. Part of char is combusted in this stage by the following reactions:



These reactions are highly exothermic and provide the necessary heat for the reduction process. The oxidation is followed by a reduction, where char gasification takes place. During reduction an interactive combination of several gas-solid and gas-gas reactions take place. Solid carbon is oxidized to carbon monoxide and carbon dioxide and hydrogen is generated through the water-gas shift reaction. The gas-solid reactions of char oxidation are the slowest and limit the overall rate of the gasification process. Many of the reactions are catalyzed by the alkali metal compounds present in wood ash, but still do not reach equilibrium.

Endothermic reactions include:

- Boudouard-reaction



- Heterogeneous water gas reaction



These reactions cause a volume increase and are strongly temperature dependent. At higher temperatures and decreasing pressures they shift to an increase of the CO compound. During the reduction of CO<sub>2</sub> and water also the homogeneous water-gas reaction takes place, which shifts at higher temperatures to the CO and H<sub>2</sub>O-side



Another important reaction is the formation of methane, which is reduced at higher temperatures and increased by higher pressures.



In summary it can be seen that the gas composition is influenced by many factors such as feed composition, water content, reaction temperature and pressure, and the extent of oxidation of the pyrolysis products. Figure 4.4 shows the example of the variation of gasification reaction constants with the change of gasification temperature.

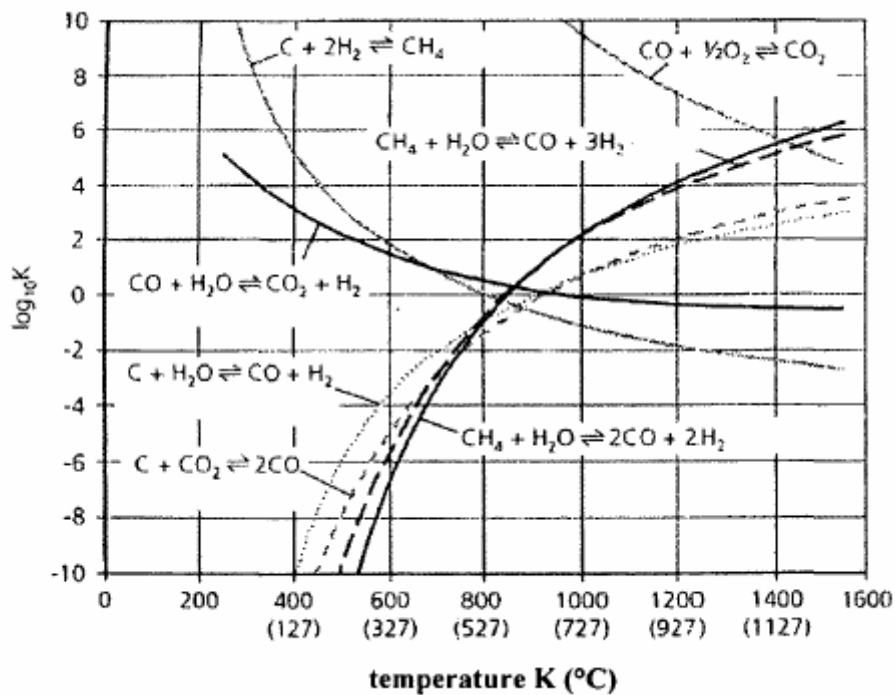


**Figure 4.4 Influence of the gasification temperature on the reaction constants (Bolhar-Nordenkamp, 2004)**

Due to the physical or geometrical limitations of the reactor and the chemical limitations of the reactions involved, some liquid products are pyrolyzed not completely and give rise to contaminant tars in the final producer gas. Owing to the higher temperatures involved in gasification compared with pyrolysis, these tars tend to be refractory, i.e. not reactive, and are difficult to remove by thermal, catalytic or physical processes.

### **4.3 Types of gasifier**

For more than a century of development, many types of gasifiers have been developed and manufactured. However, generally, gasifiers can be classified as following:

According to the gasification agent:

- Air-blown gasifier: Air is used to run the gasification process. With 79% of nitrogen in the air, the producer gas of this gasifier will contain much nitrogen and have a heating value of about 4- 6 MJ/Nm<sup>3</sup>
- Oxygen-blown gasifier: Oxygen is used as gasification agent for the gasification process. Due to N<sub>2</sub> is not present in the gasification process, these gasifiers could produce a higher quality producer gas with the a heating value of about 12- 15 MJ/Nm<sup>3</sup>
- Steam-blown gasifier: In this gasifier, heat for the gasification process has to be supplied from outside or by a combustion zone in a separated part of the gasifier. The gasification agent steam can increase the hydrogen content in the producer gas. Heating value of the producer gas of this gasifier could be 12-15 MJ/Nm<sup>3</sup>.

According to the heat supply for gasification:

- Autothermal or direct gasifiers: Heat is provided by partial combustion of biomass directly in the gasification chamber.
- Allothermal or indirect gasifiers: Heat is supplied from an external source through a heat exchanger or indirect process, i.e. separation of gasification and combustion zone.

According to the pressure in the gasifier:

- Atmospheric: The gasification process occurs under atmospheric pressure.
- Pressurized: The gasification process occurs at the higher pressure than atmospheric.

According to the design of the reactor

- Fixed bed
- Fluidized bed
- Entrained flow
- Twin bed

More detailed description of reactor designs will be given in the following section.

#### **4.3.1 Fixed bed gasifier**

Fixed bed gasifiers are gasifiers where the fuel stays in a fixed bed in the reactor. In a fixed bed gasifier, the fuel only moves downward slowly by its gravity depending on the reaction rate when the gasification consumes fuel below. Depending on the way of introducing the gasification agent into the reactor, fixed bed gasifiers can be classified as following:

- Updraft gasifier

- Downdraft gasifier
- Downdraft gasifier with open-core
- Multi-stage gasifier
- Crossdraft gasifier

### 4.3.1.1 Updraft gasifier

The updraft gasifier is the simplest type of a gasifier. The fuel is fed at the top of the reactor and moves downwards as a result of the conversion of the fuel and the removal of ashes. Figure 4.5 shows a schematic diagram of an updraft gasifier.

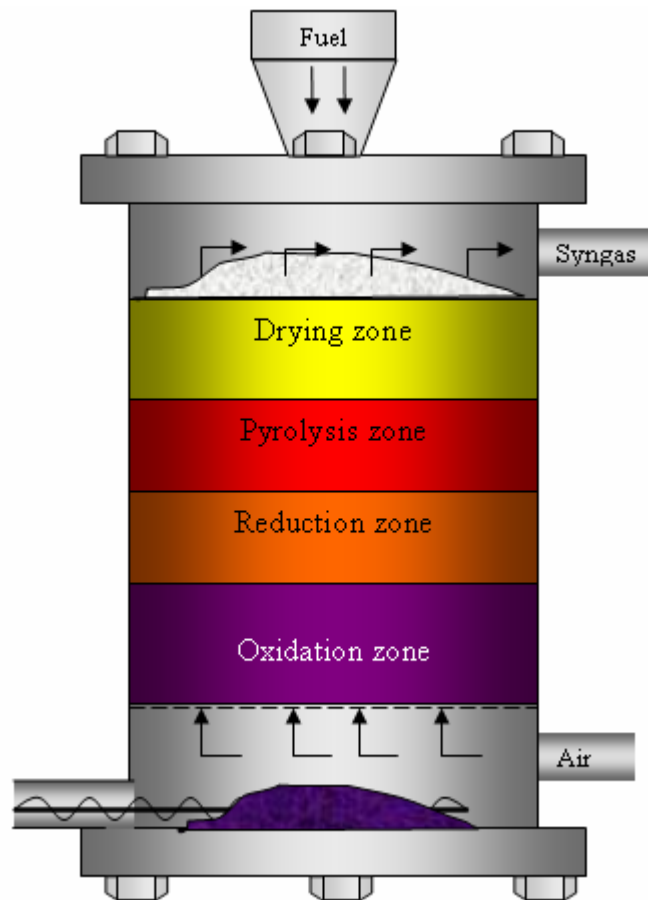


**Figure 4.5 Updraft gasifier**

The air intake is at the bottom, and then flows counter-currently to the movement of fuels and the producer gas leaves at the top of the fuel bed. The fuel at the bottom of the bed is combusted to generate the heat at high temperatures and create an oxidation zone there. The heat from the oxidation zone together with some excess air and the combustion gases from combustion zone gets in contact with the fuel above and Boudouard-reactions occur in this part of the bed. In that way, the reduction zone is above the oxidation zone. The residual heat from the reduction zone then is used for pyrolysis of the fuel above and finally for drying of the fuel in the top of the bed. The sequence of zones in the bed of fuel from the bottom to the top will be the oxidation zone, reduction zone, pyrolysis zone and the drying zone.

The major advantages of this gasifier are its simplicity, high burn out of ashes, low producer gas temperatures and high gasification efficiencies. When the fuel is going

downward from the drying zone to the oxidation zone, a good internal heat transfer is observed. Therefore fuel with high moisture contents can be used. Furthermore this gasifier can even process relatively small sized fuel particles and accepts also some size variation in the fuel feed stock.

Major drawbacks are the high amounts of tar and pyrolysis products because the pyrolysis gas is not heated up to temperatures where most of the tars would be destroyed. This is of minor importance if the gas is used for direct heat applications, in which the tars are simply burnt. In case the gas is used for power production, extensive gas cleaning is required.

### ***4.3.1.2 Downdraft gasifier***

Downdraft or co-current gasifiers are gasifiers where the air is introduced at or above the oxidation zone of the bed. Similar to the updraft gasifier, the fuel is fed at the top and moves downward with the time as the gasification process proceeds. The gas supplied moves in the same direction as the fuel and the producer gas leaves at the bottom of the bed.

Figure 4.6 shows a schematic diagram of a downdraft gasifier. The reduction zone in this gasifier is located at the bottom of the bed and consists of char at high temperature. This design will help to reduce the tar content in the producer gas and this is a main advantage of downdraft gasifier. Downdraft gasifiers produce the lowest level of tar and are therefore the best option for engine applications. However, scaling-up of this type of gasifier is limited. At low load levels, the temperature is decreasing and more tars are produced because the tar cracking becomes less efficient at low temperatures. Advantageous of low load levels is the lower entrainment of particles in the producer gas. At high load levels, the tar cracking capability is higher which results in lower tar levels. However, more particles are entrained with the gas. At too high load levels, the residence time for tar cracking become too short which will increase the tar content again, along with the particles in the producer gas.

Drawbacks for the downdraft gasifier are the high amounts of ash and dust particles in the producer gas due to the fact that the gas has to pass the oxidation zone where small ash particles are entrained. This leads also to a relative high temperature of the exiting gases resulting in lower gasification efficiencies. Downdraft gasifiers demand relatively strict requirements for the fuel like a moisture content less than 25% (on a wet basis) and an uniform size to realize regular flow, no blocking in the throat, enough "open space" for the pyrolysis gases to flow downwards and to allow heat transport from the hearth zone upwards.

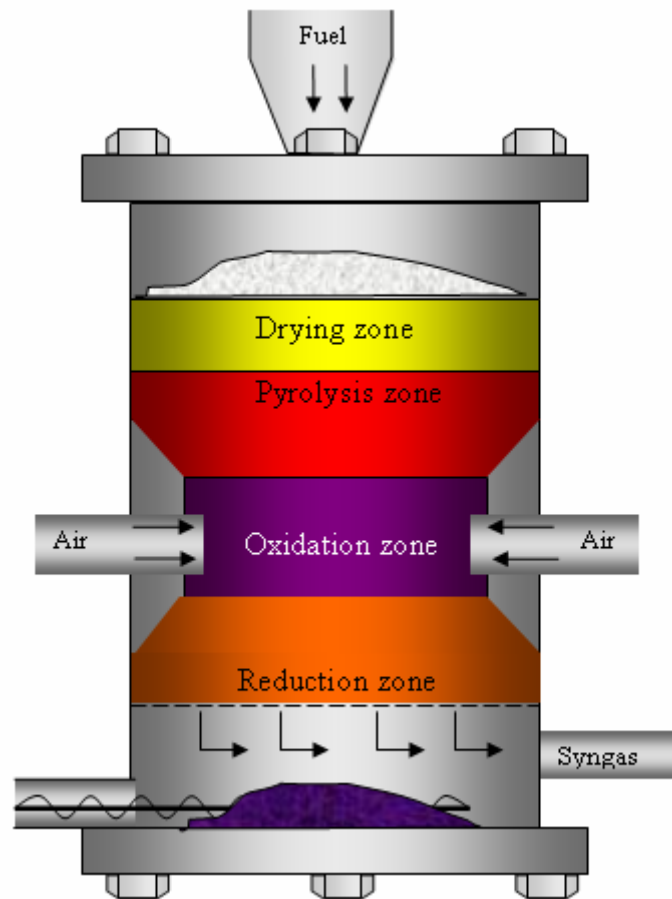


Figure 4.6 Downdraft gasifier

#### 4.3.1.3 Downdraft gasifiers: Open-core

Opencore gasifiers are especially designed to gasify fine materials with low bulk density. Because of the low bulk density of the fuel no throat can be applied in order to avoid bridging of the fuel which causes hampering or even stopping of the fuel flow. Special devices, like rotating grates, may be included to stir the fuel and to remove the ash. Particularly the rice husk gasifiers require continuous ash removal systems because of the high ash content resulting in large volumes of ash. The bottom of the gasifier is set in a basin of water by which the ash is removed.

#### 4.3.1.4 Multi-stage gasifiers

In fixed bed gasifiers, different zones can be distinguished whereas the sequence depends on the flow direction of the gasification fuel and agent. The zones are not physically fixed and move up- or downwards dependent on operating conditions; they and be also to some extent overlapping. In order to optimize each zone, several designs were developed where the combustion (oxidation zone), gasification (reduction zone) and/or pyrolysis zone are physically separated in different vessels. The basic idea is to further decrease the tar production by combustion of the pyrolysis gases since combusting a gas-gas mixture is more effective than gas-solid.

### 4.3.1.5 Crossdraft gasifiers

Crossdraft gasifiers are originally designed for the use of charcoal. Charcoal gasification results in very high temperatures ( $>1500^{\circ}\text{C}$ ) which can lead to material problems. Figure 4.7 shows a schematic diagram of a crossdraft gasifier.

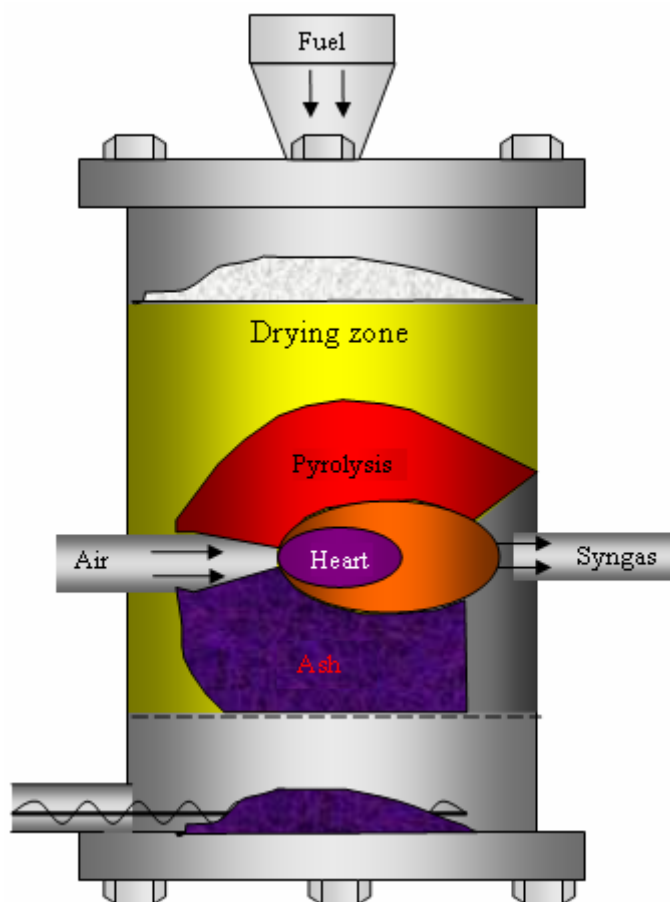


**Figure 4.7 Cross-draft gasifier**

In crossdraft gasifiers, the air is supplied into the centre of the bed of fuel and creates a hearth zone with very high temperatures in the centre with surrounding zones e.g. reduction zone, pyrolysis zone, drying zone, and the ash. These are insulation layers to protect the materials of the gasifier. The gas leaves at the side of gasifier from the reduction zone which is quite close to the hearth at high temperatures, however, the residence time for tar cracking is relatively short that can lead to tar problems in the producer gas.

Advantages of the system lie in the very small scale at which it can be operated. Installations below 10kW (shaft power) can be economically feasible under certain conditions. The reason is the very simple gas cleaning train (only a cyclone and hot filter) which can be employed when using this type of gasifier in conjunction with small engines.

A drawback is the minimal tar converting capability resulting in the need of high quality charcoals.

### 4.3.1.6 Technical and operational problems with fixed bed gasifiers

#### *Tar production*

In the fixed bed gasifiers, the problem of tar content always exists. Various different designs have been developed to reduce the tar content in the producer gas and it is not possible to create a tar free gasifier. Very low tar content can be reached with multistage gasifiers. The tar in the producer gas can condense and create problems for the gas engine. Excessive tar production may be caused by inappropriate fuel properties like morphology, size distribution and moisture content and also inappropriate flow behavior of the char. During periods of unsteady state operation or too low part load operation also excessive tars may be produced. The design of a gasifier should be appropriate to the fuel properties. Operators should be instructed to operate the plant as much as possible at steady state conditions. Operating gasifiers at part load result often in unsatisfactory performance.

### *Explosions*

Explosions may occur in case of leakage of combustible gases through the fuel feeding system, the ash discharge system or any other leakage point. When the gasifier is shut down, combustible gases will remain in the equipment. If the gasifier is ignited again without venting the equipment, the combustible gases inside gasifier could be exploded during the ignition of gasifier. To reduce the risk of explosions, gasifiers should be provided with spring-loaded top lid or busting disks and located in well vented rooms or in the open air. Operators should be taught about the risks of gasification equipment especially during start up and shut down.

### *Fuel blockages*

Fuel blockages may occur in the throat of the gasifier. These blockages are caused by an inappropriate combination of fuel properties like morphology, size distribution, ash content and ash composition, bulk density and the flow properties of the derived char. The gasifier design should be adapted to the fuel properties, the omnivorous gasifier does not exist.

### *Corrosion*

Corrosion may occur on the surface of the equipment in the high temperature areas of the gasifier (the throat). Too high temperatures can cause this corrosion and/or contaminants in the feedstock like chlorides. The gasifier design should be adapted to lower the temperature and/or to use other heat resistant materials.

## **4.3.2 Fluidized bed gasifier**

Fluidized bed gasifiers are gasifiers that working in the fluidization condition as described in chapter 2. Normally, the fuels are fed into the bed of inert or catalytically active material. The gasification agent is fed into the bed from the bottom and must be controlled to satisfy the fluidization condition and also in an amount (with reasonable equivalence ratio) to have an acceptable gas production. The gasification agents could be air, oxygen or steam depending on design of the gasifier.

The excellent heat and mass transfer characteristic of fluidized beds lead to a uniform temperature in the bed and the processes such as drying, pyrolysis, reduction, and oxidation are mixed throughout the bed. The main advantages of fluidized bed gasification are:

- Compact construction because of high heat exchange and reaction rates due to the intensive mixing in the bed

- A narrow and uniform temperature profile without hot spots
- Tolerates many feedstocks and flexible to changes in fuel characteristics such as moisture and ash content; ability to deal with fluffy and fine grained materials with high ash contents and/or low bulk densities
- Relatively low ash melting points are allowed due to the low reaction temperatures.

Drawbacks are:

- High tar and dust content of the producer gas
- High producer gas temperatures containing alkali metals in the vapor state
- Incomplete carbon burn out
- Complex operation requirements because of the need to control the supply of both air supply and solid fuel feeding
- Higher power consumption for the compression of the gas stream

Depending on the fluidization state, fluidized bed gasifiers can be classified as following:

### **4.3.2.1 . Bubbling fluidized bed (BFB)**

The bubbling fluidized bed gasifiers are gasifiers working at a bubbling fluidization condition. The bubbling condition of fluidized beds can be understood as described in figure 2.1d and 2.1e of chapter 2. In this bubbling condition, there will be a distinct interface between the fluidized bed and the freeboard above. Figure 4.8 shows a schematic diagram of a bubbling fluidized bed gasifier. The gasification agent is supplied from the bottom of the bed through a distributor plate in such amount to reach the fluidization state of the bed and also to gasify the fuel in the bed. Due to the particular characteristics, most of biomass fuels can not be fluidized alone and a "second" solid would be used as fluidization material to support the fluidization state of the fuels. The bed materials used can be quartz sand, calcite, dolomite, olivine, etc. depending on the purpose of the gasification process. The ash produced in the gasification process can be entrained and removed as fly ash in most cases. The fluidization materials can also contribute to prevent the agglomeration of the ash.

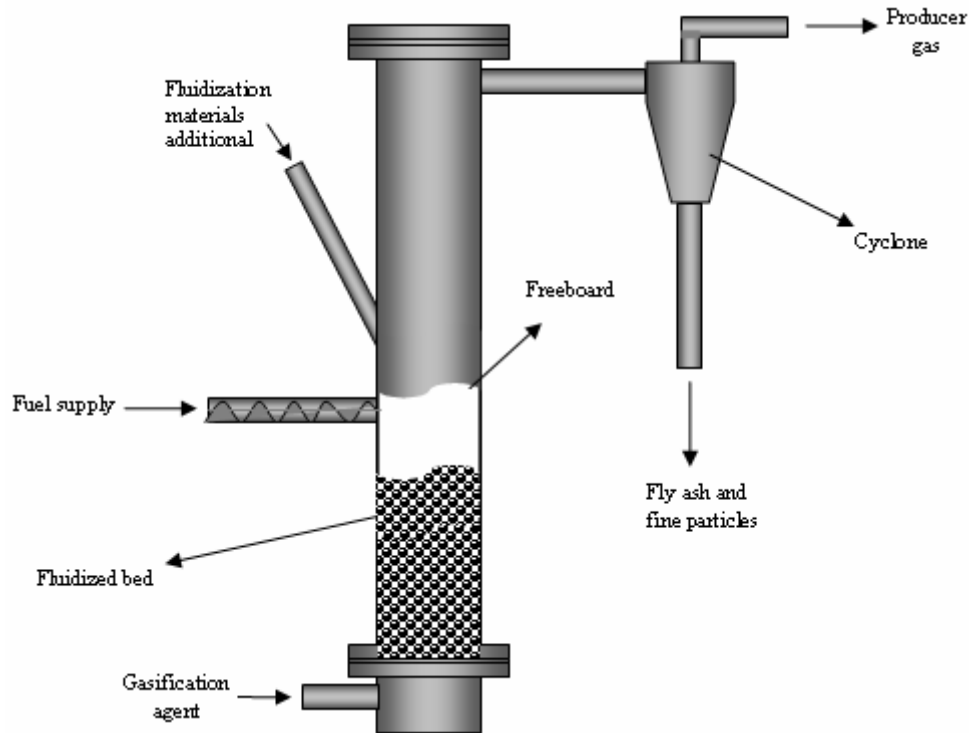


Figure 4.8 Bubbling fluidized bed gasifier

#### 4.3.2.2 Circulating fluidized bed (CFB)

The CFB gasifiers are the gasifiers that work in turbulent or fast fluidization condition. The fluidization conditions of CFB are similar to the fluidization state that was shown in figure 2.1g and 2.1h of chapter 2. In the CFB all the particles in the bed are entrained and circulate following a cycle. Figure 4.9 shows a schematic diagram of a CFB gasifiers. The distinct interface between the fluidized bed and the freeboard does not exist but there is a density gradient along the height of the reactor. Particles are transported to the top and then separated from the gas in a cyclone and recycled back to the gasifier via a system of pipes and siphon to the bottom of the bed.

In CFB, char conversion is higher and the reactor unit costs can be reduced compared to the BFB. The carbon burn out in CFB is considerably better than in BFBs.

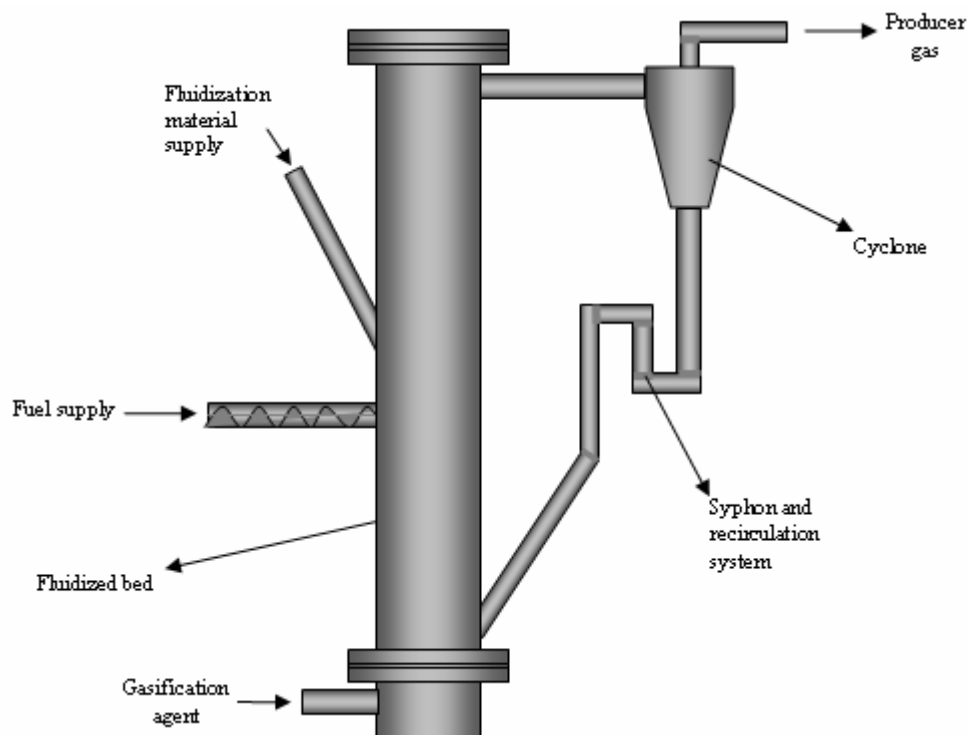


Figure 4.9 Circulating fluidized bed gasifier

### 4.3.3 Entrained flow gasifiers (EF)

An entrained flow gasifier is characterized by fuel particles dragged along with the gas stream. This generally means short residence times (typically 1 second), high temperatures (typically 1300-1500°C) and small fuel particles (solid or liquid, typically <100  $\mu\text{m}$ ). Furthermore, entrained flow gasifiers are often operated under pressure (typically 20-50 bar) and with pure oxygen. The capacity often is in the order of several hundreds of MW.

Pulverized solid fuels generally are introduced into the gasifier (after being pressurized, mostly using a lock hopper system) by pneumatic feeding. The powder is moved by inert gas and injected in a so-called burner into the gasifier. The burner intends to realize a good mixing between solid fuel and oxygen. Often vortex flow patterns are created in the burner. Local temperatures in the burner zone can be 2000°C or even higher. In the case of liquid fuels or slurries, pressurizing systems can be simply pumps. The liquid fuel subsequently is atomized and fed to the burner similarly like solid fuel powder. Since entrained flow gasifiers operate at high temperatures, the result is a CO- and H<sub>2</sub>-rich gas (and inevitably also CO<sub>2</sub> and H<sub>2</sub>O). Figure 4.10 shows a schematic diagram of an entrained flow gasifier. Two types of entrained flow gasifiers can be distinguished:

#### *Slagging entrained flow gasifier*

In a slagging gasifier, the ash forming components melt in the gasifier. The molten particles condense on the relatively cold walls and ultimately form a layer being solid close to the wall and liquid on the inner side. This slag layer serves as a protective layer for the wall. The liquid slag is removed from the bottom of the gasifier.

#### *Non-slagging entrained flow gasifier*

In a non-slugging gasifier, slag is not produced. In practice, this means that fuels should contain only little amounts of minerals/ashes. Generally 1% is the maximum allowable ash content. A certain amount of soot often is deliberately produced to generate condensation surface in the gas to prevent fouling of the walls.

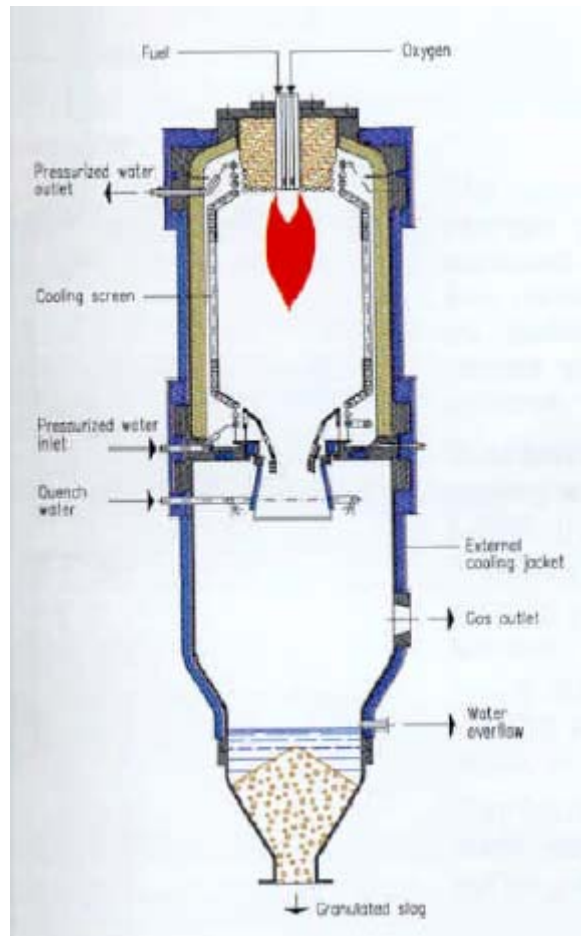


Figure 4.10 Entrained flow gasifier

### 4.4 Gasification of Biomass

The renewed interest in biomass gasification due to the awareness of greenhouse gas emissions, the Kyoto protocol and the various EU-directives stimulates the development of this technology. Several gasification plants of various sizes have been demonstrated and now the technology is close to commercialization. However each type of biomass has its own specific properties which determine its performance as a fuel in gasifier and/or depending on its own characteristics, the gasifier would be designed for the best performance.

#### 4.4.1 Biomass characteristics related to gasification

The most important properties of biomass for gasification are:

- Moisture content
- Ash content and ash composition
- Elemental composition
- Heating value

- Bulk density and morphology
- Volatile matter content
- Other fuel related contaminants like N, S, Cl, heavy metals, etc.

### **4.4.1.1 Moisture content**

The moisture content of biomass is defined as the quantity of water in the material expressed as a percentage of the materials weight. This weight can be referred to on a wet basis, on a dry basis and on a dry and ash free basis. For thermal conversion processes like gasification, preference is given to relatively dry biomass feed stock because a higher quality gas is produced, i.e. higher heating value, higher efficiency and lower tar levels. However, for the stable operation of the gasifier, moisture content in the fuel should be in the range of the design value. Natural or artificial drying is necessary in most cases to keep the moisture content of biomass in the reasonable value.

### **4.4.1.2 Ash content and ash composition**

Ash is the inorganic or mineral content of the biomass, which remains after complete combustion. The ash content of biomass varies widely from 0,1 % for wood up to 17 % in case of agricultural products. The chemical composition of the ash is also important when it affects the melting behavior of the ash. Ash melting can cause slagging and channel formation in the reactor. Slags may ultimately block the entire reactor in non-slagging gasifier. Slagging in bubbling fluidized bed gasifier can cause a large particles or even a layer that could affect the fluidization behavior of the bed. The design and operation of a gasifier is affected very much by the ash content and ash composition of biomass especially the design of the ash removal system and operating temperature of gasifier depend mainly on the ash characteristics.

### **4.4.1.3 Elemental composition**

The generic formula of biomass is  $\text{CH}_{1,4}\text{O}_{0,6}$  on dry ash free basis not taking into account elements of minor content. The elemental composition of the fuel is important with respect to the heating value and the emission levels in almost all applications. The production of nitrogen and sulphur compounds is generally small in biomass gasification because of the low nitrogen and sulphur content in biomass. Exceptions are chicken manure, sludge's, peat and other similar fuels.

### **4.4.1.4 Heating value**

The heating value is determined by the elemental composition, the ash content of biomass and in particularity by the fuel moisture content. On a dry and ash free basis, most biomass species have a heating value of about 19MJ/kg. The heating value of fuels can be measured with oxygen in a bomb calorimeter. The higher heating value (HHV) is the maximum amount of energy that can be obtained from combusting the fuel including latent heat of vaporization of water in the combustion product. However, mostly the water escape to the atmosphere as a gas and the heat evaporation of the water is no recovered. The amount of energy released in this case (water as a vapor) is referred to as the lower heating value (LHV). Energy efficiency can be calculated on LHV (Europe) or HHV (USA) basis. The heating value of fuel affects the heating value of the producer gas.

### 4.4.1.5 Bulk density and morphology

The bulk density refers to the weight of material per unit of volume. It differs for various type of biomass. Together with the heating value, it determines the energy density of the gasifier feedstock, i.e. the potential energy available per unit volume of feedstock. Biomass of low bulk density is expensive to handle, transport and store. Apart from handling and storing behavior, the bulk density is important for the performance of the biomass as a fuel inside fixed bed reactors a high voidage tends to result in channeling, bridging, incomplete conversion and a decrease in capacity of gasifier. The feeding system with a low density fuel is also a difficult problem.

Shape and size of the biomass fuel can affect the reaction rate of the gasification process in all four stages drying, pyrolysis, oxidation and reduction since the contacting area between fuels and the supplying gasification agent could be change. The bulk density of fuel is also affected by the shape and size of fuel since it can increase or decrease the porosity of the lump of fuel. In fluidized bed gasifiers, shape and size of fuel can affect to the fluidization behavior of the fluidized bed. The decisions of velocity of gasification (fluidization) agent and bed materials are depending on the shape and size of the fuel.

### 4.4.1.6 Volatile matter content

Volatile matter of fuel is the part of dry fuel released when heating a fuel to high temperature (up to 950<sup>0</sup>C) in absence of air until only char and ash is left. The volatile matter has impact on the tar production levels in gasifiers. Depending on the gasifier design, the volatiles leave the reactor at low temperatures (updraft gasifier), at moderate temperatures (fluidized bed gasifiers) or pass through a hot incandescent oxidation zone (downdraft gasifiers) where they are thermally cracked.

## 4.4.2 Problems in using biomass as a fuel for gasification process

Biomass fuels are from the living materials and could be considered as young fossil fuels. Biomass becomes an interesting fuel nowadays because it is one of the renewable energy resources. However, for proper utilization as a fuel for gasification processes, and also for other applications, some problems as described below must be solved.

**High moisture content.** Starting from the living material such as wood, grass, straw, animal manures etc. most types of biomass have quite high water content at the beginning of about 40-60%. The direct utilization at this high moisture content is impossible. Drying of fuels consume energy and time. In many cases, the drying is carried out using both natural and artificial drying.

**Low bulk density and heating value.** Most of biomasses have low density and low heating value except charcoal. Because of low density, especially with agriculture residues such as rice husk, straw, and some other grasses, the transportation cost would be higher and the feeding system also have to work harder to supply the equivalent unit of fuel compared to other fuels.

**High volatile matter is resulting high tar content in the gas production.** Volatile matter content in biomass fuel is between 50-85% except charcoal. The high volatile matter content results in relatively high tar contents in the producer gas. Tar is one of the most unpleasant constituents of the gas as it tends to deposit in subsequent part of the plant and intake valves causing sticking and troublesome operation. It is a product

of highly irreversible process taking place in the pyrolysis zone. Tar is a complex mixture of condensable hydrocarbons, which includes single ring to 5- ring aromatic compounds along with other oxygen-containing hydrocarbons and complex PAH. In the EU/IEA/US-DOE meeting, it was agreed by a number of experts to define tar as all organic contaminants with a molecular weight larger than benzene.

Tar will result in: 1) the shut-down of gasification facilities due to blocking and fouling of downstream application processes such as engines and turbines, and thus post-treatment, maintenance, and complex cleaning are required; and 2) a lower cold gas efficiency of system and lower heating value of the fuel producer gas. However, the minimum allowable limit for tar is highly dependent on the kind of process and the end user application. The physical property of tar depends upon temperature and heat rate and the appearance ranges from brown and watery (60% water) to black and highly viscous (7% water). There are approximately 200 chemical constituents that have been identified in tar so far.

Control technologies of tar production can broadly be divided into two approaches; treatments inside the gasifier (primary methods) and hot gas cleaning after the gasifier (secondary methods). Although secondary methods are proven to be effective, treatments inside the gasifier are gaining much attention due to economic benefits. In primary methods, the operating parameters such as temperature, gasifying agent, equivalence ratio, residence time and catalytic additives play important roles in the formation and decomposition of tar. Primary methods are not yet fully understood and have not to be implemented commercially. However, the utilization of some catalysts in the gasifier and the concepts of two stage gasification are of prime importance.

**Ash and slagging problem.** Ash and tar removal are the two most important processes in gasification system for its smooth running. Biomass from wood have a low ash content of 0,1-0,3% and the problems of ash are not serious however biomass from agricultural residues will have much higher ash content. The problem of ash removal would be more serious. Slagging, however, can be overcome by two types of operation of gasifier:

- Low temperature operation that keeps the temperature well below the flow temperature of the ash.
- High temperature operation that keeps the temperature above the melting point of ash.

The first method is usually accomplished by steam or water injection while the latter method requires provisions for tapping the molten slag out of the oxidation zone. Each method has its advantages and disadvantages and depends on specific fuel and gasifier design.

Table 4.1 shows a literature review of gasification characteristics of various fuels when gasifying in downdraft gasifiers.

**Table 4.1 Gasification characteristic of various fuels in downdraft gasifier (Yogi Goswami 1986)**

Fuel	Shape of fuel/Treatment Bulk density (kg/m <sup>3</sup> ) Moisture content (%)	Tar produced (g/m <sup>3</sup> )	Ash content (%)	Experience
------	--	-------------------------------------	-----------------------	------------

<b>Fuel</b>	<b>Shape of fuel/Treatment</b> <b>Bulk density (kg/m<sup>3</sup>)</b> <b>Moisture content (%)</b>	<b>Tar produced (g/m<sup>3</sup>)</b>	<b>Ash content (%)</b>	<b>Experience</b>
Alfalfa straw	Cubed 298 kg/m <sup>3</sup> 7,9 %	2,33	6	No slagging, some bridging
Bean straw	Cubed 440 kg/m <sup>3</sup> 13%	1,97	10,2	Severe slag formation
Barley straw (75% straw; 25% corn fodder and 6% orza binder)	Cubed 299 kg/m <sup>3</sup> 4 %	-	10,3	Slag formation
Coconut shell	Crushed (1-4 cm) 435 kg/m <sup>3</sup> 11,8 %	3	0,8	Excellent fuel, no slag formation
Coconut husks	Pieces 2-5 cm 65 kg/m <sup>3</sup>	Insignificant tar coconut	3,4	slag on grate but no operation problem
Corn cobs	- 304 kg/m <sup>3</sup> 11 %	7,24	1,5	Excellent fuel. No slagging
Corn fodder	Cubed 390 kg/m <sup>3</sup> 11,9 %	1,43	6,1	Severe slagging and bridging
Cotton stalks	Cubed 259 kg/m <sup>3</sup> 20,6 %	5	17,2	Severe slag formation
Peach pits	Sun dried 474 kg/m <sup>3</sup>	1,1	0,9	Excellent fuel. No slagging

## Study on Fluidization Phenomena Related to Gasification of Biomass in Fluidized Beds

Fuel	Shape of fuel/Treatment Bulk density (kg/m <sup>3</sup> ) Moisture content (%)	Tar produced (g/m <sup>3</sup> )	Ash content (%)	Experience
	10,9 %			
Peat	Briquettes 555 kg/m <sup>3</sup> 13 %	-	-	Severe slagging
Pruine pits	Air dried 514 kg/m <sup>3</sup> 8,2 %	-	0,5	Excellent fuel
Rice hulls	Pelletized 679 kg/m <sup>3</sup> 8,6 %	4,32	14,9	Severe slagging
Safflower	Cubed 203 kg/m <sup>3</sup> 8,9 %	0,88	6	Minor slag formation
Sugarcane	cut 2-5 cm 52 kg/m <sup>3</sup>	insignificant	1,6	Slag on hearthring, bridging
Walnut shell	cracked 337 kg/m <sup>3</sup> 8 %	6,24	1,1	Excellent fuel. No slagging
Wheat straw	Cubed 395 kg/m <sup>3</sup> 9,6 %	-	9,3	Severe slagging, bridging. Irregular gas production
Wheat straw and corn stalks	Cubed (50% mix) 199 kg/m <sup>3</sup> 15 %	-	7,4	Slagging
Wood blocks	5 cm cube 256 kg/m <sup>3</sup>	3,24	0,2	Excellent fuel

Fuel	Shape of fuel/Treatment Bulk density (kg/m <sup>3</sup> ) Moisture content (%)	Tar produced (g/m <sup>3</sup> )	Ash content (%)	Experience
	5,4 %			
Wood chips	166 kg/m <sup>3</sup> 10,8 %	6,24	6,26	Severe bridging and slagging

## 4.5 Gasification of rice husk

Rice is cultivated in more than 75 countries in the world. Rice husk is the outer cover of rice and it accounts for 20% of paddy produced on weight basis. The world wide annual husk output is about 80 million tones with an annual energy potential of  $1,2 \cdot 10^9$  GJ corresponding to heating value 15MJ/kg (*Natarajan et al., 1998*). Most of rice husk resources are in Asian countries and still not properly used. However, rice husk is one of the most difficult fuels to gasify because of its low bulk density, high ash content and its tendency to form bridge across the gasifier impairing flow under gravity. In spite of technical difficulties, gasification of rice husk, which is generated in rice mills where a demand for mechanical/electrical power also exists, has attracted a great deal of interest in recent years.

According to *Natarajan et al., 1998*, rice husk is a biomass fuel with relatively high ash content of 16-23%. Its ash contains more than 95% silica that gives a rigid skeleton like structure to the ash. When husk is fed at the top of the grate and the air flows from the bottom the husk loading on the grate is not so uniform. The consequence is that the air distribution in the bed is not uniform and there is significant amount of unburned carbon in the ash resulting in the loss of efficiency. As individual, husk particles usually retain their original shape even after combustion due to their rigid ash skeleton and results that the ash occupies the same volume as the original husk. The throat of downdraft gasifier is easy to slag due to high volume of ash.

### 4.5.1 Fixed bed gasifier

In small scale downdraft gasifier such as model 6250 M1 and some other similar constructions are still in use in China. Figure 4.11 shows the model of a typical Chinese rice husk gasifier.

An Indian manufacturer has developed and innovative throatless updraft rice husk gasifier. The bottom of the reactor is dipped into a water seal, from which ash is extracted manually. The producer gas passes through a ten stage cleaning system before utilization in an engine.

Some other small scale updraft and downdraft gasifier was also developed in developing countries for household cooking.

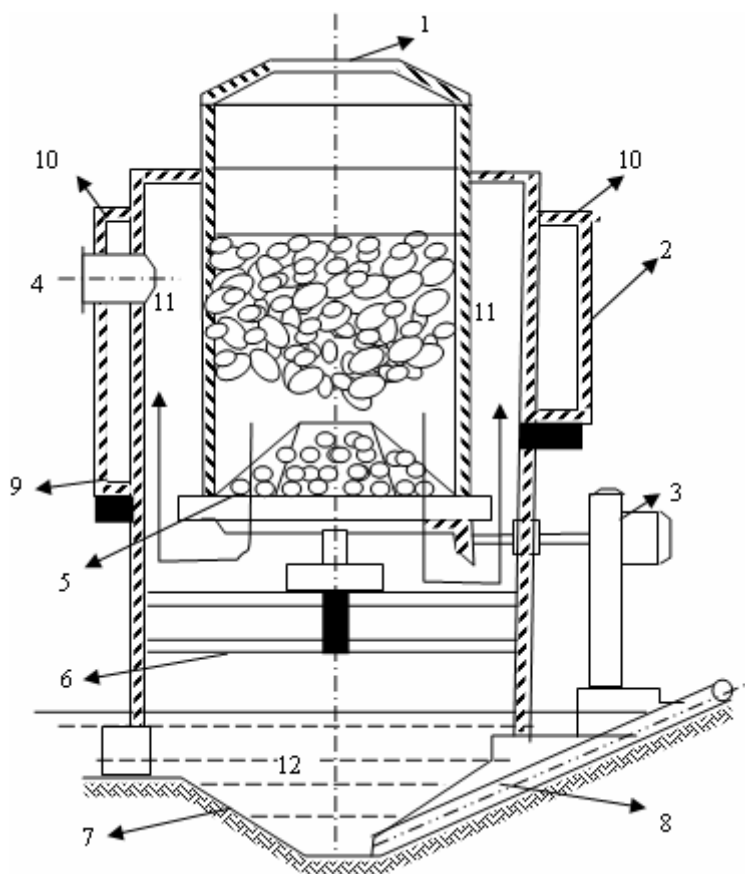


Figure 4.11 Chinese rice husk gasifier

Note:

- |                         |                          |
|-------------------------|--------------------------|
| 1. Fuel and air inlet   | 7. Ash setting pond      |
| 2. Cooling water jacket | 8. Ash removing tube     |
| 3. Gear box             | 9. Cooling water inlet   |
| 4. Gas outlet           | 10. Cooling water outlet |
| 5. Rotary grate         | 11. Gas                  |
| 6. Grate support        | 12. Ash                  |

#### 4.5.2 Fluidized bed rice husk gasifier

Fluidized bed gasifiers seem to offer some distinct advantages due to their unique operating characteristics. The turbulence due to fluidization in the bed can break the rigid ash skeleton to make the trapped carbon available for conversion. Rice husk ash can easily removed from the fluidized bed by entrainment in the gas stream, from which it can be separated by a particle separating system. The bed temperature can be kept below the ash slagging temperature by properly controlling its operating parameters and localized combustion can be avoided as long as isothermal bed condition is maintained by ensuring uniform fluidization. Hence, the fluidized bed reactors seem to be a promising choice for biomass fuels with high ash contents, particularly melting at relatively low temperatures. Table 4.2 shows fluidized bed gasification as observed by some researches.

Table 4.2 Literature review on the fluidized bed gasification of rice husk (Natarajan *et al.*, 1998)

Reference	Main observation	Main result
-----------	------------------	-------------

Reference	Main observation	Main result
Van den Aarsen et al., 1982	<ul style="list-style-type: none"> <li>• Opportunities for temperature control are optimal in fluidized bed</li> <li>• Inert fluidized bed material prevents flow problems inside the reactor and also acts as a heat fly wheel</li> <li>• Temperature profile along the height of the reactor indicates an excellent homogeneous bed temperature under all circumstances</li> <li>• Equilibrium conversion of hydrogen, water gas shift reaction</li> <li>• Gas phase conversion of 90% is observed</li> <li>• No ash sintering or ash removal problem has been observed during gasification of 1000 kg of rice husk over a period of 35 h and eve after operating up to 940 °C for 6 hours</li> </ul>	<ul style="list-style-type: none"> <li>• LHV of the gas varies between 4,5 and 6 MJ/kg, which is sufficient enough to be used as fuel in internal combustion engines</li> <li>• While the volumetric gas yield increases with temperature, its heating value and concentrations of CO and HC decrease</li> <li>• Tar content in the gas decreases rapidly with temperature from 6000 mg/Nm<sup>3</sup> at 750 °C to 800 mg/Nm<sup>3</sup> at 940 °C and deeper bed could be used for further reduction of tar</li> <li>• Carbon conversion efficiency of about 90% and cold gas efficiency of 60 to 67% could be achieved</li> </ul>
Hiller, 1982	<ul style="list-style-type: none"> <li>• Sorghum stalks, rice husk, corn cobs and cotton gin trash could be gasified to produce low energy gas in a fluidized bed</li> <li>• Gas composition is mainly influenced by equivalence ratio</li> <li>• Effect of the type of biomass fuel on the gas composition is minimal</li> </ul>	<ul style="list-style-type: none"> <li>• A 300 mm diameter gasifier can generate gas with thermal energy of 869 kW/m<sup>2</sup> of distributor area</li> <li>• Gas with a mean heating value of 6,6 MJ/m<sup>3</sup> and standard deviation of 0,8 MJ/m<sup>3</sup> has been produced at an equivalence ratio of 0,23 and bed temperature of 760°C</li> <li>• Cold gas efficiency of gasifier varies between 45 and 65%</li> </ul>
Xu et al., 1985	<ul style="list-style-type: none"> <li>• Equivalence ratio controls the bed temperature, which in turn strongly influences the gasification efficiency</li> <li>• Nearly isothermal conditions can be achieved at different temperatures</li> </ul>	<ul style="list-style-type: none"> <li>• Sand and ground husk mixture offers a good fluidization behavior. Sand to husk ratio of 3:7 is found to be desirable</li> <li>• Superficial velocity of 60-75 cm/s resulted in good fluidization and bed</li> </ul>

Reference	Main observation	Main result
	<ul style="list-style-type: none"> <li>• <math>H_2/CO</math> ratio, heating value and gas yield increase with the temperature</li> <li>• For a given air flow rate, <math>N_2</math> concentration in the product gas decreases with increasing temperature</li> <li>• Silica and potassium oxide in the ash melt at about <math>980^\circ C</math> and form a diffusion barrier for the gasification process</li> <li>• Above <math>900^\circ C</math>, water shift reaction dominates which causes only a shift in <math>H_2</math> and <math>CO</math> compositions and hence no significant improvement in heating value can be expected</li> <li>• Gasification efficiency exceeds 60% when the bed temperature is above <math>700^\circ C</math></li> </ul>	<p>expansion</p> <ul style="list-style-type: none"> <li>• To obtain near maximum efficiency, temperature range of <math>700-980^\circ C</math> is recommended</li> <li>• The gasification rate varies between 2,8 and <math>4,6 \text{ MW/m}^2</math> and the heating value between 5 and <math>8 \text{ MJ/Nm}^3</math></li> <li>• The carbon conversion efficiency is reported to be 75%</li> <li>• The bed temperature of <math>700-815^\circ C</math>, an equivalent ratio of 0,18 - 0,21, fuel flow rate of 13,6-18,2 kg/h and superficial are velocity of 60-75cm/s are found to be the optimum conditions</li> </ul>
Bingyan and Zongnan, 1987	<ul style="list-style-type: none"> <li>• Gasification process is directly affected by fluidization quality</li> <li>• When the bed is operated from 60 to 100 cm/s. The bed temperature is uniform and the bed expansion is about twice the static bed height</li> <li>• Overbed feeding for whole husk and inbed feeding for ground husk seem to be advantageous</li> <li>• Influence of temperature on the gasification reaction is dramatic up to <math>730^\circ C</math></li> <li>• Increase in temperature and fluidization quality increases the carbon conversion efficiency, gas productivity and gasification efficiency</li> <li>• Although gas quality increases, its quality deteriorates above <math>730^\circ C</math></li> <li>• Overbed feeding of whole husk offers improve performance over inbed feeding of ground husk</li> </ul>	<ul style="list-style-type: none"> <li>• Above <math>985^\circ C</math>, silica and potassium oxide fuse on the surface of the rice husk char and form a glass like barrier which prevents further reaction of the remaining material</li> <li>• Gas heating value increases from 2,64 to <math>5,5 \text{ MJ/kg}</math>, when temperature is increased from 500 to <math>730^\circ C</math></li> <li>• Optimum gasification temperature for best quality gas is found to be <math>730^\circ C</math> at an equivalence ratio of 0,26. Bed temperature range of <math>680-750^\circ C</math> is recommended</li> <li>• Product gas with <math>5,25 \text{ MJ/m}^3</math>, 90% carbon conversion, and 60% cold gas efficiency with productivity rate of <math>4,44 \text{ MW}_{th}/\text{m}^2</math> are typical results achieved</li> </ul>

Reference	Main observation	Main result
Flanigan et al., 1987	<ul style="list-style-type: none"> <li>• Ground husk is observed to have better gasification quality but it requires additional machinery and energy</li> <li>• Heating value of the gas decreases with temperature beyond 700 °C</li> <li>• The char is not blown out of the bed until it is decreased from its initial size of 5mm length to 0,4 mm</li> <li>• 25-30% of the energy in the rice husk should be carefully controlled below 900 °C, to avoid ash related problems</li> <li>• Gasifier efficiency can be improved to the extent of 10% by eliminating the heat loss by insulation and recovering the sensible heat of product gas.</li> </ul>	<ul style="list-style-type: none"> <li>• Fluidization velocity of 67-98 cm/s provides good fluidization quality and bed expansion</li> <li>• When the temperature is increased from 500-700 °C, the heating value of the gas increased from 2,6 to 5,2 MJ/m<sup>3</sup>, while the cold gas efficiency and carbon conversion efficiency are increased from 21-58% and 55-90% respectively</li> <li>• Maximum heating value of the gas is achieved at 700 °C</li> <li>• Surface heat loss from the gasifier is about 10 - 19 %</li> </ul>
Hartiniati et al., 1989 and Panaka et al., 1994	<ul style="list-style-type: none"> <li>• Increase in temperature requires higher equivalence ratio, that results in higher gas yield but decreases LHV of gas for the same fuel flow rate</li> <li>• For the same fuel flow rate, the equivalence ratio is to be raised from 0,3 -0,48 to achieve gasification temperatures from 721 -871 °C</li> <li>• Gas quality is found to vary between 4,1 to 6,3 MJ/m<sup>3</sup>, depending upon the bed temperature and/or equivalence ratio</li> <li>• Concentration of hydrocarbons decreases with increase in temperature as a result of thermal cracking</li> <li>• No operation problem was observed during 36 hours of continuous operation.</li> </ul>	<ul style="list-style-type: none"> <li>• Decrease in LHV of gas and increase in air fuel ratio with temperature for same fuel flow rate is due to higher requirement of air to burn proportionately higher amount of fuel to increase temperature</li> <li>• Maximum energy of 12,3 MJ gas/kg fuel (daf) was produced at 93 kg/h of fuel flow rate and bed temperature of 785 °C.</li> <li>• LHV of gas under this condition is found to be 4,1 MJ/kg</li> <li>• Cold gas efficiency varies from 64 - 67%</li> </ul>
Sanchez	<ul style="list-style-type: none"> <li>• Increase in equivalence ratio</li> </ul>	<ul style="list-style-type: none"> <li>• It is found that 1,4 (max 2,1)</li> </ul>

Reference	Main observation	Main result
and Lora, 1994	<p>increases the gasification efficiency initially and then decreases</p> <ul style="list-style-type: none"> <li>The hot and cold gas efficiencies are reported to be 43% (max 53,9%) and 60% (max 65%) at temperature of 759 °C and equivalence ratio of 0,55</li> </ul>	<p>m<sup>3</sup> of gas with LHV of 2,9 (max 4,0) MJ/Nm<sup>3</sup> is produced per kg of rice husk</p> <ul style="list-style-type: none"> <li>The thermal capacity of the gasifier is 1,4 (max 2,1) MW per m<sup>3</sup> of bed volume at the husk flow rate of 1000 (max 3900) kg/m<sup>3</sup>h</li> </ul>

There are the following main problems to solve when developing fluidized bed gasification of rice husk.

**Feeding system.** Biomass fuels usually make difficulties in handling and feeding due to their poor flow characteristics, its low bulk density of about 130 kg/m<sup>3</sup> and abrasive and interlocking nature. Rice husk is fed into the bed usually with a screw feeder or pneumatically by air.

In general, there is no serious difficulty in feeding rice husk into the bed using a screw feeder. However, the feed rate by screw feeder is reported to be non uniform at low feed rate. It is observed that the feed rate vary cyclically due to some sort of cyclic compression process which packs the rice husk until a minimum plug is developed before being fed (*Natarajan et al., 1998*). Fuel feeding can further be smoothened by supplying secondary air through the feeding port and by vibration of the hopper. Pneumatic feeding is also not reliable at low feed rates. Due to its low bulk density and high volumetric porosity, it could be carried with small quantities of air through the feeding port.

Due to the high volatile content in the fuel, a cooling jacket around the feeding tube is a good way to prevent the pyrolysis and carbonization of the husk before entering the bed by keeping its temperature low.

When feeding rice husk from above of the bed into the free board of a fluidized bed, the pyrolysis of husk takes place in the freeboard and the resultant char settles in the upper part of the bed. During the settling, the char is ground by the turbulent sand bed into small particles and simultaneously reduced by the gasification. Most of the remaining char is burnt by the incoming air to release the heat energy to sustain the gasification process (*Natarajan et al., 1998*).

When the whole rice husk can be conveniently fed right into the bed, the whole husk char is larger in size and heavier in weight compared to the ground husk char, they could hardly be blown out of the bed by volatiles until they are reduced to finer particles or ash (*Natarajan et al., 1998*).

The segregation tendency of rice husk and fluidization material is quite obvious due to the different of density that leads to more difficult grinding the ash and char particles by the bed material and also affects the fluidization behavior of the bed. For that reason, fuel feeding from the bottom of the bed is used. Further more, *Mansaray et al., 1999* developed a dual distributor type feeding mechanism as shown in figure 4.12.

**Equivalence ratio (ER):** Equivalence ratio determines the fraction of the fuel that is burnt and the fraction of the fuel that is gasified in the reactor. It also affects

fluidization quality and bed temperature. The lower limit of ER is decided by the minimum quantity of air to burn a part of fuel to release enough heat to support the endothermic reactions, to attain required carbon conversion efficiency, to meet the sensible heat losses in gas, char and ash, and to maintain the required temperature of the reactor. As rice husk has a high ash content, it requires relatively higher fraction of the fuel to be burnt. This ultimately demands a relatively higher ER.

The upper limit of ER is determined by the combined consideration of the reactor temperature, fluidization quality, gas heating value and tar content in the gas. An increasing of ER results an increasing of reactor temperatures since higher proportion of rice husk is burnt. It is possible to obtain different operating temperatures by adjusting the equivalent ratio. The increasing of ER also results in higher expansion and higher rates of elutriation. While the gas quantity increases continuously with the equivalent ratio, its heating value deteriorates after a certain limit due to the fact that a proportional high part of the fuel is burnt rather than gasified and partly due to dilution by nitrogen in air. Tar content in the gas drastically decreases beyond 750 °C

**Temperature limits.** The lower temperature in the gasification process is determined by the condition for complete carbon conversion. It mainly depends on the elemental composition of husk and the equivalent ratio. If the gasification temperature is less than this lower limit (750°C), part of the carbon in the fuel remains unburned and accumulates in the reactor, resulting in lower efficiencies. The higher temperature is limited by ash fusion conditions and it depends upon the ash composition and reaction atmosphere. Above this temperature, silica and potassium oxide in ash fuses on the surface of the rice husk char particles forming a glass-like barrier that prevents the further reaction of the remaining carbon. *Natarajan et al., 1998* conclude from other investigations that the temperature limits of rice husk gasification between 700-1000°C.

**Producer gas yield and gasification rate.** Producer gas yield per kg of fuel increases with ER and hence with temperature.

**Gas composition and heating value.** The concentration of CO, H<sub>2</sub>, and CH<sub>4</sub> mainly determine the heating value of the producer gas while CO<sub>2</sub> and N<sub>2</sub> are inert and other combustibles are negligibly small. The concentration of H<sub>2</sub> and CO increase and the concentrations of CO<sub>2</sub>, N<sub>2</sub>, and CH<sub>4</sub> decrease with temperature for a given equivalent ratio.

The heating value of the producer gas decreases with increasing bed temperature since it demands for higher ER and subsequent dilution.

**Gasifier efficiency.** The hot gas efficiency of the gasifier is defined as the ratio of the chemical energy plus thermal heat in the producer gas to the chemical energy in the fuel and alternatively the cold gas efficiency is the ratio of the chemical energy in the gas to that in the fuel. The cold gas efficiencies of more than 60% could be achieved.

**Tar emission.** The producer gas also contains condensable tar, which is considered highly undesirable especially for shaft power development. The tar content of the producer gas strongly depends on the reactor operating temperature and decreases from 6000mg/Nm<sup>3</sup> at 750 °C to 800 mg/Nm<sup>3</sup> at 940 °C as shown by *van den Aarsen 1982*

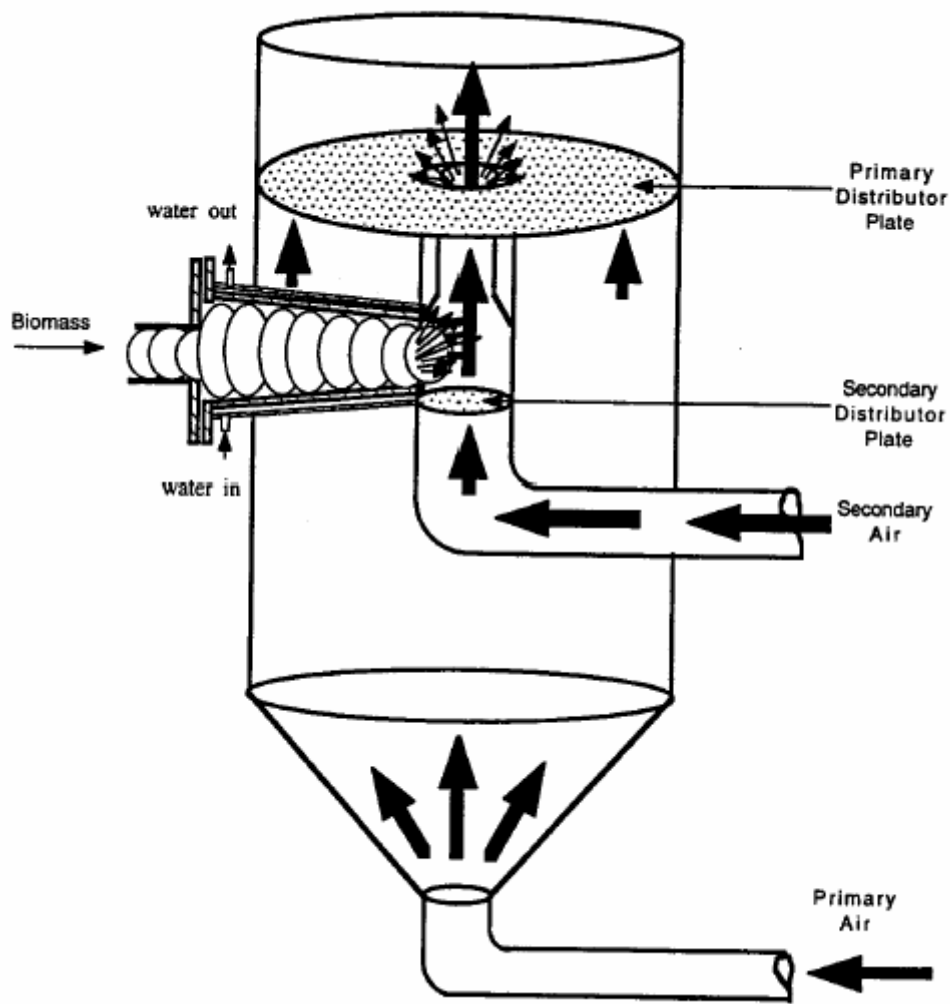


Figure 4.12 Dual distributor type feeding mechanism for rice husk into fluidized beds  
(Mansaray et al., 1999)

## 5 FLUIDIZED BED GASSIFICATION OF RICE HUSK AND WOOD PELLETS

### 5.1 Characteristic of fuel and fluidization materials

#### 5.1.1 Fuels characteristics

Fuels used for the gasification investigations are rice husk that was transported from Vietnam to Austria and milled wood pellets that was available at the institute. Wood pellets are known for its suitability for gasification in fluidized beds. Therefore, wood pellets can be considered as reference fuel. Rice husk is an important fuel for a lot of Asian countries. This was the reason for the selection of rice husk for these experiments although it is well known that rice husk is difficult to gasify in fluidized beds. An analysis of the fuels characteristics is shown in table 5.1.

**Table 5.1 Fuel Characteristics of rice husk and wood pellets**

		Wood pellets (as used) (Hrbek 2005)	Wood pellets (dry) (Hrbek 2005)	Rice husk (as used)	Rice husk (dry)
<b>Proximate analysis</b>					
Moisture	[w-%]	6,72	0	8,42	0
Ash	[w-%]	0,24	0,26	13,90	15,80
Volatile	[w-%]	-	-	62,20	67,90
Fixed carbon	[w-%]	-	-	15,50	16,60
<b>Ultimate analysis</b>					
C	[w-%]	45,71	49,00	38,52	42,06
H	[w-%]	6,08	6,52	4,84	5,28
N	[w-%]	0,11	0,12	0,36	0,39
S	[w-%]	<0,05	<0,05	0,068	0,074
Upper heating value	[kJ/kg]	18620	19962	15235	16636
Lower heating value	[kJ/kg]	17120	18530	13966	15476
Bulk density	[kg/m <sup>3</sup> ]	442	-	130	-
<b>Elemental analysis</b>					
Cl	[mg/kg]	121,26	130	820	900

		<b>Wood pellets (as used) (Hrbek 2005)</b>	<b>Wood pellets (dry) (Hrbek 2005)</b>	<b>Rice husk (as used)</b>	<b>Rice husk (dry)</b>
Na	[mg/kg]	12,13	13	-	-
K	[mg/kg]	329,28	353	-	-
Mg	[mg/kg]	121,26	130	-	-
Mn	[mg/kg]	88,61	95	-	-
Zn	[mg/kg]	8,76	9,4	-	-
Hg	[mg/kg]	<100	<100	-	-
Cd	[mg/kg]	<1	<1	-	-
Pb	[mg/kg]	<50	<50	-	-
As	[mg/kg]	<50	<50	-	-

The high ash content of rice husk can be a problem for ash removal in gasification processes. Table 5.2 describes the ash melting behavior of rice husk ash and table 5.3 shows the component analysis of the rice husk ash.

**Table 5.2 Melting behavior of rice husk ash**

(ashing temperature: 710 °C; reducing atmosphere: 55 vol % CO + 45 vol CO<sub>2</sub>%)

	Rice husk
Sintering Temperature (°C)	749
Deformation (°C)	>1450
Sphere temperature (°C)	>1450
Hemisphere temperature (°C)	>1450
Flow temperature (°C)	>1450

*Remark: The upper temperature limit for the analytical device (heating microscope) is 1450oC. This temperature is high enough for the gasification purposes.*

**Table 5.3 Rice husk ash analysis (Pham, 1999)**

<b>Component</b>	P <sub>2</sub> O <sub>5</sub>	SiO <sub>2</sub>	Fe <sub>2</sub> O <sub>3</sub>	Al <sub>2</sub> O <sub>3</sub>	CaO	MgO	Na <sub>2</sub> O	K <sub>2</sub> O	SO <sub>3</sub>
<b>Percentage (%)</b>	na	90-97	0,4	na	0,2-1,5	0,1-2	1,75	1,1	1,13

na: not analysed

Figures 5.1 and 5.2 show a sample of milled wood pellets and rice husk as they were used in the gasification experiments. Wood pellets in the original form could not be

used as the particle was too large for the feeding system. Therefore, wood pellets were milled before they were used for the gasification experiments.



**Figure 5.1 Milled wood pellets**



**Figure 5.2 Rice husk**

### **5.1.2 Characteristics of the fluidization bed material**

Due to the particular characteristics, rice husk and milled wood pellets are difficult to fluidize alone so in the experiments of fluidized bed gasification, quartz sand is used

as fluidization bed material. The figure 5.3 shows a sample of Austrian quartz sand with following characteristics.

- Chemistry:  $\text{SiO}_2$ , Silicon dioxide
- Class: Silicates
- Group: Quartz
- Hardness: 7
- Mean diameter:  $250\mu\text{m}$
- Density:  $2600 \text{ kg/m}^3$ .



**Figure 5.3 Quartz sand used as bed material**

The minimum fluidization velocity of quartz sand was measured at  $660^\circ\text{C}$ , a similar temperature where the gasification reaction taking place in the experiments. The results are shown in figure 5.4. The figure shows that  $U_{mf}$  of the quartz sand used for the experiments is  $5,68\text{cm/s}$ . The operation of the test rig has been carried out with an air velocity about three times the minimum fluidization velocity of quartz sand (around  $17\text{cm/s}$ ).

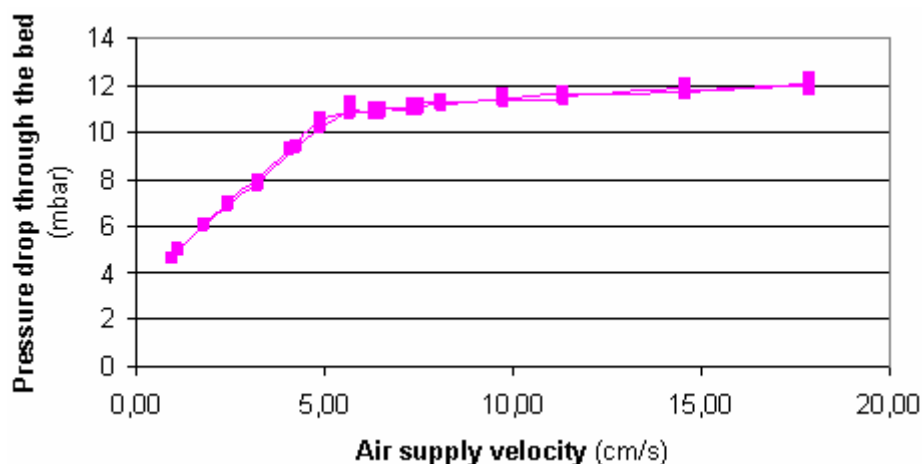


Figure 5.4 Pressure drop of a bed of quartz sand at 660 °C

## 5.2 Gasification equipments

Experiments of rice husk and wood pellets gasification have been performed in a laboratory of fluidized bed gasification test rig. A schematic diagram of the fluidized bed gasifier can be seen in figure 5.5. Figure 5.6 shows a picture of the actual test rig in the laboratory of the Institute of Chemical Engineering. The gasification system could be divided into four parts.

- Feeding system to supply biomass fuel into the for the gasification reactor.
- Gasification reactor, where the gasification reaction takes place
- Producer gas distribution system
- Measuring and analysis equipment.

### 5.2.1 Biomass feeding system

The biomass feeding system have the duty of supply biomass fuel continuously and controllable accurately for the gasification reaction. The biomass feeding system includes:

Biomass hopper:

A biomass hopper made of steel with a volume of 16,5 liters and it is available to contain about 2 kg rice husk or 7,2 kg wood pellets.

Screw feeders:

Two screw feeders which are powered by two electromotors coupled with gear boxes. The upper screw feeder was rotation controlled to set the correct rotation for the desired rate of fuel from the hopper to the second screw feeder. The second screw feeder was used only for fast transportation of the fuel to the gasification zone of the reactor.

Nitrogen purge:

The feeding system with the two screw feeders can avoid leakage of hot gases coming out from the reactor to the fuel hopper and could pyrolyse the fuel in the hopper. Therefore, a small amount of nitrogen was fed to the hopper from the top to keep the fuel cool and ensure no pyrolysis can occur in the fuel hopper.

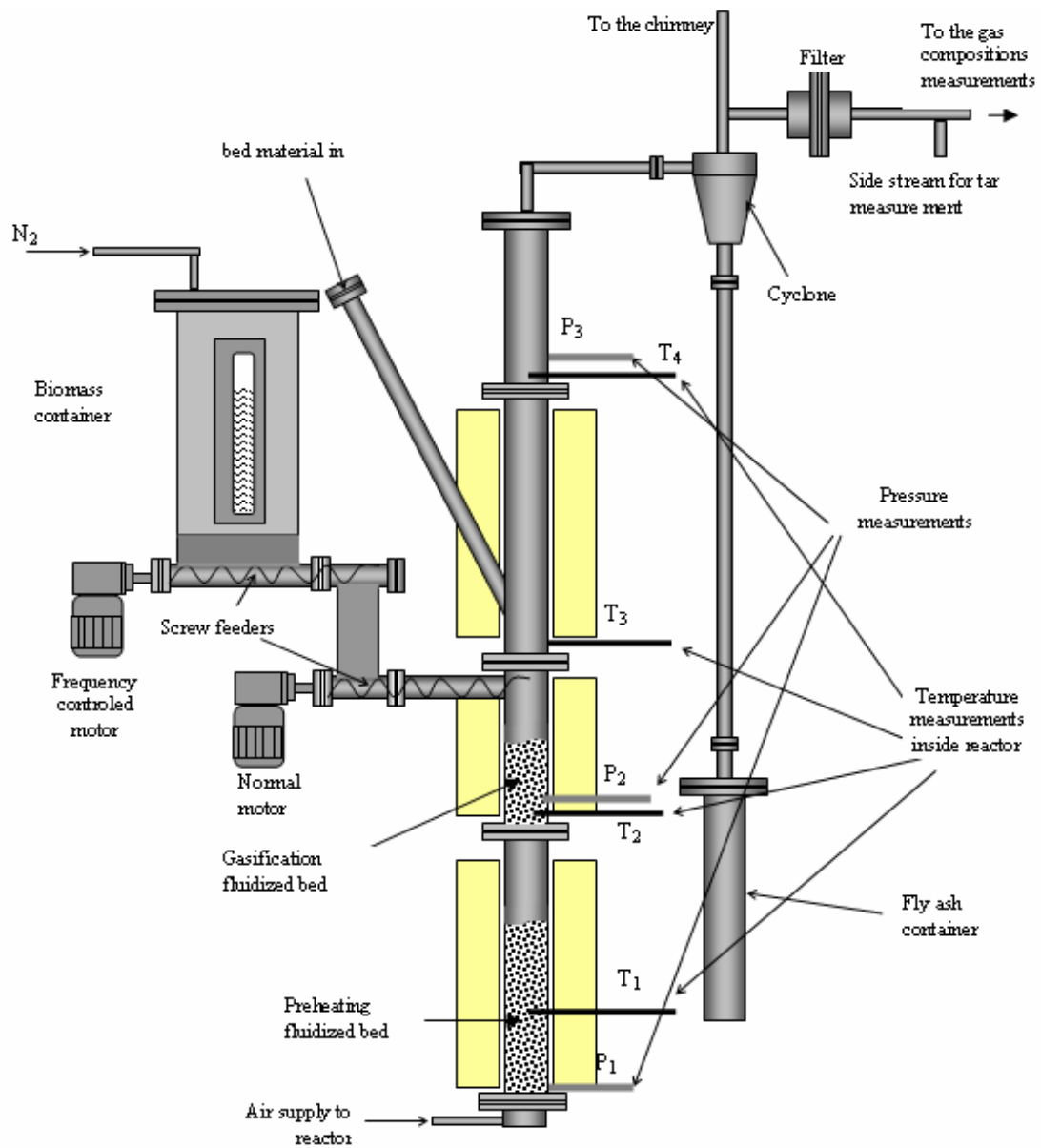


Figure 5.5 Laboratory scale fluidized bed gasifier



**Figure 5.6 Fluidized bed gasifier**

### 5.2.2 The reactor

The reactor is the place where the gasification reactions take place. The design and construction of the reactor influences the efficiency and composition of the producer gas. For the laboratory test rig, the reactor was designed as following:

The reactor made of high temperature resistant steel (1.48.41) with 66mm inner diameter 2200mm height and is divided into three zones:

-Preheating zone:

The preheating zone is located at the lower end of reactor and contains about 800g of quartz sand at 350 $\mu$ m sieving diameter. The fluidization agent (air) is preheated in this zone before it is supplied into the gasification zone.

- Gasification zone:

The gasification zone is located in the middle of the reactor where the gasification reactions take place. This zone contained 600 g of quartz sand with a mean diameter of 250 $\mu$ m

- Freeboard:

The freeboard is located at the upper end of the reactor and plays the role as free zone for further reaction of the producer gas before coming out of the reactor.

To supply heat and control the temperature in different parts of the reactor, three pairs of electrical heating shells were equipped outside the wall of the reactor. The power of

Temperature of the heating shell could be controlled to set necessary heat supply from the heating shells. Set temperatures of the heating shells are as following:

- TC0: Temperature in the preheating zone of the reactor
- TC1: Temperature in the gasification zone of the reactor
- TC2: Temperature in free board of the reactor.

TC0; TC1; TC2 could be also understood as a temperatures of the reactor wall at those parts of the reactor.

### **5.2.3 Producer gas distribution system**

Gasification reactions take place in the reactor to generate a producer gas ( $\text{CO}$ ,  $\text{CO}_2$ ,  $\text{CH}_4$ ,  $\text{H}_2$ ,...), ash and tar. Because the equipment is used as laboratory equipment for experiments, most of producer gas is burned and discharged through a chimney. A part of producer gas is taken for analysis. So the distribution system includes:

- Cyclone:

A cyclone separator is a very useful equipment to separate solid particles including fly ash and some small size fluidization materials (quartz sand) from the producer gas. The cyclone has a diameter of 120mm and a height of 220mm. The cyclone was unable to separate the very small sized particles ( $<10\mu\text{m}$ ). It is heated with the electrical heating belt to  $450^\circ\text{C}$  to avoid condensation of tar.

- Chimney

A chimney for discharge of the off gas

- Ash container

An ash container was installed to collect the solid particles (mainly fly ash) separated from stream of producer gas

- Filters

A filter in the producer gas line was used to separate fine solid particles before entering the analysis equipments. The filter was formed by two flanges to fix the filter paper in the middle. The filter paper consisted of the glass fibers and was suitable to separate very fine particles of  $0,3 - 1\mu\text{m}$  at the temperature up to  $500^\circ\text{C}$ . The filter paper was changed for each experiment. The filter was also heated with an electrical heating belt to avoid condensation of tar.

Furthermore, 3 bottles containing diesel were foreseen to separate the tar from producer gas before feeding the producer gas into the analysis equipments.

### **5.2.4 Measuring and analysis equipments**

#### **5.2.4.1 Thermal analysis**

For the thermal analysis of the gasification process, a system of thermocouples was installed to measure and record online every second several temperatures inside reactor. This procedure includes the following temperatures:

- $T_1$ : Temperature inside the fluidized bed of the preheating zone (15 cm above bottom of the bed)

- T<sub>2</sub>: Temperature inside the fluidized bed of the gasification zone (4 cm above distributor of the bed)
- T<sub>3</sub>: Temperature above the fluidized bed of gasification zone at lower part of freeboard (26 cm above the top of the bed)
- T<sub>4</sub>: Temperature in the middle of freeboard (82 cm above the top of the bed).

The locations of thermocouple are shown in figure 5.5.

#### **5.2.4.2 Pressure measurements**

Beside the temperatures, also pressures inside the reactor were recorded online every second. These measurements include:

- P<sub>1</sub>: Pressure at the bottom of preheating fluidized bed
- P<sub>2</sub>: Pressure at the bottom of gasification fluidized bed
- P<sub>3</sub>: Pressure in the free board.

#### **5.2.4.3 Producer gas analysis**

To analyze the composition of the producer gas, two types of analysis equipment are used as described in table 5.4

**Table 5.4 Gas analysis equipments**

<b>Device name</b>	<b>Measured components</b>	<b>Measuring principle</b>	<b>Range</b>	<b>Sampling rate</b>
GC	CO <sub>2</sub> , CO, N <sub>2</sub> , CH <sub>4</sub> , C <sub>2</sub> H <sub>4</sub> , C <sub>2</sub> H <sub>6</sub> , higher hydrocarbons	Gas chromatography	0-100%	20 minutes
NGA 2000	CO	IR absorption	0-100%	every second
	CO <sub>2</sub>		0-100%	
	O <sub>2</sub>	Paramagnetic behavior of oxygen	0-100%	

#### **5.2.4.4 Tar sampling and analysis**

Tar is an organic ‘contaminant’ formed as undesirable by-product of the gasification process. It is a common perception that such toxic by-products will have detrimental effects on down-stream treatment plant and power generation packs, and if emitted to atmosphere, on the local environment. Tars are formed when biomass is heated, causing molecular bonds of the biomass materials to break. The smallest molecules that form in this way are gaseous; the larger molecules are called primary tars. The primary tars can react to so called secondary tars by further reactions at the same temperature and to the so called tertiary tar at high temperature.

The definition of which components belong to the tar is varied dependent on the different methods of tar measurement. An exact tar definition or measuring procedure

is necessary to compare gasification processes or plants. At the Institute of Chemical Engineering, Vienna University of Technology, a measuring method was developed based on the tar protocol "gravimetric tar" (Neeft *et al.*, 1999). With this method, the dust, coke and tar content in the producer gas together with the water content are measured. The measurement of dust content is done according to ÖNORM M5861-1 (Österreichisches Normungsinstitut, 1993). The term "gravimetric tar" is used for the tar amount gathered with the following method:

A bypass stream of the producer gas after a filter paper is taken isokinetically for a period of time (about 10 minute). The stream of gas then is led through 6 wash bottles containing toluene. A low boiling tar ( $T_B < 200^\circ\text{C}$ ) is washed out by toluene in the washing bottles that is cooled at  $-20^\circ\text{C}$ . The dry gas flow is measured by a volume flow measurement and a thermocouple. Figure 5.7 shows the scheme of the tar measuring arrangement.

Toluene in the washing bottles then is unified and one small sample is taken for the characterization of tar using a gas phase chromatograph coupled with mass spectrometer (GC- MS). Toluene then is evaporated in a rotorvapor and most of toluene can be then condensed for further use again. A remaining condensed toluene then is transferred to a Petri dish and dried in a drying chamber. The remaining part in the Petri dish after drying are the low boiling tars.

To determine the quantity of tar in the product gas as well as the tar composition a gas phase chromatograph (Perkin Elmer, Auto system XL) coupled with a quadrupole mass spectrometer (Perkin Elmer, Turbo Mass) is used. The internal standard of the GV-MS covers more components than displayed to ensure that no component is missed.

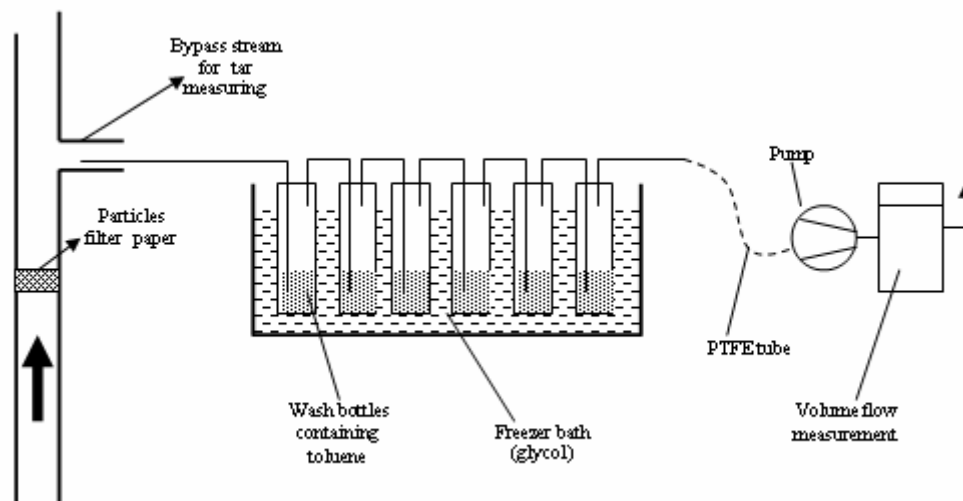


Figure 5.7 Scheme of tar measuring arrangement

### 5.3 Operation procedure of biomass gasification in the unit

Once the fuel hopper was filled, and all connections were ready, the procedure of starting the operation of the gasifier test rig was as following:

- Supply air to the reactor from the bottom of the unit with sufficient velocity so that the bed materials (quartz sand) in the preheating zone and in the gasification zone are fluidized. This is to ensure a uniform heat transfer from the walls to the bed materials.

- Turn on the electrical heating shelf to supply heat to the reactor. Set TC0, TC1, and TC2 at the desired temperature depending on purpose of the experiment.
- Supply nitrogen to the fuel hopper to ensure that no pyrolysis can take place in the fuel hopper.
- Turn on electrical heating belt to heat up the cyclone and the filter to ensure that no condensation of tar can take place.
- Turn on the online measuring programme and record online measurements from the reactor.
- Once each part of the reactor is heated up to the desired temperature, turn on the screw feeding system and supply fuel to the reactor. Control the rate of fuel feeding and air supply to secure the desired equivalent ratio.
- Wait for a steady state operation and record all parameters. Then change the input parameters such as air supply, and temperature depending on purpose of a new experiment.

## **5.4 Results and discussion of biomass gasification**

### **5.4.1 Gasification of milled wood pellets**

#### **5.4.1.1 Procedure of gasification experiments**

Experiments have been carried out using milled wood pellets as fuel. A typical experimental run is shown in figure 5.8. In this figure temperatures and pressures at different locations in the reactor and CO and CO<sub>2</sub> content in the producer gas can be seen versus time. The procedure of a typical experimental run is explained as following:

- Once the desired temperatures are reached (e.g. TC0 = 500 °C; TC1 = 700 °C; TC2 = 800 °C), the online measurement of temperatures inside the reactor (T<sub>1</sub>, T<sub>2</sub>, T<sub>3</sub>, T<sub>4</sub>), CO and CO<sub>2</sub> content, and the pressure P<sub>1</sub>, P<sub>2</sub>, P<sub>3</sub> is turned on to record sequences of values of the gasification process. At the beginning, the temperatures inside the reactor are stable with temperatures inside the bed of T<sub>1</sub> = 476 °C; T<sub>2</sub> = 677 °C; T<sub>3</sub> = 626 °C; T<sub>4</sub> = 648 °C. Figure 5.5 shows that, T<sub>1</sub> is heated up by heating shell TC0, T<sub>2</sub> and T<sub>3</sub> are heated up by TC1, and T<sub>4</sub> is heated up by TC2. The fluidized bed was chosen to have a good heat transfer from the wall to the middle of the reactor column. This is leading to T<sub>2</sub> > T<sub>3</sub> and close to TC1.
- After about 2 minutes the fuel feeding is turned on to supply fuel to the reactor. The equivalent ratio (ER) is controlled in this example at a value of 0,2. Gasification reactions take place which lead to an increasing of CO and CO<sub>2</sub> contents in the producer gas measured online until constant value were reached (CO = 16,2 - 17,5; CO<sub>2</sub> = 10,9 - 11,3).

The temperatures increase as following:

- T<sub>1</sub>: The temperature in the preheating zone stays at a constant value because the preheating zone is not affected by the gasification reactions.

- $T_2$ : The temperature in the fluidized bed of the gasification zone is increased from 674 °C to 730 °C. The gasification and partial combustion process occurring in the bed leads to an increase of  $T_2$
- $T_3$ : The temperature above the fluidized bed and under the fuel feeding point  $T_3$  is not changing and even slightly reduced because it shows the temperature close to the fuel feeding point. Pyrolysis can already occur in this region which is a heat consuming process.
- $T_4$ : The temperature in the free board is slightly increased from 648 °C to 670 °C.

Pressures in reactor including  $P_2$  (pressure at the bottom of the bed) and  $P_3$  (pressure in the freeboard) are increased since the volumetric flow of gas inside reactor are increased considerably when gasification reactions occur. However, the pressure drop through the bed remained constant with an increasing amplitude of the fluctuations.

The first set of parameters for wood pellets gasification was remained constant for 49 minutes then the setting values for the temperatures were increased to  $TC0=500$  °C;  $TC1 = 800$  °C;  $TC2=900$  °C. With the increase of these setting values for the temperatures, the gasification process in the reactor changed as following

- CO was increasing up to values of 20 - 20,8 %
- $CO_2$  was decreasing down to values of 9,5 - 9,8%.
- Temperatures  $T_2$ ,  $T_3$ ,  $T_4$  were increasing with  $T_2$  increasing faster due to the uniform of heat transfer from the wall to the fluidized bed.  $T_1$  was remaining constant.
- Pressures  $P_2$ ,  $P_3$  increased because the increased of temperatures lead to decreasing of gas density. The amplitude of pressure drop fluctuation through the fluidized bed was higher.

These conditions of wood pellets gasification were remaining constant for 49 minutes. Then equivalent ratio (ER) was increased from 0,2 to 0,24 by increasing the air supply.

- At this stage, CO decreased and had afterwards a value of 17,9- 19% and  $CO_2$  increased up to a value of 10,5 - 10,7 %.
- The temperatures inside the reactor ( $T_1$ ,  $T_2$ ,  $T_3$ ,  $T_4$ ) remained constant
- The pressure inside reactor was increased due to the higher volumetric of gas flow inside reactor.

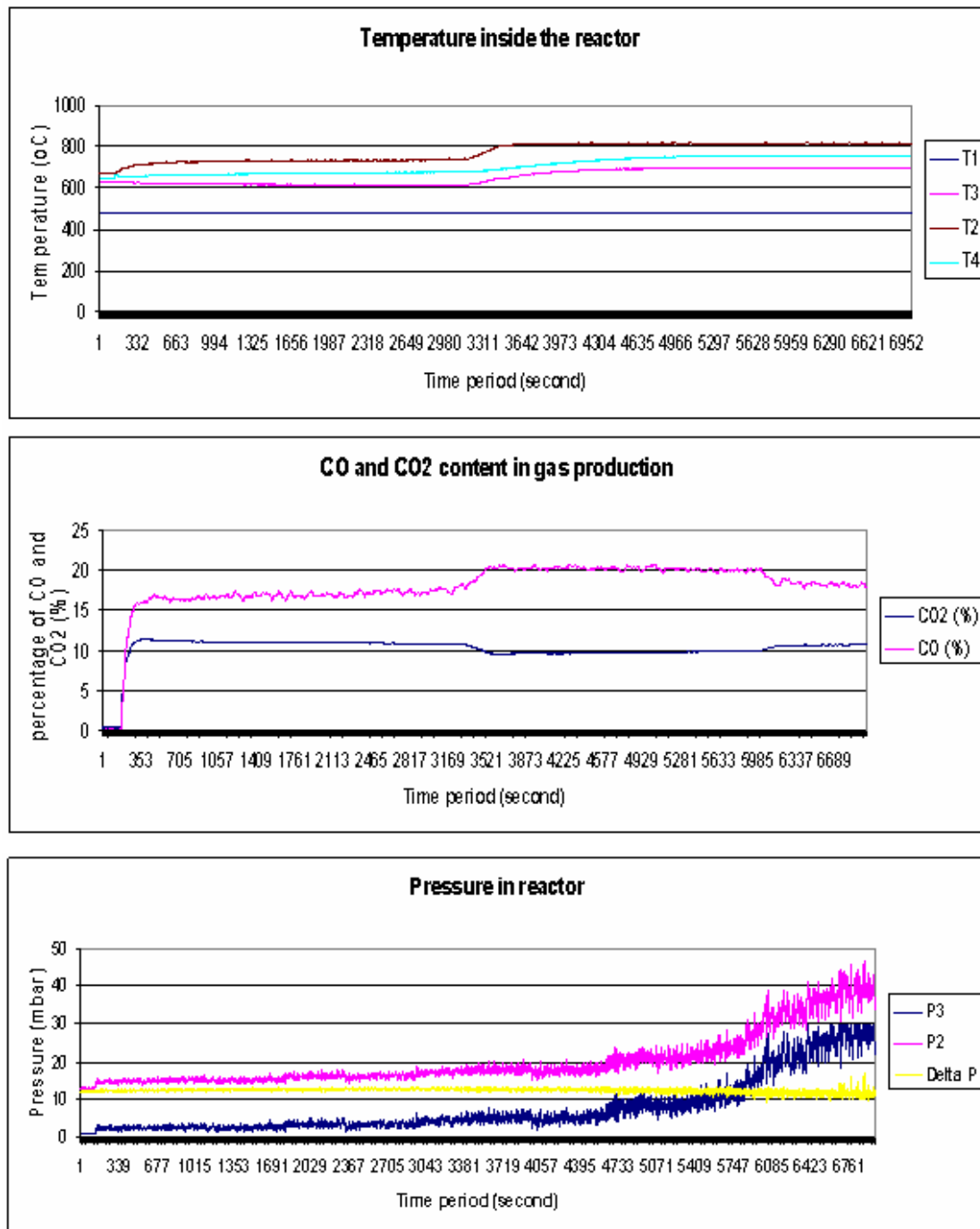


Figure 5.8 Typical gasification run for wood pellets

#### 5.4.1.2 Gas composition and heating values

Using gas chromatography for analysis of the producer gas, the contents of CO, CO<sub>2</sub>, CH<sub>4</sub>, C<sub>2</sub>H<sub>4</sub>, C<sub>2</sub>H<sub>6</sub>, N<sub>2</sub>, and higher hydrocarbon (KW) were recorded every 20minute. The value of H<sub>2</sub> content in the producer gas was calculated as following:

$$H_2 = 100\% - CO - CO_2 - CH_4 - C_2H_4 - C_2H_6 - N_2 - KW$$

#### Influence of the temperature

Figure 5.9 shows the composition of the producer gas at different temperatures inside the reactor in case of an equivalent ratio ER = 0,22. The increase of the temperatures

in the reactor results in clearly increasing amount of CO and H<sub>2</sub>. CH<sub>4</sub> and C<sub>2</sub>H<sub>4</sub> remained constant but C<sub>2</sub>H<sub>6</sub>, CO<sub>2</sub>, N<sub>2</sub> and KW (higher hydrocarbons) are decreasing. The percentage of C<sub>2</sub>H<sub>6</sub> and KW in the producer gas are quite small (C<sub>2</sub>H<sub>6</sub> < 0,3%; KW < 0,8% in all experiments) but the heating values of them are very high (C<sub>2</sub>H<sub>6</sub> = 64,345 MJ/Nm<sup>3</sup>; KW = 87,575 MJ/Nm<sup>3</sup>).

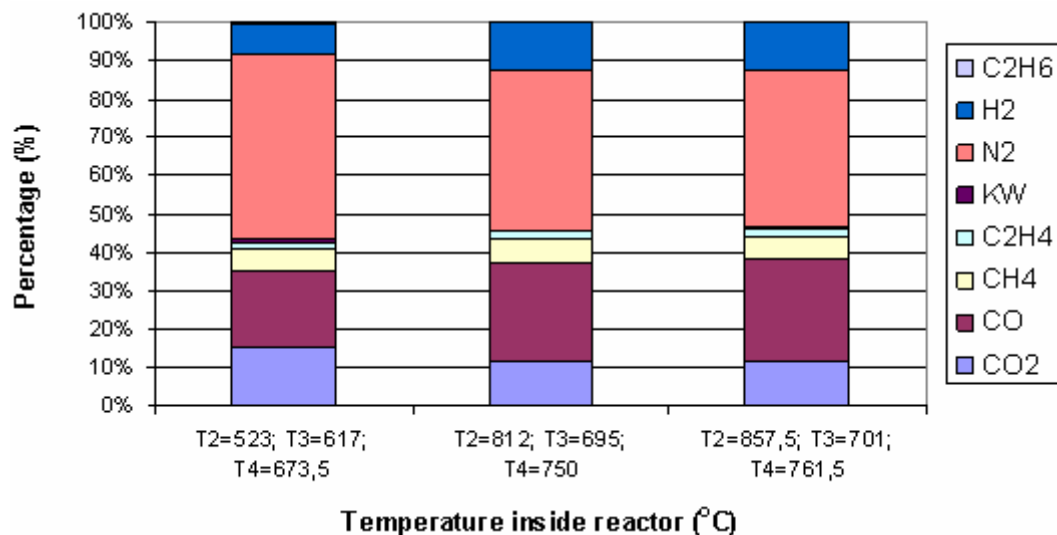


Figure 5.9 Composition of the producer gas for different reactor temperatures (ER=0,22)

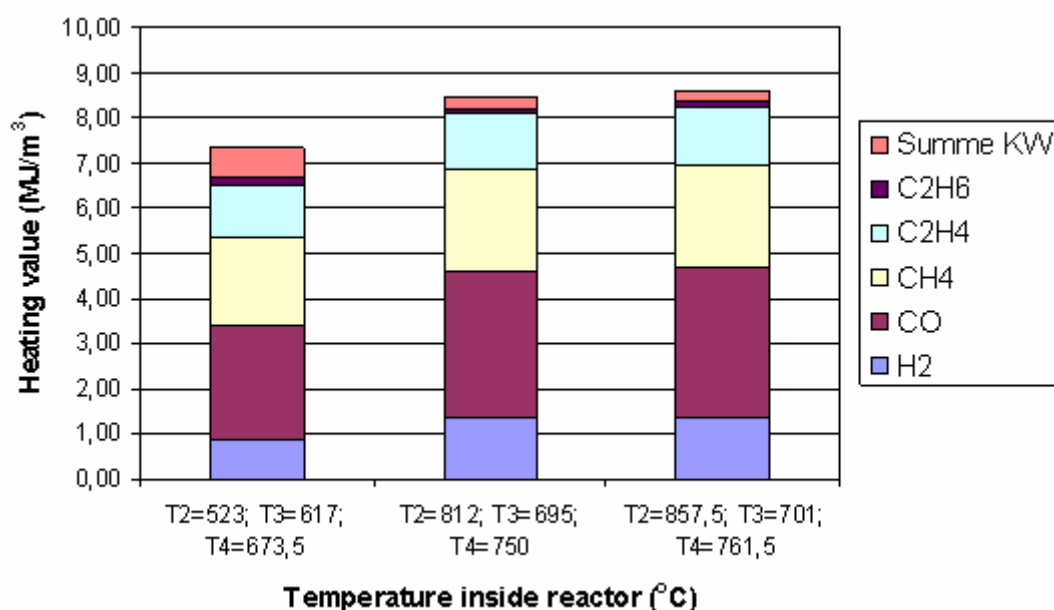
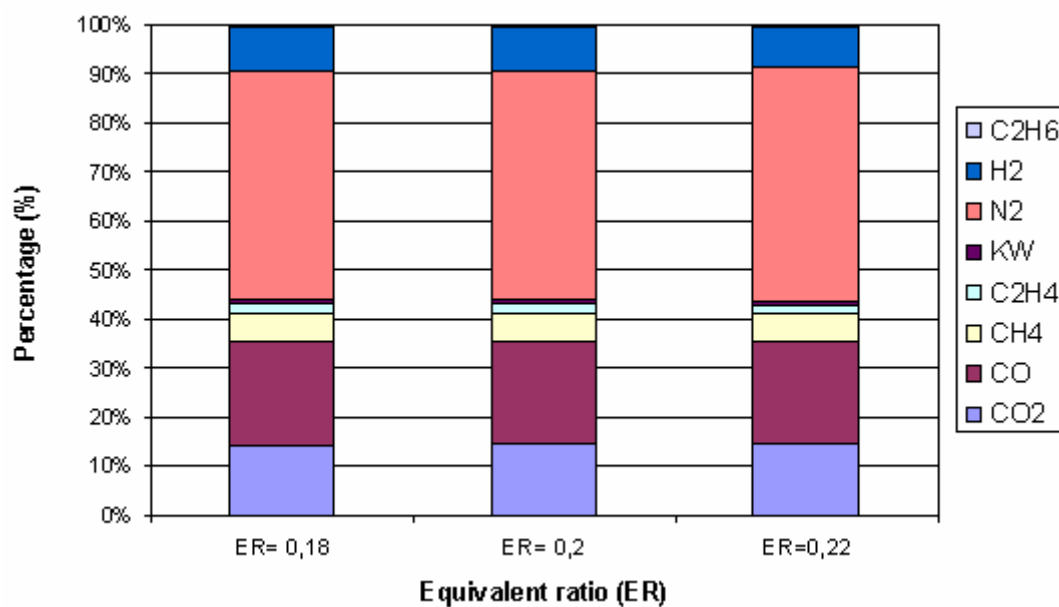


Figure 5.10 Heating value of the producer gas for different reactor temperatures (ER=0,22)

The heating value of the producer gas is increasing with increasing reactor temperatures as shown in figure 5.10. This is because the temperature increase is due to a higher power input by the electric heating shells. Figure 5.10 also shows the contribution of the main components to the heating value of the producer gas which are CO, CH<sub>4</sub>, H<sub>2</sub>, C<sub>2</sub>H<sub>4</sub>, and C<sub>2</sub>H<sub>6</sub>. Although the percentage of CH<sub>4</sub>, C<sub>2</sub>H<sub>4</sub> and C<sub>2</sub>H<sub>6</sub> in the producer gas is low these components contribute significantly to the heating value.

### *Influence of the equivalent ratio (ER)*

Experiments also have been carried out varying the equivalent ratio (ER) with quite similar reactor temperatures. The figures 5.11 and 5.12 show the compositions and heating values of the producer gas when changing the ER from 0,18 to 0,22 in case of  $T_2=725-728^\circ\text{C}$ ;  $T_3=607-617^\circ\text{C}$ ;  $T_4=679-682^\circ\text{C}$ .  $\text{CO}$ ;  $\text{H}_2$ ;  $\text{CH}_4$ ;  $\text{C}_2\text{H}_4$ ;  $\text{C}_2\text{H}_6$ ; and KW are decreasing with an increasing of ER. Contrary  $\text{N}_2$  and  $\text{CO}_2$  are increasing. This results in a decreasing of heating value of the producer gas with an increasing of ER. However, the differences are quite small due to the small change of ER.



**Figure 5.11 Composition of the producer gas for different equivalent ratios (ER)**  
( $T_2=725-728^\circ\text{C}$ ;  $T_3=607-617^\circ\text{C}$ ;  $T_4=679-682^\circ\text{C}$ )



**Figure 5.12 Heating values of the producer gas for different equivalent ratios (ER)**  
( $T_2=725-728^\circ\text{C}$ ;  $T_3=607-617^\circ\text{C}$ ;  $T_4=679-682^\circ\text{C}$ )

The figure 5.13 and 5.14 show the composition and heating value of the producer gas at higher reactor temperatures ( $T_2=803-817^\circ\text{C}$ ;  $T_3=704-712^\circ\text{C}$ ;  $T_4=754-762^\circ\text{C}$ ) with

a variation of the ER from 0,2 -0,24. Results show that with an increasing ER the heating value of the producer gas is decreased.

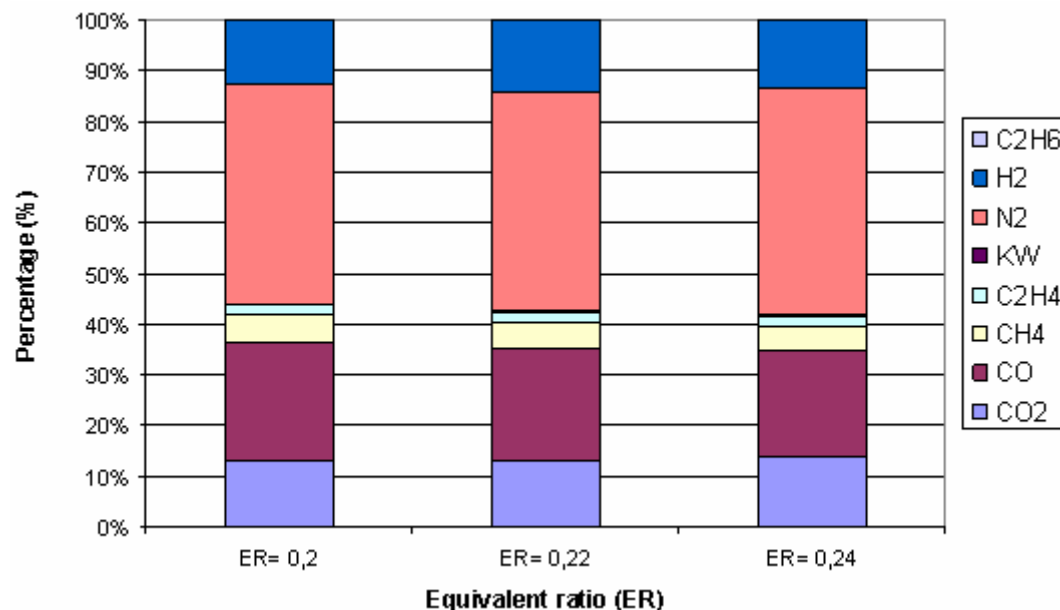


Figure 5.13 Composition of the producer gas at higher temperatures when changing ER (T<sub>2</sub>=803-817 °C; T<sub>3</sub>=704-712 °C; T<sub>4</sub>=754-762 °C)

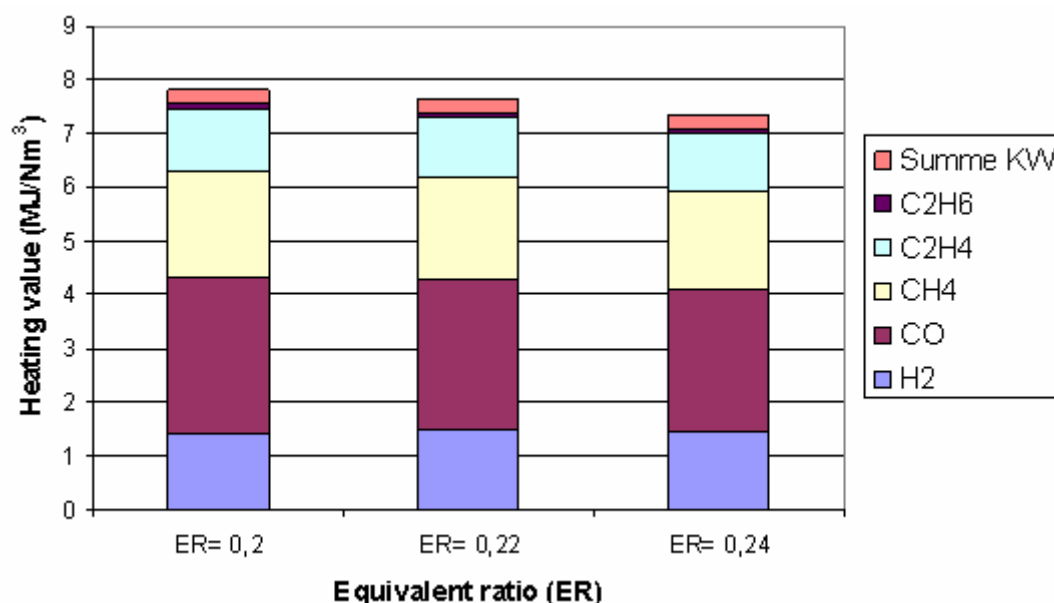


Figure 5.14 Heating value of the producer gas at higher temperatures when changing ER (T<sub>2</sub>=803-817 °C; T<sub>3</sub>=704-712 °C; T<sub>4</sub>=754-762 °C)

#### 5.4.1.3 Tar content in the producer gas

The tar content of the producer gas was measured at different temperatures. As a result of thermal cracking, higher temperatures result in lower tar contents in the producer gas as shown in the figures 5.15 and 5.16. This is in good agreement with the experience made with other gasifiers and fuels.

The dependence of tar content on ER is not clear because the variation of the ER in experiments is not high enough.

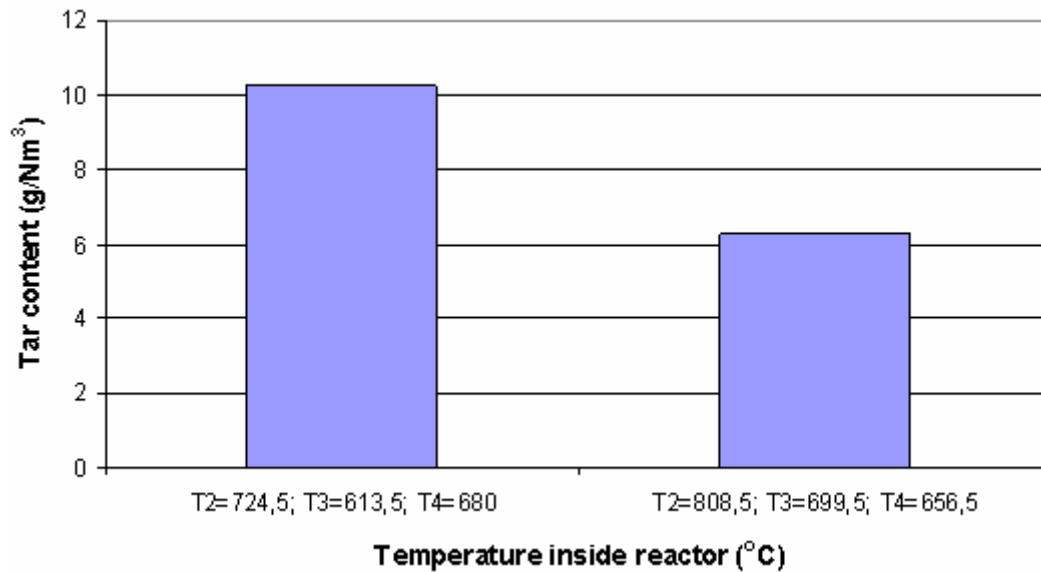


Figure 5.15 Tar content with ER = 0,22

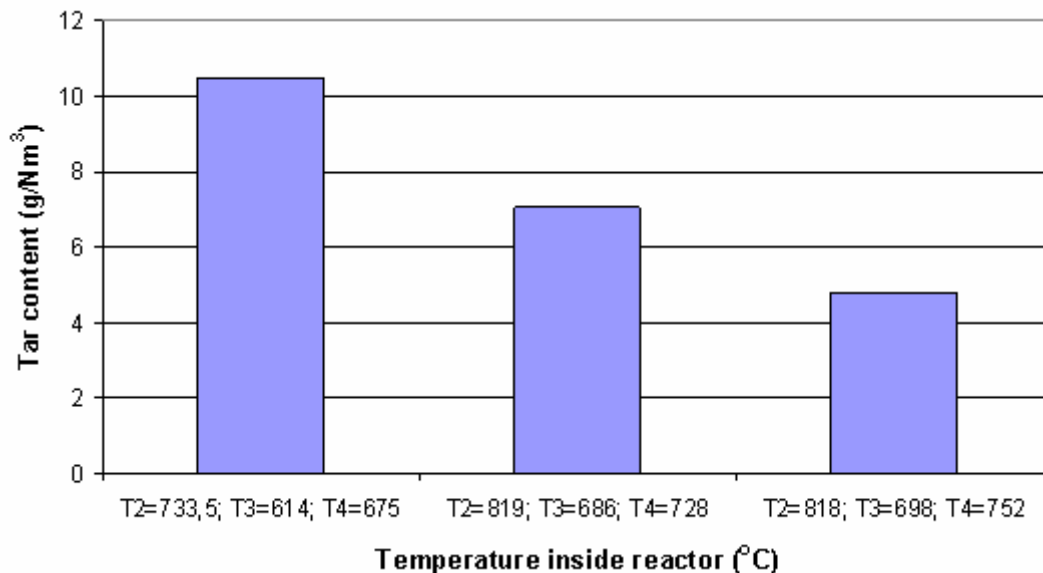


Figure 5.16 Tar content with ER = 0,2

## 5.4.2 Experiments with rice husk

### 5.4.2.1 Procedure of gasification experiments

Due to some particular characteristics, the gasification process of rice husk in the reactor is quite different compared to wood pellets. A typical experimental run of one and a half hour of rice husk gasification is shown in figure 5.17. The procedure of this experiment can be described as following:

- First the temperatures of the heating shells TC0, TC1, TC2 were set to the desired temperatures: TC0= 500°C; TC1= 650°C; and TC2 = 750°C.
- Once the setting temperatures reached desired values, the software programme "vergas" were turned on to start the recording of the temperatures, pressures, and CO and CO<sub>2</sub> online every second.

- The first 14 minutes were designated to stabilize the temperatures and the other conditions in the reactor. The temperatures at steady state conditions were  $T_2 = 626^\circ\text{C}$ ;  $T_3 = 596^\circ\text{C}$ ;  $T_4 = 589^\circ\text{C}$ .

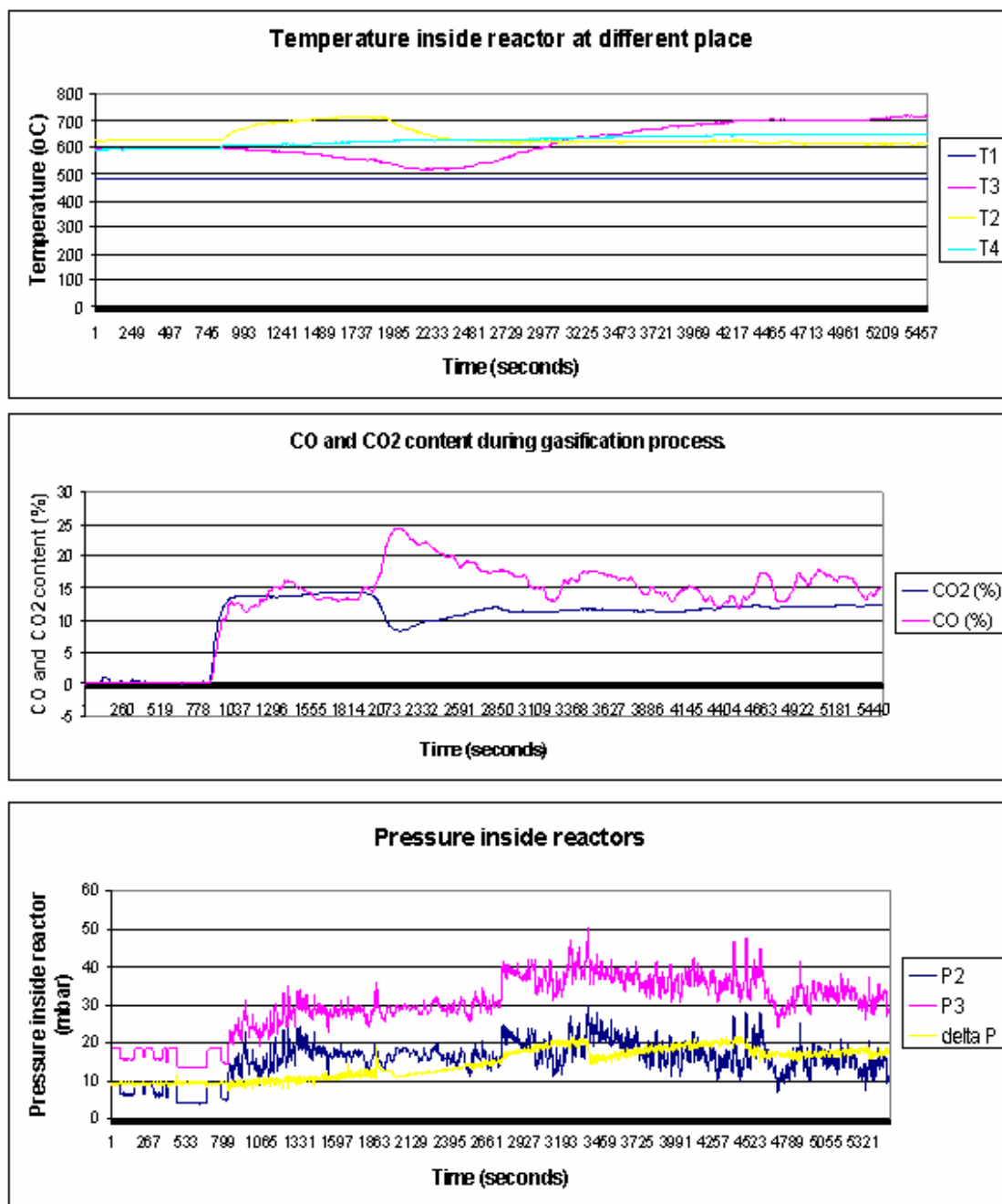


**Figure 5.17 Typical example of a gasification run with rice husk**

- Then the feeding system was turned on to supply rice husk into the reactor. At the beginning,  $T_2$  was higher than  $T_3$ . Once the feeding system was started to feed rice husk into the reactor, the gasification reaction took place and led to an increasing of CO and  $\text{CO}_2$  content in the producer gas. The temperature  $T_2$  also increased however a decrease of temperature  $T_3$  were recognized. At this time, the amount of air was controlled so that an  $\text{ER} = 0,36$  was obtained. Temperature  $T_3$  is located about 25 cm above the top of the bed and shows the temperature of producer gas just after gasification. This decreasing temperature  $T_3$  shows that the drying process and may be some endothermic reactions may

take place above the fluidized bed. This suppose have been consolidated with the unstable of CO and CO<sub>2</sub> content recorded.

- After 15 minutes of operation in that condition, the air supply was reduced to and ER of about 0,24. T<sub>2</sub> was decreased. The reason is that the endothermic gasification reactions were enhanced and at the same time the exothermic reactions were reduced. Temperature T<sub>3</sub> is still decreasing for some time.
- Due to the reduction of ER CO was increased and CO<sub>2</sub> was decreased. After 8 minute, T<sub>3</sub> started to increase meanwhile T<sub>2</sub> became stable. Now, CO is starting to decrease and CO<sub>2</sub> to increase.
- The supposition in this case is that the rice husk ash and ungasified rice husk became too much and were collected at the top of the fluidized bed. From the experiments in chapter 3 it is well known that the ash and rice husk can not really be mixed with quartz sand. This separation happened also with the new fuel coming in. Gasification reaction now takes place at the top of the bed and leads to an increasing of T<sub>3</sub>. No gasification reactions takes place in the bed anymore which leads to the stable of temperature T<sub>2</sub> at the same value as at the beginning. T<sub>3</sub> was increased to the value of about 700-715 °C and become stable in this temperature range.

### 5.4.2.2 *Producer gas composition and heating value for different conditions*

As described above, the gasification process of rice husk in the experimental equipment could be carried out in fluidized bed with good mixing for short time period. In most of the experimental runs the mixing quality was not sufficient so that the ash and the new fuel coming from the feeder were mainly above the bed.

The figure 5.18 and 5.19 show the compositions and heating values of the producer gas at the beginning of the gasification process. At the beginning, rice husk supplied was at a small amount. The mixing and fluidization behavior of the mixture between rice husk and sand was still in good condition with this low amount of rice husk in the bed. The gasification process occurred in the fluidized bed and not above. This fact was confirmed by  $T_2 > T_3$

The results in the figure 5.18 and 5.19, which were obtained with quite temperatures, show that an increasing ER gives a decreasing heating value of the producer gas. Furthermore, an increase of nitrogen in the producer gas can be clearly observed with an increasing ER. In consequence, this is a dilution of the producer gas and all other components tend to decrease. However, due to the quite high volatile matter of rice husk and low mass of a single rice husk, pyrolysis reaction occurs partly already on the way from the feeding inlet to the top of the fluidized bed. These reactions are not steady state and lead to the variation of hydrocarbon components in the producer gas such as CH<sub>4</sub>, C<sub>2</sub>H<sub>6</sub>, and KW.

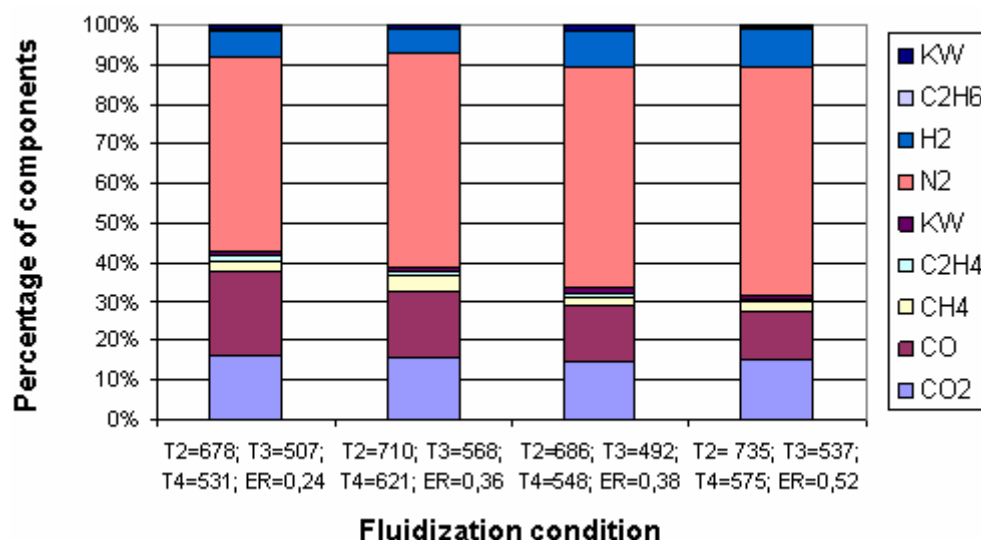


Figure 5.18 Composition of the producer gas dependent on ER

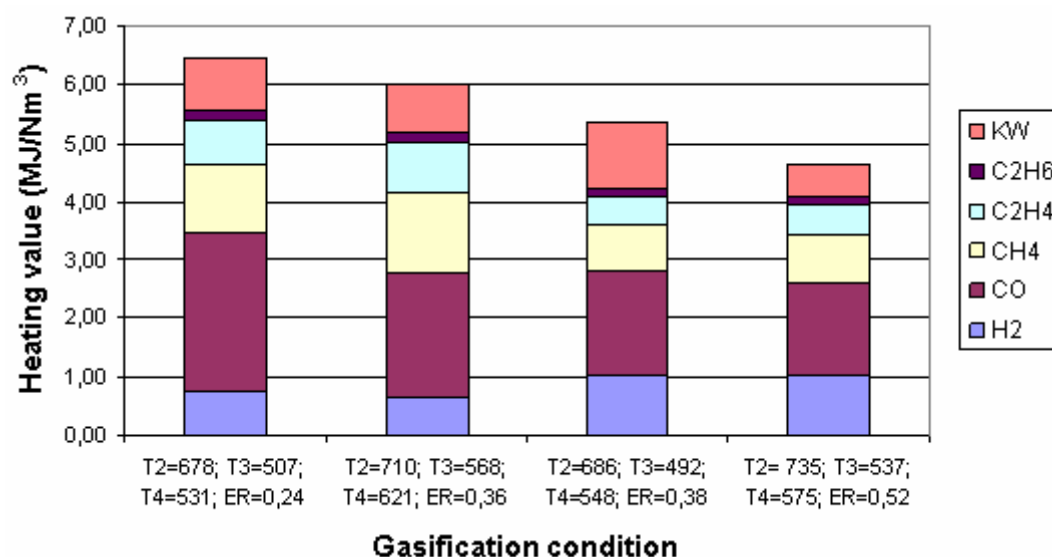


Figure 5.19 Heating value of the producer gas dependent on ER

The figures 5.20 and 5.21 show compositions of the producer gas when the gasification reactions occur above the bed. Particular trait of this period is  $T_3 > T_2$ . In this case,  $T_3$  is supposed to be the gasification temperature. At that time the amount of rice husk, rice husk char and ash in the bed was too much that bad mixing with the bed material can be assumed. All the oxidation, reduction and pyrolysis reactions occur above the bed and that leads to a gasification process similar to an updraft fixed bed gasifier. However, the heating value of the producer gas is still in accordance with the experience of a decreasing heating value with an increasing the ER. The same result is valid for the producer gas composition as explained above.

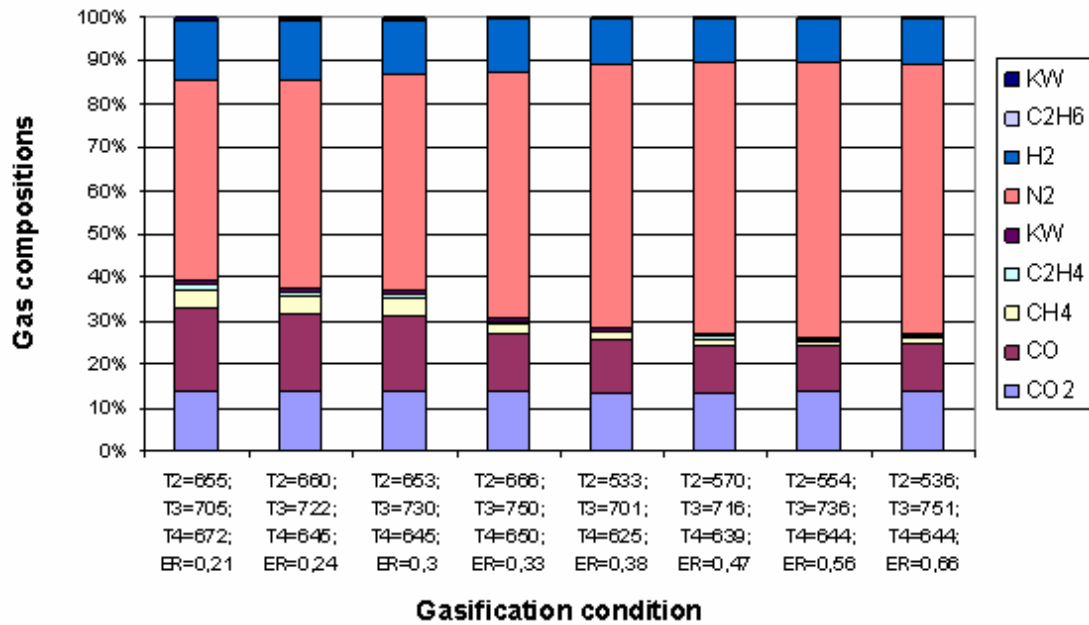


Figure 5.20 Composition of the producer gas when gasification process of rice husk takes place at the top of the bed

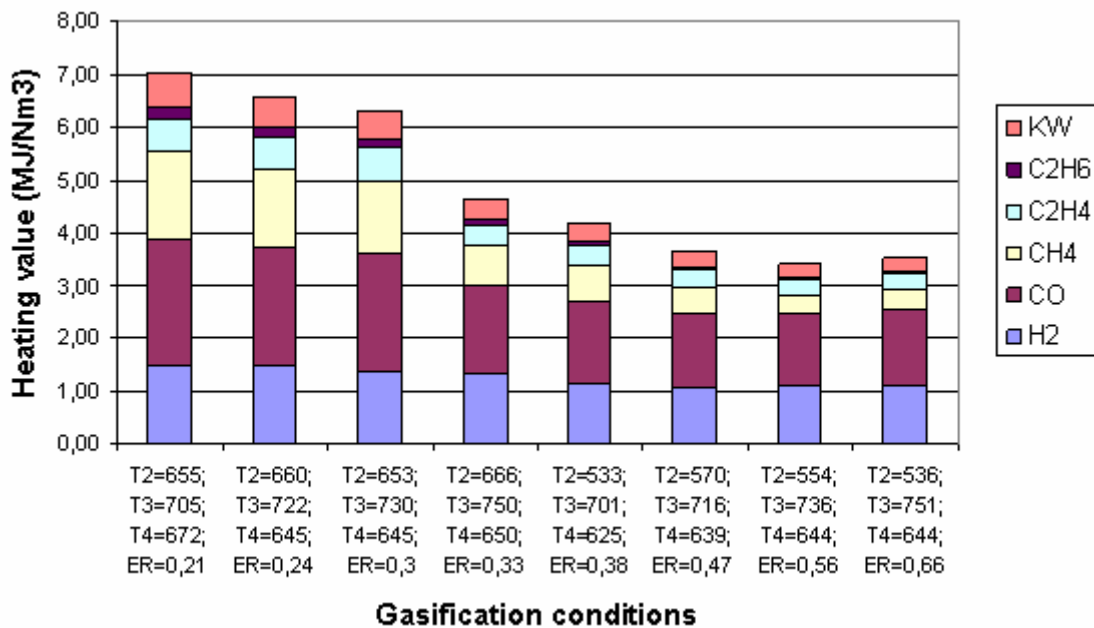


Figure 5.21 Heating value of the producer gas when gasification process of rice husk takes place at the top of the bed

#### 5.4.2.3 Tar content in the producer gas

In all experiments gasification of rice husk in good mixing condition was only possible for a duration of 15 to 20 minutes. The tar measurements have been taken in case of gasification in the bed as well as above the bed. Selected results are shown in figure 5.22.

As it can be seen in the figure, that the tar content for the "in-bed" measurements in case of lower temperature and ER is lower compared to the tar content in case of higher temperature and ER. These contrary results are because of the pyrolysis reactions on the way of the fuel falling down from the supplying point to the bed. It is

known that tar is a product of pyrolysis reactions occurred faster and stronger at higher temperature and ER. The time of falling down is also too short for the thermal cracking reaction for the pyrolysis products and therefore results in a higher tar content in the producer gas. However, this hypothesis needs more experiments to be confirmed.

In case when the gasification process occurs above the bed, a higher temperature  $T_3$  higher resulted in a lower tar content. This is in accordance to the normal rules that the tar content decreased with an increasing of the temperature.

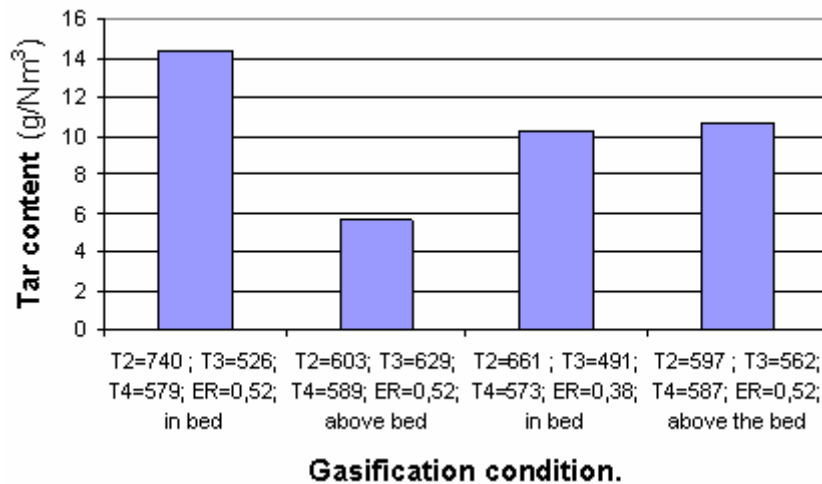


Figure 5.22 Tar content in the producer gas

#### 5.4.2.4 Problems of rice husk gasification

With the experiments it was shown that gasification of rice husk is possible in a fluidized bed. The composition of the producer gas, the calorific values, and also the tar content (e.g. 5-15 g/Nm<sup>3</sup>) were obtained in the same order of magnitude as it was observed for wood pellets gasification. Furthermore, the results are comparable to those found in literature.

With the particular characteristics of rice husk as described in section 5.1.2, experiments with rice husk gasification were not as stable as with wood pellets. The following problems were recognized:

- Problem with the feeding system.** Because of the very low bulk density compared to wood pellets ( $\rho_{rh} = 130 \text{ kg/m}^3$  while  $\rho_{wood \text{ pellet}} = 440 \text{ kg/m}^3$ ), the feeding system must work harder to supply the same amount of fuel (referred to energy) compared to the wood pellets. The feed rate is not uniform and this leads to the difficulties in calibration of the feeding system. Also, because the feeding system has to transport more volume per time, the screw must be operated at higher rotations. These higher rotations lead to the friction problems between the screw and rice husk. Figure 5.23 shows the microscope picture of rice husk skin. The rice husk skin is rough, hard and there are quite many needles on the surface. Figure 5.24 shows the effect of the friction force on the screw after about 20 hours of operation.

One further problem is the small size of the feeding screw in case of the laboratory size test rig. But this is not a real problem and will be no more present for each large scale.

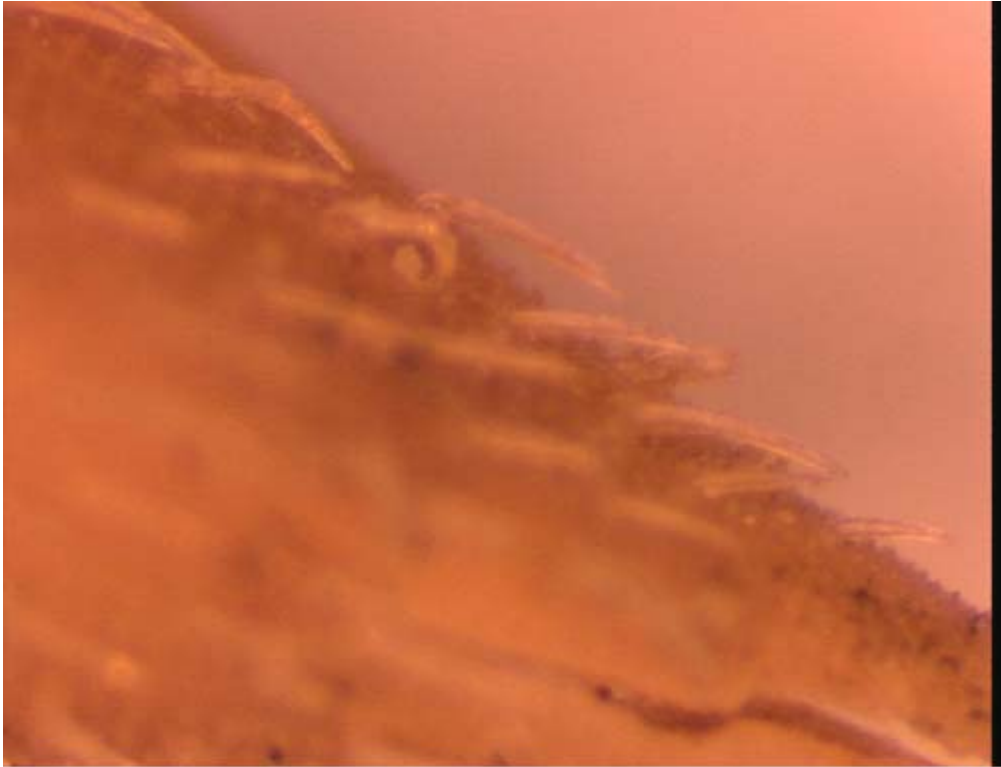


Figure 5.23 Outer surface of rice husk particle



Figure 5.24 Screw feeder after 20 hours of feeding rice husk

- **Ash removal problem.** As described in 4.4.1, rice husk used in the experiments have an ash content of 15,18% with more than 95% silica content and gives a rigid skeleton like structure to the ash. Ash was formed containing the same structure of a single rice husk particle and was not easy to break. Figure 5.25

shows an examples of a rice husk ash taken from the reactor after the experiment. The carry over of such large pieces of ash is quite small compared to the new formed ash in the bed for example in case of wood pellets gasification. Furthermore, the cylindrical shape of rice husk ash was very difficult to be pneumatically transported so that most of the ash remained in the bed.



**Figure 5.25 Shape of one a rice husk ash particle**

Figure 2.26 shows the ash remaining in the bed after one experiment. The picture also shows that the unburned carbon in the ash is quite high which can be assumed by the black color of the ash. Even some rice husk seems to be still in the early stage of conversion.



**Figure 5.26 Rice husk ash remaining in the bed after one experiment**

**Rice husk mixing problem.** The rice husk supply rate to the reactor was 6g/minute. After 20 minute of operation, there would be 15,6 g ash inside reactor assuming an ash content of 13,9 % and no elutriation. Having the same shape of rice husk with a little smaller size, rice husk ash particles with a lower mass will have also a lower bulk density. The measurement of rice husk ash bulk density including more than a half broken particles gives  $\rho_{\text{ash}}=125\text{kg/m}^3$ . With this low bulk density rice husk ash is difficult to mix with the bed materials (Quartz sand) and therefore tend to float on the top of the bed.

Figure 5.27 shows the experiment of fluidization behavior of rice husk ash and sand in the cold model of fluidized bed made of Plexiglas. Even with a uniform mixing at the beginning, rice husk ash and quartz sand quickly tend to segregate due to the different in density. Rice husk ash became flotsam and sand became jetsam. As shown in figure 5.25 at high air supply velocities ( $4U_{\text{mf}}$  of sand), a part of the rice husk ash is completely separated from the sand bed and both of them were fluidized in separated parts of one column.



**Figure 5.27 Fluidization behavior of rice husk ash and sand**

**Ash melting point problem.** Rice husk ash starts melting at a temperature of  $749^{\circ}\text{C}$ . For the gasification experiments, the setting of temperatures was controlled not to exceed this temperature. However when more ash was produced in the reactor and the mixing process was not as good as necessary, there would be a higher probability to have hot spots so that ash melting and sticking together can occur as shown in figure 5.28. With the time, rice husk ash agglomerated together and formed a block as it can be seen in figure 5.29. In this case, heat transfer and air distribution were very poor and the combustion of char was incomplete.



Figure 5.28 Rice husk ash particle stucked together in a small spot



Figure 5.29 Rice husk ash agglomerated together to form a block

#### ***5.4.2.5 Proposed ideas for the rice husk gasification***

The laboratory test rig of fluidized bed gasification at the Institute of Chemical Engineering was designed mainly for gasifying wood residues. It operates well when gasifying wood pellets. However, for special characteristic fuels such as rice husk, some modifications are necessary for the appropriate operation of the gasifier.

**Screw feeder:** A screw feeder is still a best way for feeding rice husk into the fluidized bed gasifier since the ability of controlling the feeding rate of the fuel. However with the a low density fuel like rice husk, a longer thread pitch may be better since it can reduce the rotation rate of the screw and reduce also the attrition between the screw and rice husk particles. The proper selection of the material to manufacture the screw, the structure of the feeding system have further affects on the long life and stable working of feeding system.

**Feeding methodology.** The low bulk density characteristic of rice husk and also of rice husk ash cause a strong segregation tendency between rice husk or rice husk ash and the quartz sand in the bed with rice husk or rice husk ash floating on the top of the bed. Fuel feeding from the top of the bed may not be suitable for these characteristics. *Mansaray et al., 1999* supposed that fuel feeding from the bottom may be better for the rice husk. Furthermore, a dual distributor feeding mechanism where the fuel is fed at the secondary fluidized bed column below the main fluidized bed have been proposed as shown in figure 4.12. The observation during experiments with rice husk gasification shows that rice husk feeding from the bottom of the bed is better for the gasification process because:

- Heat and mass transfer in the fluidized bed are more uniform comparing to that process when feeding above the bed. This can contribute to a more stable gasification process.
- On the way of floating from the bottom to the top of the bed, rice husk have more chance to be burnt or gasified and more ash is broken by the turbulence of the fluidization of the sand particles. In this case the ash removal through fly ash is more efficient.
- Under the turbulent condition of fluidization, a uniform temperature is created all over the bed. Therefore, hot spots can be avoided and the tendency for the ash to agglomerate is much lower.

**Ash removal methodology.** Rice husk have a very high ash content and the ash particles have the same structure like original rice husk particles. This is leads to a fast increase of the ash volume in the bed that affects to the fluidization behavior of the mixture. Increasing the quantity of sand is one method to extend the time that ash really affects the fluidization behavior of the bed. So in case of rice husk gasification, mass of fluidization materials needed to be increase as much as possible. This also helps to increase the efficiency of a complete gasification of the fuel, and the fly ash removal. The rate of ash removal through fly ash is relatively small compared to the new formation of ash. In a continuously operated gasifier with rice husk as a fuel, material segregation will be a problem. Therefore, such a gasifier should be equipped with a removal system for ash from the bed. This could be a floating based on the principle that ash has the tendency of floating to the top of the bed. If the amount of ash exceeded a certain level, it can automatically falling down to the floating ash container based on its gravity.

Figure 5.30 shows the proposed modifications for the recent laboratory gasifier so that it can be used properly for rice husk gasification.

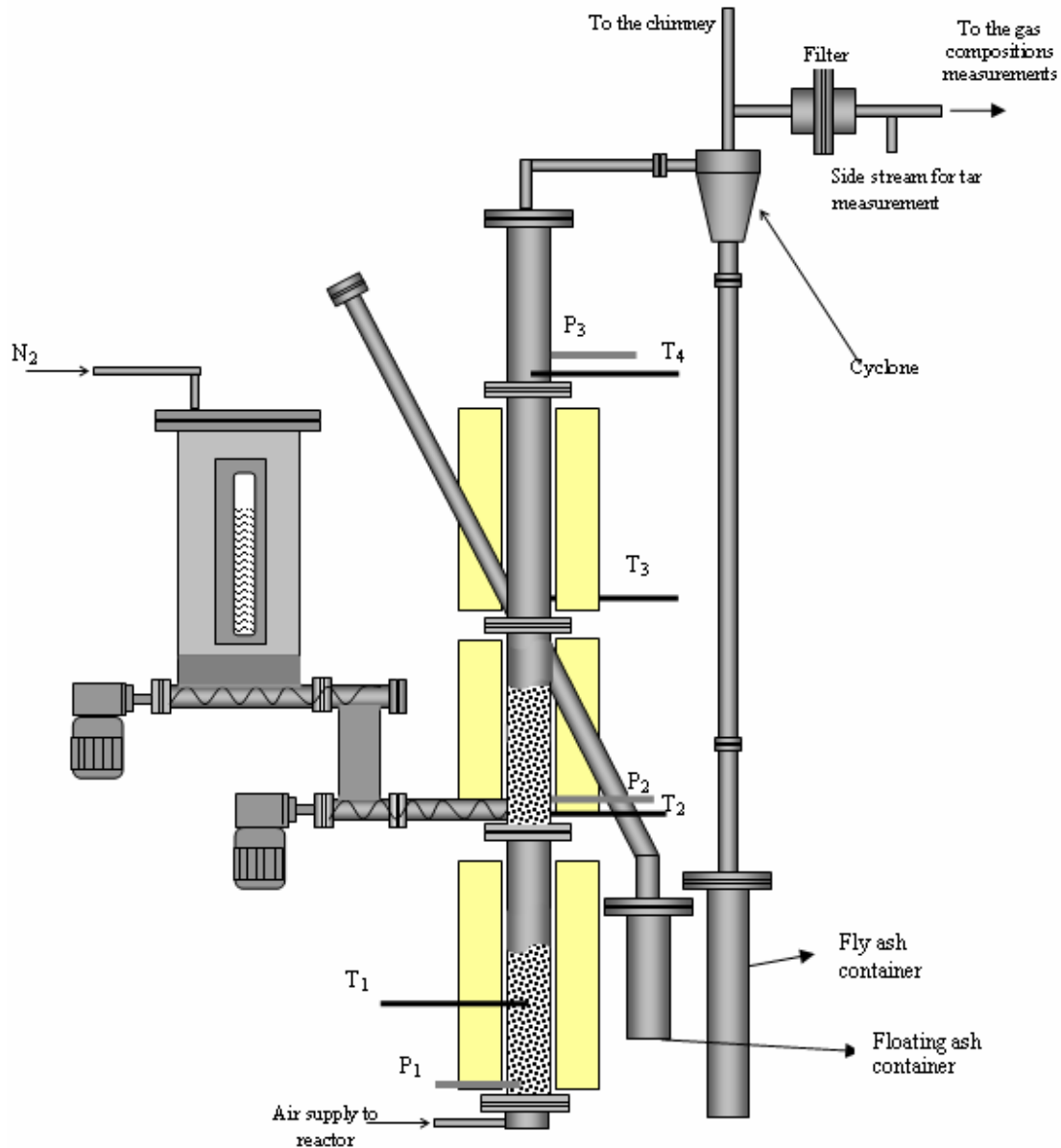


**Figure 5.30 Proposed improvements for the laboratory scale gasifier for rice husk gasification**

The improvements are mainly referred to the gasification zone of the reactor with the following activities:

- Equip the screw feeder with a higher thread pitch.
- Increase the sand or other bed material in the gasification bed as much as possible.
- The feeding point should be changed to the bottom of the fluidized bed.
- Equip the plant with a floating ash removal. The height of the floating ash removal point should be variable so that it is possible to adapt for different amounts of bed materials in the bed and also with the variation of volume flow of the air.

## **5.5 Conclusions**

Experiments have been carried out for gasifying rice husk and wood pellets in a laboratory scale fluidized bed gasifier. The fuel characteristics of the two fuels are quite different in bulk density, ash content, and shape of particles that lead to the different gasification results. The gasification of wood pellets occur continuously with a stable operation while there are quite many problems occur when gasifying rice husk. The most important problems were:

- The feeding system had not worked well. High friction forces were the reason for the damaging of the screw feeder. Calibration of the feed rate was difficult which resulted in relatively low accuracy.
- Ash removal had not properly worked as expected that led to the abundant ash remaining in the reactor which affected the fluidization behavior of the bed. Ash melting led to the agglomeration of rice husk ash and the problem of ash removal became more severe.
- Pyrolysis occurred at the top of the fluidized bed. Heat and mass transfer in this area were not as good as in the fluidized bed area. Furthermore the reaction rate was not stable which led to variation in gas composition and tar content in the producer gas.

However, many experiments have been carried out with the analysis of the producer gas, temperature in the reactor and pressure drop through the bed material. On the base of these experiments the gasification process is now understood quite well and also the influence of temperatures and other conditions on the formation of the gas components and tar content in the producer gas is quite clear. The observations made also give an opportunity to propose a modification of the gasifier for properly working with rice husk as fuel. However, those modifications have to be proofed by further research work.

## **6 CONCLUSION AND RECOMMENDATION**

Rice husk and wood pellets are among the most popular biomass used in the world that could be used for energy generation. Among the technologies used, fluidized bed gasification is a well known technique that gives many advantages. In the fluidized bed gasifier and other fluidized bed applications, kinetic of fluidization mechanism play a very important role for the proper work of the processes. With the particular characteristics, biomasses such as wood pellets and rice husk are not possible to fluidize alone in a proper way thus the addition of a second fluidization material is necessary. The mixture of two materials with different characteristics will affect the fluidization behavior of the fluidized bed so that it also can affect its applications.

The research on fluidization behavior of mixtures of biomass and sand concentrated on the analysis of pressure drop and its fluctuations at different percentages of biomass in the mixture and the mixing behavior of the mixture at different conditions lead to the following results:

- Fluidization behavior of biomass alone is similar to the behavior of group C particles in Geldart classification. Due to the particular characteristic of particles, biomass is easy to agglomerate so that it is impossible to fluidize. At very high air supply velocity, channeling appears and the fuel in the top was blown upward. Big holes appear when the bed column is low or could be divided when the bed column is high enough.
- Fluidization behavior of the fluidization material becomes complicated when introducing biomass to the bed. Changing porosity and the changing location of biomass particles in the bed lead to the partial defluidization and the curve of pressure drop vs. air supply velocity can vary in each experiment. The curves received when gradually increasing and decreasing air supply velocity are completely different. Determining an accurate value for the minimum fluidization velocity of the mixture seems not to be possible.
- Fluctuation of pressure drop that appears and increases with the formation of bubbles is reduced when introducing biomass into the bed. It means the biomass in the bed can reduce the bubbles and influences the fluidization behavior. For the actual application it is important to understand how pressure drop fluctuations are related to the fluidization behavior.
- Mixing of biomass and sand in the fluidized bed was studied by determining the mixing index (MI) based on the concept of real volume of biomass in the mixture. The mixing is mainly caused by the formation of bubbles. However, when biomass and sand are initially separated, and biomass is placed at the bottom of the bed, the agglomeration characteristic of biomass is a reason for bad mixing at a low air supply velocities. The mixing quality is essentially increased when the air velocity is high enough to break the biomass layer.
- When biomass initially is placed at the top of the bed, the gap of no mixing and a very well mixed bed is quite small. The bed is quickly mixed above a certain level of air velocity and at lower velocities nearly no mixing can be observed. In general, the mixing quality decreased by increasing the percentage of biomass in the bed.

- Continuous feeding of biomass leads to a good mixing even at low air supply velocity. However, the mixing indexes are different even when all other parameters such as air supply velocity, percentage of biomass, and fluidization time were kept constant. Equations or methods for prediction of the mixing index are very difficult to develop.
- Experiments also showed that rice husk due to its low density, affected the fluidization behavior more than wood pellets at the same biomass percentage.

In the actual application of biomass gasification in fluidized bed, beside the difficulties in particles characteristics, there are some difficulties in the fuel characteristics of rice husk including:

- The heating value of rice husk is low (HHV dry basis is 16,636 MJ/kg) compare to of wood pellets (19,962 MJ/kg).
- The ash content in the fuel is relatively quite high (15,18% dry basis). The ash with more than 95% silica can form a structure similar to rice husk particles giving the difficulty of ash removal and affection on the fluidization behavior of the bed. The low ash melting point compels the gasifier to be operated at low temperatures what can reduce the efficiency.
- The low bulk density of rice husk and the hard surface with the prickles lead to difficulties for the screw feeding system. One screw was damaged due to friction force when feeding rice husk. The calibration of the feeding rate is also difficult.
- Results of experiments, which have been performed with gasification of wood pellets and rice husk show that gasification of wood pellets is much more stable compared to rice husk.

The gasifier designed in this way may not be very suitable to be operated with special fuels, such as rice husk. Based on the experiences obtained when gasifying rice husk, some modifications can be proposed as follows:

- Increase the thread pitch of the screw feeder and select a suitable material that can stand with high friction force.
- Adding as much as possible fluidization materials into the fluidized bed.
- Feeding rice husk from the bottom of the bed.
- Equipping a floating ash removal system.

## Reference

- Abrahamsen, A.R., and Geldart, D. (1980a): *Behaviour of Gas-Fluidized Beds of Fine Powders, Part 1. Homogeneous Expansion*, Powder Technol., Vol. 26, pp. 35-46.
- Abrahamsen, A.R., and Geldart, D. (1980b): *Behaviour of Gas-Fluidized Beds of Fine Powders, Part 2. Voidage of the Dense Phase in Bubbling Beds*, Powder Technol., Vol. 26, pp. 47-55.
- Adanez, J., and Abanades, J.C. (1991): *Minimum Fluidization Velocities of Fluidized-Bed Coal-Combustion Solids*, Powder Technol., Vol. 67, pp. 113-119.
- Aznar P. M. , Gracia-Gorria F. A. , Corella J. , (1992a). *Minimum and maximum velocities for fluidization for mixtures of agricultural and forest residues with a second fluidized solid. I. Preliminary data and results with sand-sawdust mixtures*. International Chemical Engineering 32, No1, pp 95-102
- Aznar P. M. , Gracia-Gorria F. A. , Corella J. , (1992b). *Minimum and maximum velocities for fluidization for mixtures of agricultural and forest residues with a second fluidized solid. II. Experimental results for different mixtures*. International Chemical Engineering 32, No1, pp 103-113
- Babu, S.P., Shah, B., and Talwalkar, A. (1978): *Fluidization Correlations for Coal Gasification Materials – Minimum Fluidization Velocity and Bed Expansion Ratio*, AIChE Symp. Ser., Vol. 74, No. 176, pp. 176-186.
- Baeyens, J. (1973): Ph.D. thesis, University of Bradford, UK.
- Baeyens, J., and Geldart, D. (1974a): *Particle Mixing in a Gas Fluidized Bed*, Int. Symp. on Fluidization and Its Applications, Oct. 1-5, 1973, Toulouse, France, Cepadues Editions, Toulouse, France, pp. 182-195.
- Bai D., Shibuya E., Nakagawa N., Kato K. (1996). *Characterization of gas fluidization regimes using pressure fluctuations*. Powder technology. 87:105-111.
- Baskakov, A. P., Tuponogov, V.G. and Filippovsky, N.F. (1986). *A study of pressure fluctuations in a Bubbling fluidized bed*. Powder technology, 45, 113-117
- Bena, J., Ilavsky, J., Kossaczky, E., (1960). *Calculation of the boundary velocity of fluidization*. Chemicky Prumysl . 10, pp. 285-90..
- Bi H. T., Ellis N., Abba I. A., Grace J. R. (2000). *A state-of-the-art review of gas-solid turbulent fluidization* Chemical Engineering Science 55, pp. 4789-4825
- Bi H. T., Grace J. R. (1996). *Radial pressure differences and their fluctuations in dense fluidized beds*, Chemical Engineering Science, Vol. 51, No. 4, pp. 663-665.
- Bi, H., and Fan, L.-S. (1992): *Existence of Turbulent Regime in Gas-Solid Fluidization*, AIChE J., Vol. 38, No. 2, pp. 297-301.
- Bi, H.T., and Grace, J.R. (1994): *Transition from Bubbling to Turbulent Fluidization*, AIChE Ann. Meeting, San Francisco, 13-18 November.

- Bi, H.T., and Grace, J.R. (1995): *Effects of Measurement Methods on Velocities Used to Demarcate the Transition to Turbulent Fluidization*, Chem. Eng. J., Vol. 57, pp. 261-271.
- Bilbao, R., Lezaun, J. and Abanades, J.C., (1987) *Fluidization velocities of Sand/straw Binary mixtures*. Powder Technology, 52; 1-6
- Bilbao, R., Lezaun, J., Menendez, M., and Izquierdo, M.J., (1991). *Segregation of Straw/sand mixtures in fluidized beds in non-steady state*. Powder Technology, 68, 31-35
- Bingyan, X., and Zongnan, L., (1987) *A study of fluidized bed gasification of rice hulls*. Advances in Solar Energy Technology, Bienial congress, Hamburg, Germany, 2312-2316
- Bolhar-Nordenkamp, M., (2004) *Techno-Economic Assessment on the gasification of Biomass on the large scale for heat and power production*. Ph.D thesis. Institute of Chemical Engineering, TU Vienna.
- Bourgeois, P. and Grenier, P. (1968): *Ratio of Terminal Velocity to Minimum Fluidizing Velocity for Spherical Particles*, Can. J. Chem. Eng., Vol. 46, pp. 325-328.
- Briens, L. A., and Ellis, N.,. (2005) *Hydrodynamics of three-phase fluidized bed systems examined by statistical, fractal, chaos and wavelet analysis methods* Chemical Engineering Science 60 6094 – 6106
- Briongosa, J. V., Guardiolab, J., (2005). *New methodology for scaling hydrodynamic data from a 2D-fluidized bed*. Chemical Engineering Science 60 5151 – 5163
- Broadhurst, T.E., and Becker, H.A. (1975): *Onset of Fluidization and Slugging in Beds of Uniform Particles*, AIChE J., Vol. 21, pp. 238-247.
- Brotz, W. (1956): Chem. Eng. Technol., Vol. 28, pp. 165.
- Brown, R. C., and Brue, E., (2001). *Resolving dynamical features of fluidized beds from pressure fluctuations*. Powder Technology, , 119:68-80
- Brue, E., and Brown, R. C., (2001). *Use of pressure fluctuations to validate hydrodynamic similitude in fluidized media: bubbling beds*. Powder Technology, , 119:117-127
- Cai, P., Chen, S.P., Jin, Y., Yu, Z.Q., and Wang, Z.W. (1989): *Effect of Operating Temperature and Pressure on the Transition from Bubbling to Turbulent Fluidization*, AIChE Symp. Ser., Vol. 85, No. 270, pp. 37-43.
- Cheung, L., Nienow, A. W., Rowe, P. N., (1974). *Minimum fluidization velocity of a binary mixture of different sized particles*. Chemical Engineering Science. 29 (5), 1301-3.
- Chiba, S. M.Sc. Thesis, University of Hokkaido, Japan (1977)
- Chiba, S., Chiba, T., Nienow, A. W., Kobayashi H., (1979). *The minimum fluidization velocity, bed expansion and pressure-drop profile of binary particle mixtures*. Powder Technology . 22(2), 255-69

- Chiba, S., Nienow, A.W., Chiba, T. and Kobayashi., (1980). *Fluidized Binary Mixtures in which the Denser component may be Flotsam*. Powder Technology, 26, 1-10
- Chiba, T., and Kobayashi, H., (1977). *Solids Exchange between the Bubble Wake and the Emulsion in a Gas-fluidized Bed*, J. Chem. Eng. Jpn., Vol. 10, pp. 206-210.
- Chitester, D.C., Kornosky, R.M., Fan, L.S., and Danko, J.P. (1984): *Characteristics of Fluidization at High Pressure*, Chem. Eng. Sci. , Vol. 39, pp. 253-261.
- Coltters, R., and Rivas, A.L., (2004). *Minimum fluidation velocity correlations in particulate systems*. Powder Technology 147 34– 48
- Costa, A.M.S., and Souza-Santos, d.M.L.. (1999). *Studies on the Mathematical Modeling of Circulation Rates of Particles in Bubbling Fluidized Beds*, Powder Technol., Vol. 103, pp. 110-116.
- Cuong, N. D., (2004). *Biomass for Electricity generation in Vietnam*, The information for the commercialisation of renewables in ASEAN, Institute of Energy, Vietnam.
- David F. and Brown R. C., (2004) *Analysis of Pressure fluctuations in fluidized bed*. Ind. Eng. Chem. Res., 43, 5721.
- Davies, L., and Richardson, J.F. (1966): *Gas Interchange between Bubbles and the Continuous Phase in a Fluidized Bed*, Trans. Instn. Chem. Eng., Vol. 44, pp. 293-305.
- Davtyan, G. A.; Ainshtein, V. G.; Grigoryan, R. V.; Amamchyan, M. G., (1976) *Starting velocity of the fluidization of some industrial granular materials under actual working conditions*. Izvestiya Akademii Nauk Armyanskoi SSR, Seriya Tekhnicheskikh Nauk , 29(5), 36-44.
- Doichev, K., and Akhmakov, N.S. (1979): *Fluidization of Polydisperse Systems*, Chem. Eng. Sci., Vol. 34, pp. 1357-1359.
- Dunham, G.E., Mann, M.D., and Grewal, N.S. (1993). *Dependence of Transition to Turbulent Fluidization on the Static Bed Depth in a Fluidized Bed*, Int. Conference on Circulating Fluidized Bed, A.A. Avidan (Ed.).
- Ellis N. , Briens L.A. , Grace J.R. , Bi H.T. , Lima C.J., (2003). *Characterization of dynamic behaviour in gas–solid turbulent fluidized bed using chaos and wavelet analyses*. Chemical Engineering Journal. 96, 105–116
- Fan, L.T. (1990): *Recent Developments in Solids Mixing*, Powder Technol., Vol. 61, pp. 255-287.
- FAO (1986). *Wood gas as engine fuel*. FAO forestry paper 72. M-38. ISBN 92-5-102436-7
- Flanigan V.J., Xu B.Y. and Huang E., (1987). *Fluidized bed gasification of rice hulls*. The Tenth Annual energy sources technology conference and Exhibition, Dallas, Texas, 19-34.
- Frantz, J.F. (1966): *Minimum Fluidization Velocities and Pressure Drop in Fluidized Beds*, Chem. Eng. Prog. Symp. Ser., Vol.62, pp. 21-31.

- Geldart, D. (1973). *Types of Gas Fluidization*, Powder Technol., Vol. 7, pp. 285-292.
- Gonzales, A., Chaouki, J., Chehbouni, A., Guy, C., and Klavna, D. (1994): *Effect of Temperature on the Onset of Turbulent Fluidization*, 4th Int. Conf. Circulating Fluidized Beds, A. Avidan (Ed.), AIChE, New York, pp. 681-688.
- Gonzalez, A., Chaouki, J., Chehbouni, A., Guy, C., and Klvana, D. (1995): Eighth Engineering Foundation Conf. Fluidization, Tours, France, Engineering Foundation, pp. 681-688.
- Goossens, W. R. A., Dumont, G. L., Spaepen, G. J., (1971). *Fluidization of binary mixtures in the laminar flow region.* AIChE Symposium Series , 67(116), 38-45.
- Goroshko, V.D., Rozembaum, R.B., and Todes, O.M. (1958). Izv. Vyssh., Uchebn. Zaved. Neft. Gaz, Vol. 1, pp. 125.
- Grace, J.R. (1982). *Fluidized Bed Hydrodynamics*, in Handbook of Multiphase Systems, G. Hetsroni (Ed.), Washington Hemisphere Publishing, Washington.
- Grace, J.R. (1986). *Contacting Modes and Behaviour Classification of Gas-Solid and Other Two-Phase Suspensions*, Can. J. Chem. Eng., Vol. 64, p. 353-363
- Gwyn, J.E., Moser, J.H., and Parker, W.A. (1970). *A Three-phase Model for Gas-Fluidized Beds*, Chem. Eng. Prog. Symp. Ser., Vol. 66, pp. 19-27.
- Han, G.Y., Lee, G.S, and Kim, S.D. (1985). *Hydrodynamics of a Circulating Fluidized Bed*, Korean J. Chem. Eng., Vol. 2, pp. 141-147.
- Hartiniati, A., Soemardjo, A. and Youvial, M., (1989). Performance of a pilot scale fluidized bed gasifier fuelled by rice husks. Proc. Int. Conf. Pyrolysis and Gasification, 257-263.
- Hiby, J. W. (1967) Periodic phenomena connected with gas-solid fluidization. *Proceedings of the International Symposium on Fluidization*, Eindhoven, The Netherlands,; The Netherlands University Press: Amsterdam, p 99.
- Hofbauer, H. (2004). *Wirbelschichttechnik*, Unterlagen zur vorlesung No 159220, Institute für Verfahrenstechnik, Umwelttechnik und Techn. Biowissenschaften, TU Wien.
- Horio, M., (1991). *Hydrodynamics of Circulating Fluidization: Present Status and Research Needs*, Circulating Fluidized Bed Technology III, P. Basu, M. Horio, and M. Hasitani (Eds.), Pergamon Press, Oxford, UK, pp. 3-14.
- Horio, M., Nonaka, A., Hoshiba, M., Morishita, K., Kobukai, Y., Naito, J., Tachibana, O., Watanabe, K., Yoshida, N. (1986). *Coal Combustion in a Transparent Circulating Fluidized Bed*, in Circulating Fluidized Bed Technology, P. Basu (Ed.), Pergamon, New York, pp. 255-262.
- Hrbek, J., (2005). Experimental investigation of selected elements behaviour during biomass pyrolysis and gasification. Ph.D dissertation, Institute of Chemical Engineering, TU Vienna.

- Jin, Y., Yu, Z.Q., Wang, Z., and Cai, P. (1986). *A Criterion for Transition From Bubbling to Turbulent Fluidization*, in Fluidization V, K. Ostergaard, and A. Sorensen (Eds.), Engineering Foundation, New York, pp. 33-40.
- Kang, W.K., Sutherland, J.P., Osberg, G.L., (1967). *Pressure fluctuations on a fluidized bed with and without screen cylindrical packings*. Ind. Eng. Chem. Fundam., 6 (4), 499-504.
- Knoef, H. A. M., (2005). *Handbook biomass gasification*. BTG biomass technology group, Netherlands.
- Kumar, A. and Sen Gupta, P. (1974). Industrial journal Technology, 12, 225-228
- Kunii, D. and Levenspiel, O. (1991): *Fluidization Engineering*, Second Edition, Butterworth-Heinemann, Boston.
- Kunii, D., and Levenspiel, O. (1969): *Fluidization Engineering*, Wiley, New York, USA.
- Lee, G.S., and Kim, S.D. (1989): *Gas mixing in Slugging and Turbulent Fluidized Beds*, Chem. Eng. Comm., Vol. 86, pp. 91- 111.
- Lee, G.S., and Kim, S.D. (1990): *Bed Expansion Characteristic and Transition Velocity in Turbulent Fluidized Beds*, Powder Technol., Vol. 62, pp. 207-215.
- Letzel, H. M. , Schouten, J. C., Krishna, R., van den Bleek, C. M.. (1997) *Characterization of regimes and regime transitions in bubble columns by chaos analysis of pressure signals*, Chemical Engineering Science, Vol. 52:.. 4447- 4459,
- Leu, L.-P., Hsia, J.-W., and Gua, B.-B. (1990). *Axial pressure Distribution in Turbulent Fluidized Beds*, Proc. of the 2nd Asian Conference on Fluidized Bed and Three-Phase Reactors, pp. 71-79.
- Leva, M. (1959). *Fluidization*, McGraw-Hill, New York.
- Leva, M., Shirai, T., and Wen, C.Y. (1956). Genie Chim., Vol. 75, pp. 33.
- Li Xiaodong, Yan Jianhua, Ni Mingjiang, Cen Kefa, (2001). *Study on mixing performance of municipal solid waste (MSW) in differential density fluidized beds (FBs)*. Chemical Engineering Journal. 84, 161–166
- Li, Z., Kobayashi, N. , Hasatani, M., (2005). *Characteristics of pressure fluctuations in a fluidized bed of Binary mixtures*. Journal of chemical Engineering of Japan, , Vol 38; 12:960-968.
- Lien, N. T. K., (2001). Country Paper Vietnam, Regional Seminar on Commercialization of Biomass Technology, Guangzhou, China.
- Lim, K.S., Zhu, J.X., and Grace, J.R.,(1995). *Hydrodynamics of Gas-Solid Fluidization*, Int. J. Multiphase Flow, Vol. 21, pp. 141-193.
- Lin, C.-L., Wey, M.-Y., You, S.-D., (2002). *The effect of particle size distribution on minimum fluidization velocity at high temperature..* Powder Technology 126 297– 301

- Lin, J.S., Chen, M.M., and Chao, B.T. (1985). *A Novel Radioactive Particle Tracking Facility for Measurement of Solids Motion in Gas Fluidized Beds*, AIChE J., Vol. 31, pp. 465-473.
- Lin, T. J. , Juang, R. C. , Chen, Y. C., Chen, C. C., (2001a). *Predictions of flow transitions in a bubble column by chaotic time series analysis of pressure fluctuation signals*. Chemical Engineering Science 56 1057-1065
- Lin, T. J. ., Juang, R.C., Chen, C. C., (2001b). *Characterizations of flow regime transitions in a high-pressure bubble column by chaotic time series analysis of pressure fluctuation signals*. Chemical Engineering Science 56 6241–6247
- Lirag, R.C., Litman, H., (1971). Statistical study of the pressure fluctuations in a fluidized bed, AIChE Symp. Ser. 166 67 11–22.
- Loeffler, G., (2001). *A Modeling Study on Fuel-nitrogen Conversion to NO and N2O related to Fluidized Bed Combustion*. Ph.D dissertation. Institute of chemical Engineering, TU Vienna.
- Lucas, A., Arnaldos, J., Casal, J., and Puigjaner, L. (1986). *High Temperature Incipient Fluidization in Mono- and Polydisperse Systems*, Chem. Eng. Commun., Vol. 41, pp. 121-132.
- Mansaray, K.G., Ghaly, A.E., Al-Taweel, A.M., Hamdullahpur, F., Ugursal, V.I. (1999). *Air gasification of rice husk in a dual distributor type fluidized bed gasifier*. Biomass and Bioenergy 17. 315-332
- May, W.G. (1959). *Fluidized-Bed Reactor Studies*, Chem. Eng. Prog., Vol. 55, No. 12, pp. 49-56.
- Miller, C.O., and Logwinuk, A.K., (1951). *Fluidization Studies of Solids Particles*, Ind. Eng. Chem., Vol. 43, pp. 1220-1226.
- Ming-Chang Shou and Lii Ping Leu ,(2005). *Identification of transition Velocities in fluidized beds using wavelet analysis*. Journal of Chemical Engineering of Japan., Vol 38, (6), pp409-421.
- Ming-yan liu and Zong-ding Hu, (2004). *Studies on the Hydrodynamics of Chaotic bubbling in Gas-Liquid bubble column with a single nozzle*. Chemical Engineering Technology, 27, (5), pp. 537-547
- Molerus, O. (1982), *Interpretation of Geldart's Type A, B, C, and D Powders by Taking into Account Interparticle Cohesion Forces*, Powder Technology, 33, pp. 81-87.
- Nakagawa, N., Bai, D., Shibuya, E., Kinoshita, H., Takarada, T., Kato, K., (1994). *Segregation of particles in binary solids circulating fluidized beds*. Journal of chemical engineering of Japan. Vol 27, No2. pp 194-198.
- Nakajima, M., Harada, M., Asai, M., Yamazaki, R., and Jimbo, G. (1991). *Bubble Fraction and Voidage in an Emulsion Phase in the Transition to a Turbulent Fluidized Bed*, in Circulating Fluidized Bed Technology III, P. Basu, M. Horio, and M. Hasatani (Eds.), Pergamon, Oxford, UK, pp. 79-84.

- Nakamura, M.; Hamada, Y.; Toyama, S.; Fouda, A. E.; Capes, C. E., (1985). *An experimental investigation of minimum fluidization velocity at elevated temperatures and pressures*. Can. J. Chem. Eng. 63 pp. 8-13
- Natarajan E., Nordin A., Rao A. N. (1998). *Overview of combustion and gasification of rice husk in fluidized bed reactors*. Biomass and Bioenergy, Vol 14, 533-546.
- Nienow, A.W., Naimier, N.S., and Chiba, T. (1987). *Studies of Segregation/Mixing in Fluidized Beds of Different Size Particles*, Chem. Eng. Commun., Vol. 62, pp. 53-66.
- Nienow, A.W., Rowe, P.N., and Cheung, L.Y.-L. (1978). *A Quantitative Analysis of the Mixing of Two Segregating Powders of Different Density*, Powder Technol., Vol. 20, pp. 89-97.
- Noda, K.; Uchida, S.; Makino, T.; Kamo, H. (1986). *Minimum fluidization velocity of binary mixture of particles with large size ratio*. Powder Technology, 46(2-3), 149-54
- Obata, Eiji; Watanabe, Haruo; Endo, Naotoshi. (1982). *Measurement of size and size distribution of particles by fluidization*. Journal of Chemical Engineering of Japan, 15(1), 23-8.
- Österreichisches normungsinstitut (1993). *ÖNORM M 5861-1: Manuelle Bestimmung von staubkonzentrationen in strömenden gasen*. Wien
- Otero, A. R., and Corella, J. (1971). *Fluidization of mixtures of solids of distinct characteristics. I. Fluidization velocities*. Anales de Quimica, 67(12), 1207-19.
- Panaka, P., (1994). *Operating experience with biomass gasifiers in Indonesia*. In Adv. Thi
- Peeler, J.-P.K., and Huang, J.R., (1989). *Segregation of Wide Size Range Particle Mixtures in Fluidized Beds*, Chem. Eng. Sci., Vol. 44, pp. 1113-1119.
- Perales, J.F., Coll, T., Llop, M.F., Puigjaner, J., Arnaldos, J., and Casal, J., (1991). *On the Transition from Bubbling to Fast Fluidization Regimes*, in Circulating Fluidized Bed Technology III, P. Basu, M. Horio, and Hasatani, M. (Eds.), Pergamon, Oxford, UK, pp. 73-78.
- Pham, H.L., (1999), *Wood Energy Basiss*, FAO/RWEDP.
- Pillai, B.C., and Rao, M.R. (1971): *Pressure Drop and Minimum Fluidization Velocities in Air-fluidized Beds*, Indian J. Technol., Vol. 9, pp. 77-86.
- Qingjie Guo, Guangxi Yue, and Joachim Werther., (2002). *Dynamics of Pressure Fluctuation in a Bubbling Fluidized Bed at High Temperature*. Ind. Eng. Chem. Res., 41, 3482-3488
- Rao, T. R., and Bheemarasetti, J. V. Ram., (2001). *Minimum fluidization velocities of mixtures of biomass and sands*. Energy, 26; 633-644.
- Rhodes, M., and Geldart, D., (1986). *Transition to Turbulence*, in Fluidization V, K. Ostergaard and A. Sorensen (Eds.), Engineering Foundation, New York, pp. 281-288.

- Rice, R.W., and Brainovich, J.F., (1986). *Mixing/Segregation in Two- and Three-dimensional Fluidized Bed: Binary Systems of Equidensity Spherical Particles*, AIChE J., Vol. 32, pp. 7-16.
- Richardson, J.F., and Jeronimo, M.A., (1979). *Velocity-voidage Relations for Sedimentation and Fluidization*, Chem. Eng. Sci., Vol. 34, pp. 1419-1422.
- Rincon, J., Guardiola, J., Romero, A., Ramos, G., (1994). *Predicting the minimum fluidization velocity of multicomponent systems*. Journal of Chemical Engineering of Japan , 27(2), 177-81
- Rowe, P. N.; Nienow, A. W. (1975). *Minimum fluidization velocity of multicomponent particle mixtures*. Chemical Engineering Science , 30(11), pp. 1365-9.
- Rowe, P.N. (1971). *Experimental Properties of Bubbles*, in Fluidization, J.F. Davidson and D. Harrison (Eds.), Academic Press, London, pp. 121-191.
- Rowe, P.N., and Henwood, G.A. (1961). *Drag Forces in a Hydraulic Model of a Fluidised Bed – Part I*, Trans. Instn. Chem. Eng., Vol. 39, pp. 43-54.
- Rowe, P.N., and Partridge, B.A. (1962). *Symp. Interaction between Fluids and Particles*, Instn. Chem. Eng., pp. 135.
- Rowe, P.N., and Partridge, B.A. (1965). *An X-Ray Study of Bubbles in Fluidised Beds*, Trans. I. Chem. Engrs., Vol. 43, pp. 157-175.
- Rowe, P.N., Nienow, A.W., Agbim, A.J., (1972a). The mechanisms by which particles segregate in gas fluidised beds-binary systems of near-spherical particles. Trans. Instn Chem. Engrs, Vol 50, pp 310-323
- Rowe, P.N., Nienow, A.W., Agbim, A.J., (1972b). A preliminary quantitative study of particle segregation in gas fluidized beds-binary systems of near spherical particles. Trans. Instn Chem. Engrs, Vol 50, pp 324-333
- Ruud van Ommen J., Robert-Jan de Korte, van Den Bleek Cor M. (2004) *Rapid detection of defluidization using the standard deviation of pressure fluctuations*. Chemical Engineering and Processing. 43; 1329-1335.
- Sahoo A., and Roy, G.K., (2005). *Mixing characteristic of homogeneous binary mixture of regular particles in a gas–solid fluidized bed..* Powder Technology 159 150–154
- Sanches, C. G and Lora, E.S., (1994). *Biomass fluidized bed gasification research in the state University of Campinas*, Energy for sustainable development, 1 (4), 31-33.
- Sangeetha V., Swathy R., Narayanamurthy N., Lakshmanan C. M. and Miranda L. R., (2000). *Minimum Fluidization Velocity At High Temperatures Based on Geldart Powder Classification* Chem. Eng. Technol. 23 pp. 713-719
- Sathyanarayana, K., and Rao, P. G., (1989). Short Communication, I. Chem. Eng. 31 No. 2, pp. 79-81.
- Saxena, S.C., and Vogel, G.J., (1977). *The Measurement of Incipient Fluidization Velocities in a Bed of Coarse Dolomite at Elevated Temperature and Pressure*, Trans. Instn. Chem. Eng., Vol. 55, pp. 184-189.

- Schaaf, J.v.d., Johnsson, F., Schouten, J.C., Bleek, C.M. v.d., (1999). *Fourier analysis of nonlinear pressure fluctuations in gas-solids flow in CFB risers-observing solids structures and gas/particle turbulence*. Chemical Engineering Science, 54:5541-5546.
- Schouten, J.C., Vander Stappen, M.L.M., and Van Den Bleek, C.M., (1996). *Scale-Up of Chaotic Fluidized Bed Hydrodynamics*. Chemical Engineering Science, Vol. 51, (10), pp. 1991-2000,
- Stiegel, G. J., and Maxwell, R. C., (2001). *Gasification technologies: the path to clean, affordable energy in the 21st century*. Fuel Processing Technology 71 79-97
- Stringer, J., (1989). *Proc. 10th Int. Conf. on FBC*, Vol. 1, pp. 265-272.
- Sun, G., and Chen, G. (1989). *Transition to Turbulent Fluidization and its Prediction*, in Fluidization VI, J.R. Grace, L.W. Shemilt and B.A. Bergougnou (Eds.), Engineering Foundation, New York, pp. 33-40.
- Tamarin, A. I. (1964). *The origin of self-excited oscillations in fluidized beds*. Int. Chem. Eng., 4 (1), 50-54.
- Thonglimp, V. (1981). Ph.D. thesis, Institut National Polytechnique, Toulouse.
- Thonglimp, V., Hiquily, N. and Laguerie, C. (1981). *Vitesse minimale de fluidisation et expansion des couches de mélanges de particules solides fluidisées par un gaz*. Powder technology 39: 223-239.
- Tsukada, M., (1995). *Fluidized Bed Hydrodynamics, Heat Transfer and High Temperature Process Developments*, Ph.D. thesis, Tokyo University of Agriculture and Technology, Tokyo, Japan.
- Tsutsui, T., Furusaki, S., and Miyauchi, T. (1980). *Behavior of Bubbles and Circulating Flow of the Emulsion Phase in a 60 cm – Diameter Fluidized Catalyst Bed*, Kagaku Kogaku Ronbunshu, Vol. 6, pp. 501-507.
- Uchida, S., Yamada, H., Tada, I., (1983). *Minimum fluidization velocity of binary mixture*. Journal of the Chinese Institute of Chemical Engineers , 14(2), 257-64
- van Deemter, J. J. (1961). *Mixing and Contacting in Gas-solid Fluidized Beds*, Chem. Eng. Sci., Vol. 13, pp. 143-154.
- Van den Aarsen F. G., Beenackers A. A. C. M. and van Swaij W. P. M., (1982). *Performance of rice husk fluidized bed pilot plant gasifier*. In producer gas. First Int. Conf.. Srilanka, pp 381-391.
- Verloop, J.; Heertjes, P. M., (1974). *Periodic pressure fluctuations in fluidized beds*. Chem. Eng. Sci. 29, 1035-1042.
- Wen, C.Y., and Yu, Y.H. (1966). *A Generalized Method for Predicting the Minimum Fluidization Velocity*, AIChE J., Vol. 12, pp. 610-612.
- Werther, J., and Molerus, O., (1973). *The Local Structure of Gas Fluidized Beds. II. The Spatial Distribution of Bubbles*, Int. J. Multiphase Flow, Vol. 1, No. 103, pp. 123-128.

- Whitehead, A.B., (1985). *Distributor Characteristics and Bed Properties*, in Fluidization, J.F. Davidson, R. Clift, and D. Harrison(Eds.), Academic Press, London, UK, pp. 173-199.
- Wirsum, M.C., and Fett, F.N. (1997). *Mixing and Segregation of Flotsam Fuel Particles in Bubbling Fluidized Beds*, 14th Int. Conference on Fluidized Bed Combustion, ASME, New York, USA, pp. 251-265.
- Wu, S.Y., and Baeyens, J., (1991). *Effect of Operating Temperature on Minimum Fluidization Velocity*, Powder Technol., Vol. 67, pp. 217-220.
- Wu, S.Y., and Baeyens, J., (1998). *Segregation by Size Difference in Gas Fluidized Beds*, Powder Technol., Vol. 98, pp. 139-150.
- Xu, B.Y., Huang, W.C., Hlanigan, V.J. and Sittong, O.C., (1985). *Design and operation of a 6 inch fluidized bed gasifier for rice hulls*. Symposium on Energy from biomass and waste IX. pp595-613
- Yamazaki, M., Fukuta, K., and Tokumoto, J., (1986). 3rd World Congress of Chem. Eng., Tokyo, Japan.
- Yan Cao, Yang Wang, Riley John, T., Wei-Ping Pan, (2006). *A novel biomass air gasification process for producing tar-free higher heating value fuel gas*. Fuel Processing Technology 87 343 – 353
- Yang, W.C. (1984). *Mechanistic Models for Transitions between Regimes of Fluidization*, AIChE J., Vol. 30, pp. 1025-1027.
- Yerushalmi, J., and Cankurt, N.T. (1979). *Further Studies of the Regimes of Fluidization*, Powder Technol., Vol. 24, pp. 187-205.
- Yogi Goswami Ed. D., (1986). *Alternative Energy in Agriculture*. Vol2, chapter 4. CRC Press.
- Yong-guo Chen, Zi-ping Tian, Zheng-quiring Miao., (2006). *Analysis of the pressure fluctuations in binary solids circulating fluidized bed*. Energy Conversion and Management,; 47: 611-623.
- Zheng, Z. X.; Yamazaki, R.; Jimbo, G., (1985). Kagaku Kogaku Ronbunshu, 11 pp. 115.
- Zhong, W., Zhang, M., (2005). *Characterization of dynamic behavior of a spout-fluid bed with Shannon entropy analysis*. Powder Technology 159 121 – 126

# CURRICULUM VITAE

## PERSONAL DATA

Name: Nguyen Xuan Quang  
Title: Master of Engineering  
Date of birth: 03.12.1973  
Nationality: Vietnam  
Marital status: Married and 1 daughter.  
Home address: 39/12 Le Thanh Nghi, Ha noi, Vietnam.

## EDUCATION AND WORKING EXPERIENCE

Until 1990                      Graduated high school in Vietnam  
1990 - 1995.                  Bachelor study in Thermal-Electrical Department, Energy Faculty, Hanoi University of Technology  
1996- 1997                   Working for Electricity design consultant company No.1, Vietnam.  
1997 - 1999                  Master study in Energy Technology, School of Environmental resources and development, Asian Institute of Technology, Thailand.  
1999- 2003                  Working for Institute of Heat Engineering and Refrigeration, Hanoi University of Technology as a Teacher.  
2003- 2006                  PhD studies at the Institute of Chemical Engineering, Vienna University of Technology. *Topic: Study on Fluidization behavior related to gasification of biomass in fluidized bed*

## PUBLICATION

Quang, N.X., Reichhold, A., Hofbauer, H., (2005). *Fluidization behavior of binary mixture of biomass and sand in fluidized bed*. 14th European biomass conference and exhibition, Paris, France.

## HOBBY AND INTEREST

Wingchun and Buddhist Zen